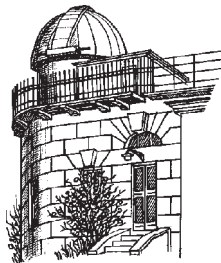


ODESSA ASTRONOMICAL PUBLICATIONS

Volume 23
(2010)



Odessa
«AstroPrint»

FOREWORD

The present 23-th volume of the "Odessa Astronomical Publications" (OAP) contains 46 papers submitted by the participants of the international scientific conference "Variable Stars - 2010", after revising the reports and taking into account discussions. The papers are published in an alphabetical order of the authors. The journal is edited in the research institute "Astronomical Observatory" of the Odessa National University (ONU) named after I.I.Mechnikov and published by the "Astroprint" publishing house. The papers will be listed in the international "Astrophysics Data System" (ADS).

The conference took place on August 16-21, 2010 in the "Chernomorka" summer camp of ONU, just near the Black Sea, 15 km far away from Odessa.

This conference is traditional. It was first organized in Odessa in 1980, exactly 30 years ago. At that time, it was organized by Professor Vladimir Platonovich Tsessevich (1907–1983), the director of the Odessa observatory in 1945-1983 years. He was an outstanding variable star researcher of the twentieth century, eminent scientist, lecturer, popularizer and supervisor of science.

Other conferences "Variable stars" were devoted to the memory of Prof. of V.P.Tsessevich - in 1987, then with a 4-year cycle in 1993, 1997, 2001, 2005. In between, there were conferences on "Interacting binary stars", which are also related to variable stars.

The main topics discussed at the conference were: Interacting Binary Stars (with special sections on Cataclysmic and Symbiotic Variables); Pulsating Variables; Eruptive Variables; Chemical Composition and Evolutionary Status; Discoveries and Classification of New Variables; Mathematical Modeling of Variable Astrophysical Objects and Processes; Variable Radio, Gamma and X-Ray sources; Occultations of Stars and Extraterrestrial Planet Transits; Small Telescopes in Variable Star Research; Advanced Methods and Instruments for Astrophysical Observations.

Among the authors of 83 reports presented at the conference, there 185 astrophysicists of Ukraine, Russia, Azerbaijan, Belorussia, USA, Koorea, Canada, Hungary, Poland, Germany, Slovakia, Czechia, Greece, Finland, France, UK, Chile, Brasil. There were 24 review, 36 oral and 23 poster reports.

Co-chairs of the SOC were Kovtyukh V.V. (AO ONU, Odessa, Ukraine) and Andronov I. L. (ONMU, Odessa, Ukraine), Responsible Editor of this volume. Vice-Chair was Mishenina T.V. (AO ONU, Odessa, Ukraine), secretaries: Melikyants S.M. and Marsakova V.I. (DA ONU, Odessa, Ukraine). World-wide members of the SOC: Andrievsky S.M. (AO ONU, Odessa, Ukraine; LOC chair), Berdnikov L.N. (SAI, Moscow, Russia), Chochol D. (AI SAS, Slovakia), Grinin V.P. (MAO RAS, St.Peterburg, Russia), Hegedus T. (Baja Observatory, Hungary), Henden A. (AAVSO, Harvard, USA), Hric L. (AI SAS, Slovakia), Karetnikov V.G. (AO ONU, Odessa, Ukraine), Kim Chun-Hwey (AO CBNU, Cheongju, Korea), Kudzej I. (Vihorlat Observatory, Slovakia), Mikulasek Z. (MUNI, Brno, Slovakia), Panchuk V.E. (SAO RAS, Russia), Pavlenko E.P. (CrAO, Ukraine), Pavlenko Ya.V. (MAO NANU, Kiev, Ukraine), Pogodin M.A. (MAO RAS, St.Peterburg, Russia), Ryabov M.I. (Odessa obs. RI NAS, Ukraine; ONU, Ukraine), Samus' N.N. (IA RAS; SAI, Moscow, Russia), Szabados L. (Konkoly Observatory, Hungary), Szczerba R. (Nicolaus Copernicus Astronomical Center, Torun, Poland), Turner D. (StMU, Halifax, Canada), Yushchenko A.V. (ARCSEC, Seoul, Korea)

The Web page of the conference is <http://uavso.org.ua/?page=vs2010>, and the Web page of this volume is <http://oap23.pochta.ru>. The photogalleries, are available at <http://photo.online.ua/vs2010/>, <http://uavso.org.ua>, <http://foto.mail.ru/mail/il-a> and <http://foto.mail.ru/mail/pikhun>.

The participants of the conference got a good opportunity to discuss different topics of one of the most actual and dynamically evolving part of astrophysics - the theoretical and observational research of variable stars. SOC and LOC plan to continue the tradition of these conferences in future.

Ivan L. Andronov

CONTENTS

<i>Andronov I.L.</i>	
Foreword	2
Contents	3
<i>Alentjev D.V., Mkrtichian D.E.</i>	
Preliminary Results of Doppler Imaging Analysis of roAp Star α Cir	6
<i>Andronov I.L., Antoniuk K.A., Baklanov A.V., Breus V.V., Burwitz V., Chinarova L.L., Chochol D., Dubovsky P.A., Han W., Hegedus T., Henden A., Hric L., Chun-Hwey Kim, Yonggi Kim, Kolesnikov S.V., Kudzej I., Liakos A., Niarchos P.G., Oksanen A., Patkos L., Petrik K., Pit' N.V., Shakhovskoy N.M., Virnina N.A., Yoon J., Zola S.</i>	
"Inter-Longitude Astronomy" (ILA) Project: Current Highlights And Perspectives. I. Magnetic vs. Non-Magnetic Interacting Binary Stars	8
<i>Baklanova D.N., Plachinda S.I.</i>	
High-Accuracy Magnetic Field Measurements on Cool Giant β Geminorum	11
<i>Barsunova O., Grinin V., Arkharov A., Sergeev S., Shugarov S.</i>	
Observations of Low-Amplitude Brightness Oscillations in the Unusual Eclipsing System V718 Per (HMW 15, H 187)	13
<i>Basak N.Yu., Mishenina T.V., Soubiran C., Kovtyukh V.V., Belik S.I.</i>	
n-Capture Elemental Abundances in Active and Non-Active Stars	17
<i>Breus V.V., Andronov I.L., Dubovsky P.A., Hegedus T., Kudzej I., Petrik K.</i>	
Improved Photometric Characteristics of the Newly Discovered EW-Type System GSC 04370-00206	19
<i>Butkovskaya V.V., Baklanova D.N., Plachinda S.I.</i>	
Spectroscopic Study of the Hot Supergiant ζ Persei	21
<i>Bychkov V.D., Bychkova L.V., Madej J., Schatilo A.V.</i>	
The mCP Star HD 9996 - Precession or Not?	23
<i>Chinarova L.L.</i>	
Wavelet Analysis of 173 Semi-Regular Variables	25
<i>Chinarova L.L., Andronov I.L., Gubin E.G.</i>	
VR CCD Observations of the Intermediate Polars BG CMi and PQ Gem	27
<i>Chekhonadskikh F.A.</i>	
The Abundances of the Elements of the Magellanic Clouds.....	29
<i>Glagolevskij Yu.V., Shavrina A.V., Chuntunov G.A.</i>	
Non-Stationary He-Weak Star HD182255 ?	33
<i>Godłowski W., Szpanko M.</i>	
Abilities of Celestial Observations in Astronomical Observatory of Physics Institute in Opole	37

<i>Gopka V.F. , Ulyanov O.M., Andrievsky S.M., Shavrina A.V., Yushchenko V.A.</i>	
Some Statistical Picture of Magnetic CP Stars Evolution	41
<i>Gorbaneva T.I., Mishenina T.V.</i>	
Eu Abundances in Active and Non-Active Stars.....	44
<i>Ismailov N.Z., Alimardanova F.N., Baheddinova G.R., Adygezalzade H.N.</i>	
Ultraviolet Spectrum Variability of BP Tau	46
<i>Ismailov N.Z., Khalilov O.V.</i>	
Spectral Observations of AB Aur	49
<i>Ismailov N.Z., Adigozalzade H.N.</i>	
Spectral and Photometric Researches of RY Tau	53
<i>Ivanyuk O., Pavlenko Ya.V., Jenkins J.S., Jones H.R.A., Lyubchik Yu., Kaminsky B., Kuznetsov M.</i>	
Iron Abundances in Atmospheres of HD10700 & HD146233	57
<i>Ivanyuk O., Pavlenko Ya.V., Jones H.R.A., Pinfield D., Clarke J.R.A.</i>	
TiO Isotopes Bands in M Dwarf Spectra	60
<i>Kim Chun-Hwey, Lee Jae Woo, Kim Duck Hyun, Andronov Ivan L.</i>	
Four New Binary Stars in the Field of CL Aurigae. II.....	62
<i>Kudashkina L.S., Andronov I.L.</i>	
Atlas of Light Curves of Faint Mira-Type Stars. Statistical Relations Between the Characteristics of Smoothed Phase Light Curves	65
<i>Kudashkina L.S., Andronov I.L.</i>	
Periodogram and Wavelet Analysis of the Semi-Regular Variable Supergiant Y Cvn ...	67
<i>Kudzej I., Dubovsky P.A.</i>	
One-Meter Telescope in Kolonica Saddle - 4 Years of Operation.....	70
<i>Kuznetsov M.K., Pavlenko Y.V., Pinfield D., Jones H.</i>	
Spectral Investigations of CM Dra	74
<i>Litvinchova A.A., Pavlenko E.P.</i>	
The Photometric Investigation of the Active Post-Nova CP Lac in High and Low State of Brightness in 2006-2008 yrs.....	76
<i>Maryeva O., Abolmasov P.</i>	
Modeling the Optical Spectrum of Romano's Star in Minimum Brightness.....	79
<i>Mishenina T.V., Glazunova L.V., Soubiran C., Kovtyukh V.V.</i>	
The New Absolute Parameters of OU Gem - The Star of BY Dra Type	83
<i>Moncrieff K.E., Turner D.G., Short C.I., Bennett P.D., Balam D.D., Griffin R.F.</i>	
Spectral Type and Radial Velocity Variations in Three SRc Variables	86
<i>Pavlenko Ya.V., Jenkins J.S., Jones H.R.A.</i>	
Modelling of Late Type Spectra and Abundances: New Observed Data and Approaches	90

<i>Pogodin M.A., Drake N.A., Jilinski E.G., Ortega V.G., de la Reza R.</i> Spectral Variability of the Unusual Southern Be Star HD 152478	94
<i>Samsonov D.A., Pavlenko E.P., Andreev M.V., Sklyanov A., Zubareva A.M., Voloshina I.B., Metlov V.G., Shugarov S.Yu., Golovin A.V., Antoniuk O.I.</i> Positive and Negative Superhumps of the Dwarf Nova MN Dra.....	98
<i>Samus N.N., Antipin S.V., Kolesnikova D.M., Sat L.A., Sokolovsky K.V.</i> New Variable Stars in the Field of 66 Oph on Digitized Moscow Plates.....	101
<i>Samus N.N., Kazarovets E.V., Kireeva N.N., Pastukhova E.N., Durlevich O.V.</i> General Catalogue of Variable Stars: Current Status and New Name-Lists	102
<i>Szabados L.</i> Open Questions on Cepheids and Their Period-Luminosity Relationship.....	106
<i>Szymański T., Zola S., Siwak M., Ogłóza W.</i> Unusual Accretion Disk in Algol - Type Binaries - KU Cyg	112
<i>Tkachenko A., Lehmann H., Tsymbal V., Mkrtichian D.</i> Spectroscopic Analysis of Oscillating Algol-Type Systems.....	115
<i>Turner D.G., Majaess D.J., Lane D.J., Rosvick J.M., Henden A.A. Balam D.D.</i> The Galactic Calibration of the Cepheid Period-Luminosity Relation and its Implications for the Universal Distance Scale.....	119
<i>Turner D.G., Majaess D.J., Lane D.J., Percy J.R., English D.A., Huziak R.</i> HDE 344787, the Polaris Analogue that is Even More Interesting Than Polaris.....	125
<i>Turner D.G., Berdnikov L.N., Percy J.R., Abdel-Sabour Abdel-Latif M.</i> The Onset of Chaos in Pulsating Variable Stars.....	129
<i>Udovichenko S.N., Dubovsky P.A., Kudzej I.</i> Photometry and Blazhko Effect in RR Lyr Type Star DM Cyg.....	133
<i>Usenko I.A., Berdnikov L.N., Kravtsov V.V., Knyazev A.Yu., Chini R., Hoffmeister V.H., Stahl O., Drass H.</i> Spectroscopic Investigations of Cepheids in Carina.....	136
<i>Usenko I.A., Bychkov V.D., Bychkova L.V., Plachinda S.I.</i> Magnetic Field of Polaris	140
<i>Virnina N.A.</i> New Binary Systems With Asymmetric Light Curves	143
<i>Virnina N.A., Panko E.A., Sergienko O.G., Murnikov B.A., Gubin E.G., Klabukova A.V., Movchan A.I.</i> Modeling and O-C Analysis of the Close Binary BM UMa	148
<i>Wszolek B., Kuźmicz A.</i> Search for Spectroscopic Families Among Diffuse Interstellar Bands	152
<i>Author index</i>	154

PRELIMINARY RESULTS OF DOPPLER IMAGING ANALYSIS OF roAp STAR α Cir

D.V. Alentjev¹, D.E. Mkrtichian²

¹ Tavrian National University Vernadskiy's Avenue 4, Simferopol, Crimea, 95007, Ukraine.
e-mail: *sl4m@ukr.net*

² Crimean Astrophysical Observatory, Nauchny, Crimea, 98409, Ukraine.

ABSTRACT. Based on high-resolution spectra, we investigate the abundance distribution of chromium and silicon on the surface of α Cir using Doppler Imaging technique. Results of our analysis show the presence of chromium and silicon spots on the surface of α Cir as well as large gradients of the abundances of these elements.

Key words: Stars: Alpha Circini; methods: Doppler imaging mapping

1. Introduction

α Cir (HD 128898; HR 5463) is one of the brightest rapidly oscillating Ap (roAp) stars. Despite of the fact that this is one of the best studied roAp stars showing vertical stratification of several chemical elements (see Kochukhov et al. 2009), Doppler Imaging (DI) analysis of this star was not carried out so far. In this paper we fill in this gap in the study of α Cir and represent preliminary results of DI mapping based on chromium and silicon lines. In Sect.2, we shortly describe the observational material that we have at our disposal as well as the data reduction procedure. Sect.3 is devoted to the description of DI technique while the results are presented in Sect.4. Finally, Sect.5 gives the summary of our study.

2. Observations and data reduction

We have obtained 5 high-resolution spectra with the UCLES coude echelle spectrograph installed at the 3.9-m Anglo-Australian Telescope (AAT) and 6 high-resolution spectra with the UVES echelle spectrograph installed at the 8.2-m Very Large Telescope (VLT). The spectra cover wavelength range from 6115 Å to 6155 Å. Although the UVES spectra have been reduced with the standard pipeline installed at the telescope, we had to reduce the spectra from UCLES. For this aim, an automatic data reduction procedure have been developed.

Table 1: Journal of observations. HJD is the heliocentric Julian Date, ϕ is the corresponding rotational phase.

Seq.	Source	HJD	ϕ
1	UCLES	2453510.844	0.812
2	UCLES	2453511.851	0.037
3	UCLES	2453512.891	0.269
4	UCLES	2453513.902	0.495
5	UCLES	2453514.892	0.716
6	UVES	2451945.894	0.430
7	UVES	2451946.895	0.654
8	UVES	2451947.889	0.876
9	UVES	2451953.895	0.217
10	UVES	2451954.893	0.440
11	UVES	2451955.900	0.665

Table 1 gives the journal of observations. Rotational phases have been computed in accordance to the Julian Dates calculated for all spectra as follows:

$$HJD = 2453937.2086 + 4.4790 * E. \quad (1)$$

3. Doppler Imaging technique

Stellar surface inhomogeneities, such as a nonuniform distribution of temperature or chemical composition, lead to characteristic distortions in the profiles of Doppler broadened stellar spectral lines. In the course of stellar rotation these distortions will move across the line profiles due to the changes in visibility and Doppler shifts of individual structures at the stellar surface.

The Doppler imaging (DI) technique utilizes the information contained in the rotational modulation of the absorption line profiles and reconstructs features at the surfaces of stars by inverting a time series of high-resolution spectra into a map of the stellar surface.

4. Results

We started with the selection of the spectral line profiles showing variability with rotational phase. For

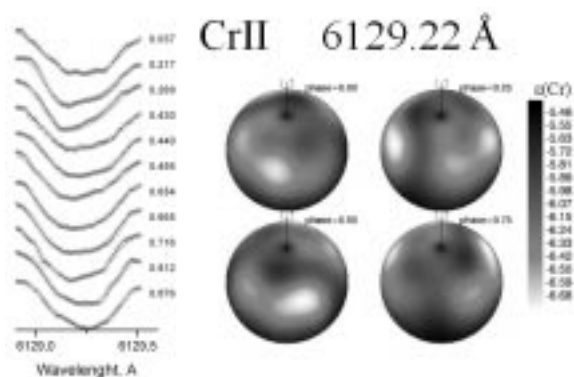


Figure 1: Stellar surface abundance map for Cr in spherical projection obtained based on Cr II 6129.22 Å line. Comparison between observed (crosses) and computed (solid lines) spectra are given to the left. Scale is in dex.

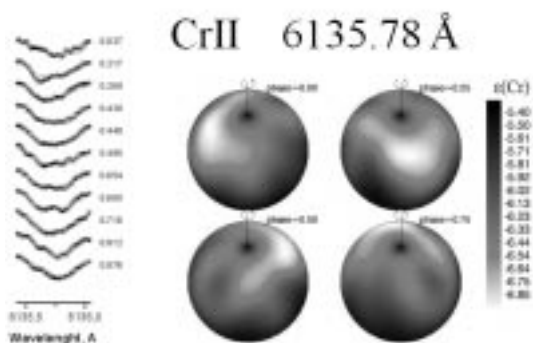


Figure 2: Same as Fig. 1 but for Cr II 6135.78 Å line.

our analysis, we have selected three Cr II lines (Cr II 6129.22 Å, Cr II 6135.78 Å, Cr II 6147.15 Å) and one Si I line (Si I 6125.02 Å).

For the DI analysis, we used the INVERS8 program (Piskunov & Rice 1993) which uses Tikhonov regularization delivering results in the sense of the smoothest map in terms of stellar surface abundances that is possible to fit the observations at a certain level. The program uses pre-calculated tables of intrinsic line profiles which have been computed with the SynthV code (Tsymbal 1996) using the LLmodels atmosphere models (Shulyak et al. 2004). Atomic line lists were taken from the VALD database (Kupka et al. 2000).

Figs. 1–3 show the abundance distribution for Cr in spherical projection. Comparison between observed (crosses) and computed (solid lines) line profiles are shown to the left. The bright spots of lower chromium abundance are clearly seen on the surface of the star and the observed line profiles are well fitted. The rotational velocity of 12.5 km s^{-1} and the inclination angle of the rotation axis to the line of sight of 35° were adopted in the model.

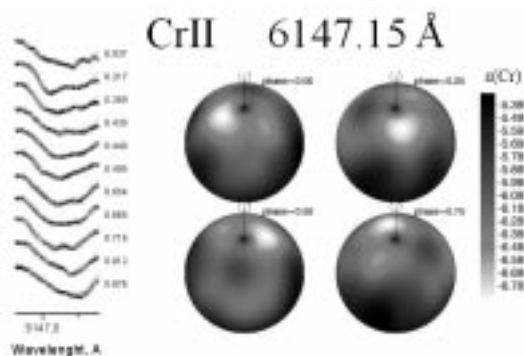


Figure 3: Same as Fig. 1 but for Cr II 6147.15 Å line.

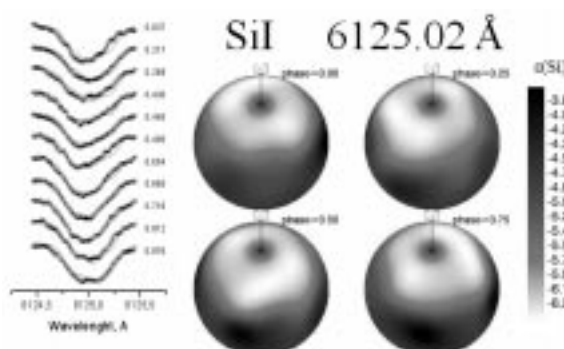


Figure 4: Same as Fig. 1 but for Si I 6125.02 Å line.

As shown in Fig.4, the abundance distribution of Si on the surface of α Cr is characterized by a large spot of lower abundance located at the rotational pole of the star. Both, Cr and Si show large gradients of the abundances of about 2.4 dex.

5. Discussion

Based on high-resolution spectra obtained with two different instruments, we have carried out Doppler Imaging analysis of roAp star α Cr. Despite of the small number of spectra that we had at our disposal, we could show that both Cr and Si are inhomogeneously distributed on the star's surface showing large gradients of about 2.4 dex.

In future, we plan to carry out a more detailed study of α Cr based on extended spectroscopic observations.

References

- Kochukhov O., Shulyak D., Ryabchikova T.: 2009, *A&A*, **499**, 851
- Kupka F., Ryabchikova T.A., Piskunov N.E. et al.: 2000, *Baltic Astronomy*, **9**, 590
- Piskunov N.E., Rice J.B.: 1993, *PASP*, **105**, 1415
- Shulyak D., Tsymbal V., Ryabchikova T., et al.: 2004, *A&A*, **428**, 993
- Tsymbal V.: 1996, *ASP Conf. Series*, **108**, 198

"INTER-LONGITUDE ASTRONOMY" (ILA) PROJECT:
CURRENT HIGHLIGHTS AND PERSPECTIVES.
I. MAGNETIC VS. NON-MAGNETIC
INTERACTING BINARY STARS

I.L. Andronov^{1,2}, K.A. Antoniuk², A.V. Baklanov², V.V. Breus^{1,3}, V. Burwitz⁴,
L.L. Chinarova³, D. Chochol⁵, P.A. Dubovsky⁶, W. Han⁷, T. Hegedus⁸, A. Henden⁹,
L. Hric⁵, Chun-Hwey Kim¹⁰, Yonggi Kim^{10,11}, S.V. Kolesnikov³, I. Kudzej⁶,
A. Liakos¹², P.G. Niarchos¹², A. Oksanen¹³, L. Patkos¹⁴, K. Petrik¹⁵, N.V. Pit²,
N.M. Shakhovskoy², N.A. Virnina¹, J. Yoon¹⁰, S. Zola^{16,17}

- ¹ Department "High and Applied Mathematics",
Odessa National Maritime University, Odessa, Ukraine, *tt_ari@ukr.net*
- ² Crimean Astrophysical Observatory, Nauchny, Ukraine
- ³ Department of Astronomy and Research Institute "Astronomical Observatory",
Odessa National University, Odessa, Ukraine
- ⁴ Max-Planck Institut für Extra-Terrestische Physik, Garching, Germany
- ⁵ Astronomical Institute of the Slovak Academy of Sciences, Stara Lesna, Slovakia
- ⁶ Vihorlat Astronomical Observatory, Humenne, Slovakia
- ⁷ Korea Astronomy and Space Science Institute, Daejeon, Korea
- ⁸ Baja Astronomical Observatory, Baja, Hungary
- ⁹ American Association of Variable Stars Observers, Harvard, USA
- ¹⁰ University Observatory, Chungbuk National University, Cheongju, Korea
- ¹¹ Institute for Basic Science Research, Chungbuk National University, 361-63, Korea
- ¹² Department of Astrophysics, Astronomy and Mechanics, University of Athens, Greece
- ¹³ Hankasalmi Observatory, Hankasalmi, Finland
- ¹⁴ Konkoly Observatory, Hungarian Academy of Sciences, Budapest, Hungary
- ¹⁵ Astronomical Observatory, Hlohovec, Slovakia
- ¹⁶ Astronomical Observatory, Jagiellonian University, Cracow, Poland
- ¹⁷ Mt. Suhora Observatory, Pedagogical University, Cracow, Poland

ABSTRACT. We present a review of highlights of our photometric and photo-polarimetric monitoring and mathematical modeling of interacting binary stars of different types: classical, asynchronous, intermediate polars with 25 timescales corresponding to different physical mechanisms and their combinations (part "Polar"); negative and positive superhumpers in nova-like and dwarf novae stars ("Superhumper"); symbiotic ("Symbiosis"); eclipsing variables with and without evidence for a current mass transfer ("Eclipser") with a special emphasis on systems with a direct impact of the stream into the gainor star's atmosphere, which we propose to call "Impactors", or V361 Lyr-type stars. Other parts of the ILA project are "Stellar Bell" (pul-

sating variables of different types and periods - M, SR, RV Tau, RR Lyr, Delta Sct) and "New Variable".

Key words: Variable stars: cataclysmic, pulsating, eclipsing, interacting binary

The monitoring of the first star of our sample AM Her was initiated by Prof. V.P. Tsessevich (1907-1983). More than 300 papers were published, with a total number of studied variable stars exceeding 1400. The previous review of the "Inter-Longitude Astronomy" ("ILA") campaign was published by Andronov et al. (2003). For the CCD observations, we mainly use the BVRI calibration of A.Henden.

The "top of the top" of the recent highlights are:

- **TT Ari** (nova-like superhumper): discoveries of a back switch between the states of positive and negative superhumps (Andronov et al., 1999, 2005a); of a "loop" at the "Period of Quasi-Periodic Oscillations (QPO) brightness", contrary to a previous suggestion on dependence of characteristics of superhumps and QPOs on brightness (Kim et al., 2009); of drastic brightness variations up to 2 mag during a prolonged exotic "low luminosity state" started in October, 2009 and continued for one year, finished just before final version of this paper, passing through stages (with increasing luminosity) of positive superhumps, double wave of positive superhumps; negative superhumps.
- **DO Dra** (an "outbursting intermediate polar" or a "magnetic dwarf nova"): discoveries of the new type of variability "Transient Periodic Oscillations" (TPO), which are interpreted by model of plasma blobs spiralling down to the magnetic white dwarf; correlation of the decay rate and outburst brightness; out-of-outburst luminosity variations (Andronov et al., 2008);
- **V1432 Aql** (asynchronous polar): discovery of a third type of eclipses in the system, self-consistent model for the arc-shaped accretion structure (Andronov and Baklanov, 2007); determination of the most accurate value of the synchronization time of 96.5 ± 1.5 years (Andronov and Baklanov, 2006) in an excellent agreement with former theoretical prediction for another system AM Her with similar physical parameters (Andronov, 1987ab);
- **AM Her** (synchronous polar): Discovery of two-component nature of the "shot noise" with characteristic time-scales of 9.8 and 170 sec based on the 24117 seconds of CHANDRA observations, which justifies the "Z-pinch"-type magneto-hydrodynamic instability in falling plasma blobs "spaghetti" (Andronov et al., 2003, 2005b). More detailed self-review was published by Andronov (2008);
- **BY Cam** (asynchronous polar): detailed study of previously discovered switching of accretion from pole to pole with a phase of spin-orbital beat; correlation between the color index and brightness, which is an agreement with a cyclotron emission of the accretion column (Andronov et al., 2008); detection of drastic changes of the amplitude of variations of polarization which may be explained by variations of the accretion structure dependent on periodically changing angle between the line of centers and the magnetic axis (Breus et al., 2007);
- **Intermediate polars** (BG CMi, MU Cam =1RXS J062518.2+733433, FO Aqr, AO Psc, 1RXS J063631.9 +353537, 1RXS J070407.9 +262501, 1RXS J180340.0 +401214, 1RXS J192626.8 +132153, 1RXS J213344.1 +510725, PQ Gem, V405 Aqr): study of the rotational evolution of magnetic white dwarfs in these systems based on long-term monitoring; some systems exhibit acceleration (Andronov, Ostrova and Burwitz, 2005) or deceleration (Kim et al., 2005) of rotational acceleration (i.e. negative or positive d^2P/dt^2), for interpretation of which a model of precession was proposed (Andronov, 2005); the statistical dependence of phases of spin pulses on orbital phase was detected in MU Cam, indicating modulation of the accretion structure with a periodically changing angle between the magnetic axis and the line of centers (Kim et al., 2005);
- **OT J071126.0+440405** (synchronous polar with 3 types of eclipses): discovery of 3 distinctly separate luminosity states based on 100+ nights of mono and multi-color observations; determination with best accuracy of the parameters of the light curve; elaboration of self-consistent theoretical model for structure of the system, which is dependent on luminosity (i.e. the accretion rate);
- **Eclipsing nova-like variables** (DW UMa, BH Lyn, PX And, other SW Sex stars): besides superhumps and QPOs, they exhibit an ultra-violet excess (seen in the U-B color index) at the eclipse (e.g. Andronov et al., 2001), indicating an extended hot emission region (like an accretion disk corona) and thus a physical unreliability of thin disk models;
- **Positive vs. Negative Superhumps** in non-eclipsing Nova-Like variables: besides a large international campaign on TT Ari, we arrange occasional campaigns for V603 Aql. In 2004 the system was found to exhibit either positive superhump with a period 0.14813(10), or the statistically significant waves with 3^d9 , 1^d4 , 0^d135 , which may be interpreted as the negative superhump-orbital, the beat periods (negative superhump - positive superhump) and the negative superhump with low amplitude, respectively (Andronov et al., 2005c). Similarly to TT Ari, another star MV Lyr showed dependence of colors of variations with time scale - the most "blue" spectral energy distribution correspond to the quasi-periodic oscillations (QPO), the most "red" is time-averaged emission and the negative superhumps are intermediate in color temperature (Andronov and Antoniuk 2005). Using advanced methods for mathematic modeling of multi-component signals, from the observations obtained during 6 nights following "the king of superoutbursts" in WZ Sge, we succeeded to detect not only a orbital variability

with prominent eclipses of the accretion disk, but also “early superhumps”, which have become dominating only two weeks later (Andronov et al., 2002).

- **Symbiotic stars:** photographic photometry and time series analysis was made for dozens stars during an international campaign initiated by Hric and Skopal (1989). For recent studies of these stars, we use different methods: periodogram, wavelet, scalegram analysis and global (polynomial + trigonometric polynomial fits) and local (running parabolae, running sine fits), see e.g. Andronov and Chinarova (2003).
- **New Eclipsing and Pulsating variables:** from the database of BV Hipparcos-Tycho observations, we have found 863 new variables (Andronov et al., 1999), the majority of which are eclipsing or pulsating variables. For such a study, we have used trigonometric polynomial fits of 1, 2, 3 orders and than specially developed algorithms of “EAC” (“EA catcher”, which is effective for noisy observations not only of the EA-type systems, but also for the types EB and EW) and “RR Catcher” (Andronov, Cuypers and Piquard, 2010). More than fifty new variable stars were discovered, studied and classified by N.Virgina. From those, 27 discoveries were reported separately in this volume (Virgina, 2010b). It should be noted that, from this sample, 10 systems (i.e. $\sim 37\%$) exhibit statistically significant difference between the brightness at maxima arguing for a presence of spots.
- **VSX J052807.9+725606:** discovery of large asymmetry of the newly detected variable (Virgina, 2010a, Virgina and Andronov, 2010) with an amplitude increasing towards shorter wavelengths, which were interpreted in terms of the model proposed for V361 Lyr (Andronov and Richter, 1987), i.e. an extremely bright hot spot caused by a direct impact of an accretion stream from the donor to the accretor’s atmosphere at a pre-contact stage; this allows to propose a new class of “Impactors”.

References

- Andronov I.L.: 1987a, *ApSS*, **131**, 557
 Andronov I.L.: 1987b, *SvA*, **31**, 49
 Andronov I.L.: 2005, *ASPC*, **334**, 447
 Andronov I.L.: 2008, *JPhSt*, **12**, 2902
 Andronov I.L., Antoniuk K.A.: 2005, *ASPC*, **330**, 505
 Andronov I.L., Antoniuk K.A., Augusto P., Baklanov A.V., Chinarova L.L., Chochol D., Efimov Yu.S., Gazeas K., Halevin A.V., Kim Y., Kolesnikov S.V., Kudashkina L.S., Marsakova V.I., Mason P.A., Niarchos P.G., Nogami D., Ostrova N.I., Patkos L., Pavlenko E.P., Shakhovskoy N.M., Tremko J., Yushchenko A.V., Zola S.: 2003, *AAT*, **22**, 793
 Andronov I.L., Antoniuk K.A., Breus V.V., Chinarova L.L., Han Wonyong, Jeon Young Beom, Kim Yonggi, Kolesnikov S.V., Oh Joon Young, Pavlenko E.P., Shakhovskoy N.M.: 2008, *CEJPh*, **6**, 385
 Andronov I.L., Arai K., Chinarova L.L., Dorokhova N.I., Dorokhova T.N., Dumitrescu A., Nogami D., Kolesnikov S.V., Lepardo A., Mason P.A., Matsumoto K., Oprescu G., Pajdosz G., Passuelo R., Patkos L., Senio D.S., Sostero G., Suleimanov V.F., Tremko J., Zhukov G. V., Zola S.: 1999, *AJ*, **117**, 574
 Andronov I.L., Baklanov A.V.: 2006, *AA*, **452**, 941
 Andronov I.L., Baklanov A.V.: 2007, *Ap*, **50**, 105
 Andronov I.L., Burwitz V., Reinsch K., Barwig H., Chinarova L.L., Kolesnikov S.V., Shakhovskoy N.M., Hambaryan V., Beuermann K., Yukhanov D.A.: 2003, *OAP*, **16**, 7
 Andronov I.L., Burwitz V., Chinarova L.L., Gazeas K., Kim Y., Niarchos P.G., Ostrova N.I., Patkos L., Yoon J.N.: 2005a, *IBVS*, **5664**, 1
 Andronov I.L., Burwitz V., Reinsch K., Barwig H., Chinarova L.L., Kolesnikov S.V., Shakhovskoy N.M., Hambaryan V., Beuermann K., Yukhanov D.A.: 2005b, *ASPC*, **330**, 407
 Andronov I.L., Chinarova L.L.: 2003, *ASPC*, **292**, 211
 Andronov I.L., Chinarova L.L., Han W., Kim Y., Yoon J.-N.: 2008, *AA*, **486**, 855
 Andronov I.L., Cuypers J., Piquard S.: 2000, *ASPC*, **203**, 64
 Andronov I.L., Kolesnikov S.V., Niarchos P.G., Shakhovskoy N.M., Zola S.: 2001, *OAP*, **14**, 15
 Andronov I.L., Ostrova N.I., Burwitz V.: 2005, *ASPC*, **335**, 229
 Andronov I.L., Ostrova N.I., Kim Yong-Gi, Burwitz V.: 2005c, *JASS*, **22**, 211
 Andronov I.L., Richter G.A.: 1987, *AN*, **308**, 235
 Andronov I.L., Yushchenko A.V., Niarchos P.G., Gazeas K.: 2002, *ASPC*, **261**, 459
 Breus V.V., Andronov I.L., Kolesnikov S.V., Shakhovskoy N.M.: 2007, *AAT*, **26**, 241
 Hric L., Skopal A.: 1989, *IBVS*, **3364**, 1
 Kim Y.G., Andronov I.L., Park S.S., Jeon Y.-B.: 2005, *AA*, **441**, 663
 Kim Y., Andronov I.L., Cha S.M., Chinarova L.L., Yoon J.N.: 2009, *AA*, **496**, 765
 Kim Yong-Gi, Andronov I.L., Park Sung-Su, Chinarova L.L., Baklanov A.V., Jeon Young-Beom: 2005, *JASS*, **22**, 197
 Virgina N.A.: 2010a, <http://sas.astro.sk/docs/bezpoz10eng3.pdf>
 Virgina N.A.: 2010b, *OAP*, **23**, 143
 Virgina N.A., Andronov I.L.: 2010, *OEJV*, **119**, 1

HIGH-ACCURACY MAGNETIC FIELD MEASUREMENTS ON COOL GIANT β GEMINORUM

D.N. Baklanova, S.I. Plachinda

Crimean Astrophysical Observatory
Nauchny, Crimea 98409 Ukraine, *dilyara@crao.crimea.ua*

ABSTRACT. Pollux is a weakly-active yellow giant neighbor of the Sun with known regular surface magnetic field about 1 Gauss. We present new high-accuracy magnetic field measurements of β Gem which were obtained during 2010 at Crimean Astrophysical Observatory with 2.6-m telescope and Stokesmeter.

Key words: Stars: magnetic field; stars: individual: β Gem.

1. Introduction

Pollux (β Geminorum, HD 62509, HR 2990) is a single bright and well-studied star, classified as a K0 IIIb giant. The distance to Pollux was measured by Hipparcos and equals to 10.3 pc. Interferometric measurements have determined stellar diameter of $8.8 \pm 0.1 R_{\odot}$ (Nordgren et al., 2001). Published parameters differ for different investigators. Values of effective temperature $T_{eff} = 4660 \div 4920$ K, a surface gravity $\log g = 2.52 \div 3.15$, metallicity $[Fe/H] = -0.07 \div 0.19$, and stellar mass $M_{*} = 1.7 \div 2.3 M_{\odot}$. The radial velocity variations with a period of 554 days have been discovered for β Gem by Hatzes & Cochran (1993). The main hypothesis for these variations is that they due to a planetary companion with a mass of $2.9 M_{Jup}$. Subsequently Hatzes et al. (2006), Reffert et al. (2006) and Han et al. (2008) confirmed this explanation with a revised period in the range of 590–596 days. Aurière et al. (2009) reported the detection a weak magnetic field about 1 Gauss on the surface of Pollux changing with radial velocity's period of 589.64 days.

2. Observations

Spectropolarimetric observations of β Gem were carried out at the Crimean Astrophysical Observatory using coude spectrograph of 2.6-meter Shajn telescope and Stokesmeter. Our data overlap interval of 9 nights from 25 February to 2 May 2010. 194 circular polarization spectra were collected with resolution ~ 30000 and signal-to-noise ratio from 270 to 580.

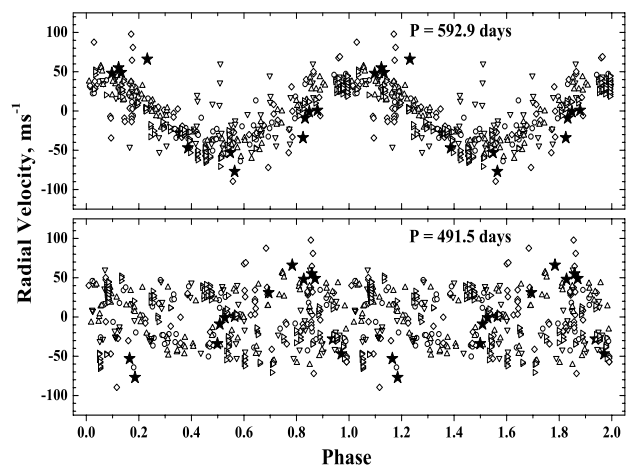


Figure 1: Radial velocities folded in phase with the orbital period of 592.9 days (upper panel) and the magnetic field's 491.5 days period (lower panel). The different symbols correspond to different source of radial velocity data. Diamonds are data from Larson et al. (1993), upside down triangles – from Hatzes and Cochran (1993), upward triangles – from Reffert et al. (2006), circles – from Hatzes et al. (2006), right triangles – from Han et al. (2008), and asterisks are from Aurière et al. (2009).

3. Results

We performed search for periodicity with the program Period04 (Lenz & Berger, 2004). Using all available radial velocity measurements from literature we re-determined the planetary companion rotation period, $P_{pl} = 592.9 \pm 0.6$ days. The upper frame in Fig. 1 shows the variations of radial velocity with orbital period of 592.9 days (phases were computed with ephemeris $P_{RVmax} = 2444158.8 + 592.9$ days). The lower frame in Fig. 1 shows the variation of radial velocity with magnetic field period. In the last case there is no periodic variations for all data, as it should have been, in spite of the radial velocities measurements from Aurière et al. (2009) which shown by asterisks.

From the analysis of power spectrum of magnetic

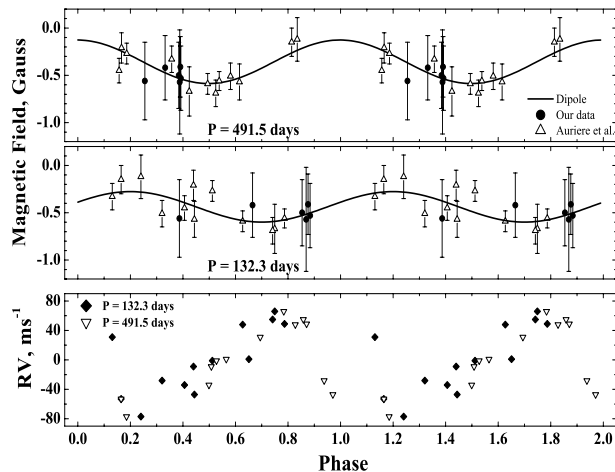


Figure 2: Longitudinal magnetic field folded in phase with the axial rotation period of 491.5 days (upper panel) and with period of 132.3 days (middle panel). Filled circles are our measurements of magnetic field; open triangles – data from Aurière et al.; dipole fit is shown by solid line. Bars are rms errors of measurement. Lower panel shows radial velocity's variations with the periods 132.3 days (filled diamonds) and 491.5 days (open triangles) using data from Aurière et al.

field measurements the axial rotation period of star, 491.5 days, was evaluated with 98% statistical significance (see Fig. 2, upper panel). For clear analysis we excluded lie out points. Using the Hipparcos photometry Hatzes et al. (2006) estimated a best fit period of 132.3 days the origin of which was not determined. The same period presents in power spectrum of the magnetic field measurements, but its statistical significance is only 77% (see Fig. 2, middle panel). In addition, because $2/(1/132^{d.3} - 1/491^{d.5}) = 362.2$ days is very closed to year, we concluded that this period is artifact of frequency beating of star rotation period and year's season observations. The best fit to the magnetic field data in the case of the centered dipole gives the following results: the angle between spin axis and line of sight $i = 31^\circ \pm 1^\circ$ is in agreement with Hatzes' et al. (2006) $i = 28^\circ \pm 3^\circ$, and the angle between both the spin and dipole axes $\beta = 133^\circ$.

In the lower panel of Fig. 2 the radial velocity from paper by Aurière et al. (2009) are phase-folded with two periods, 491.5 and 132.3 days. One can see the discrepancy between other authors' data and measurements by Aurière et al. (2009). The methods of RV measurements of both arrays of data differ from each other. In contrast to the nonpolarimetric data of other authors, the RV obtained by Aurière et al. (2009) were calculated using spectropolarimetric observations. The last RV data demonstrate the presence of both periods while the magnetic period, 491.5 days, is absent in data

of other authors. We do not know the nature of such discrepancy between RV data from Aurière et al. (2009) and others authors.

In Fig. 3 all points of the magnetic field measurements are presented. We suppose that four lie out points of the curve fitting are the result of the active regions emergence on the stellar surface as it was discovered for solar-like star 61 Cyg A (Plachinda, 2004). Additional data, which will require further observations, are needed in order to confirm this result.

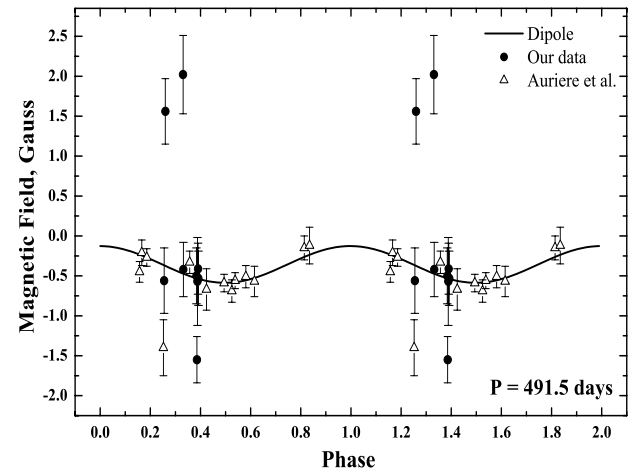


Figure 3: Magnetic field measurements folded in phase with the axial rotation period of 491.5 days. All points of the magnetic field measurements are presented. Filled circles are our measurements of magnetic field; open triangles – data from Aurière et al.; dipole fit is shown by solid line.

References

- Aurière M., Wade G. A., Konstantinova-Antova R., et al.: 2009, *A&A*, **504**, 231.
 Han I., Lee B.-C., Kim K.-M., Mkrtychian D. E.: 2008, *JKAS*, **41**, 59.
 Hatzes A. P., and Cochran W. D.: 1993, *ApJ*, **413**, 339.
 Hatzes A. P., Cochran W. D., Endle M., et al.: 2006, *A&A*, **457**, 335.
 Hatzes A. P. and Zechmeister M.: 2007, *ApJ*, **670**, 37.
 Larson A. M., Irwin A. W., Yang Stephenson L. S., et al.: 1993, *PASP*, **105**, 825.
 Lenz P. and Berger M.: 2004, *IAU Symp.* **224**, eds. Zverko J. et al., Cambridge Univ. Press, 786.
 Nordgren T. E., Sudol J. J., and Mozurkewich D.: 2001, *AJ*, **122**, 2707.
 Plachinda S. I.: 2004, *IAU Symp.* **223**, eds. Stepanov A. V. et al., Cambridge Univ. Press, 689.
 Reffert S., Quirrenbach A., Mitchell D. S., et al.: 2006, *ApJ*, **652**, 661.

OBSERVATIONS OF LOW-AMPLITUDE BRIGHTNESS OSCILLATIONS IN THE UNUSUAL ECLIPSING SYSTEM V718 PER (HMW 15, H 187)

O. Barsunova¹, V. Grinin^{1,2}, A. Arkharov¹, S. Sergeev³, S. Shugarov⁴

¹ Central Astronomical Observatory (Pulkovo), St. Petersburg, Russia, *monoceros@mail.ru*

² Sobolev Astronomical Institute, St. Petersburg State University, St. Petersburg, Russia

³ Crimean Astrophysical Observatory, Nauchny, Crimea, Ukraine

⁴ Sternberg Astronomical Institute, Moscow State University, Moscow, Russia

ABSTRACT. The unusual young star V718 Per is known its prolonged eclipses with a period of 4.7 years. In addition we have discovered that for the last observational seasons (2008–2010) the low-amplitude oscillations are presented at the star's light curve and their period is approximately a factor of 8 shorter than the main one. In contrast to the large-scale eclipses accompanied by the star's reddening, the low-amplitude oscillations are neutral in character. So bimodal behavior can be the result of the division of a circumstellar disk into two parts: an inner, dense region, and an outer, less dense disk, with a large cavity between them. Such structures emerge in the presence of a fairly massive perturbing body (or bodies) in the disk. In this case, density waves rotating with different angular velocities can be formed in each of these parts. Therefore, when such a system is observed nearly edge-on, two oscillation modes with different periods can be present in the extinction variations. We suggest that such a situation takes place in the case of V718 Per. In that case the perturbing body (or bodies) can be either a giant planet or a brown dwarf, because of this star exhibits no signatures of spectroscopic binarity.

Key words: young eclipsing systems, photometry, protoplanetary disks; stars: individual: V718 Per.

1. Introduction

The star V718 Per belongs to the subclass of young weak-line T Tauri stars characterized by a low level of accretion activity and weak infrared excesses, indicative of a small amount of circumstellar dust. It is, therefore, very surprising the fact that this star exhibits

photometric activity caused by large-scale circumstellar extinction variations. The pattern of this activity, a sequence of extensive eclipses whose duration (3.5 yr) is comparable to the period between them (4.7 yr), is also unusual.

The results of our (Barsunova et al. (2005), Grinin et al. (2006, 2008)) and other authors (Cohen et al. (2003), Nordhagen et al. (2006)) photometric observations are shown that the eclipses parameters and shape rather close. Hence, it followed that the stars eclipses are produced by the passages of the same extended dust (or gas-dust) structure through the line of sight. A Fourier analysis of this light curve obtained yields a period of $P = 4.7$ yrs.

During the eclipse, the star reddened according to a law that did not differ greatly from the standard interstellar reddening law (Grinin et al. (2008)). Note that the shape of the color-magnitude diagram indicate on changing of the characteristic size of the dust particles in the extended structure.

The arrows in the light curve (Fig.1) show dates with the spectroscopic observations. Analysis of two high-resolution spectra taken by G. Herbig with the Keck telescope showed that the spectrum of V718 Per had no spectroscopic signatures of the secondary component. So, V718 Per is most likely a single star and that only a low-mass companion (a brown dwarf) or a proto-planet could be a source of perturbations in the circumstellar disk causing periodic extinction variations.

It was found from the spectral energy distribution for V718 Per (Grinin et al.(2008)) that the circumstellar disk has an inner matter-free gap with a radius of the order of several astronomical units. At the same time, the high extinction toward the star, much of which is produced by circumstellar extinction, indicates that

the disk is seen nearly edge-on.

In this paper we present last results of our optical and near-infrared photometry for V718 Per obtained during the 2008-2010 observing seasons.

2. Observations

The optical observations of V718 Per were carried out at the 0.7-m AZT-8 telescope of the Crimean Astrophysical Observatory. The observations were reduced to the Johnson-Cousins photometric system. We measured the stars brightness by the method of aperture photometry. The resulting accuracy of the aperture photometry for V718 Per is determined by the errors of the method and the brightness fluctuations of the comparison stars; it is $0^m.03$ in the V and R bands and about $0^m.02$ in the I band. The photometric technique and information about the comparison stars are presented in more detail in Grinin et al. (2008).

Our infrared photometry in the J,H,K bands was performed with the Pulkovo 1.1-m telescope at the Campo Imperatore Observatory (Italy). We reduced the observations to the standard Johnson system. The accuracy of the photometry is about $0^m.02$ in all three bands.

3. Results

3.1. The Optical Light Curve

Figure 1 shows the I-band light curve of V718 Per from our observations supplemented by the observations of the previous eclipse from Cohen et al. (2003) and by the data of Nordhagen et al. (2006). One can see from this figure that, in addition to the large scale brightness variations with a period of 4.7 yr, the star exhibits also the low-amplitude oscillations with a shorter characteristic time. They are also clearly seen in the V- and R-band light curves.

Such oscillations were not detected earlier due to large gaps in the previous observations.

3.2. O-C Analysis

Using the standard procedure of O-C analysis, we attempted to isolate the low-amplitude oscillations from the stars light curve. Figure 2 shows the results of our Lomb-Scargle periodogram analysis of the O-C residual. We see that a strong peak exists in the power spectrum. The corresponding period is 213 days, or approximately 1/8 of the period between the eclipses.

Figure 3 shows the O-C residual folded with this period. The thin line indicates the model (a sine wave with the 213-day period) providing the best fit to the

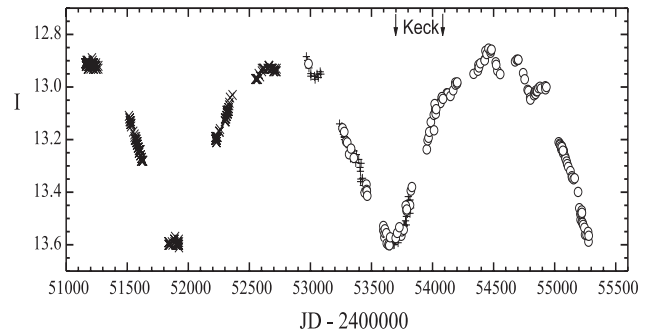


Figure 1: I-band light curve of V718 Per from our observations (\circ) and the data of Cohen et al. (2003) (\times) and Nordhagen et al. (2006) ($+$). The arrows indicate the times of the spectroscopic observations.

observations. We see that the scatter of points in the O-C residual about the model is rather large due to both the small amplitude of the oscillations and the insufficient accuracy of the smoothed light curve based only on two eclipses.

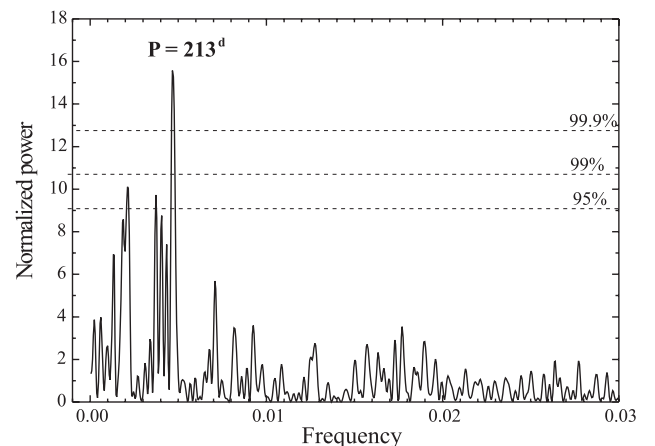


Figure 2: Lomb-Scargle periodogram for the O-C residual of the light curve for V718 Per.

3.3. The Neutral Character of the Low-amplitude Brightness Oscillations

Analysis of the low-amplitude oscillations showed that they have the neutral character. It is clearly seen from Figure 4 with the fragment of the out-of-eclipse light curve in the VRI bands. The same conclusion follows also from the analysis of the IR bands.

The IR observations are more fragmentary than the optical photometry due to the schedule of the infrared observations. Nevertheless, the low-amplitude oscillations are also can be seen in all three JHK light curves (Fig. 5). They occur synchronously with the optical brightness oscillations and, what is particularly inter-

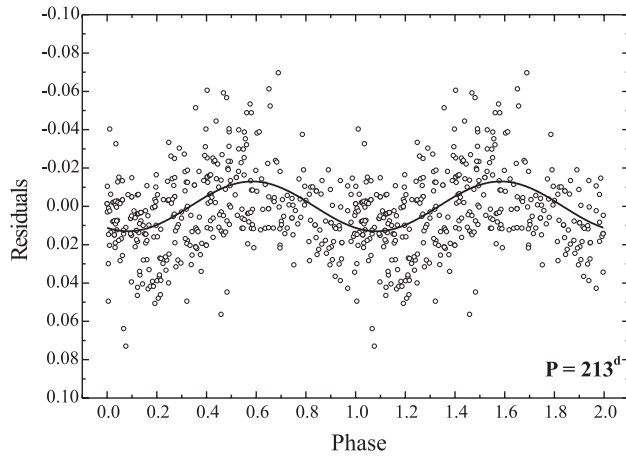


Figure 3: Phase light curve of the O–C residual folded with a 213–day period. The thin line indicates the model (a sine wave with the 213–day period).

esting, the amplitude of these oscillations, does not depend (or depends very weakly) on the wavelength.

This is clearly seen from Figure 6 which shows the same fragment of the light curve. The magnitudes in these bands are normalized in the same way as for the VRI bands.

So, the low-amplitude oscillations differ greatly from the large-scale eclipses whose amplitude increases toward the short-wavelengths (as can be clearly seen from Fig. 5).

4. Discussion

The SPH simulations (Sotnikova and Grinin (2007), Grinin et al. (2010)) show that the bimodal brightness oscillations caused by variations of circumstellar extinction can appear in young binary systems. Interestingly, the ratio of the periods of two brightness oscillation modes in such models is about 5–7, i.e., it is close to what is observed in our case. Nevertheless, despite this coincidence, the model is unsuitable, because the assumption about the binarity of V718 Per is in conflict with the results of its radial-velocity measurements, indicating that the star is a single one.

The neutral character of the low-amplitude brightness oscillations means that the periodic extinction variations causing these oscillations are attributable mainly to large particles with characteristic sizes greater than one micrometer. At the same time, small dust grains with sizes of the order of several tenths of a micrometer make a major contribution to the extinction in large-scale eclipses whose amplitude grows with decreasing wavelength. This fact suggests that the bimodal brightness oscillations in V718 Per can be due to a two-component structure of the circumstellar disk, which consists of inner and outer disks separated

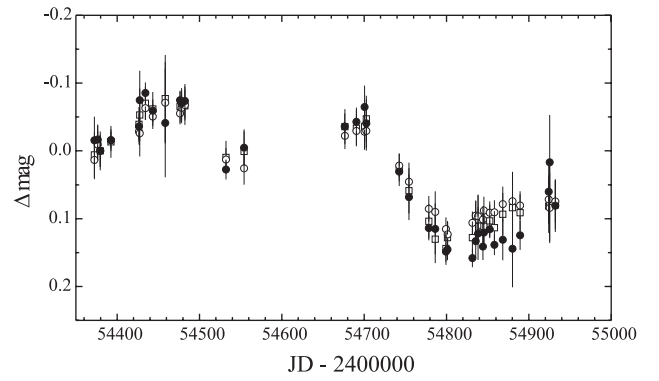


Figure 4: Diagram illustrating the neutral character of the low-amplitude brightness oscillations in V718 Per in the V, R, I bands. Fragments of the stars normalized V (\bullet), R (\square), and I (\circ) light curves in the interval JD = 2 454 372–2 454 789 are shown. The magnitudes in all three bands are taken to be zero at JD = 2 454 382.5.

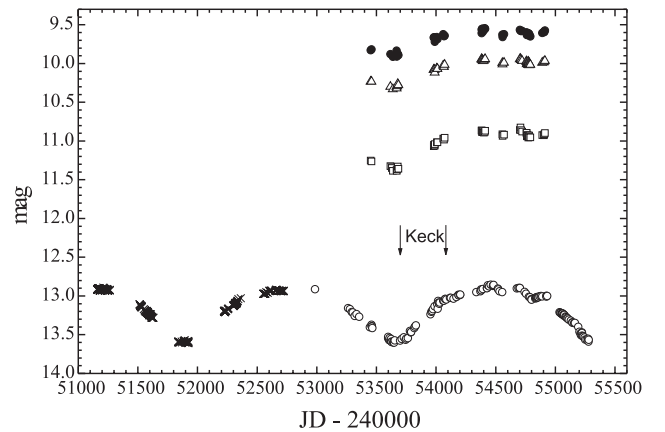


Figure 5: J (\square), H (\triangle), and K (\bullet) light curves of V718 Per. The I-band light curve of the star from the data of Cohen et al. (2003) (\times) and our observations (\circ) is shown below for comparison.

by a matter-free (or almost matter-free) gap (see Fig. 7). The grain coagulation processes have a higher rate in the inner disk because of the higher matter density. Therefore, the contribution of large particles to the extinction here will be greater than that in the outer disk.

A two-component structure of the circumstellar disk like that shown in Figure 7 is well known from the theory of protoplanetary disks perturbed by a giant planet or a substellar companion (see, e.g., de Val-Borro et al. (2007)).

The calculations by these authors show that cyclonic structures can arise in a protoplanetary disk perturbed by a giant planet. In the course of evolution, they form two giant cyclones that move with local Keplerian velocities on opposite sides of the inner gap in the disk. If such disk is inclined at a small angle to the line

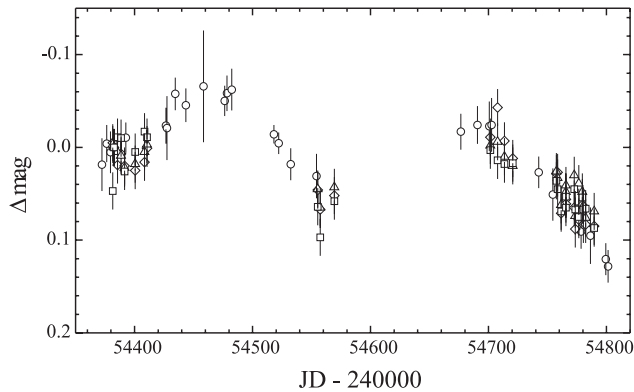


Figure 6: Diagram illustrating the neutral character of the low-amplitude brightness oscillations in V718 Per in the I, J, H, K bands. Fragments of the stars normalized I (\circ), J (\diamond), H (\triangle), and K (\square) light curves in the time interval JD = 2 454 372-2 454 789 are shown. The magnitudes in all four bands are taken to be zero at JD = 2 454 382.5.

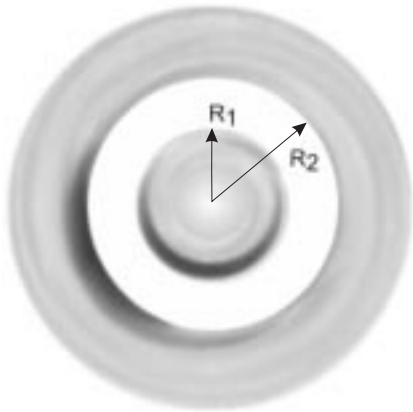


Figure 7: Scheme of the two-component circumstellar disk model for V718 Per.

of sight, then extinction variations with two different periods can be observed due to the rotation of the two giant cyclones.

Thus, the bimodal pattern of extinction variations observed in V718 Per is, in principle, compatible with the present-day models of circumstellar disks perturbed by low-mass companions or protoplanets.

The observationally very unusual photometric variability of V718 Per described above actually has a certain similarity with the activity cycles of UX Ori stars. This similarity means that, in both cases, the cyclic brightness variations are due to recurrent passages of giant gasdust structures through the line of sight. We associated such structures with periodic perturbations in the circumstellar disks generated by low-mass companions or protoplanets.

So, V718 Per has analogues among young stars. However, it should be noted that the cyclic activity of UX Ori stars is observed against the background of strong stochastic variability, making its study difficult. In contrast, in the case of V718 Per, we are dealing with an object that is considerably more convenient for studying fine features of the light curve.

Acknowledgements. We are grateful to N.Ya. Sotnikova, D.V. Bisikalo, N.N. Chugai, and A.A. Kilpio for helpful discussions. We also thank S.V. Klimanov for help with the observations and K.N. Grankin for consultations on the statistical methods for reducing observations. This work was performed in the context of the Origin and Evolution of Stars and Galaxies Program of the Presidium of the Russian Academy of Sciences and was supported by grants NSh-6110.2008.2 and NSh-1318.2008.2.

References

- Barsunova O. et al.: 2005, *Astrofizika*, **48**, 5
 Cohen R. et al.: 2003, *AJ*, **596**, L243
 Grinin V. et al.: 2006, *PAZh*, **32**, 918 (2006, *AstrL*, **32**, 827)
 Grinin V. et al.: 2008, *A&A*, **489**, 1233
 Grinin V. et al.: 2010, *PAZh*, **36**, in print
 Nordhagen S. et al.: 2006, *AJ*, **646**, L151
 Sotnikova N., Grinin V.: 2007, *PAZh*, **33**, 667 (2007, *AstL*, **33**, 594)
 de Val-Borro M. et al.: 2007, *A&A*, **471**, 1043

n-CAPTURE ELEMENTAL ABUNDANCES IN ACTIVE AND NON-ACTIVE STARS

N.Yu. Basak¹, T.V. Mishenina¹, C. Soubiran², V.V. Kovtyukh¹, S.I. Belik¹

¹ Department of Astronomy, Odessa National University

T.G.Shevchenko Park, Odessa 270014 Ukraine, *tamar@deneb.odessa.ua*

² Observatoire Aquitain des Sciences de l'Univers,
CNRS UMR 5804, BP 89, 33270 Floirac, France

ABSTRACT. Abundances of Y, Zr, La, Ce, Nd, and Sm have been obtained under LTE approximations. The program stars were observed at high resolution, high signal to noise ratio with the ELODIE echelle spectrograph (OHP, France). Among them more than 30 stars are active stars with a fraction of BY Dra and RS CVn type stars. Comparison of the behavior of n-capture elemental abundance in active and non active stars was made.

Key words: Stars: fundamental parameters; stars: abundances; stars: kinematics; stars: atmospheres; Galaxy: stellar content.

1. Introduction

Studying of the stars of the lower part of the Main Sequence we have found about 30 active stars (BY Dra type) and the difference in Li abundance for active and non active stars (Mishenina et al., 2008). In this work we continue the chemical abundance investigation of these stars and have turned our attention to the elements of neutron capture.

2. Observations and spectra processing

The spectra of 89 stars were obtained in the region of the $\lambda\lambda$ 4400–6800 Å and with S/N about 100–350 using the 1.93 m telescope at the Observatoire de Haute-Provence (OHP, France) equipped with the echelle-spectrograph ELODIE (Barrane et al., 1996), resolving power is $R = 42000$. The spectral processing carried out by (Katz et al., 1998; Galazutdinov, 1992).

3. Parameter and abundance determination

Effective temperatures T_{eff} were estimated by the line depth ratio method (Kovtyukh et al., 2003). The relations combine the effective temperature with a set

of spectral line depth ratios. The internal accuracy of the effective temperature determined in this way is rather high in the temperature range 4000 K to 6000 K: typically 150 K or less (standard deviation or 10 to 20 K for the standard error). Another very important advantage of this method (or any spectroscopic method) is that it produces the reddening-free T_{eff} estimates.

Surface gravities $\log g$ were determined by two methods: parallaxes and ionization balance of iron. The microturbulent velocity V_t was determined on the independence of the iron abundance $\log A(\text{Fe})$ obtained from given Fe I line from equivalent width EW of this line.

Abundances of Y, Zr, La, Ce, Nd, and Sm have been obtained under LTE approximations with 9–12 lines of YII, 3–4 lines of ZrII, 5–6 lines of LaII, 10–13 lines of CeII, 8–11 lines of NdII, 4–5 lines of SmII with the solar oscillator strengths (Kovtyukh & Andrievsky, 1999). Model of the atmospheres and the code WIDTH9 of Kurucz were used (Kurucz, 1993).

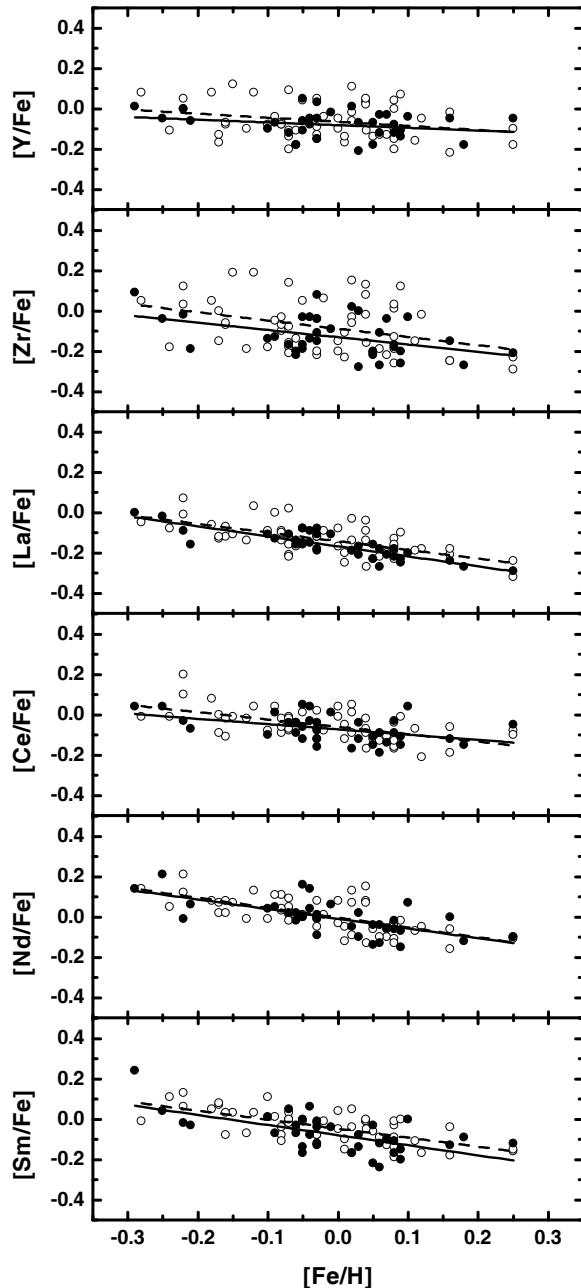
Influence of parameters determination and spectra processing (Sp) on n-capture elemental abundance determination for example of stars HD 139813 ($T_{\text{eff}}/\log g/V_t/[\text{Fe}/\text{H}] = 5408/4.5/1.2/0.0$) given in Table 1.

4. Results and conclusion

Comparison of the behavior of n-capture elemental abundance $[\text{El}/\text{Fe}]$ vs. $[\text{Fe}/\text{H}]$ in active (filled circles) and non active (open circles) stars in the region of metallicities from $[\text{Fe}/\text{H}] = -0.3$ to $[\text{Fe}/\text{H}] = +0.3$ was presented in Fig. 1 (see below). As can see from Figures, in the region of metallicities from $[\text{Fe}/\text{H}] = -0.3$ to $[\text{Fe}/\text{H}] = +0.3$ all elements (except Y) demonstrate the trend of abundance with $[\text{Fe}/\text{H}]$ and the deficient of abundance at $[\text{Fe}/\text{H}] > -0.2$. This trend of the elemental abundance corresponds to the received earlier results for this region of $[\text{Fe}/\text{H}]$.

Table 1: Influence of parameter determination and spectra processing (Sp) on abundance determination.

Elem	ΔT_{eff}	$\Delta \log g$	ΔV_t	$\Delta[\text{Fe}/\text{H}]$	Sp	Total
Y	0.00	-0.11	-0.02	0.07	0.02	0.13
Zr	0.01	-0.12	0.00	0.07	0.02	0.14
La	0.00	-0.12	0.00	0.07	0.02	0.14
Ce	-0.01	-0.12	-0.01	0.07	0.02	0.14
Nd	-0.02	-0.13	-0.01	0.07	0.02	0.15
Sm	-0.02	-0.13	-0.01	0.08	0.02	0.15

Figure 1: Trends of studied elements with $[\text{Fe}/\text{H}]$ of non active (open circles, dashed line) and active (black circles, solid line).

For active and non active stars we observed the insignificant difference between elemental abundance that it is in the limits of determination errors. It permit to us use the obtained data in the galactic chemical evolution investigation.

Acknowledgements. This work was supported by the Swiss National Science Foundation (SCOPES project No. IZ73Z0-128180/1)

References

- Baranne A., Queloz D., Mayor M. et al.: 1996, *A&AS*, **119**, 373.
Galazutdinov G.A.: 1992, *Prepr. SAO RAS*, **92**, 27.
Katz, D., Soubiran, C., Cayrel, R. et al.: 1998, *A&A*, **338**, 151.
Kovtyukh V.V., Andrievsky S.M.: 1999, *A&A*, **351**, 597.
Kovtyukh V.V., Soubiran C., Belik S.I., Gorlova N.I.: 2003, *A&A*, **411**, 559.
Kurucz R.L.: 1993, *CD ROM n13*.
Mishenina T.V., Soubiran C., Bienayme O. et al.: 2008, *A&A*, **489**, 923.

IMPROVED PHOTOMETRIC CHARACTERISTICS OF THE NEWLY DISCOVERED EW-TYPE SYSTEM GSC 04370-00206

V.V. Breus¹, I.L. Andronov¹, P.A. Dubovsky², T. Hegedus³, I. Kudzej², K. Petrik⁴

¹ Department “High and Applied Mathematics”, Odessa National Maritime University, Odessa, Ukraine, *bvv_2004@ua.fm*, *il-a@mail.ru*

² Vihorlat Astronomical Observatory, Humenne, Slovakia, *var@kozmos.sk*

³ Baja Astronomical Observatory, Baja, Hungary, *hege@bajaobs.hu*

⁴ Astronomical Observatory, Hlohovec, Slovakia, *kpetrik@astronyx.sk*

ABSTRACT. We present results of two-color photometric study of the newly discovered EW-type eclipsing binary star GSC 04370-00206 in the field of the intermediate polar MU Cam. CCD V,R observations were obtained in the Astronomical Observatories in Hlohovec, Baja and Kolonica in 2007-2009. Improved photometric elements for the primary minimum were determined: $\text{Min.BJD}=2454805.75635+0.44264511(27)\text{E}$. The range of the brightness variations is 13.79-14.13 (V) and 13.07-13.44 (R). The accuracy of the period determination is by a factor of $\sim 7,000$ times better than the one published by the discoverers based on only one night of observations. We report on the night-to-night variability of the shape of the light curve which is interpreted by a presence of spots in the atmosphere of one or both components (O’Connell effect).

Key words: stars: variables, eclipsing binaries

During monitoring of the intermediate polar MU Cam = 1RXS J062518.2+733433 in frame of the international campaign “Inter-Longitude Astronomy” (see Andronov et al. (2010) for recent highlights on variable stars of different types), Kim et al. (2005) discovered a new EW-type star GSC 04270-00206 and estimated the orbital period of $P_{orb} = 0.^d4421 \pm 0.^m0018$ and an initial epoch of 2454805.75635.

The observations were obtained in 2007-2009 using 60cm Zeiss Cassegrain in Hlohovec, Slovakia; the 50cm reflector in Baja, Hungary and the 1m VNT (“Vihorlat National Telescope”) in Kolonica, Slovakia. The V (14 nights, 66 hours, $n = 1011$) and R (16 nights, 72 hours, $n = 1163$) filters were used for observations. The photometric data were reduced the using C-Munipack software package (Motl, 2007). The calibration of the comparison stars was discussed by Kim et al. (2005) based on Henden (2004). The time series

analysis was carried out using the MCV program (Andronov and Baklanov, 2004). The periodograms for observations in both filters were computed using the sine fit, then the period was doubled and re-analyzed using the best fit trigonometric polynomial (TP) fit of statistically optimal order s (see Andronov (1994, 2003) for a description). The range of the brightness variations is $13.^m792\text{-}14.^m169$ (V) and $13.^m067\text{-}13.^m444$ (R) based on this fit. For both filters, we obtained $s = 4$. Finally, the initial epoch for the primary minimum is $\text{Min.BJD}=2454805.75635$ by Kim et al. (2005) and the a weighted mean for the period of $P = 0.^d44264511(27)$.

The accuracy of our period determination is by a factor of $\sim 7,000$ times better than the one published by the discoverers based on only one night of observations.

Our improved light elements were confirmed by Chinarova et al. (2010) based on two nights of observations.

From original light curves, we have determined timings of the primary and secondary minima. They are listed in Table 1, as well as the corresponding brightness. For the determination of the characteristics of extrema, we have used the “asymptotic parabola” (AP) method by Marsakova and Andronov (1996). As the majority of minima were covered in two colors (VR), we also computed the color index and the weighted mean minimum timings (also listed in Table 1). Unexpectedly, it was found to be the same for either primary ($V - R = 0.^m758(6)$), or secondary ($V - R = 0.^m755(6)$) minima. The mean values (integrated over a period) are $V = 13.^m948(1)$ and $R = 13.^m213(2)$, respectively. This corresponds to the mean color index $V - R = 0.^m735(2)$, only slightly “hotter” than at minima.

Phase curves are shown in Fig. 1. There are systematic changes from night to night. So we may suggest that there is a variability of brightness of star which can be interpreted as the O’Connell’s effect, i.e. the presence of the migrating spots in the atmosphere.

Table 1: Characteristics of minima.

HJD 24.....	mag	Min
54308.44674±0.00097	14.199± 0.019	2 V
54309.55169±0.00063	14.207± 0.022	1
54312.43015±0.00068	14.167± 0.012	2
54314.41964±0.00044	14.240± 0.007	1
54315.53010±0.00086	14.160± 0.014	2
55069.57531±0.00192	14.115± 0.053	1
55094.58453±0.00049	14.225± 0.006	2
55220.51604±0.00039	14.200± 0.006	1
55304.39825±0.00053	14.148± 0.007	2
54308.44544±0.00068	13.441± 0.008	2 R
54309.55017±0.00137	13.457± 0.029	1
54312.43004±0.00114	13.303± 0.010	2
54314.42057±0.00085	13.504± 0.009	1
54315.53097±0.00140	13.457± 0.023	2
55094.58345±0.00036	13.491± 0.006	2
55220.51562±0.00034	13.434± 0.004	1
55304.39859±0.00077	13.397± 0.010	2
54308.44587±0.00056	0.757± 0.021	2 V - R
54309.55142±0.00057	0.750± 0.037	1
54312.43012±0.00058	0.865± 0.016	2
54314.41984±0.00039	0.736± 0.011	1
54315.53034±0.00073	0.703± 0.027	2
55094.58383±0.00029	0.734± 0.008	2
55220.51580±0.00026	0.767± 0.007	1
55304.39836±0.00044	0.751± 0.012	2

Systematic changes of brightness from one minimum to another at the trigonometric polynomial are significant only in the R filter and are negligible in V .

The $(V - R)$ color variations are rather strange. The largest value of $V-R$ corresponding to smallest temperature occurs unexpectedly at the phase 0.5 of the secondary minimum, whereas the largest color temperature is observed at phase 0.9, i.e 0.1 prior to the main minimum, practically at the middle of the descending branch. This differs from expectations for deformed stars, for which a double-hump wave is observed with a temperature maximum at phases of 0.25 and 0.75.

To check results of fitting of complete light curves using the TP fit, we also computed mean characteristics using the AP fit: $R_1 - R_2 = 13.^m448 - 13.^m439 = 0.^m0090(15)$, and, in the V filter: $V_1 - V_2 = 14.^m215 - 14.^m190 = 0.^m0252(15)$. This differs from results from the TP fit. One of possible explanations may be due to significant variability of the shapes of the individual light curves discussed above: the AP fit characterizes only parts of minima covered by observations (either descending, or ascending branch of the light curve), whereas the TP fit uses all the nights and phases. Thus systematic night-to-night variations may strongly affect mean values of estimated parameters.

This interesting object is recommended for further observations.

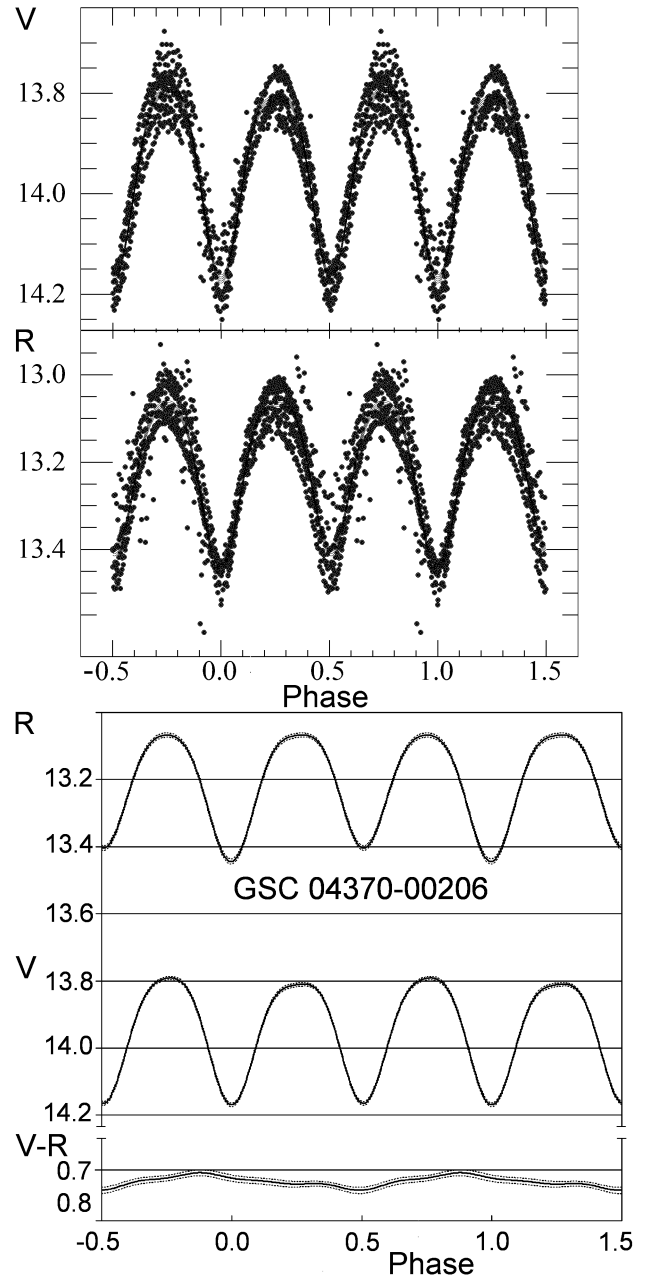


Figure 1: Phase light curves of GSC 04370-00206 (up) and 4-th order trigonometric polynomial fits (bottom).

References

- Andronov I.L.: 1994, *OAP*, **7**, 49
 Andronov I.L.: 2003, *ASPC*, **292**, 391
 Andronov I.L. et al.: 2010, *OAP*, **23**, 8
 Andronov I.L., Baklanov A.V.: 2004, *Astronomy School Reports*, **5**, 264, <http://uavso.pochta.ru/mcv>
 Henden A.: 2004, <ftp.aavso.org/public/calib/j0625.dat>
 Chinarova L.L., Andronov I.L., Gubin E.G.: 2010, *OAP*, **23**, 27
 Kim Y., Andronov I.L., Park S.S., Chinarova L.L., Baklanov A.V., Jeon Y.B.: 2005, *JASS*, **22**, 197
 Marsakova V.I., Andronov I.L.: 1996, *OAP*, **9**, 127
 Motl D.: 2007, C-Munipack Project v1.1, <http://integral.physics.muni.cz/cmunicipack/index.html>

SPECTROSCOPIC STUDY OF THE HOT SUPERGIANT ζ PERSEI

V.V. Butkovskaya, D.N. Baklanova, S.I. Plachinda

Crimean Astrophysical Observatory
98409 Nauchny, Crimea, Ukraine, *varya@crao.crimea.ua*

ABSTRACT. The preliminary results of the high-resolution spectroscopic study of the hot supergiant ζ Persei (B1 Ib) are presented. It was found that the radial velocity of ζ Persei measured in the He I 6678 Å line varies from night to night probably in the α Cygni manner.

Key words: Stars: oscillations stars: early-type - stars: massive, supergiants; stars: individual: ζ Per.

1. Introduction

α Cygni variables are nonradially pulsating supergiants covering the whole range of effective temperatures of β Cephei and SPB (Slowly Pulsating B-stars) variables. The typical periods of α Cygni-type stars are from few days to more than 10 days.

Progenitor of this class of pulsating variables is α Cygni (A2 Iae). Paddock (1935) found that the radial velocity of α Cygni varies with average quasi-period of 11.7 day and amplitude of 2.6 km/s. Luccy (1976) has reanalyzed the data of Paddock and provided 16 pulsation modes from 6.9 to 100.8 day as well as more long-period variation (about 800 days) was supposed by him due to orbital motion.

Waelkens et al. (1998) discovered a sample of B-supergiants to be periodically variable with SPB-type periods from the Hipparcos mission. These stars and additional several ones were subjected to detail spectroscopic and frequency analyses by Lefever et al. (2006), who found their photometric periods to be from 1.5 to 24 days. Saio et al. (2006) detected both p and g modes in the B2Ib/II star HD 163899 from MOST space-based photometry.

The radial velocity of ζ Persei (HD 24398, B1 Ib) was found to be variable by Bouigue (1950) using photographic spectra of the star, obtained by the author during 17 nights in 1948. Bouigue proposed 1.765-day period of radial velocity variations and explained it by orbital motion of the star. Calculated by him orbital parameters are: $T = 2432865.600$ d, $P = 1.765$ d, $K = 6.0$ km/s, $\gamma = 22.2$ km/s, $e = 0.45$, $\omega = 349^\circ$, $asin i = 130000$ km. But the later investigation of Muller

et. al. (1956) has not confirmed a possible binarity of the star. In this paper we present the result of high-resolution spectroscopic study of ζ Persei from 1997 to 2010.

2. Observations

High-accuracy 262 spectroscopic observations of ζ Persei have been performed in the line He I 6678 Å during 25 nights from 1997 to 2010 using coude spectrograph of the 2.6-m Shajn telescope at the Crimean Astrophysical Observatory (Butkovskaya & Plachinda 2007). Signal-to-noise ratios of a single spectrum were typically 300-900 with resolving power of spectra approximately 25000.

3. Results

Fourier analysis of the radial velocity of ζ Persei was performed using Period04 code. The results of this study are summarized in Table 1. In the top part of Table 1 the multifrequency solution obtained with using only our time-string are presented ($Nyquist = 23.1$ d $^{-1}$, $step = 1.34 \times 10^{-5}$ d $^{-1}$). In the bottom part of the Table 1 the multifrequency solution calculated with using our data and data of photographic measurements of Bouigue (1950) and Muller et. al. (1956) are presented ($Nyquist = 45.5$ d $^{-1}$, $step = 2.22 \times 10^{-6}$ d $^{-1}$). All data cover 62 years. In order to obtain the uniform time-string, the radial velocity data from paper of Bouigue (1950) were corrected on -1.26 km/s and radial velocity data from paper of Muller et. al. (1956) were corrected on -4.03 km/s. From Table 1 one can see, that obtained in these two calculations results are well coincided.

The radial velocity data folded in phase with the main period of 51 day are presented in the Fig. 1.

In our study we found also the period 1.734 day closed to one obtained by Bouigue (1950) and explained by him as the orbital period. But in our opinion, this period and other two periods presented in Table 1, can be explained by the non-radial oscillations in

Table 1: Multifrequency solutions for ζ Persei radial velocity data.

Frequency (d^{-1})	Amplitude (km/s)	Period (d)
Our data		
0.019442	1.98	$51.433 \pm 3.5 \times 10^{-2}$
0.106212	1.20	$9.4151 \pm 1.2 \times 10^{-4}$
0.573990	1.02	$1.74220 \pm 1.1 \times 10^{-5}$
All data		
0.019444	1.59	$51.429 \pm 5.9 \times 10^{-3}$
0.106241	0.97	$9.4126 \pm 2.0 \times 10^{-4}$
0.576688	1.18	$1.734040 \pm 6.7 \times 10^{-6}$

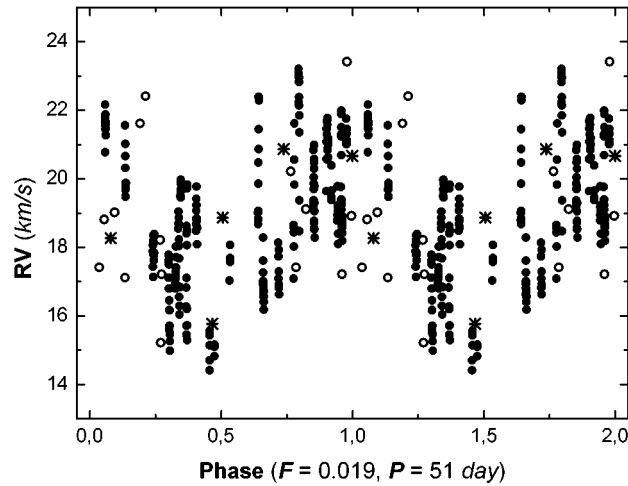


Figure 1: Our radial velocity data (*closed circles*) and single radial velocity measurements of Bouigue (*open circles*) and Muller et. al. (*stars*) folded in phase with the period of 51 day.

the atmosphere of ζ Persei. So we suppose that ζ Persei is one of the α Cygni-type variable supergiant stars. In the Fig. 2 the examples of the three-frequency fit of our data (middle and bottom panels) and data of other authors (top panel) are presented.

We found also that the shot-term radial velocity variations with amplitude 1 - 4 km/s exist within some nights and these shot-term variations cause the scattering of our data. The shot-period oscillations with amplitude 0.5 - 1.2 km/s were also reported by Paddock (1935) for α Cygni.

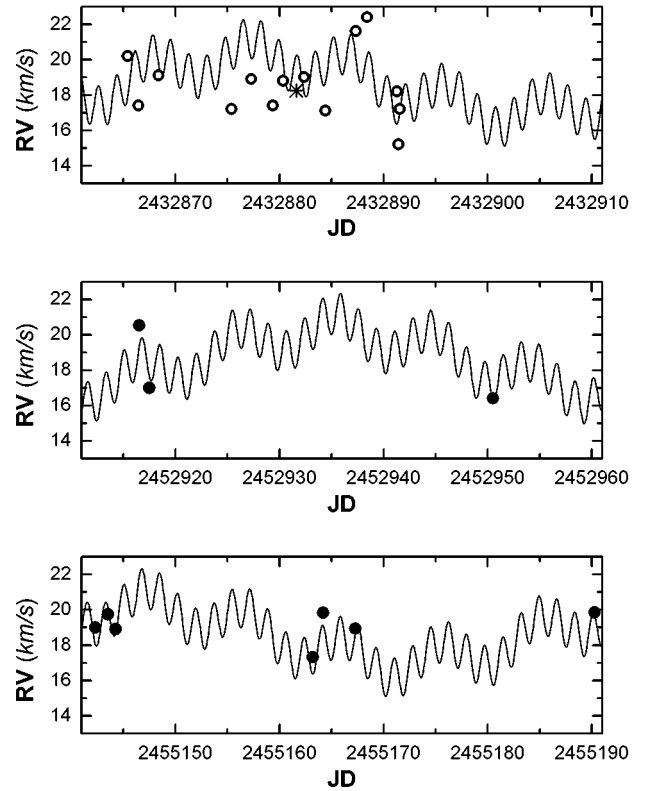


Figure 2: The examples of the three-frequency fit of our data (*closed circles* on middle and bottom panels) and data of other authors (Bouigue (*open circles*) and Muller et. al. (*stars*) on top panel) are presented.

References

- Bouigue M.R.: 1950, *Annales de l'Observatoire Astron. et Meteo. de Toulouse*, **20**, 47
- Butkovskaya V.V. & Plachinda S.I.: 2007, *A&A*, **463**, 1093
- Lefever K. et al.: 2007, *A&A*, **469**, 1069
- Lucy L.B.: 1976, *ApJ*, **206**, 499
- Muller A.B. et. al.: 1956, *BAN*, **13**, 51
- Paddock G.F.: 1935, *LicOb*, **17**, 99
- Saio H. et al.: 2006, *ApJ*, **650**, 1111
- Waelkens C. et al.: 1998, *A&A*, **330**, 215

THE mCP STAR HD 9996 - PRECESSION OR NOT?

V.D. Bychkov¹, L.V. Bychkova¹, J. Madej², A.V. Schatilov¹

¹ Special Astrophysical Observatory Russian Academy of Sciences

North Caucasus, Nizhnij Arkhyz, Karachai-Cherkesia, 369167, RUSSIA *vbych@sao.ru*

² Warsaw University Observatory

Al.Uesdowskie 4, Warsaw, Poland

ABSTRACT. The star HD9996 have a long-period magnetic field of variations. On long-term variability was impose shorter variations conterminous with the orbital period.

Key words: Stars: magnetic field; stars: individual: HD9996.

1. Long-period magnetic phase curve.

Compilation of early photometric measurements for HD9996 allowed to constrain the corresponding period P in range $7750 < P_{ph} < 8550$ dayes, Pyper & Adelman, (1986). Period from magnetic measurements $P_{mag} = 7842$, Bychkov et al.,(1997), $P_{mag} = 7692$, Bychkov et al.,(2005). Since the magnetic phase curve still was poorly constrained, monitoring project for HD9996 was continued until now. Because this object is a realitively bright, magnetic monitoring were done in coude-focus of 1-m reflector SAO, equipped with CEGS spectrometer and analyzer of circular polarization (Bychkov, 2008). Finally we collected 41 measurements of B_e during 15 recent years. Fig.1 shows long-period magnetic phase curve. All data for 60 years of supervision have been used. We have found the best magnetic period $P_{mag} = 8019.24$. The magnetic curve has a double wave with parameters $B_0 = -429G$, $B_1 = 1330G$, $B_2 = 332G$. The wide scatter of B_e specifies possible availability to short time variability.

2. Short-term magnetic variability.

We used only B_e received by us for search of the short period. We measured $V_e \sin I$ on all spectra and have received $\leq 8km/s$. The star has radius nearly 2.4 solar radius - the period should be more than 15.2 days. We have found using evasion from the average curve short magnetic period. It has coincided with the orbital period $P_{orb} = 272.99$ days (Scholz, 1978). On Fig.2 shows variability with imposing this period. Fig.3 shows a phase curve of this variability with

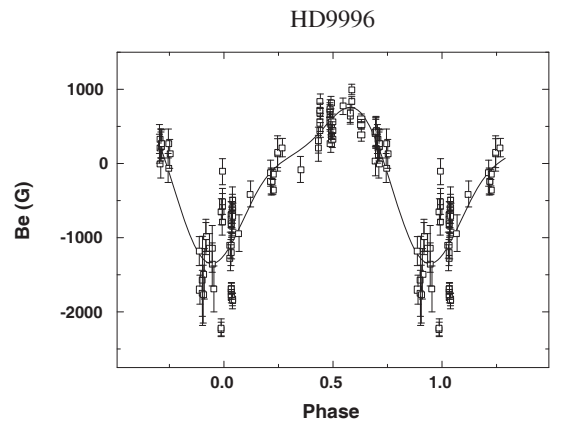


Figure 1: Long-period magnetic phase curve.

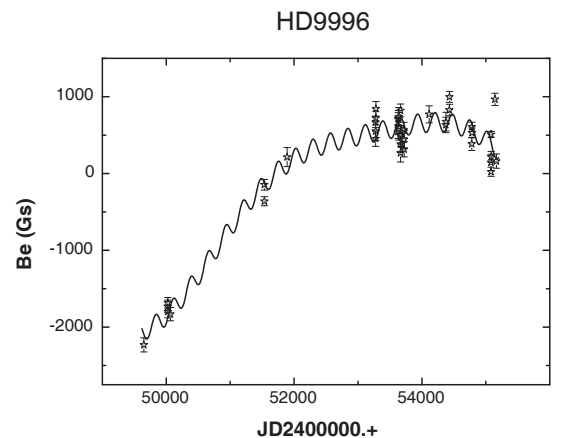


Figure 2: Magnetic behaviour HD9996 for last 15 years of our observation.

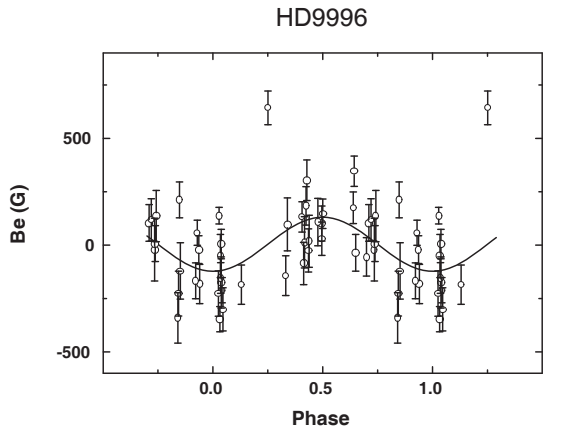


Figure 3: Short-period magnetic phase curve.

parameters $B_0 = 4$, $B_1 = 128G$ about the long-term magnetic mean phase curve.

3. Discussion.

We tried to explain magnetic behaviour precession axes rotations of the main star in double system with the period of 8020 days as well as Lehmann (1987), the period of rotation of a star is synchronized with the orbital period and makes 272.99 days, angle $\beta = 18$ degrees, Eulers angle $\Theta = 43$ degrees. We took structure of a magnetic field of the main component as the central not displaced dipole described standard formalism of Preston (1967).

This assumption is contradicted by following data:

1. The amplitude should be maximal at short variability in a phase when mean $B_e = 0$ (the axis of rotation lays in a plane of the sky) and minimal when mean $B_e = max$ (the angle i is minimal).

2. Slow precession variability should be strictly harmonious, not have a double wave.

4. Our plans for the future.

We plan to continue regular magnetic monitoring of this object.

1. We wish to study its magnetic behaviour in more detail.
2. Modulation of a magnetic field with the orbital period is very interesting. Probably it not only tidal effects. Probably it is interoperability of magnetic fields if the second component the magnetic white dwarf.
3. We wish to understand, the rotation of the main component with the orbital period is synchronized or not.

Acknowledgements. We acknowledge support from Polish Ministry of Science and Higher Education grant No. N N203 511638.

References

- Bychkov V.D., Gerth E., Kroll R., Shtol' V.G.: 1997, *Stellar Magnetic Fields, Proc. Int. Conf., Special Astrophysical Observatory Press, Nizhnij Arkhyz.*, 204.
- Bychkov V.D., Bychkova L.V., Madej J.: 2005, *A&A*, **430**, 1143.
- Bychkov V.D.: 2008, *Astrophysical Bulletin*, **63**, 83.
- Preston G.W.: 1967, *Ap.J.*, **150**, 547.
- Pyper D.M., Adelman S.: 1986, *IAPPP Commun.*, **25**, 76.
- Lehmann T.: 1987, *Astron.Nachr.*, **308**, 333.
- Scholz G.: 1978, *Astron.Nachr.*, **299**, 81.

WAVELET ANALYSIS OF 173 SEMI-REGULAR VARIABLES

L.L. Chinarova

Research Institute "Astronomical Observatory"
Odessa National University, Odessa 65014, Ukraine

ABSTRACT. We made the wavelet analysis of 173 semi-regular pulsating variable stars of different sub-types. For the analysis, we have used 1,000,000 individual brightness estimates from the published international databases of the VSOLJ (Japan) and AFOEV (France). They were visually checked using the program OL (I.L.Andronov, 2001OAP...14..255A), and bad points were removed from the data files. The wavelet analysis was performed using the program WWZ (I.L.Andronov, 1998KFNT...14..490A) which improves the discrete Morlet-type wavelet transform to the case of irregularly spaced data. Mean weighted wavelet periodograms are presented, as well as wavelet maps. Dependences of the wavelet-based periods and amplitudes on time are presented for the investigated stars. Some stars exhibit switchings between preferred periods, which are interpreted as switchings of the pulsation mode. Additional criteria for classification of the pulsating variables based on the stability of periods and amplitudes are discussed. Results are shown for the semi-regular star RU And, for which the semi-amplitude varies drastically from 0.027 ("nearly constant star") to 1.204 mag ("Mira"- type pulsating variable. The phase of pulsations also varies drastically by 0.7P, and the wavelet estimates of the period - from 210 to 270 days.

Key words: Variable stars: pulsating: Semi-Regular: RU And; Data analysis.

We introduce the "Atlas and Catalogue ..." which is an extended version of the "Catalogue of main characteristics of pulsations of 173 semi-regular stars" by Chinarova and Andronov (2000) taking into account observations from the AFOEV international databases obtained during 10 more years of photometric monitoring. Statistical study of semi-regular variables using scalegram-based characteristics was made by Andronov and Chinarova (2003). Comparison of different methods for determination of characteristic time scales in semi-regular stars was made by Andronov and Chinarova (2001). In this work, we use for the analysis improved values of the parameters based on more extensive time series and more individual pulsation cycles.

Results are shown for one of the stars from our sample - RU And.

For the analysis, we have used 1446 observations from the AFOEV (2010) international database. Also we have used the data from the VSOLJ (2000) international database, which were analyzed by Chinarova and Andronov (2000). After the filtering of the merged dataset for bad points (or groups of points by some observers) using the program OL (Andronov, 2001), the final number of data points covering the time interval from October 14, 1979 to March 13, 2010, is 1638.

The wavelet analysis was performed using the program WWZ (I.L.Andronov, 1998, 1999) using a standard decay coefficient $c = 0.0125$. The wavelet periodogram is shown in Fig.1. The test function computed as a time-weighted mean of the function WWZ proposed by Foster (1995) and improved by Andronov (1999). The highest peak at the periodogram corresponds to the period of 247^d , although some smaller peaks are present. Consequently, we used another value of the decay coefficient $c = 0.003125$, which corresponds to a twice larger time interval for each trial period and time. The corresponding periodogram has become higher and thinner. And finally, we made a periodogram analysis using the sine fit for all data (i.e. $c = 0$ using the programs Four (Andronov 1994) and MCV described by Andronov and Baklanov (2004). The test function S is a square of the correlation coefficient between the observed and calculated (for a given period) values. It is also shown in Fig. 1. Because of large time base, the peaks at this periodogram are more narrow than for the wavelet periodograms, and some peaks are splitted, what is not seen at the local wavelet fits.

The statistically optimal sine fit to the observations corresponds to a mean value $C_1 = 11.^m775 \pm 0.^m012$, semi-amplitude $r = 0.^m493 \pm 0.^m017$, period $P = 246.^d99 \pm 0.^d11$ and initial epoch for maximum brightness $T_0 = 2450577.8 \pm 1.3$.

Using the wavelet analysis, we have determined best fit values of the period and semi-amplitude as functions of trial time. They are shown in Fig. 2. Both these parameters show significant variations. The wavelet period varies mainly from 210 to 270 days, sometimes formally going out of this interval. This is caused by observational gaps between annual seasons.

To avoid this problem, we used $c = 0.003125$, which corresponds to twice better period resolution in cost of twice worse time resolution. For such a parameter, the problem of seasonal gaps is solved, however, the smoothing function has wider and less prominent peaks. Thus we conclude that the variations are present and significant. The third wavelet-related method is the method of “running sine” with a rectangular weight function (see Andronov 1997, 1998b for a description). We used the filter half-width $\Delta t = P/2$.

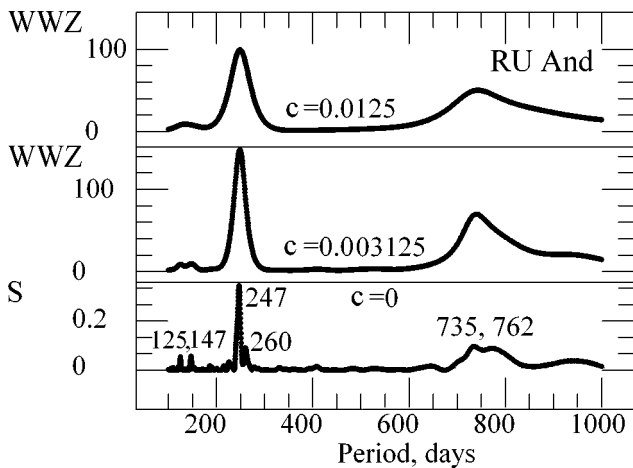


Figure 1: Wavelet periodograms for observations of RU And for different values of the decay coefficient c .

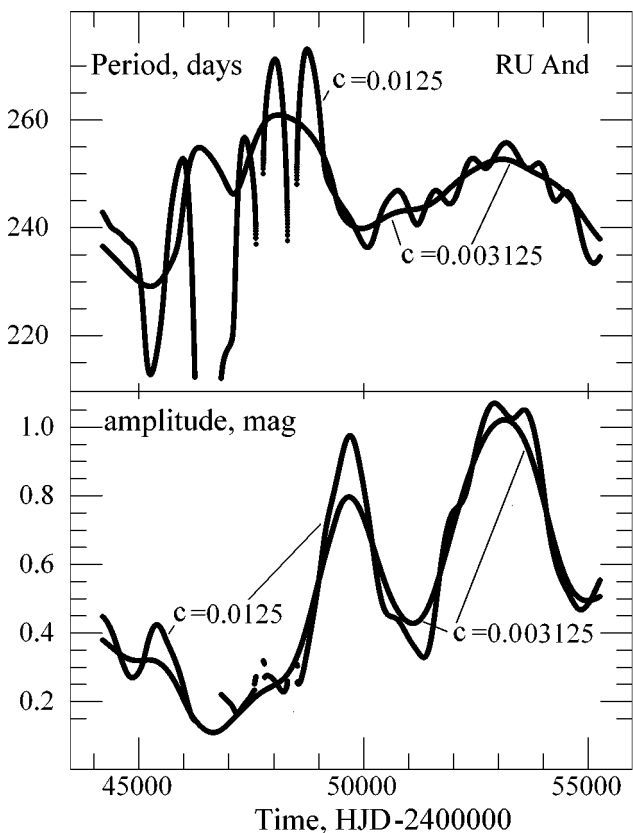


Figure 2: Dependence of the period and amplitude on trial time for different values of the decay coefficient c .

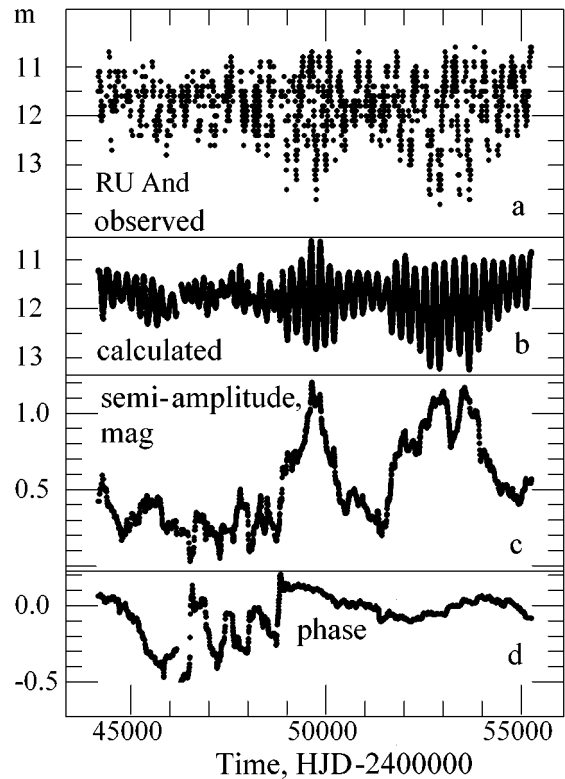


Figure 3: “Observed” and “calculated” data and time variations of the semi-amplitude and phase of individual pulsation cycles using the method of ‘running sines’ according to the ephemeris $\text{Max.HJD} = 2450577.8 + 246.99 \cdot E$.

The semi-amplitude varies drastically from 0.027 (“nearly constant star”) to 1.204 mag (“Mira”- type pulsating variable). The phase of pulsations also varies drastically by $0.7P$, indicating transitions between relatively stable periods.

Acknowledgements. The author is thankful to the observers and the staff of the AFOEV and VSOLJ international databases for the free access to the observations and to Prof. Ivan L. Andronov for helpful discussions and supervision of this work.

References

- AFOEV, 2010, <ftp://cdsarc.u-strasbg.fr/pub/afoev>
 Andronov I.L.: 1994, *OAP*, **7**, 49
 Andronov I.L.: 1997, *A&AS*, **125**, 207
 Andronov I.L.: 1998, *KFNT*, **14**, 490
 Andronov I.L.: 1999, *sss.conf...57A*
 Andronov I.L.: 2001, *OAP*, **14**, 255
 Andronov I.L.: 2003, *ASPC*, **292**, 391
 Andronov I.L., Baklanov A.V.: 2004, *Astronomy School Reports*, **5**, 264, <http://uavso.pochta.ru/mcv>
 Andronov I.L., Chinarova L.L.: 2001, *OAP*, **14**, 113
 Andronov I.L., Chinarova L.L.: 2003, *ASPC*, **292**, 401
 Chinarova L.L., Andronov I.L.: 2000, *OAP*, **13**, 116
 Foster G.: 1996, *AJ*, **112**, 1709
 VSOLJ: 2000, <http://vsolj.cetus-net.org>

CCD OBSERVATIONS OF THE INTERMEDIATE POLAR MU CAM AND GSC 04370-00206

L.L. Chinarova¹, I.L. Andronov², E.G. Gubin¹

¹ Research Institute "Astronomical Observatory"

Odessa National University, Odessa 65014, Ukraine

² Department "High and Applied Mathematics", Odessa National Maritime University,
Odessa, Ukraine, *il-a@mail.ru*

ABSTRACT. Results of CCD observations of MU Cam and GSC 04370-00206 obtained at the 60 cm telescope of the RSI "Astronomical Observatory" of the Odessa National University.

Key words: Variable stars: intermediate polars, eclipsing.

Cataclysmic variable stars are excellent natural laboratories to study various astrophysical processes (cf. Warner 1995). Among them, there is a very interesting class of intermediate polars with rapidly rotating magnetic white dwarf (see Patterson 1994 for a review). The spin period variations have been discovered for many of these objects, showing either increase, or decrease. This depends on arbitrary dimensions of the co-rotation radius and radius of the magnetosphere. Andronov (2005) proposed a model, according to which, the variations may be explained by a precession of the white dwarf, even if the accretion rate does not undergo significant changes.

To study rotational evolution of the white dwarf, a regular monitoring is needed. Thus intermediate polars are included in the part "Polar" of the international campaign "Inter-Longitude Astronomy" (see Andronov et al. 2010 for recent highlights). One of the objects is a newly discovered intermediate polar 1RXS J062518.2+733433 (Araujo-Betancor et al. 2003, Staude et al. 2003). Results of our previous study of this object (now known as MU Cam) were published by Kim et al. (2005).

In this paper, we report on first CCD observations of cataclysmic variable stars obtained in Odessa (Mayaki). Totally, 1817 unfiltered data were obtained during 12.6 hours during the nights on December 15 and 20, 2006 with time resolution of 16 seconds.

To study the instrumental system, we have used secondary photometric standards for 7 comparison stars published by Kim et al. (2005). The instrumental magnitude m was determined using the "artificial comparison star" method (Andronov and Baklanov, 2004; Kim et al. 2005) using the V calibration of the comparison

star C2 ($V = 13.^m842$, $B - V = 0.^m920$) by Henden (2002). The color transformation equations are

$$m - V = 0.026(30) - 0.844(160) \cdot (B - V - 0.774),$$

$$m - V = 0.026(30) - 1.390(264) \cdot (V - Rc - 0.547)$$

with the unit weight error of $\sigma_0 = 0.^m080$. Here "(numbers)" are error estimates in units of the last decimal digit. Excluding two outstanding points at the diagram, we recomputed the coefficients, so

$$m - V = 0.111(8) - 0.942(120) \cdot (V - Rc - 0.422)$$

with much smaller $\sigma_0 = 0.^m018$. In other words, the unfiltered instrumental system is close to the standard Rc within statistical error estimates. Thus finally we have used for calibration the extrapolated value of brightness of C2 in the Cousins' Rc system of $Rc = 12.^m936$. The r.m.s. accuracy of the "artificial comparison star" is $0.^m0095$, i.e. by a factor of 1.4 better than an accuracy of the "most stable" comparison star C2. The accuracy estimate is $\sigma = 0.^m019$ for $R = 13.^m5$ and $\sigma = 0.^m066$ for $R = 15.^m0$ for exposures of 15 seconds.

The first step is to determine nightly "mean timings". For this purpose, we have used a two-period approximation

$$m_C(t) = m_0 - r_1 \cos\left(\frac{2\pi(t-T_1)}{P_1}\right) + r_2 \cos\left(\frac{2\pi(t-T_2)}{P_2}\right),$$

where we have adopted $P_1 = P_{spin} = 0.^d01374116815$ and $P_2 = P_{orb} = 0.^d19661$ are the spin and the orbital periods, respectively (Kim et al. 2005). For the two nightly runs, we determined initial epochs for the spin maximum $T_1 = HJD2454085.50661(12)$, $2454090.52210(9)$; semi-amplitudes of the spin pulse $r_1 = 0.^m055(3)$, $0.^m084(4)$; initial epochs for the orbital minimum $T_2 = 2454085.45826(81)$, $2454090.57783(263)$, semi-amplitudes of the orbital variations $r_2 = 0.^m114(3)$ and $0.^m045(4)$ and mean brightness $m = 14.^m739(2)$ and $14.^m766(3)$. As the parameters vary from night to night, we have used the second step - the "running sine" fit

$$m_C(t) = m_0 - r_1 \cos(2\pi((t - T_{01})/P_1 - \phi)),$$

where the "initial epoch" for maximum is $T_{01} = 2452893.78477$ (Kim et al. 2005) and ϕ is the phase of maximum. For such a "running approximation", we have used a filter half-width of $\Delta t = 0.5P_1$.

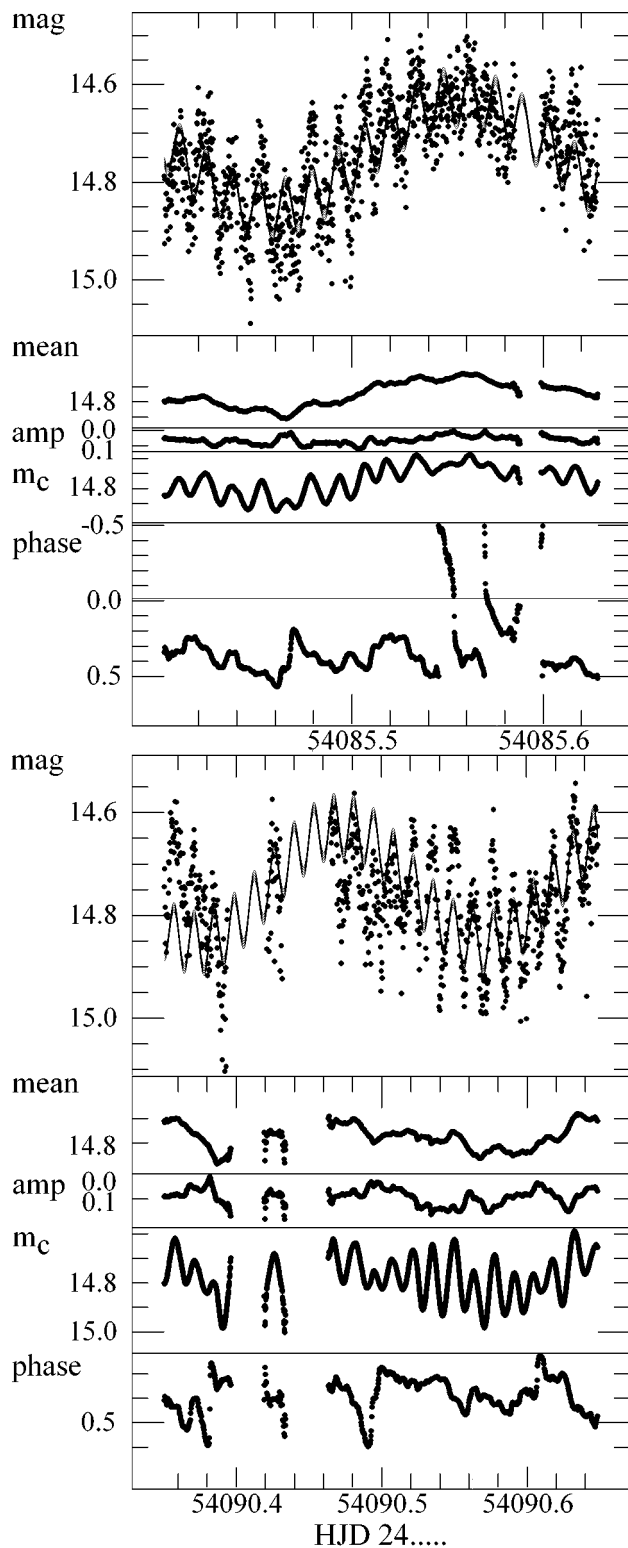


Figure 1: Light curves of MU Cam and their approximations: (up) two-periodic fit (spin+orbital) and (bottom) parameters of approximation using the “running sine” (Andronov 1997): “mean” m_0 , semi-amplitude r_1 (“amp”) and ϕ (“phase”) of the spin maximum according to the ephemeris by Kim et al. (2005). Contrary to the two-period fit, where the mean, amplitude and phase are suggested to be constant, the “running sine” shows significant variability of all three parameters.

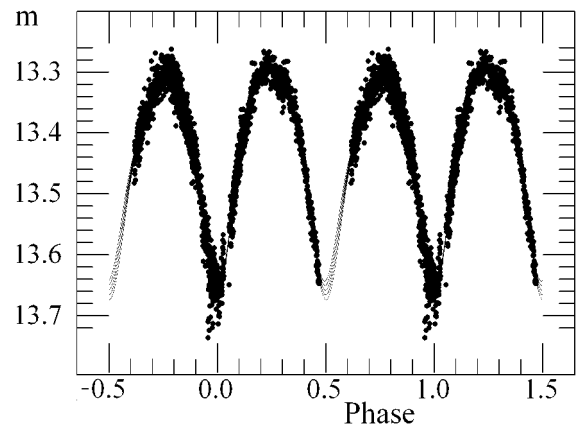


Figure 2: Phase light curve of GSC 04370-00206 and 6-th order trigonometric polynomial fit with $\pm 1\sigma$ and $\pm 2\sigma$ error corridors.

All the parameters of the running approximations significantly vary with time, indicating cycle-to-cycle instability of the shape. The phase is significantly shifted from zero, indicating that the photometric ephemeris needs an improvement. Moreover, period variations may be suggested.

During our first study of MU Cam, we have discovered a new EW-type variable GSC 04370-00206. It is studied in more detail separately in this volume by Breus et al. (2010). The phase light curve according to an improved ephemeris $Min.HJD = 2454805.7548 + 0.4426448 \cdot E$ by Breus et al. (2010) is shown in Fig. 2 along with the 6-th order polynomial fit and “ 1σ ” and “ 2σ ” corridors (Andronov 1994). There is no statistically significant shift of the primary minimum. To determine individual minima (only primary ones were covered), we have used the “asymptotic parabola fit” (Marsakova and Andronov, 1996). The timings are 2454085.57243(53) and 2454090.43569(126). The magnitude estimates 13.652(7) and 13.669(10) are the same within error estimates. The deviations from the phase zero are 0.0016(12) and $-0.0116(28)$ are negligible.

References

- Andronov I.L.: 1994, *OAP*, **7**, 49
 Andronov I.L.: 1997, *A&AS*, **125**, 207
 Andronov I.L.: 2005, *ASPC*, **334**, 447
 Andronov I.L. et al.: 2010, *OAP*, **23**, 8
 Andronov I.L., Baklanov A.V.: 2004, *Astronomy School Reports*, **5**, 264, <http://uavso.pochta.ru/mcv>
 Araujo-Betancor S. et al., 2003, *A&A*, 406, 213
 Breus V.V., Andronov I.L. et al.: 2010, *OAP*, **23**, 19
 Henden A.: 2004, <ftp.aavso.org/public/calib/j0625.dat>
 Kim Y., Andronov I.L., Park S.S., Chinarova L.L., Baklanov A.V., Jeon Y.B.: 2005, *JASS*, **22**, 197
 Marsakova V.I., Andronov I.L., 1996, *OAP*, 9, 127
 Patterson J.: 1994, *PASP*, **106**, 209
 Staude A. et al.: 2003, *A&A*, 406, 253
 Warner B.: 1995, *Cataclysmic Variable Stars*

THE ABUNDANCES OF THE ELEMENTS OF THE MAGELLANIC CLOUDS

F. A. Chekhonadskikh

Department of Astronomy, Odessa National University
T. G. Shevchenko Park, Odessa 65014 Ukraine
chehonadskikh@gmail.com

ABSTRACT. The results of the spectroscopic researches of classical Cepheids of the Magellanic Clouds (MC) are presented in this paper. 21 spectra for the Large Magellanic Cloud (LMC) and 10 for the Small Magellanic Cloud (SMC) were investigated. I obtained highly accurate values of effective temperatures (T_{eff}), of the logarithm of the surface gravity ($\log g$), of the microturbulence velocity (V_t), of abundances of elements for all of the objects. There is a good agreement with previous studies, some data were obtained for the first time.

Key words: Classical Cepheids: parameters of stellar atmosphere; Magellanic Clouds: abundances.

1. Introduction

There were the great telescopes allowing to obtain high-quality spectra of high resolution in recent years. The classical Cepheids are known as yellow supergiants which one of the brightest stars. And modern tools allow to obtain spectra of satisfactory quality for the brightest stars in nearby galaxies. The Magellanic Clouds represent for my research special interest as the most close galaxies. These facts provide an excellent opportunity to explore in detail a variety of abundances of chemical elements there.

Luck et al spent a lot of work to determine the chemical composition of the Magellanic Clouds using 22 Cepheids (Luck, 1998). Atmospheric parameters and abundances for more than 20 chemical elements were identified for all of them. The detailed study with high accuracy was carried out. They got some interesting conclusions which agreed well with data of other authors. But I want to note that previous data were fragmented, while in (Luck, 1998) is collected a good statistic based on a large number of elements. Luck got theoretically predicted content of elements of the CNO and of the iron peak, but it was also found an excess of heavy elements ($Z \geq 56$).

The new high-dispersion spectra and the results of processing are presented by Romaniello et al (2008).

They got the atmospheric parameters and metallicities for 32 Galactic Cepheids and for 36 MC Cepheids and analyzed the influence of chemical composition on the PL-relationship.

In my article I would like to present new data on the chemical composition of MC Cepheids based on high-quality spectra obtained with the help of a new generation tool.

2. Observations and measurements

The spectra of the program stars which I employed were obtained using facilities of 8.2 m VLT Unit 2 (Kueyen) equipped with echelle-spectrograph UVES (Bagnulo et al, 2003). The detector in the Red Arm is a mosaic of two CCDs (EEV + MIT/LL) with 15 micron pixels (2048 x 4096 pixels). The spectral resolution is about 25 000 and the accessible wavelength range is from 4800 to 6800 Å. The signal-to-noise ratios vary between 50 and 70 for most of the spectra. 1-D extracted spectra with primary reduction were download from electronic spectra database of ESO.

The next processing of the spectra (continuum level location, line identification, measuring of line depths and equivalent widths) was carried out using the DECH20 software (Galazutdinov, 1992). Line depths R_λ were measured by means of Gaussian fitting.

Atmospheric parameters were obtained by the agency of last achievements. Thus, effective temperatures were calculated using the original and powerful method proposed by Kovtyukh (2007). The microturbulence velocities V_t and surface gravities $\log g$ were derived using a modification of the standard analysis proposed by Kovtyukh & Andrievsky (1999). The WIDTH9 code and grids of atmospheric models (Kurucz, 1992) were used to derive the abundances of the chemical elements.

3. Conclusions.

The Table 1 shows comparison of my obtained data

Table 1: Atmospheric parameters and metallicities of Cepheids. Comparison table.

LMC								
HV	T_{eff}	$logg$	V_t	$[FeI/H]$	T_{eff}^*	$logg^*$	V_t^*	$[FeI/H]^*$
877	4831	1.0	6.0	-0.25	4690	0.5	5.4	-0.44
879	5809	1.2	5.3	-0.11	5630	1.0	3.05	-0.14
971	5943	1.9	4.0	-0.36	5930	1.4	2.3	-0.29
997	5782	1.5	6.0	-0.28	5760	1.2	3.1	-0.21
1013	4662	0.3	5.3	-0.40	4740	0.2	5.35	-0.59
1023	5909	1.5	4.5	-0.18	5830	1.1	3.1	-0.28
2260	5898	1.8	4.0	-0.06	5770	1.6	3.4	-0.38
2294	5232	0.9	5.0	-0.16	5080	0.5	3.9	-0.42
2337	5489	1.5	4.5	-0.12	5560	1.6	3.3	-0.35
2352	6300	1.8	5.5	-0.26	6100	1.6	3.65	-0.49
2369	4794	0.15	4.0	-0.11	4750	0.3	6.0	-0.62
2405	5985	1.8	5.0	-0.24	6170	2.3	4.2	-0.27
2580	5461	1.2	3.5	-0.06	5360	0.7	2.75	-0.24
2733	5473	1.6	5.0	-0.25	5470	1.8	2.9	-0.28
2793	5505	1.0	3.5	-0.07	5430	0.9	2.9	-0.1
2827	4892	0.3	4.7	-0.20	4790	0.0	4.0	-0.38
2836	5471	1.1	4.0	-0.13	5450	1.0	2.85	-0.16
2864	5799	1.6	3.7	-0.17	5830	1.5	2.8	-0.19
5497	5206	0.6	6.1	-0.29	5100	0.3	3.4	-0.25
12452	5548	1.5	4.0	-0.16	5460	1.0	2.9	-0.35
12700	5451	1.4	4.1	-0.22	5420	1.4	3.15	-0.36
SMC								
HV	T_{eff}	$logg$	V_t	$[FeI/H]$	T_{eff}^*	$logg^*$	V_t^*	$[FeI/H]^*$
817	5940	1.4	4.7	-0.61	5850	1.0	3.25	-0.82
824	5333	1.1	4.5	-0.54	5170	0.7	3.0	-0.73
829	5350	1.0	7.0	-0.62	5060	0.2	3.3	-0.76
834	6016	1.6	6.0	-0.38	5750	1.2	2.95	-0.63
837	5355	1.0	4.6	-0.55	5140	0.0	2.9	-0.83
847	4817	0.4	4.5	-0.66	4790	0.0	2.8	-0.75
1954	5974	1.6	5.2	-0.61	5890	1.0	2.47	-0.76
2064	5832	1.5	5.3	-0.39	5550	0.7	3.1	-0.64
2195	6211	1.6	6.8	-0.47	5970	1.0	2.9	-0.67
11211	5067	0.8	4.0	-0.58	4830	0.0	2.6	-0.83

* data from (Romaniello et al, 2008)

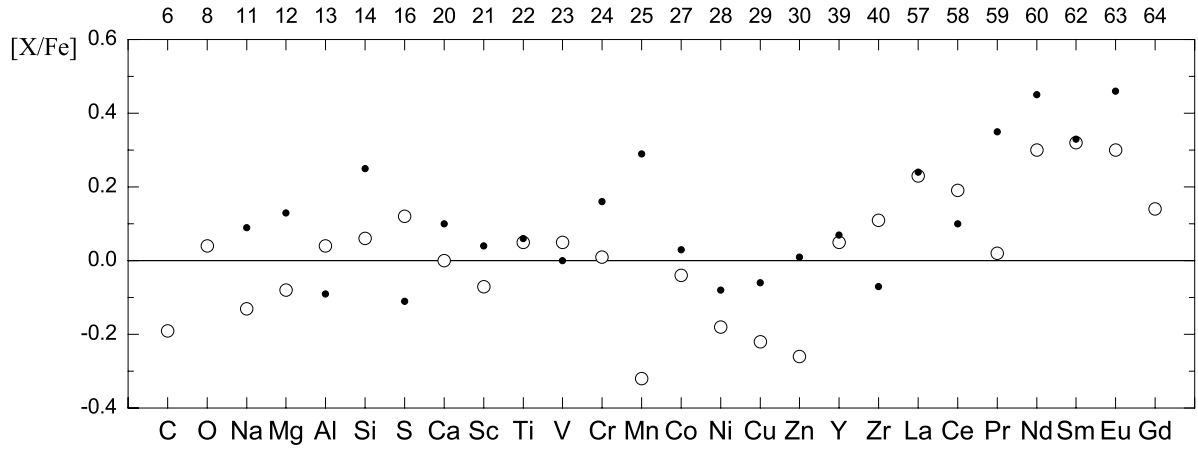


Figure 1: Abundances of the LMC. Open circles – this paper, black points – data from (Luck, 1998).

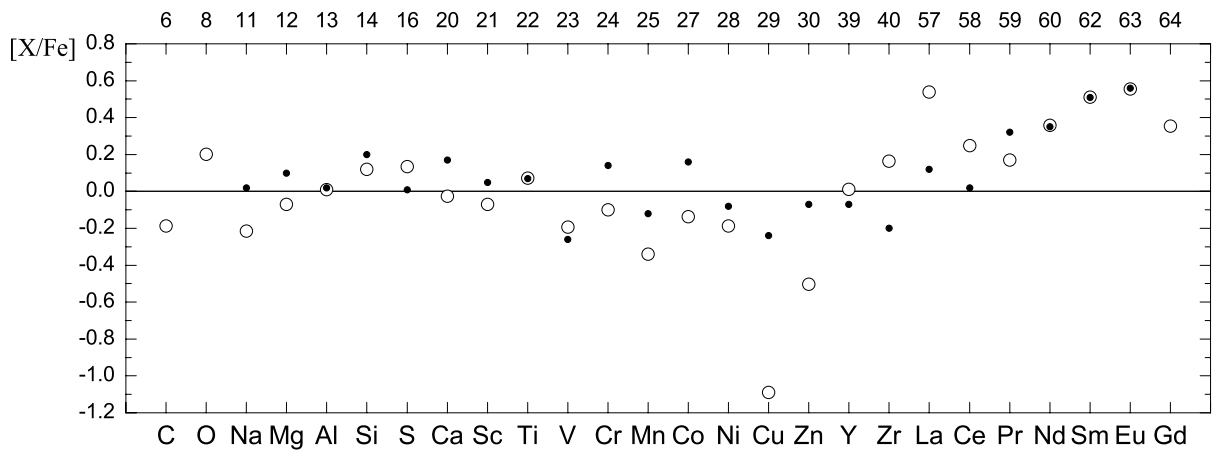


Figure 2: Abundances of the SMC. Open circles – this paper, black points – data from (Luck, 1998).

and data from (Romaniello et al, 2008). The difference in effective temperatures can be explained by the using more outdated method (Kovtyukh & Gorlova, 2000) in (Romaniello et al, 2008), whereas I used newer calibrations of Kovtyukh (2007). But you can also see a big difference in microturbulence velocities V_t and surface gravities $\log g$. It also speaks distinctions in methods: still Kovtyukh & Andrievsky (1999) noticed that if find microturbulence velocity along the $Fe I$ lines then the values to be considerably underestimated. For this reason, I used the $Fe II$ lines as suggested by Kovtyukh & Andrievsky (1999) unlike Romaniollo's research.

In Fig. 1 and Fig. 2 you can see abundances of the MC. Data are presented in comparison with (Luck, 1998) and can note that they are in good agreement. Now, if to compile all the data then I can summarize the following few points:

1. The values of $[Fe/H]$ for the LMC Cepheids vary around the mean value of -0.2 , while the SMC have higher deficiency compared with the solar value at about -0.5 . The standard error is ± 0.2 .
2. The α -elements in the SMC and LMC are not overabundant or yield values of excess within the errors of determination.
3. The heavy elements ($Z \geq 56$) and n-capture

elements are in evident excess for the LMC and the SMC which is consistent with the earlier conclusion of Luck (1998).

Acknowledgments. I would like to express one's thanks to Dr. Kovtyukh V. V. for his help and useful discussions. This work was supported by the Swiss National Science Foundation (SCOPES project No. IZ73Z0-128180/1)

References

- Bagnulo, S., Jehin, E., et al.: 2003, *ESO Messenger*, **114**, 10.
- Galazutdinov, G.A.: 1992, *Prepr. SAO RAS*, **92**.
- Kovtyukh, V.V., Andrievsky, S.M.: 1999, *As.&Ap.*, **351**, 597.
- Kovtyukh, V.V., Gorlova, N.I.: 2000, *As.&Ap.*, **351**, 597.
- Kovtyukh, V.V.: 2007, *Mon. Notic. RAS*, **378**, 617.
- Kurucz, R. L.: 1992, *IAU Symp. 149*, 225.
- Luck, R.E., et al.: 1998, *Astron. J.*, **115**, 605.
- Romaniello, M., Primas, F., et al: 2008, *As.&Ap.*, **488**, 731.

NON-STATIONARY HE-WEAK STAR HD182255?

Yu.V. Glagolevskij¹, A.V.Shavrina², G.A. Chuntunov³

¹ Special Astrophysical Observatory of Russian Academy of Sciences,
glagol@sao.ru

² Main Astronomical Observatory of National Academy of Sciences of Ukraine,
shavrina@mao.kiev.ua

³ Special Astrophysical Observatory of Russian Academy of Sciences,
chunt@sao.ru

ABSTRACT. It is known that the chemical elements distribution on the surface of chemically peculiar (CP) stars are associated with the distribution of the magnetic field. It is interest to study CP stars of various types and temperatures for the distribution of chemical elements on the surface. To this aim our research program includes HgMn star HD 182255 with no magnetic field, but with spectral and photometric variability, which is unusual in terms of the aforementioned. We suspect that the non-uniform distribution of helium and silicon on the surface of the star is due to the influence of the weak magnetic field.

Key words: Stars: He-weak: magnetic field; stars: individual: HD182255, 3 Vul

1.Introduction

So far there have no doubt that the distribution of chemical elements on the surface of CP stars associated with the distribution of the magnetic field. For example, in the atmospheres of He-rich stars He is weaker at the magnetic equator and accumulated at the magnetic poles due to the influence of solar-type wind (Vauclair, Dolez, Gough, 1991). Silicon, on the contrary, accumulates at the magnetic equator (Vauclair, Hardorp, Peterson, 1979). The calculations are supported by observational data. For example, for He-weak star HD 21699 the intensity of the helium line reaches its maximum at the magnetic poles, while the intensity of the silicon lines reaches its minimum in the same place. Silicon abundance is maximal in the regions where the magnetic field is predominantly tangential to the stellar surface (Shavrina et al. 2010). On the other hand the work of Megessier (1984) argued that the concentration of silicon at the equator is not stable. It gradually migrates along the magnetic

lines toward the magnetic pole. Depending on the age of the star the distribution of silicon changes. Young stars have a maximal excess of silicon on the magnetic equator, and the stars with the age over 10^8 years, have a mild excess at the equator and other areas. In the oldest stars the silicon excess is observed only at the poles and consist only of 5 - 10 times. In this connection it is interest to investigate chemically peculiar stars of various types and temperatures for the distribution of chemical elements on the surface. Our research program included HgMn star HD 182255 (Jashek, Egret, 1985) with no magnetic field (Hubrig et al. 2006), but with spectral and photometric variability (Catanzaro, Leone, Catalano 1999), which is unusual in terms of the above mentioned. In the paper Catanzaro, Leone, Catalano (1999) the star HD 182255 is represented as a He-weak star. In the plot of equivalent widths - T_{eff} for the He I line 5876 Å this star falls in the region occupied by stars of luminosity class III, although it has $\log g = 4.17$. Consequently, the line of helium slightly weakened, making the star to be closer to the He-weak stars, than to HgMn stars. In this case one can suspect that it has a weak magnetic field of several tens of gauss. In the papers of Lesh, 1968; Hoffleit and Jaschek, 1982, the spectral class V6III is indicated, but Palmer et al., 1968, reported B7-B8V, depending on the criteria used. All the authors show that the star belongs to the chemically peculiar objects. HD182235 is a one-lined spectroscopic binary system with an orbital period of 367 days (Hube, Aikman, 1991). This work also reported that the lines of Si II 4128, 4130, 6347 Å experience rapid fluctuations in shape and intensity during the night, which is unusual for typical CP stars. In addition, there are secular spectral changes. For example, in 1987 the line Si II 6347A have a complex structure in the center, and in

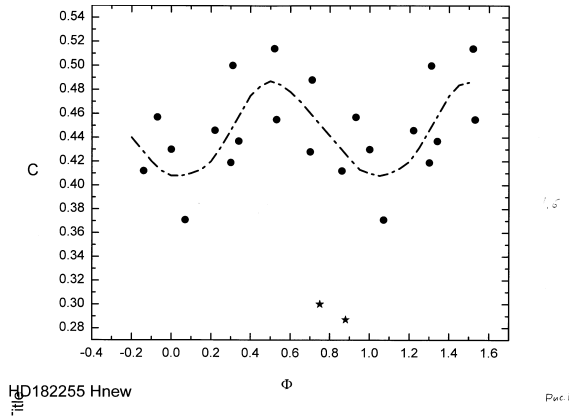


Figure 1: The points show the central intensity of the H_{δ} line in 2008-2009, and asterisks - the same in 2002-2003 (EA spectra).

1988, these lines were without distortion during three nights. The authors note that these changes are not associated with rotation and non-periodic changes in radial velocity are observed. Thus, there are signs of non-stationary processes. In the paper of Mathias, Aerts and Briquet, 2001, the evidence of the non-radial pulsations in the star's atmosphere is provided and the assumption that the star belongs to variables of 53 type is made. However it is unclear why the Si II 6347 Å line in 1988 for three nights have not been distorted by non-radial pulsations. Perhaps the pulsations sometimes disappear? It is also unclear why there are changes of the spectrum and brightness with the phase of the rotation (Catanzaro, Leone, Catalano, 1999). Our goal is the further study of helium and silicon distributions on the surface of chemically peculiar B-stars by the example of HD182235.

2. The observational data and calculations

Our spectra with resolution $R = 15000$ were obtained on Main stellar spectrograph of the 6-m telescope for the period of 68 nights, from November 2008 to January 2009. Spectral range 4000 - 4240 Å was recorded on a matrix 2Kh2K with the image slicer (Chountonov, 2003). Signal to noise ratio was 300. We also used the spectra of The ELODIE Archive (hereinafter EA), obtained in September 2002 and November 2003.

Synthetic spectra of HD 182255 were calculated by the program SYNTHV [Tsybal, 1996], version 2009. The Kurucz model atmospheres (1993) and lists of atomic lines VALD (Kupka et al. 1999) of version of 2009 were used. From the comparison of the calculated synthetic spectra with observations the averaged abundances of chemical elements were determined

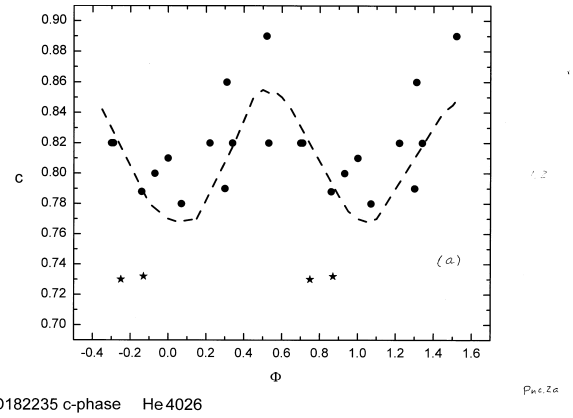


Figure 2: Central intensities of He I 4026 Å. The points show the central intensity of the H_{δ} line in 2008-2009, and asterisks - the same in 2002-2003 (EA spectra).

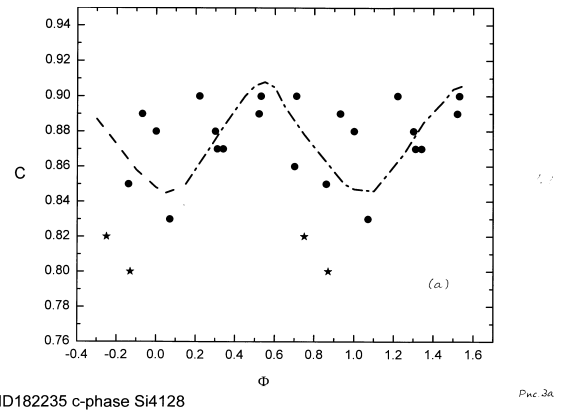


Figure 3: Central intensities of Si II 4128, 4130 Å. The points show the central intensity of the H_{δ} line in 2008-2009, and asterisks - the same in 2002-2003 (EA spectra).

at first without accounting their stratification. The stratification of helium and silicon has been studied using the sensitivity of the calculated profiles to given distribution of elements with depth in the atmosphere (the two-steps approximation was used). The wings of lines allow to determine the abundance of the element in the deep layers of the atmosphere, the central part of the lines - the abundance in the upper layers and the layer of the abundance jump.

3. Preliminary results

1) The star undergoes spectral variability linked with rotation, as well as fast variability. It follows, in particular, from Fig.1, where the points show the central intensity of the H_{δ} line in 2008-2009, and asterisks -

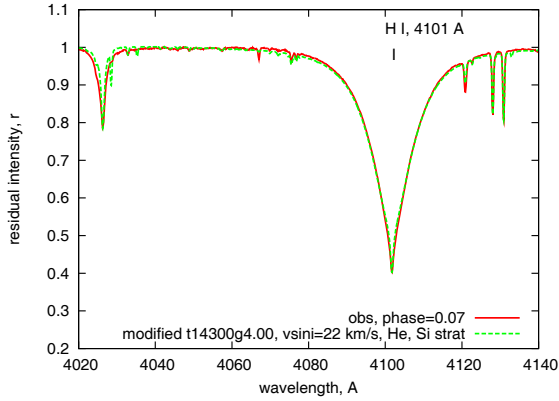


Figure 4: The fit of model profile of H_{δ} to observed one in the phase 0.07 taking into account modified T-P distribution and He, Si stratification.

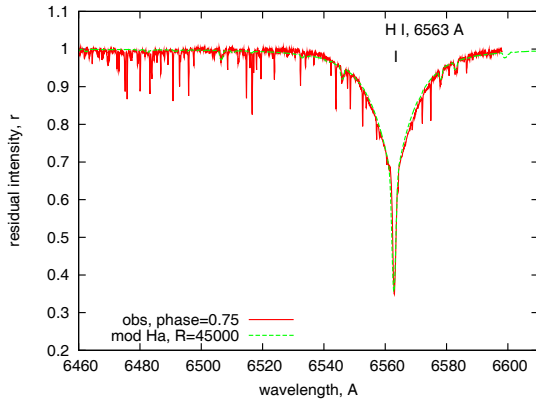


Figure 5: The fit of model H_{α} profile to observed one in the phase 0.75 (EA spectrum) taking into account modified T-P distribution.

the same in 2002-2003 (the EA spectra).

2) Central intensities of He I 4026 Å line behave similarly (Fig.2). The estimation of the He abundance shows, that together with general underabundance over the surface, it is intensified in the phase $\phi=0$. It is also means that the star belongs to the He-weak type.

3) The fact that the helium abundance is increased in the magnetic poles in the comparison with other regions can be an indication of the presence of wind on the magnetic poles.

4) Central intensities of Si II 4128, 4130 Å lines (Fig.3) behave similarly, but the silicon abundance determined with full line profiles modeling is opposite to helium one, i.e. the silicon is weakened where the helium is strengthened.

5) As silicon (theoretically Vauclair et al.1979, 1991) accumulates in the areas between the magnetic poles, where the magnetic force lines are located horizontally

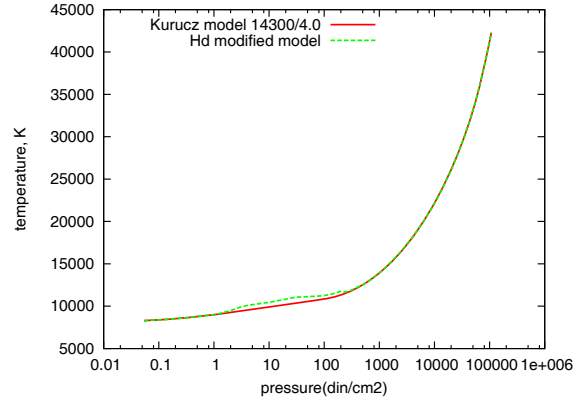


Figure 6: Dependence T-P for phase $\phi=0.07$ in 2008-2009 obtained with the H_{δ} profile.

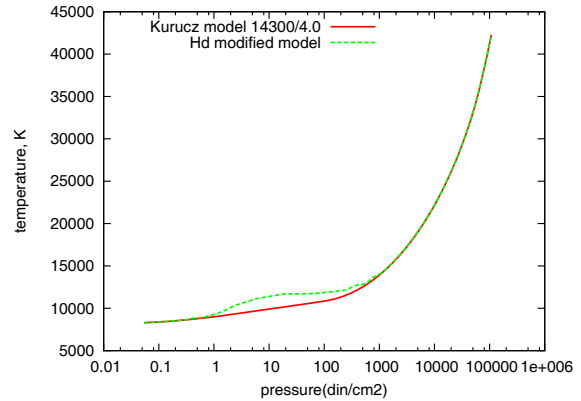


Figure 7: Dependence T-P for phase $\phi=0.53$ in 2008-2009 obtained with the H_{δ} profile.

($\phi=0.5$), it is possible to assume that the star has a magnetic field with the magnetic pole, passing through the central meridian in $\phi=0$.

6) The structure of the atmosphere changes with time. Fig.6,7 demonstrate the distribution of temperature in the atmosphere of HD 182255 in different phases of the rotation period, obtained from the profiles of hydrogen lines in 2008-2009. Fig.8 shows the same as Fig. 6,7 in 2002-2003, EA spectra. Different structures of the atmosphere at different epochs are evident.

7) A two-level stratification of helium in Fig.9 shows its general deficiency and strengthening in the phase $\phi=0.07$ near the presumable magnetic pole.

8) A two-level stratification of silicon in Fig.10 shows its general overabundance and strengthening between presumable positions of poles.

9) Basing on its parameters we can conclude that the star HD182255 is probably a young CP star, which has just arrived on the Main Sequence.

10) The results have a preliminary character.

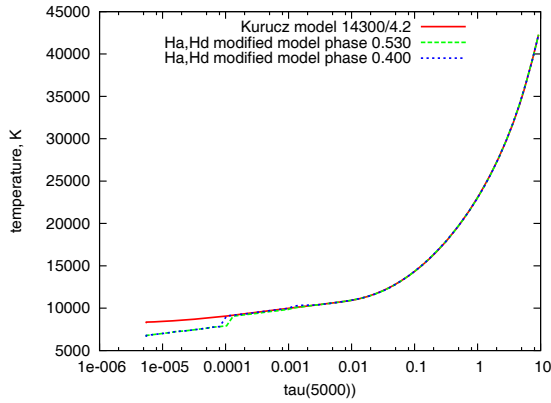


Figure 8: Dependence T-P for 2 phases of EA spectra from H_{δ} and H_{α} profile.

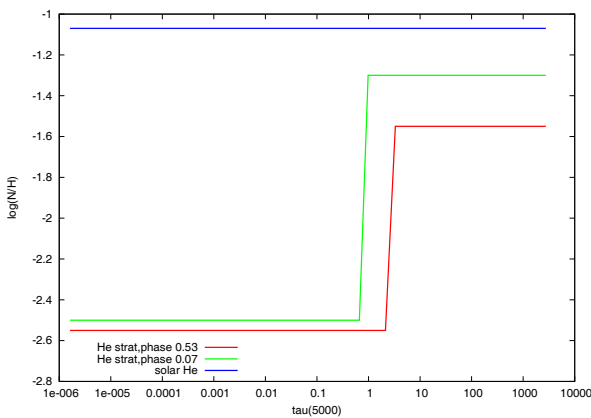


Figure 9: The He stratification, obtained with He I, 4026 Å profile in two phases $\phi = 0.07$ (dash line) 0.53 (solid line). Solar abundance of He (horizontal line) was taken from Grevesse, Asplund, Sauval, 2007).

Acknowledgements. We appreciate V. Tsymbal for the code SYNTHV. This work was partially supported by the Microcosmophysics program of National Academy of Sciences and National Space Agency of Ukraine.

References

- Catanzaro G., Leone F., Catalano F.A.: 1999, *Astron. Astrophys.*, **134**, 211
 Chountonov G.A.: 2003, in *Magnetic stars*, ed. Glagolevskij Yu.V., Kudryavtsev D.O., Nizhnij Arkhyz, p.286

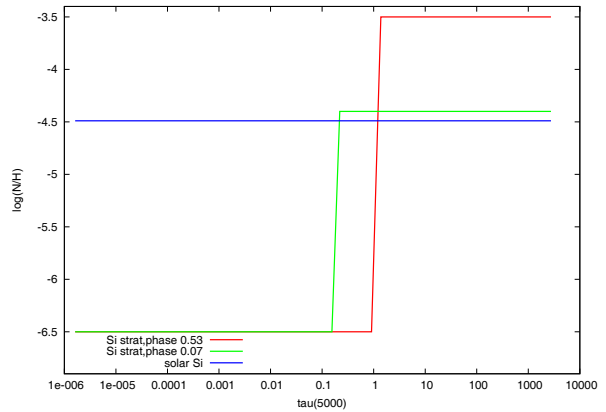


Figure 10: The Si stratification, obtained with Si II 4128, 4130 Å profiles in two phases $\phi = 0.07$ (dash line) 0.53 (solid line). Solar abundance of Si (horizontal line) was taken from Grevesse, Asplund, Sauval, 2007).

- Grevesse N., Asplund M., Sauval A.: 2007, *J. Space Science Reviews*, **130**, Issue 1-4, pp. 105
 Hoffleit D., Jaschek C.: 1982, *The Bright Star Catalogue*, (4-th ed. New Haven, Yale Univ. Observatory)
 Hube D.P., Aikman G.C.L.: 1991, *PASP*, **103**, 49
 Hubrig S., Briquet M., Scholler M. et al.: 2006, *MNRAS*, **369**, 61
 Jashek M., Egret D.: 1985, *Catalogue of stellar groups*, Liege
 Kurucz R.L., *Data Bank, CD-ROM NN 1-22* (1993-1994)
 Kupka F., Piskunov N., Ryabchikova T.A. et al.: 1999, *Astron. Astrophys.*, **138**, 119
 Lesh J.R., 1968: *Astrophys.J. Suppl.*, **17**, 371
 Mathias P., Aerts C., Briquet M. et al.: 2001, *Astron. Astrophys.*, **379**, 905
 Megessier C.: 1984, *Astron. Astrophys.*, **138**, 267
 Palmer D.R., Walker E.N., Jones et al.: 1968, *Roy. Obs.Bull.*, **135**, 385
 Shavrina A.V., Glagolevskij Yu.V., Silvester J. et al.: 2010, *MNRAS*, **401**, 1882
 Tsymbal V.: 1996, in: *Model Atmospheres and Spectrum Synthesis*, eds. S. J. Adelman, F. Kupka, W.W. Weiss, *ASP Conference Series*, **108**, 198
 Vauclair S., Hardorp J., Pederson D.M., *Astrophys. J.*, 1979, **227**, 526
 Vauclair S., Dolez N., Gough D.O.: 1991, *Astron. Astrophys.*, **252**, 618

ABILITIES OF CELESTIAL OBSERVATIONS IN ASTRONOMICAL OBSERVATORY OF PHYSICS INSTITUTE IN OPOLE

W. Godłowski, M. Szpanko

Institute of Physics, Opole University
Oleska 48 45-052 Opole Poland,
godlowski@uni.opole.pl

ABSTRACT. We present possibilities of astronomical investigation in Astronomical Observatory in Opole. Our observatory uses two telescopes: Celestron CGE-1400 XLT (35 cm) and Meade LX200 (30 cm) with spectrograph and CCD Camera. Main topic of our observational investigation is connected with observations of variable stars, minor bodies of the solar system, blazars and the Sun.

Key words: instrumentation; methods: observational;

1. Introduction

Our Observatory (named prof Teodor Kaluza) was created in the year 2006. However, because of technical problems it has been efficiently working since 2009. It is located on top of "Niechcic", the highest building in Opole ($50^{\circ}40'21''N$, $17^{\circ}56'01''E$). It is in the city centre which is mostly commercial area, free during night time. As a result the light pollution is not a big problem. Presently our Observatory is equipped with two main telescopes, Celestron CGE-1400 XLT (35 cm) and Meade LX200 (30 cm) with spectrograph and CCD Camera. Our observational investigation is focused on observations of variable stars, minor bodies of the solar system, blazars and the Sun. The aim of the paper is to show that even with small telescopes located inside the city it is possible to obtain important scientific observations.

2. Instrumentation

The Celestron CGE-1400 is optically designed Schmidt-Cassegrain telescope with aperture 356 mm (14.02 in), focal length 3910 mm (153.94 in) and focal ratio 10. Meade LX200 is also optical design Schmidt-Cassegrain telescope with aperture 305 mm (12 in) focal length 3048 mm (120 in) and focal ratio 10.98.

Our observatory is equipped with two CCD cameras. The first one is SBIG ST-7E, Kodak KAF-0401E CCD NABG (715x510, pixel 9 microns, max QE - 0.6 at 6000 Angstroms, front side illuminated, thermoelectric cooling). It is equipped with filter wheel with UBVRI and RGB filters. The field of view for LX200 telescope is (for focal ratio $f/10$) 5.3×7.9 arcmin. The second one is FLI IMG-6303E Kodak KAF-6303E CCD NABG (3088x2056, pixel 9 microns, max QE - 0.7 at 6000 Angstroms, front side illuminated, tree-stage thermoelectric cooling) with filter wheel UBVRI where field of view for LX200 telescope is (for $f/10$) 21.2×31.9 arcmin. For both cameras maximum photometry range is 14 mag. The picture from our CCD Camera is presented in the Figure 1.

We possess the spectrograph SBIG SGS with custom modification - we added two calibration lamps - Ne and Xe. The spectrograph has two gratings with 150 and 600 lines per mm and two slit 18 and 72 microns respectively. The wavelength range of the spectrograph is from 3800 to 7500 Angstroms, the dispersion is 1.07 or 4.3 Angstroms per pixel while the spectral coverage per frame is 750 or 3200 Angstroms respectively. As a result, depending on configuration, the resolution is: for slit 18 and grating 150 - 2.4 Angstroms per pixel, for slit 18 and grating 600 - 10 Angstroms per pixel, for slit 72 and grating 150 - 10 Angstroms per pixel and for slit 72 and grating 600 - 38 Angstroms per pixel.

We have also used two smaller telescopes: Schmidt-Cassegrain Celestron NexStar 8i with aperture 203mm and focal length 2032mm and Carl Zeiss Jena Meniscas Telescope with aperture 180 and focal length 1800. We also have 40 millimetre Sun Telescope Coronado PST (H-alpha) with focal ratio 10.

3. Observations in Astronomical Observatory in Opole.

Observations in our Astronomical Observatory of Physics Institute in Opole University is focused on a

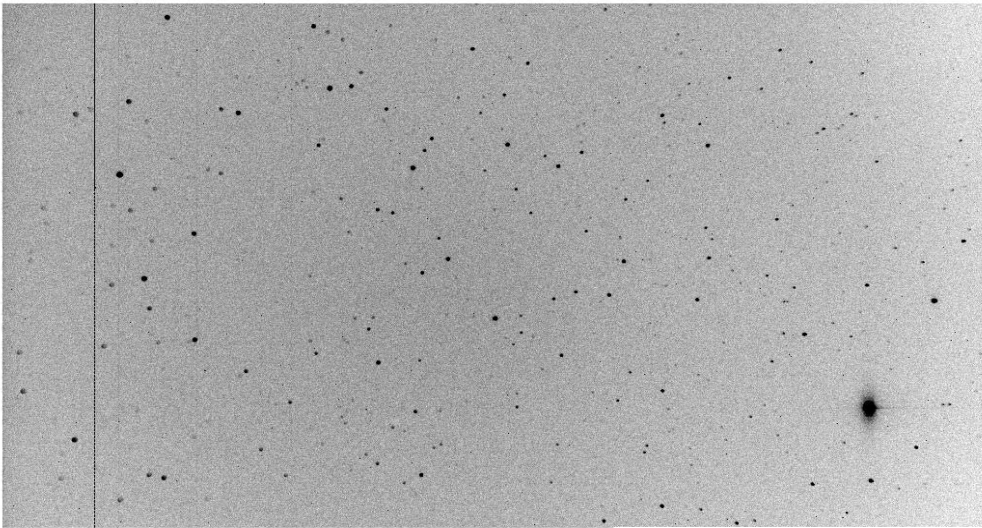


Figure 1: The picture TZ Bootis from CCD Camera in Opole.

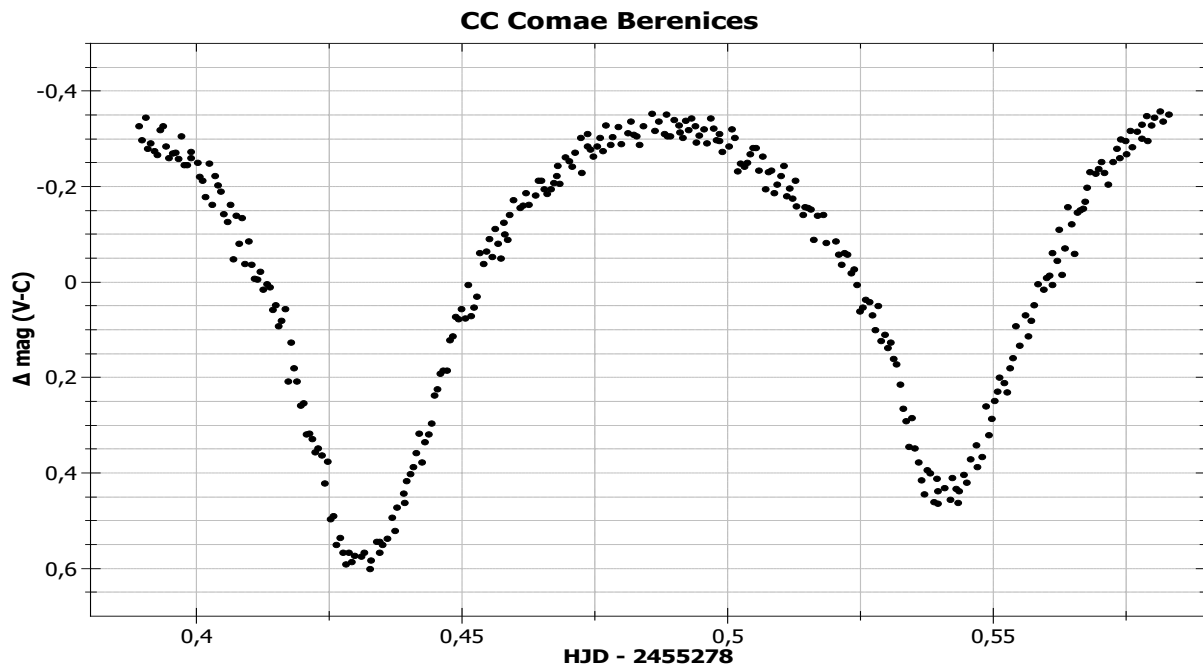


Figure 2: Light curve for CC Comae Berenices from Observations in Opole.

Table 1: Theoretical and observed efemerydes for Messalia 20.

Messalia data	NASA Efemerydes		Observed	
	α	δ	α	δ
05.11.2009; 20:44:44	23h 37m 23,68s	$-02^{\circ}10'33,0''$	23h 37m 23,61s	$-02^{\circ}10'32,4''$
20.11.2009; 20:53:33	23h 38m 50,12s	$-02^{\circ}07'03,2''$	23h 38m 50,06s	$-02^{\circ}07'02,2''$
07.12.2009; 19:22:27	23h 47m 42,94s	$-01^{\circ}15'10,8''$	23h 47m 42,98s	$-01^{\circ}15'11,0''$

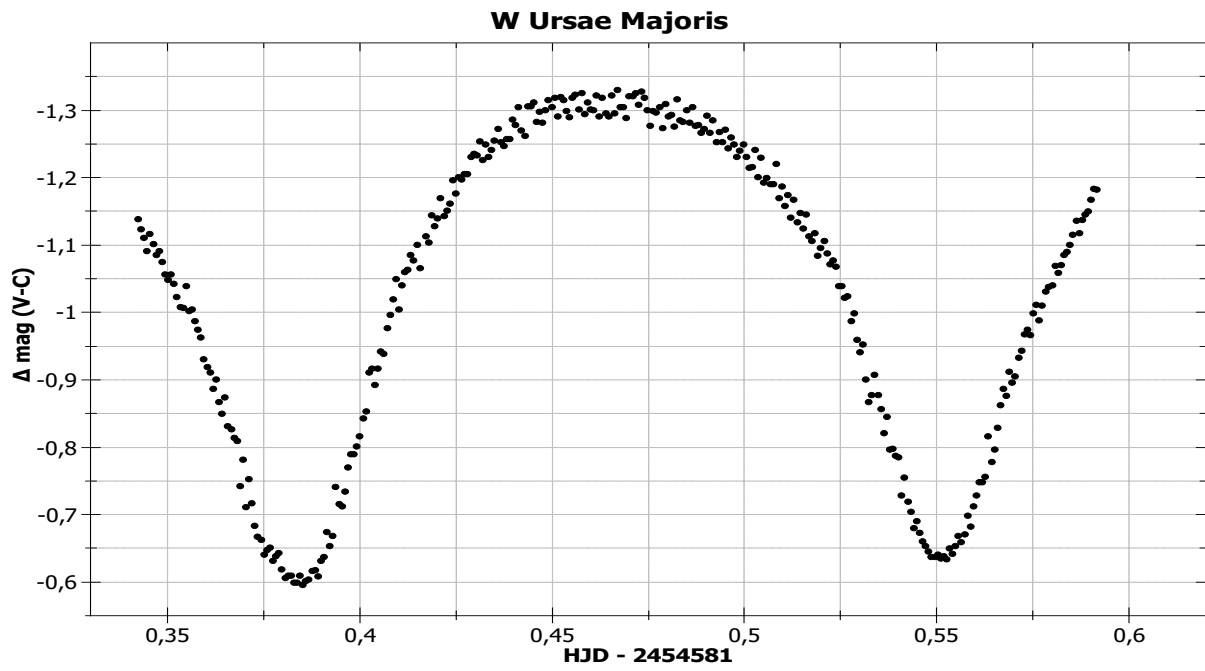


Figure 3: Light curve for W Ursea Majoris from observations in Opole.

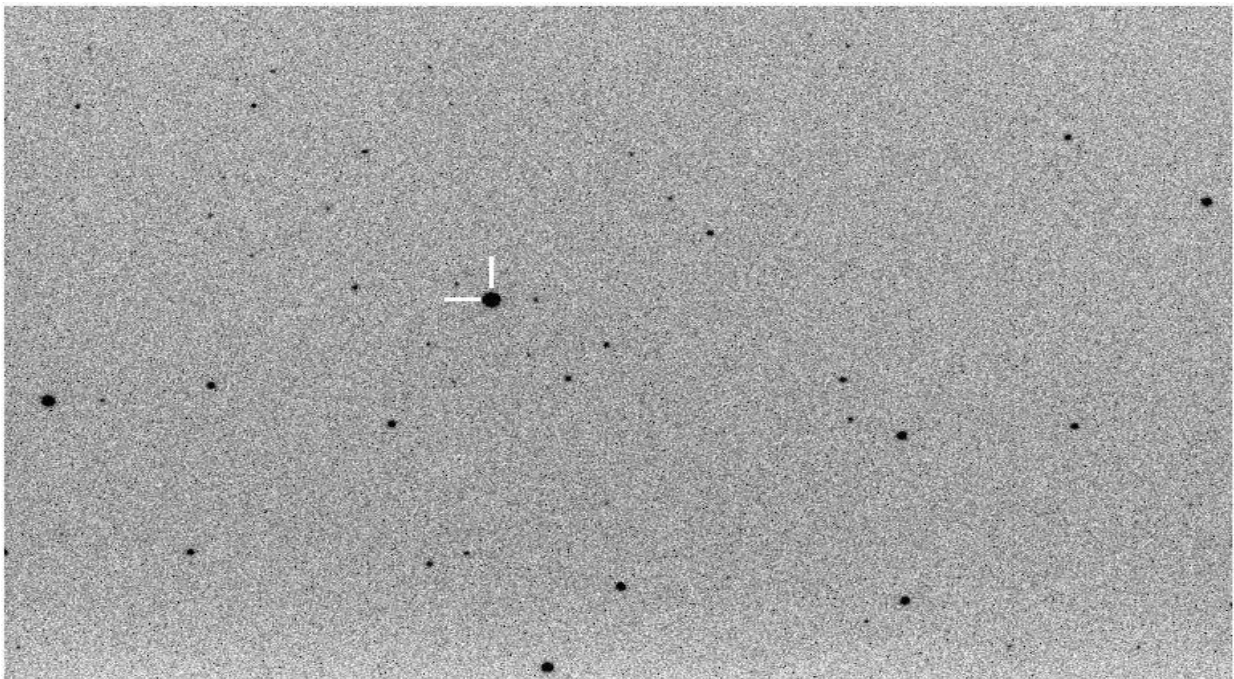


Figure 4: The picture Melpomena 18 from CCD SBIG ST-7E Camera in Opole.

Table 2: Differences between efemerydes and observed position Messalia 20 (in arcsec)

Messalia	α			δ		
data	α^*	$\Delta\alpha$	$\sigma = \alpha^*/\Delta\alpha $	δ^*	$\Delta\delta$	$\sigma = \delta^*/\Delta\delta $
05.11.2009; 20:44:44	1,049"	1,188"	0,883	0,600"	1,432"	0,419
20.11.2009; 20:53:33	0,889"	0,947"	0,950	1,000"	0,775"	1,290
07.12.2009; 19:22:27	0,600"	4,980"	0,120	0,200"	2,068"	0,097

few topics, namely: variable stars, small bodies of the Solar System, Blazars Observations and observations of the Sun.

First observational program started in the year 2006 was observations of the variable stars. Due to observational condition - inside the city, very few night with very good weather for us the best object for observations are variables type WUma or long terms variables. In the figures 2 and 3 we present light curves obtained in our observatory for two variables W Ursae Majoris and CC Coma Berenices. One should not that presently we start also program of the observation cataclismic variables.

Another type of our activity is observing small bodies of the Solar System. Such programs are very interesting not only because of pure science but also in connection with the program of preventing Earth from cosmic impacts. It is comonly accepted that astreoid or comet kill dinosaurs 65 milion years ago. Such huge impact is unlikely but even astreoid that has only 100 meter diameter can cause significant damage on the Earth. During last year we observed three planetoids: Juno (3), Melpomene(18) and Messalia (20). The picture of Melpomene (18) obtained in November 2009 in our observatory is presented in the Figure 4. The results of observation from November and December 2009 for Messalia (20) is presented in the Tables 1 and 2. Unfortunately, during the whole autumn and winter 2009/2010 we did not have good weather in Opole. We present theoretical NASA efemerydes and observed positions of Messalia (20) as well as differences between theoretical and observed positions of this small celestial body. One can observe that differences both in right ascension and declination: $\alpha^* = \cos\delta|\alpha_{the} - \alpha_{obs}|$ and $\delta^* = |\delta_{the} - \delta_{obs}|$ not exceeding $1arcsec$, which is a criterion of well done observation. One can observe that even for in the case not very well weather it was possible to obtain reasonable observations.

Since present year we have started the observations of blasars. Presently, because of observational conditions, our observational program is connected with blazars OJ287, 3C273 and 3C279.

Another important subject of our scientific work are observations of the Sun. The Sun is interesting not only because it allows life on the Earth, but also have influence on our present life. Even with our small Coronado telescope it is possible to investigate the Sun activities.

One of important aspects of the Solar influence is the Space Weather. A solar wind stream is buffeting Earth's magnetic field, and this could cause geomagnetic activity at high latitudes. The one-hour blast does not produce a bright flash of electromagnetic radiation nor a substantial coronal mass ejection. However, huge halo coronal mass ejections are likely to be geoeffective. The strength of geomagnetic storms is highly correlated with source location and space velocity of a given event (Michalek et al. 2006). Activities of the Sun is also important for both, present Earth climate (Friis-Christensen 1991, Abdussamatov 2005, Wilson 2008) and for the Earth climate in the past i.e. for Climate Optimum in X century and Maunder's Minimum XVII century (Mangini 2005).

4. Conclusions.

With the abilities of Astronomical Observatory Institute of Physics Opole University we are able to participate in scientific programs connected with observations of variable stars, minor bodies of Solar System, blazars and investigations of Solar activities. Even small telescopes give possibilities to obtain important scientific results!

References

- Abdussamatov H.I.: 2005 *Kinematyka i Fizika Niebiesnych Tel* **21**, 471.
- Friis-Christensen E., Lassen K.:1991, *Science*,**254**,698.
- Mangini A., Spotl C., Verdes P: 2005, *Earth and Planetary Science Letters* **235**, 741
- Michalek G., Gopalswamy N., Lara A., Yashiro S.: 2006, *Space Weather* **4**, 10003
- Wilson I.R.G., Carter B.D., Waite I.A.: 2008, *Publications of the Astronomical Society of Australia*, **25**, 85.

SOME STATISTICAL PICTURE OF MAGNETIC CP STARS EVOLUTION

V.F. Gopka¹, O.M. Ulyanov², S.M. Andrievsky¹, A.V. Shavrina³, V.A. Yushchenko¹

¹ Department of Astronomy, Odessa National University
T.G.Shevchenko Park, Odessa, 65014, Ukraine, *gopka.vera@mail.ru*

² Institute of Radio Astronomy of NASU,
Chervonoprapona str. 4, Kharkov, 61002, Ukraine

³Main Astronomical Observatory of NASU,
Zabolotnogo str. 27, Kyiv, 03680, Ukraine

ABSTRACT. We discuss some statistical results on the evolution of magnetic CP stars in the framework of the supposition about their binary nature.

Key words: star, magnetic chemically peculiar stars, evolution, binary stars, neutron star.

1. Introduction

It is well known that CP stars of upper main sequence can be divided on magnetic chemically peculiar stars (MCP stars or Bp-Ap stars) and non-magnetic (Hg-Mn stars and Am-Fm stars). Hg-Mn stars have temperatures more than 10 000 K, Am-Fm stars are cooler than 10 000 K. Some authors concluded that there exists a relationship between Hg-Mn stars and Am-Fm star (Adelman, Adelman & Pintado, 2003).

MCP stars are overlapped with Hg-Mn stars in the region of the hot temperatures of HR diagram and with Am-Fm stars in the region of the cooler temperatures. Evolutionary state of chemically peculiar (CP) stars of upper main sequence is the subject of some working hypotheses and numerous debates. The new observational facts on these stars cause more and more questions. Some reviews of specialists include the list of unsolved problems concerning this topic. Thus, it should be stated that origin of CP stars is not completely understood at present.

The MCP stars show more complicated phenomena among CP stars (Rudiger & Scholz, 1988). Now we do not have a hypothesis that could be able to explain an origin of anomalies of their chemical abundances and their kinematics, as well as an origin of their magnetic field. Some characteristics of MCP stars show that they do not support old ideas about chemical evolution. Some existing inexplicable facts (Gopka et al., 2004, Gopka et al., 2006) force us to suppose that MCP stars are the binary systems consisting of the two intermediate-mass stars experienced mass

transfer between the originally less massive star and its more massive companion in the state of the pre-supernova explosion with mass near to $8M_{\odot}$. As a result, the present day MCP star was permanently influenced by the supernova remnant (neutron star, NS) and some its properties were formed under this influence (Gopka, Ulyanov & Andrievsky, 2008a,b). Such a model is supported by the results of the numerous investigations of MCP stars from IR to X-rays observations. The evolutionary change of the MCP star properties with mass reflects the change of the system's mass ratio (both for visible and invisible neutron star companion, Gopka, Ulyanov, Yushchenko et al., 2010).

2. On the increasing of rotational period of the low-mass MCP stars in the framework of model MCP star binarity

For some MCP stars an intensive mass-loss from magnetic poles is known. As an example, for the helium-strong stars σ Ori E and HD 37017 Drake et al. (1994) estimated mass-loss rate is near $10^{-9} M_{\odot}$ per year with observed significant outflow velocity of about 600 km s^{-1} . Such a phenomenon can be easily understood in our phenomenological model of MCP stars (see Fig. 1). Important consequence of this conclusion is supported by statistical results of an increasing of the rotational period for low-mass MCP stars.

Fedorova (1997) investigated the qualitative changes of the low-mass X-ray binary evolution. When the matter is accreted by the low-mass star, the hard radiation occurs.

Fedorova obtained the theoretical dependence of the semimajor axis size upon the companion masses supposing that all accreted matter is lost by the X-ray binary. Fig. 1 schematically shows how this process works in binary system where one companion is NS.

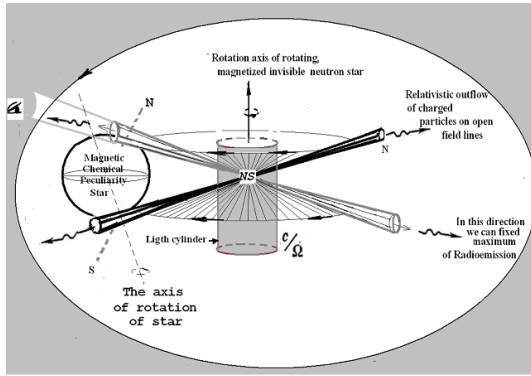


Figure 1: Schematic model of MCP star as a binary system with neutron star companion.

Some part of the matter of MCP star falls onto NS, while some part is removed away from the system due to magnetic stellar wind. This scenario is in the base of our assumption that MCP star is a donor and NS is an acceptor.

When so-called Jeans mode conditions are realized in the binary system, the change of the system semimajor axis (A_m) due to the mass-loss is given by the follow equation:

$$\left(\frac{dA_m}{dt}\right)_{los} = \frac{-A_m}{(M_{star} + M_{ns})} \cdot \left(\frac{dM_{star}}{dt}\right)_{los}, \quad (1)$$

where A_m is the semimajor axis, M_{star} is the mass of the MCP star, M_{ns} is the NS mass.

Integration of this equation produces so-called Jeans invariant:

$$A_m \cdot (M_{star} + M_{ns}) = const. \quad (2)$$

We simulated the dependence of the semimajor axis size upon the mass of MCP star in an interval from $8M_\odot$ to $1.6M_\odot$. We found that semimajor axis of the binary system increases if MCP component has the mass in the range $1.6M_\odot - 8M_\odot$ and NS component has the mass near to $1.35M_\odot$. The semimajor axis of the close binary system increases more rapidly for the MCP stars in combination with lower mass NS (Fig. 2). This qualitatively confirms the statistical dependence obtained by Kochukhov & Bagnulo (2006). According to these authors rotation braking (an increase of the rotational period) takes place within the range of small masses of the star which is companion of NS.

We also used observation data from ATNF pulsar catalogue (atnf.csiro.au). Among 1879 pulsars that are present in the ATNF pulsar catalogue only 141 PSRs are the binary system components. As a rule their non-relativistic star-companions are the low mass objects. Only 18 system show the star-companion masses in the

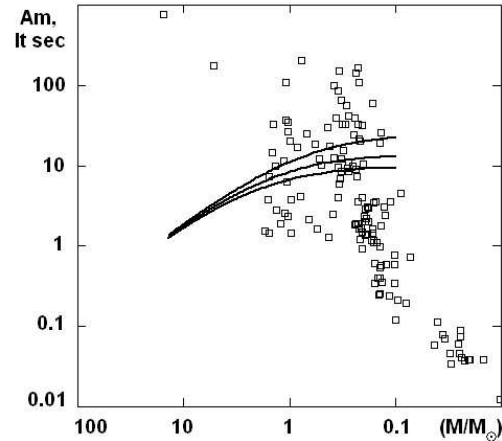


Figure 2: Distribution of the semimajor axis of the binary system (A_m) depending on the median mass of the star-companion. Solid lines illustrate qualitative behavior under the Jeans mode conditions corresponding to $0.8M_\odot$, $1.4M_\odot$, $2.0M_\odot$ of NS mass (from the top to bottom respectively).

range $8M_\odot$ to $1.6M_\odot$ (that is appropriate for MCP star masses).

For the low-mass star-companion, when $M_{star} \ll M_{NS}$, the semimajor axis of the system does not increase even in the case of a strong stellar wind from the donor (Fig. 2).

We give the orbital period distribution as a function of the mass of the non-relativistic star-companion in Fig.3.

One can assume that for the binary systems in the range of star masses from $0.3M_\odot$ to $2M_\odot$ an increase of the orbital period can occur (Fig. 3.). Unfortunately, in the ATNF catalogue there is some deficiency of the pulsar companions in the mass range from $2M_\odot$ up to $8M_\odot$ (it is MCP mass range), and this prevents complete statistical analysis.

Fig. 3 shows that the behavior with the Jeans mode condition corresponds to another range of masses of the star-companion: $M_{star} \in [0.3M_\odot, 2.0M_\odot]$.

3. Conclusion

We have adopted the model of MCP stars as a close binary system with undetected NS as one of the components. This model explains many properties of MCP stars, in particular: secular decrease of the semimajor axis of the binary systems, statistical distribution of the MCP star orbital periods as a function on their masses, and some other properties.

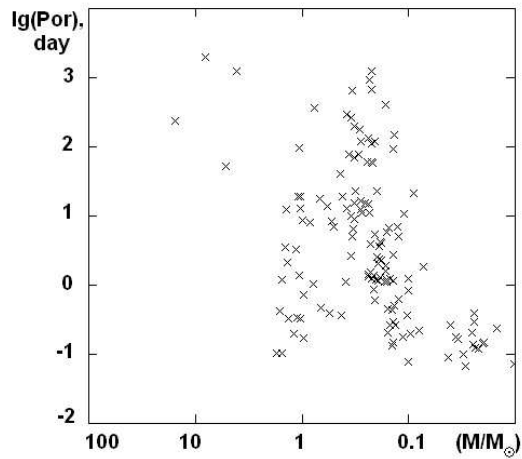


Figure 3: Distribution of the orbital periods (P_{or}) as a function of the star-companion median mass (M/M_{\odot}).

References

Adelman S.J., Adelman A.S., Pintado O.J.: 2003,

A&A, **337**, 2267.

Drake S.A., Lynsky J.L., Bookbinder J.A.: 1994, *Ap.J*, **108**, 2203.

Fedorova A.V.: 1997, *Binary systems*, Moskow, 179.

Gopka V., Yushchenko A, Shavrina A., et al. : 2004, *AIP Conf. Proc.*, **224**, 119.

Gopka V., Yushchenko A, Goriely S., et al. : 2006, *AIP Conf. Proc.*, **843**, 389.

Gopka V.F., Ulyanov O.M., Andrievsky S.M. : 2008, *AIP Conf. Proc.*, **1016**, 460.

Gopka V.F., Ulyanov O.M., Andrievsky S.M. : 2008, *KFNT*, **24**, 50.

Gopka V.F., Yushchenko A.V., Yushchenko V.A., et al. : 2008, *KFNT*, **24**, 43.

Gopka V.F., Ulyanov O.M., Yushchenko A.V., et al. : 2010, *AIP Conf. Proc.*, **1269**, 454.

Kochukhov O., Bagnulo S. : 2006, *A&A*, **450**, 763.

Rudiger G. and Scholz G. : 1988, *Astron. Nachr.*, **309**, 181.

<http://www.atnf.csiro.au/research/pulsar/psrcat/>

EU ABUNDANCES IN ACTIVE AND NON-ACTIVE STARS

T.I. Gorbaneva, T.V. Mishenina,

Astronomical Observatory, Odessa National University
T.G.Shevchenko Park, Odessa 65014 Ukraine, *clumpstars@rambler.ru*

ABSTRACT. Eu abundances have been determined for stars observed at high resolution, high signal to noise ratio with the ELODIE spectrograph at the 1.93-m telescope of the Observatoire de Haute Provence (France). Among them more than 30 stars are active stars with a fraction of BY Dra and RS CVn type stars for which spectral peculiarities were investigated. For all stars fundamental parameters were determined earlier. We find the mean abundances of the majority of elements in active and non-active stars. Active and non active cool dwarfs show similar dependencies of elemental ratios vs $[\text{Fe}/\text{H}]$.

Key words: Stars: fundamental parameters; stars: Eu abundances.

1. Introduction

Studying of the 75 stars of the lower part of the Main Sequence it was found about 30 active stars (BY Dra type) and the difference in Li abundance for active and non active stars (Mishenina et al.2008). We continue the chemical abundance investigation of these stars and have turned our attention to the elements of neutron capture. The aim of this paper is to provide Eu abundances with a high accuracy for a large sample of cool main sequence stars. We present the abundance determination of Eu and the analysis of abundance trends.

2. Observations and stellar parameters.

The spectra of stars were obtained in the region of the lambda 4400-6800 Å and with S/N about 100-350 using the 1.93 m telescope at the Observatoire de Haute-Provence (OHP, France) equipped with the echelle-spectrograph ELODIE (Barrane et al., 1996), resolving power is $R = 42000$. The spectral processing carried out by (Katz et al., 1998; Galazutdinov, 1992).

3. Atmospheric parameters and abundance determination.

For all stars fundamental parameters were determined earlier (Mishenina et al. 2008) Effective

temperatures T_{eff} were estimated by the line depth ratio method (Kovtyukh et al. 2003). Surface gravities $\lg g$ were determined by two methods: parallaxes and ionization balance of iron. Determination of the Eu abundance was made by STARSP LTE spectral synthesis code (Tsymbal, 1996) from the EuII subordinate line 6645 Å with taken into account the hyperfine structure. Recent NLTE calculation for EuII have been carried out by Mashonkina et al., (2000). For Eu 6645 Å the correction NLTE ranges from 0.04 dex to 0.06 dex. The example of comparison of synthetic and observed spectra for Eu line is shown in Fig.1 Three synthetic spectra with different Eu abundances, in steps of 0.05 dex have been plotted for each line.

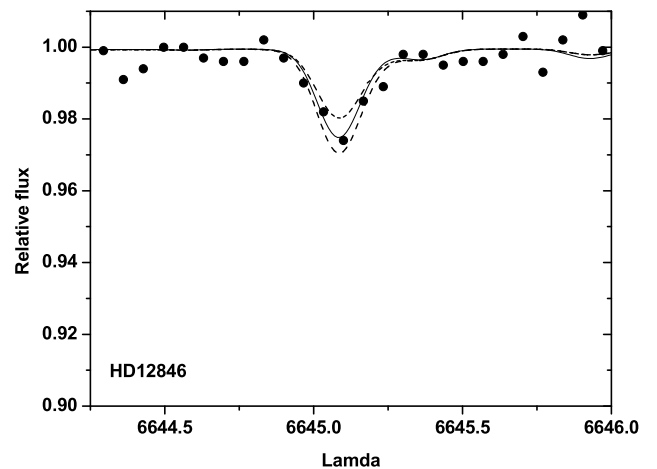


Figure 1: Synthetic LTE (continuous line) flux profiles of the Eu II line compared with the observed spectrum (bold dots).

4. Results and conclusions

Comparison of the behavior of Eu abundance in active (black circles) and non active (red circles) stars captures in the region of metallicities from $[\text{Fe}/\text{H}] = -0.7$ to $[\text{Fe}/\text{H}] = +0.4$ was presented in Fig. 2. The abundance of europium show appreciable trend with $[\text{Fe}/\text{H}]$ (the increase of the relative abundance $[\text{Eu}/\text{Fe}]$ at the low metallicity). We observe in our sample of stars the trend of $[\text{Eu}/\text{Fe}]$ vs. $[\text{Fe}/\text{H}]$ similar to the

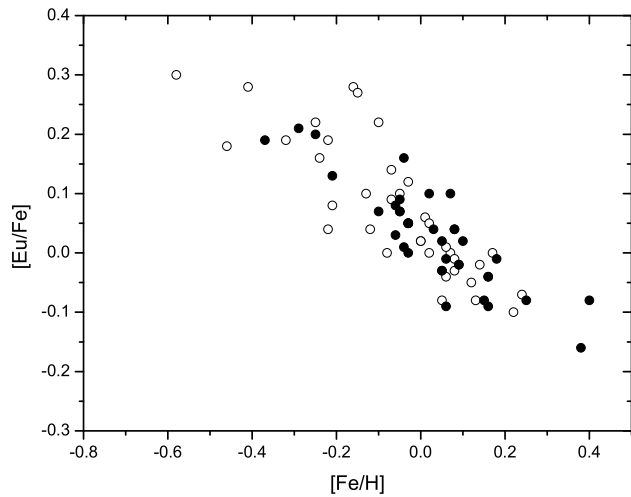


Figure 2: The run of $[Eu/Fe]$ with $[Fe/H]$. Active stars are marked as filled circles, and non active stars as open circles

those for stars studied in our early works and works of other authors. As can see from the figure active and

non active cool dwarfs show similar dependencies of elemental ratios vs $[Fe/H]$. The mean values of $[Eu/Fe]$ for non active stars is 0.06 ± 0.1 and for active stars is 0.03 ± 0.09 .

Acknowledgements. This work was supported by the Swiss National Science Foundation (SCOPES project No. IZ73Z0-128180/1)

References

- Baranne A., Queloz D., Mayor M. et al.: 1996, *A&A*, **119**, 373.
 Galazutdinov G.A.: 1992, *Prepr.SAORAS*, **92**, 28.
 Katz D., Soubiran C., Cayrel R., et al.: 1998, *A&A*, **338**, 151.
 Kovtyukh V.V., Soubiran C., Belik S.I., Gorlova N.I.: 2003, *A&A*, **411**, 559.
 Kurucz R.L.: 1993, CD ROM n13.
 Mishenina, T.V., Soubiran, C., et al.: 2008, *A&A*, **489**, 923.
 Mashonkina, L., Gehren, T.: 2000, *A&A*, **364**, 249.

ULTRAVIOLET SPECTRUM VARIABILITY OF BP TAU

N.Z. Ismailov^{1,2}, F.N. Alimardanova², G.R. Baheddinova², H.N. Adygezalade¹

¹ Baku State University

Z.Khalilov 23, Baku AZ1148 Azerbaijan, *ismailovn@yahoo.com*

² Shamakha Astrophysical Observatory NAS of Azerbaijan

Y.Mamedaliyev v., Shamakha, Azerbaijan

ABSTRACT. Results of the ultraviolet IUE archive spectrum researches of classic T Tauri type star BP Tau had been presented. Spectroscopic parameters of mainly strong emission lines were measured. On the more full massive which had been created on the intensity values of the emission doublet Mg II $\lambda 2800 \text{ \AA}$ a variability with period $P = 8.275 \pm 0.005$ days with high confidence level was obtained. There is some group of lines, intensities of emission lines for which were showed decreasing for more than 13 years of time interval. As a rule, lines with high potential of excitation related to the first group. More probable, such lines shows periodic variability. It is showed that we have as a minimum two local physical conditions of matter in the circumstellar disk of the star.

Key words: Pre-Main Sequence Stars: UV spectrum: variability; individual: BP Tau.

1. Introduction

Studying of the UV spectra of classical T Tauri stars (TTS) represents significant interest for understanding the physical nature of young stars. Mainly it is connected with following factors: for TTS in this wavelength range of spectrum the excess of radiation in a continuum is observed; besides emission lines of extremely high temperature excitation (He II, C IV, Si IV, O I, etc.) are observed. Researches of these features of the individual TTS can be a key to understanding of mechanisms of activity of young stars.

BP Tau is one of classical Tauri type stars (CTTS) with spectral class K7V (Herbig, Bell, 1988). According to photometric *UBVRI* data's a radiation of the star can be explained with a hot spot model with temperature $8200^\circ K$, covering 0.36% of a surface of the star (Vrba et al., 1986). Simon et al. (1990) showed that a variation in the UV continuum radiation and magnitudes of the star in *UBVRI* bands shows some correlation. 14-day's monitoring executed by Gomez de Castro and Franqueira (1997) has shown that intensities of spectral lines O I, Si II, Mg II and UV light radiation in the band $\lambda 2900 \text{ \AA}$ have varied syn-

chronously. On the received from the Hubble Space Telescope archive structures of resonant lines Mg II $\lambda 2800 \text{ \AA}$ was investigated. In this work is showed that an absorption component was displaced in a red part of the spectrum.

On the analysis data optical light of BP Tau periods of variability 6.1, 7.6, and 8.3 days Simon et al.(1990), Gomez de Castro and Franqueira (1997) and Gullbring et al (1996) had been obtained. Values of these periods founded by different authors were not coordinated among themselves. Those are inconsistent results in interpretation of the activity mechanism and nature of the emission spectrum of the star. For detailed research and the statistical analysis of physical characteristics of CTTS it is necessary to receive a plenty a homogeneous spectral material. From this point of view final archive IUE is a unique source for research of such objects (Valenty et al. 2000, Johns-Crull et al. 2000, Valenty et al. 2003). The objectives of the present work are researches of UV spectrum of BP Tau on the spectral material, obtained from the IUE archive data.

2. Observations and results

The UV spectrum of the star has been investigated on the spectrograms taken from IUE archive data. It has been used only 15 SWP and 62 LWP type spectrograms. Spectral resolution is at 6 \AA . For avoiding the account of interstellar reddening in spectral lines, and also additional mistakes because of heterogeneity of the received spectrograms we applied a classical method of processing of spectrograms in which measurement is made in relative units: after carrying out of a level of the spectral continuum the central depths (residual - intensity) $R_\lambda = 1 - I/I_0$ and half widths ($\Delta\lambda_{1/2}$ - FWHM) of lines were determined. Where, I - an absolute intensity at top of the line, I_0 - an absolute intensity of line at the level of continuum. In such measurements the mainly error in intensity of the line arises because of wrong carrying out of a level of the spectral continuum. Therefore, we carried out pro-

cedure of setting of the spectral continuum level very carefully, achieving a constancy of carrying out of a continuum through stable points of the spectrum. Mean deviations are in intensity measurements at 5 %, and in half widths at 15-20 %.

For measured spectral parameters variations from day to day and during 5-6 years characteristic time have discovered. For example in Fig.1 time variability diagrams for parameters R_λ and $\Delta\lambda_{1/2}$ have presented. Full time of observation is equal nearly 13 years (1979 – 1992).

The most continuous daily long IUE observations on the star have been carried out in two series: 1) JD 2446705 – 2446730, duration about 25 days and 2) JD 2448627 – 2448641, duration about 14 days. Most numerous measurements in this interval have been carried out for a doublet Mg II $\lambda\lambda 2795, 2802 \text{ \AA}$, (further, Mg II $\lambda 2800 \text{ \AA}$) which in spectrograms are observed as one composed emission. These data allow to search of cyclic changes in the spectral parameters in an interval about 6 – 8 day.

In the Fig. 2a and 2b we show a time variability of intensity R_λ for doublet Mg II $\lambda 2800 \text{ \AA}$ for the above-mentioned two different time intervals. As it is visible from Fig.2, a change of the line intensity has a cyclic character with characteristic time 7 – 8 days.

We have analyzed time dependence for intensities of different emission spectral lines. We have found that on the character of time variability, lines are divided to 2 groups: 1) group of lines, which show monotonous decreasing during all IUE observation (for more than 10 years), 2) lines which do not show the some certain law in change of the parameter R_λ .

In fig.3 for example we presented time variability of the R_λ and FWHM for spectral lines SiIV $\lambda 1403 \text{ \AA}$, [Si III] $\lambda 1893 \text{ \AA}$ which concern to first of the named groups of emission lines. Apparently, FWHM of lines have not shown the certain dependence on time for these lines. It testifies that besides quick changes, there is also a long-time variability in emission spectrum of BP Tau.

For lines Mg II $\lambda 2800 \text{ \AA}$ nightly parameters R_λ were used for the period search, resulting in a set containing 62 points spread over 13 year interval of the observation. We use the Scargle (1982) periodogram method as recommended by Horne and Balinas (1986) to search for periods. The greatest peak in a power spectrum is observed at frequency $\nu = 0.1208 \pm 0.0005 \text{ d}^{-1}$, that corresponds to the period $8.275 \pm 0.005 \text{ day}$. The variability level of this peak is over 90 %.

In Fig.4 phase diagrams for period 8.275 days for lines Mg II $\lambda 2800 \text{ \AA}$ and SiIV $\lambda 1403 \text{ \AA}$ lines have presented. There is certain group of lines for which a periodicity does not obtain.

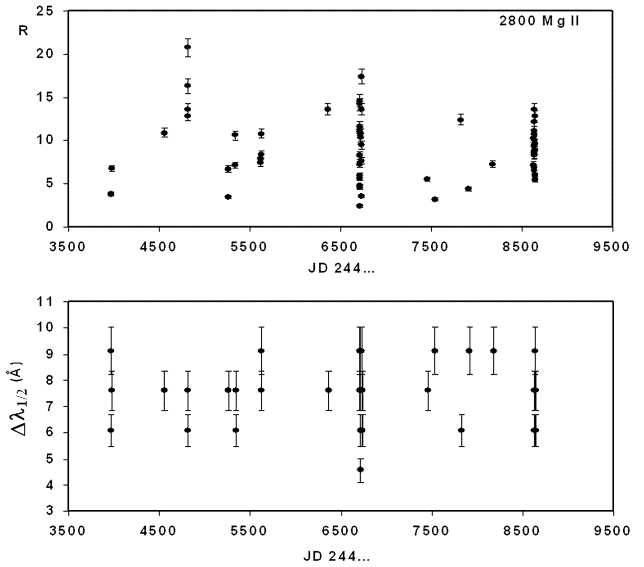


Figure 1: Time variability diagram for parameters R_λ and $\Delta\lambda_{1/2}$ for 13 years (1979 – 1992).

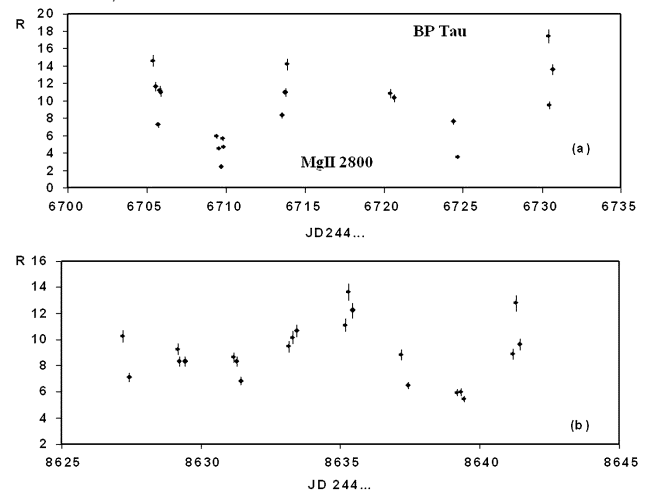


Figure 2: a and b. From day - to day time variability diagrams for intensities of doublet Mg II $\lambda 2800 \text{ \AA}$ for two separate data.

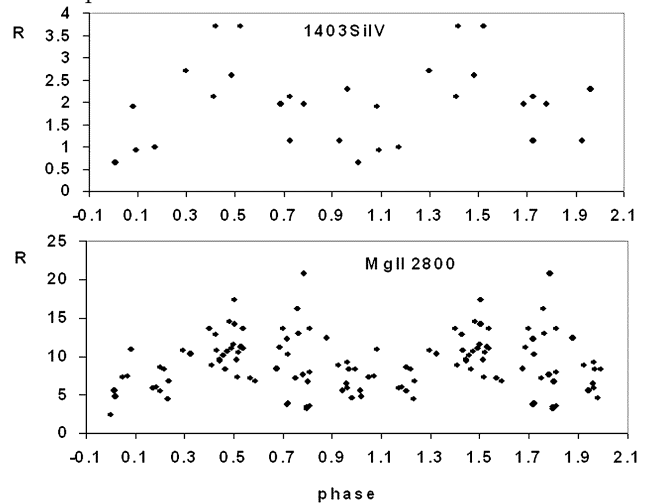


Figure 4: Phase diagrams for period 8.275 days for lines Si IV $\lambda 1403 \text{ \AA}$ and Mg II $\lambda 2800 \text{ \AA}$.

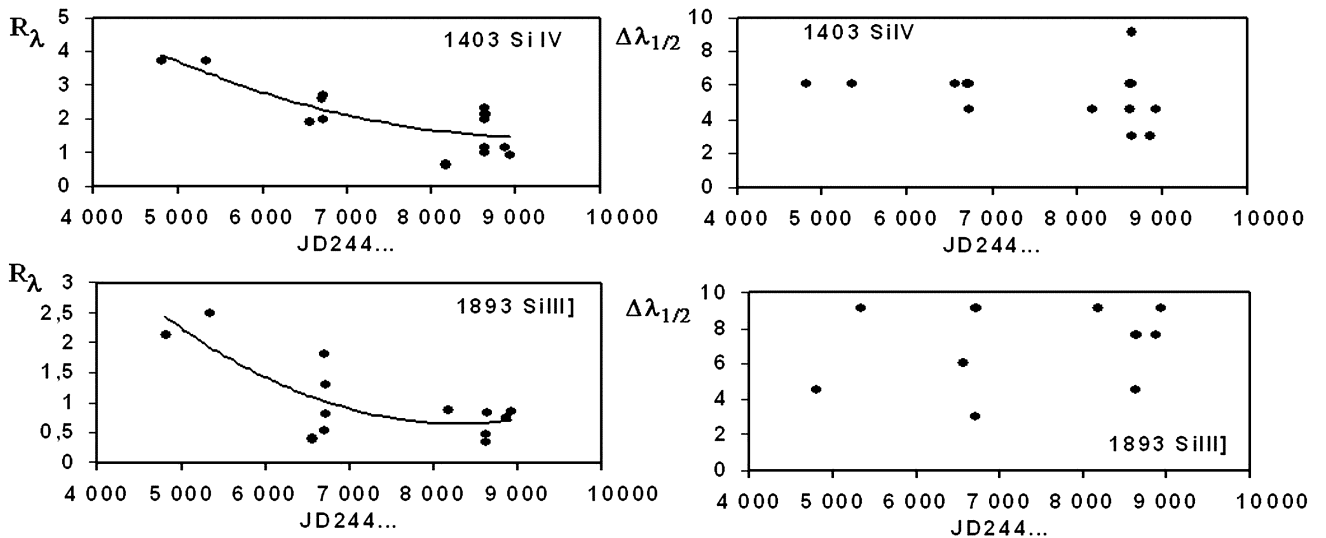


Figure 3: Time variability of the parameters R_λ and $\Delta\lambda_{1/2}$ for emission lines Si IV $\lambda 1403 \text{ \AA}$ and [Si III] $\lambda 1893 \text{ \AA}$.

3. Conclusions.

1. Intensities of emission lines showed variability from day-to day and some group of lines showed large time scale variability with characteristic time 5-6 years.
2. Variability of the central depths R_λ for Mg II $\lambda 2800 \text{ \AA}$ and some other spectral lines with probable period = 8.275 days had been discovered. It is very close value with photometric period 8.3 day obtained by Richter et al. (1992). There is certain group of lines for which a periodicity does not obtained.
3. For time interval of 13 years a character of variability of emission lines are divided into two groups: a) Intensities of lines for this time was monotonous decreased, b) Intensities of lines show irregular variability.
4. As a rule, lines with high potential of excitation related to the first group. More probable, such lines shows periodic variability. It is showed that we have as a minimum two local physical conditions of matter in the circumstellar disk of the star.

References

- Gomez de Castro A.I., Franqueira M.: 1997, *ApJ*, **482**, 465.
- Gullbring E., Barwig H., Chen P.S., Gahm G. F., Bao M. X.: 1996, *AsAp*, **307**, 791.
- Herbig G.H., Bell K.R.: 1988, *Lick Obs. Bull.*, **1111**, 90.
- Horne J.H., Balinas S.L.: 1986, *ApJ*, **302**, 757.
- Johns-Krull C.M., Valenti J.A., Linsky J.I.: 2000, *ApJ*, **539**, 815.
- Richter M., Basri G., Perlmutter S., Pennypacker C.: 1992, *PASP*, **104**, 1144.
- Scargle J.D.: 1982, *ApJ*, **263**, 835.
- Simon T., Vrba F.J., Herbst W.: 1990, *AJ* **100**, 1957.
- Valenti J.A., Fallon A.A., Johns-Krull C.M.: 2003, *ApJSS*, **147**, 305.
- Valenti J.A., Johns-Krull C.M., Linsky J.I.: 2000, *ApJSS*, **129**, 399.
- Vrba F.J., Rydgren A.E., Chugainov P.F., Shakovskaya N.I., Zak D.S.: 1986, *ApJ*, **306**, 199.

SPECTRAL OBSERVATIONS OF AB AUR

N.Z. Ismailov^{1,2}, O.V. Khalilov²¹ Baku State UniversityZ.Khalilov 23, Baku AZ1148 Azerbaijan, *ismailovn@yahoo.com*² Shamakha Astrophysical Observatory NAS of Azerbaijan

Y.Mamedaliyev v.,Shamakha, Azerbaijan

ABSTRACT. Results of spectral observations of the Herbig Ae/Be type star AB Aur carried out for 2008 – 2009 in SHAO were presented. The absorption component of the H_α line has a negative variable displacement on different dates, reaching -300 km/s. To this absorption component superimposed an emission peak, which is rather unstable and can disappear completely on time scales 3-4 day. We also studied profiles of the H_β line and found behavior completely similar to that of H_α . The line HeI $\lambda 5876$ AA has a composite structure with dominant one red and blue component. Profiles of presented lines and its spectral parameters shows variability from night to night.

Moreover we have also presented results of researches UV spectrograms of the star on the IUE archive data base. On this data we have measured intensities of 15 absorption lines. Our measurements allow us to carry out a monitoring of spectral parameters of the lines for 3, 6 days, and for 14 years. It was showed that since quick time variability from day-to day can be referred only for some group of lines, for 14 years observations in practice intensities of all spectral lines is showed variability with deviation larger 3σ level. We have discovered variability with period 6 day both for 6 day and more long time data. It was showed that some lines of different elements shows different character of variability. In some case variations of lines are in similar phase, in anti-phase and free forms with each other. We supposed that the basic variability in atmosphere Aur occurs in the bottom layers of an environment, in nearby areas to the surface of the star where matter accretion velocity reaches up to 300 km/s.

Key words: stars: emission line stars, optic and UV spectroscopy, individual: AB Aur.

1. Introduction

AB Aur (HD 31293, $d = 150$ pc; A0 Ve, van den Ancer et al., 1997) is one of the popular Herbig Ae/Be stars, with a mass of $2.4 \pm 0.2 M_\odot$ and age of 4 ± 1 Myr

(de Warf et al. 2003). The star is surrounded by a 450 AU gas and dust disk (Mannings and Sargent 1997) viewed at $i = 76^\circ$ (Miroshnichenko et al. 1997). Profiles of spectral lines H_α and h and k MgII shows conspicuous signs of strong stellar winds, like P Cyg and chromospheric activity, like e.g., the presence of CIV and Si IV resonance lines, emission in Ca II K and infrared triplet, and HeI $\lambda 5876$ Å lines (Catala et al. 1986). Catala et al.(1997) find that the photospheric lines have variable profiles on a time scale of a few hours.

AB Aur has been the subject of several synoptic observing programs documenting periodic modulation of a strong stellar wind (Praderie et al. 1986, Catala et al. 1987, 1997), including species up to CIV (Catala 1988) and NV (Bouret et al.1997). An analysis of the Mg II blue wing velocity versus time shows that the variability can be fitted with a sine curve period 45 hr, which Praderie et al.(1986) have interpret as rotation modulation period.

First part of our spectral researches in the optical range was presented in Ismailov and Khalilov (2010), where we have showed that the blue wing of hydrogen Balmer lines H_α and H_β is varied from night to night. Weak emission with component displacement -300 km/s is superimposed to the blue wing of these lines. In this report results of new researches in optical range and short-term day-by day, and 14 year variability of photospheric lines in UV range were presented.

2. Observations and results.

2.1. Visual range

Our observations of 2008–2009 was carried out using echelle spectrometer and 530×580 CCD with spectral resolution ~ 0.2 Å in spectral range $\lambda\lambda 4400 - 6700$ Å. For these spectrograms mean error for equivalent widths W_λ is at 5%, and in radial velocity Vr at ± 2 km/s. Following spectral parameters - W_λ , residual intensity R_λ , wide of lines at the half intensity (FWHM) and radial velocities Vr of lines had been measured.

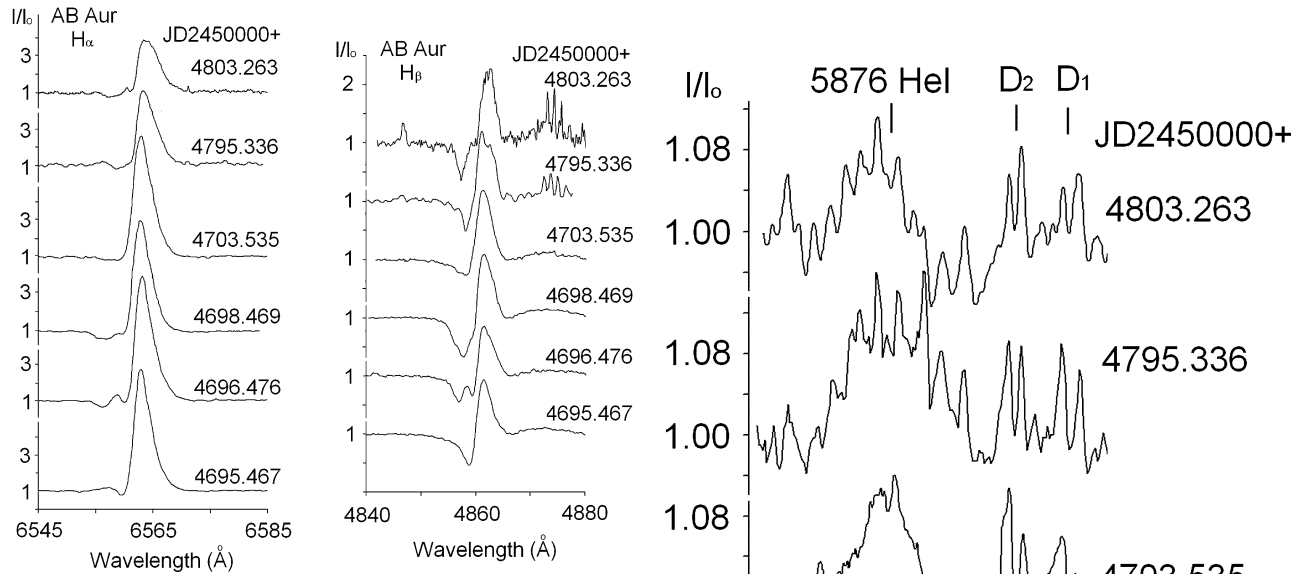


Figure 1: Profiles of emission lines H_α and H_β for 2008 observations.

The analysis of these parameters showed that they are shows a short time variability from night to night which characteristic time one day. Moreover a variability of the structure of line profiles also we have derived. In the Fig.1 line profiles of H_α , H_β and in Fig.2 profiles of the lines He I $\lambda 5876 \text{ \AA}$, D_1 , D_2 Na I for CCD spectrograms obtained in 2008 was presented. For JD2454696.476 we can clear see increasing of the emission peak on blue wings of lines H_α and H_β . During observations 2454695, 2444696, 2444698 we have discovered continuously an appearance and disappearance of this blue emission component in blue wings of lines H_α and H_β .

As one can see in Fig.2, the line He I $\lambda 5876 \text{ \AA}$ has a composite structure with dominant one red and blue component. Profiles of presented lines and its spectral parameters shows variability from night to night.

For August - December 2008 we have received only 6 pairs of spectrograms of the star. It has been shown, that the absorption component of the line has negative variable displacement in the different days, reaching up to -300 km/s .

2.2. UV spectrum.

The UV spectrum of the star has been investigated on the spectrograms taken from IUE archive data. It has been used 57 SWP and 46 LWP type spectrograms. Spectral resolution is at 6 \AA . For avoiding the account of interstellar reddening in spectral lines, and also additional mistakes because of heterogeneity of the received spectrograms we applied a classical method of processing of spectrograms in which measurement is made in relative units: after setting of a level

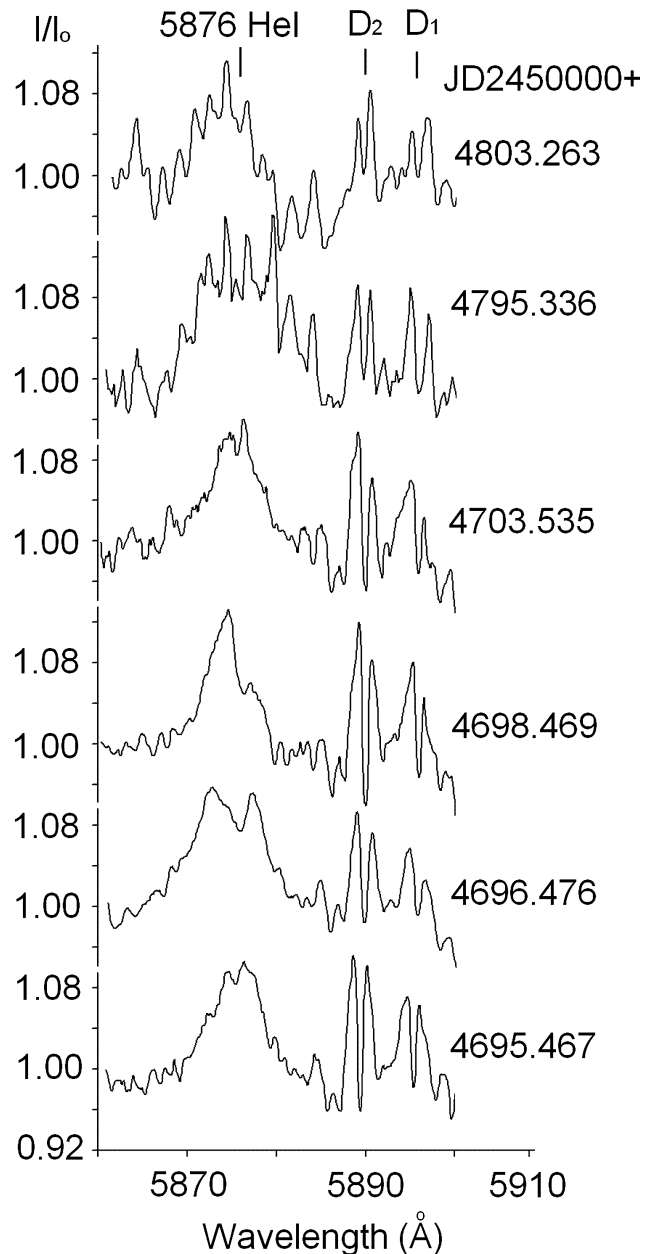


Figure 2: Profiles of He $\lambda 5876 \text{ \AA}$ and D_1 , D_2 lines for 2008 observations.

of the spectral continuum the central depths (residual - intensity) $R_\lambda = 1 - I/I_0$ and half widths ($\Delta\lambda_{1/2}$ - FWHM) of lines were determined. There, I - an absolute intensity at top of the line, I_0 - an absolute intensity of line at the level of continuum. In such measurements the mainly error in intensity of the line arises because of wrong carrying out of a level of the spectral continuum. Therefore, we carried out procedure of setting of the spectral continuum level very carefully, achieving a constancy of carrying out of a continuum through stable points of the spectrum. On the standard stars measurements mean deviations are

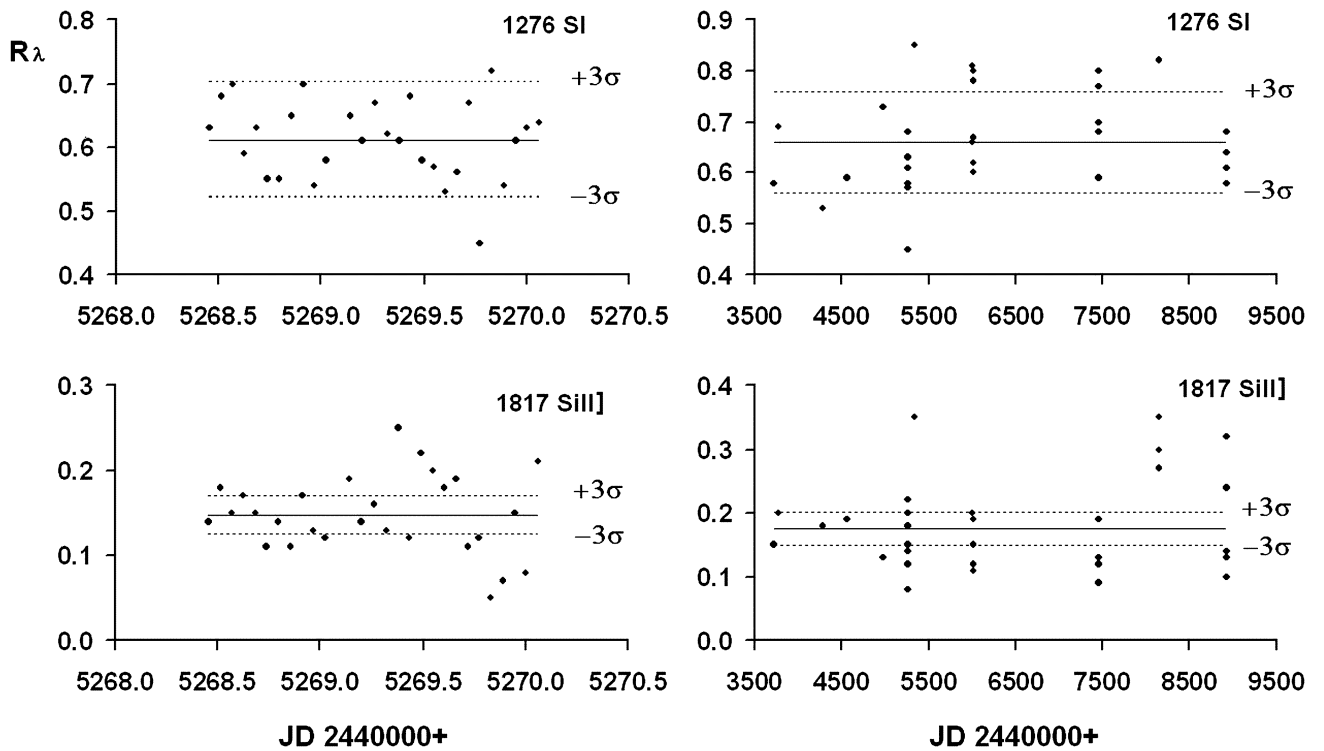


Figure 3: An example of time variability diagrams the residual intensity for 3 day monitoring (left panel) and 14 year (right panel) monitoring for lines Si I 1276 and Si II] 1817.

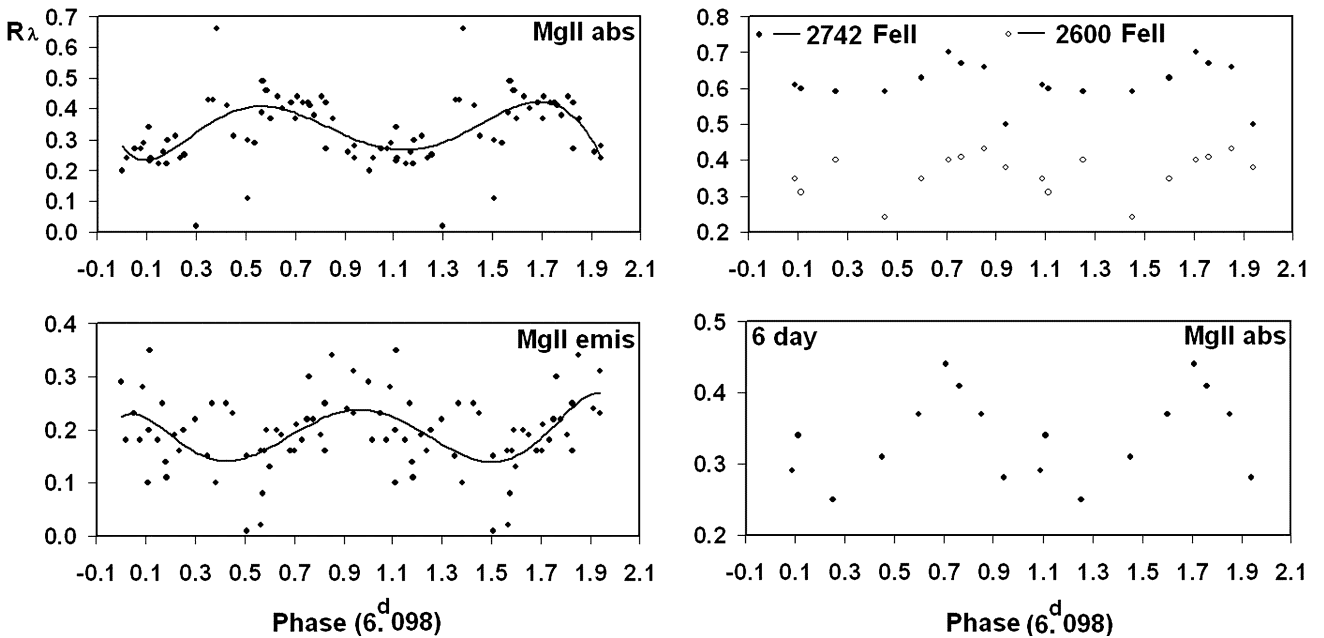


Figure 4: Phase diagrams for lines Mg II λ 2800 Å absorption and emission components (left panel), and only for 6 day monitoring of lines Fe II λ 2742, 2600 Å and Mg II λ 2800 Å absorption lines.

in intensity at 5 %, and in half widths at 15-20 %.

We have divided all observations to three contiguous sequences: I - monitoring for 3 day (JD2445268-2445270, all -27 points), II - monitoring for 6 day (JD 2446010-2446016, all - 16 points), and III - monitoring for 14 years (1978-1992, all - 57 points). We have measured photospheric absorption spectrum for more than 15 different lines in SWP and at 10 lines in LWP spectrograms. Doublet h and k Mg II λ 2795, 2802 Å, is not resolved and we had measured absorption and emission components separately as line Mg II λ 2800 Å.

We have discovered that in the short term series, as I and II, residual intensities of some photospheric lines with needs a high temperature excitation, as CIV 1549, He II 1640, Si IV 1403, Si III 1533 etc. are not shows variability in the 3 σ level. Some group of lines, as S III] 1817, H_2 1435, C III] 1915 etc., in series I and II shows active variability. But all lines shows variability in the large time interval for 14 years.

In the Fig.3 residual intensities versus time for I and III series for lines Si I 1276 and Si II] 1817 have presented. The short time series do not shows any variability in level 3 σ for line Si I 1276, since for series III both of lines shows variability higher 3 σ level.

For lines Mg II λ 2800 Å nightly parameters R_λ were used for the period search, resulting in a massive containing 46 points spread over 14 year interval of the observation We use the Scargle (1982) periodogram method as recommended by Horne and Balinas (1986) to search for periods. The greatest peak in a power spectrum is observed at frequency $\nu = 0.1641 \pm 0.0002 d^{-1}$, that corresponds to the period 6.098 ± 0.005 days.

In Fig.4 variability of intensities R_λ versus phase of period $P = 6.098$ for lines were presented.

3. Conclusions.

On results of this work it is possible to make the following conclusion:

1. The basic variability in atmosphere Aur occurs in the bottom layers of an environment, in nearby areas to

the surface of the star where matter accretion velocity reaches up to 300 km/s.

2. We have observed variations of emission component in the blue wing of lines H_α and H_β from day to day with continuously an appearance and disappearance for 3-4 day. Maximal displacement for this unstable emission component is -300 km/s.

3. For day to day short time observations shows that there are some group of absorption lines, as CIV1549, HeII1640, Si IV 1403, Si III 1533 etc. which are not vary of intensities in the 3 σ level. Group of lines, as S III] 1817, H_2 1435, C III] 1915 etc., in short time series shows active variability. For a long time all absorption lines shows variability with larger 3 σ level.

4. Some group of absorption lines including Mg II λ 2800, Fe II , etc. shows variability with period 6.098 days.

References

- Bouret J.C., et al. : 1997, *As.Ap.*, **328**, 606.
 Catala C. et al.: 1987, *As.Ap.*, **182**, 115.
 Catala C. : 1988, *As.Ap.*, **193**, 222.
 Catala C., Bohm T., Donati J.F., et al. : 1997, *As.Ap.*, **319**, 176.
 Catala C., Czarny J., Felenbok P., Praderie F.: 1986, *As.Ap.*, **154**, 103.
 Catala C., et al.: 1997, *As.Ap.*, **319**, 176.
 deWarf L.E., Septinsky J.F., Guinan J.F., et al.: 2003, *Ap.J.*, **590**, 357.
 Horne J.H., Balinas S.L.: 1986, *Ap.J.*, **302**, 757.
 Ismailov N.Z., Khalilov O.V. : 2010, *Variable Stars, The Galaktic Halo and Galaxy formation*, Russia, 12-16 October 2009, ed.C.Sterken, N.N.Samus, L.Szabados, 71.
 Mannings V.G., Sargent A.I.: 1997, *Ap.J.*, **490**, 792.
 Miroschnichenko N. et al.:1997, *B.A.A.S.*, **29**, 1286.
 Praderie et al. : 1986, *Ap.J.*, **303**, 311.
 Scargle J.D.: 1982, *Ap.J.*, **263**, 835.
 Van den Ancer M.E., The P.S., Tjin A.Djie et al.: 1997, *Ap.As.*, **324**, 33.

SPECTRAL AND PHOTOMETRIC RESEARCHES OF RY TAU

N.Z. Ismailov^{1,2}, H.N. Adigozalzade²¹ Shamakha Astrophysical Observatory NAS of Azerbaijan
Y.Mamedaliyev v., Shamakha, Azerbaijan, *ismailovn@yahoo.com*² Baku State University
Z.Khalilov 23, Baku AZ1148 Azerbaijan

ABSTRACT. The results of analysis of the total light curve of the classic T Tauri type star RY Tau were presented. For a time at last 48 years a brightness of the star is characterized by fluctuations with amplitude about $\Delta V \sim 1^m$, with characteristic time about 300 days. Firstly we were showed, that in an interval of 1983 – 2004 in V-band light variability of the star has cyclic character with the period of 377 ± 10 days. After the deepest minimum in 1995 there was some change in system therefore, since, fluctuations with amplitude about 1^m are continued, the phase of the period found before this minimum showed some displacement.

On the IUE archive data base we have studied a spectrum of RY Tau in the UV range. For 1979 – 1990 spectral observations we have measured relative intensities, FWHM (full wide at half middle) and equivalent widths of the relatively strong emission lines, as Mg II $\lambda 2800\text{\AA}$, S II, O I $\lambda 1334\text{\AA}$, C II $\lambda 1403\text{\AA}$, Si V $\lambda 1454\text{\AA}$, C IV $\lambda 1546\text{\AA}$, He II $\lambda 1640\text{\AA}$, etc. A variability of the line intensities of Mg II $\lambda 2800\text{\AA}$ emission and absorption components with period 23.2 ± 0.3 days was discovered. Some variability of emission line intensities from night to night was obtained.

Key words: stars: photometry, total light curve, UV spectroscopy: emission lines, individual: RY Tau.

1. Introduction

RY Tau is one of brightest classical T Tauri type stars (CTTS), with irregular light variability and a moderate emission spectrum. After unusual brightening in 1983/1984 from 11^m to 9^m in V (Herbst and Stine 1984, Zajtseva et al. 1985) the star has been high interest of investigators for photometric and spectroscopic observations. Full light curve for 1965 – 1985 was investigated by Herbst (1986) which have showed that a light of the star is varied with period larger 20 year. There are many works to find a periodicity in the light variations of the star. Some periods were reported on timescales from 5 to 66 days, but none

was confirmed after (Zajtseva 1986, Herbst et al., 1987, Herbst and Korett, 1988, Bouvier et al., 1993, Bouvier et al., 1995).

Spectral type obtained by Herbig (1977) and Cohen and Kuhl (1979) as *K1IV – V*, Cabrit et al. (1990) as *G2* and Petrov et al. (1996), as *G1 – 2IV*. The equivalent width of the H_α emission is about 20\AA , H_β sometimes in emission, sometimes in absorption, while higher Balmer lines are always in absorption. The flux radiated in H_α and IR CaII emission lines remained the same, in spite of the $\Delta V = 1^m$ difference in the continuum flux (Petrov et al., 1999). On the HST/STIS repeated observations of RY Tau Gomez de Castro and Verdigo (2007) the stellar wind physical parameters had been obtained.

In this work we have reporting results of the analysis a summary light curve for periodicity and UV spectral variability of RY Tau.

2. Summary light curve

The summary light curve of RY Tau has been carried out on the observations of the different authors from Wesleyan University database (Herbst et al., 1999), and also in archive (Grankin et al., 2007). In total for the analysis it has been used about 1800 individual UBV measurements received in 1962 – 2005.

On the Fig.1 the summary light curve of the star, carried out in a time interval of 1962-2004 is presented. Apparently, up to unusual increase of brightness in 1983 of the star light carries irregular character: was observed often weakening with different amplitudes, average value of the light in different seasons had been varied. The common character of the light variability RY Tau is corresponded IV photometric type of variability on the scheme of classification (Ismailov, 2004). According to results of observations of Petrov et al. (1999) and in 1996 a brightness of the star the same as and during the period, after 1983, continued fluctuations in an interval $9.^m5 - 10.^m8$. As already have noted

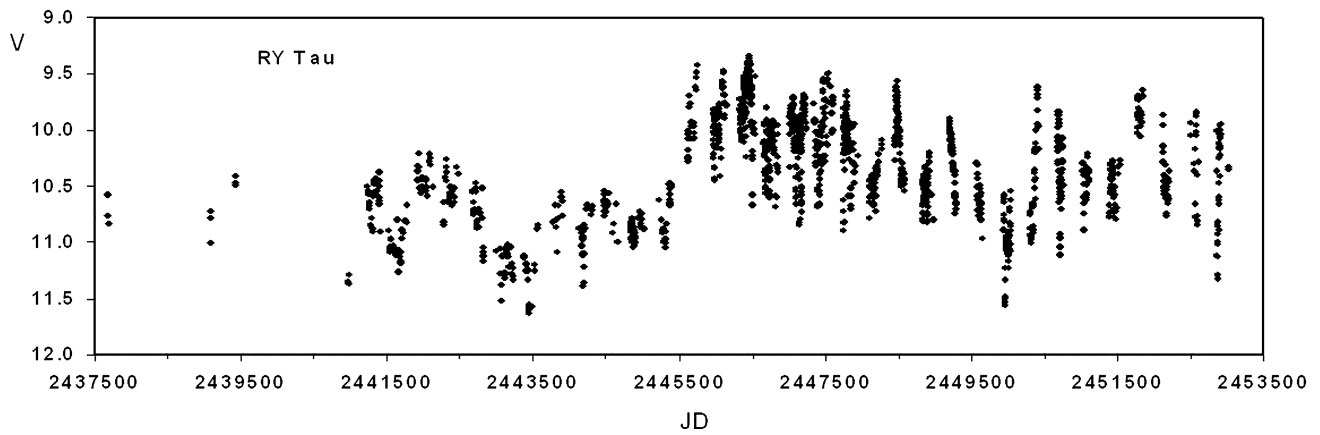


Figure 1: Summary V-light curve of RY Tau for 1962-2004.

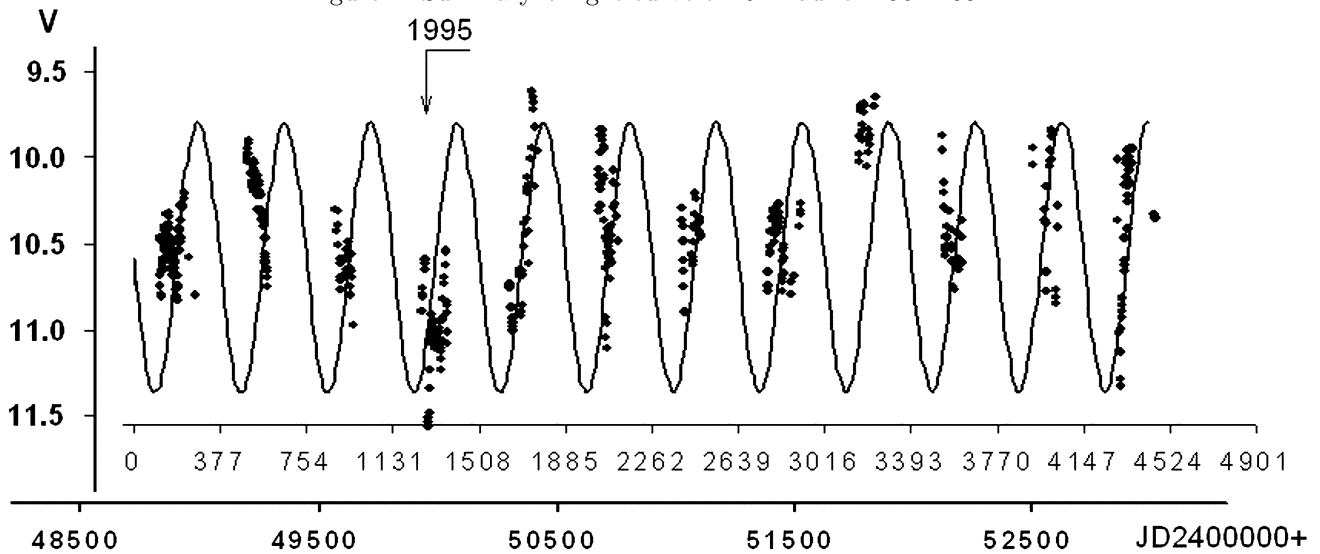


Figure 2: The fragment of light curves in range 1992 – 2004. V -values fitted with sinusoidal curve with period 377 days (solid line). A characteristic minimum in 1995 marked with the arrow.

many authors, after unusual increase of light since 1983 (JD 2445618), a character of variability a brightness of the star has a little changed: fluctuations with amplitude about 1m with characteristic time of 300-400 day was observed. After of this time the light variability of the star began to have cyclic character. As it is visible from Fig.1 a mean value of the V -magnitudes is slow change with characteristic time about 11 years, where superimposed fluctuations with amplitudes about 1m with characteristic time at 350 days. This feature of the light curve demands detailed search of the possible periodic component on the light curve. As we see from Fig.1 in different time intervals a brightness of the stars are carried cyclic character, but sometimes under irregular events this cyclic variability is destroyed. For carry out statistical fourye analysis all measurements we have divided into 3 separate massive with different quantity of the data, and for each of massive has been search of the period separately. The first file contains

all data before event of 1983, the second - from 1983 up to 1996 (JD 2450318), and the third - from 1996 on 2004. For performance of the statistical frequency analysis we use a method Scargle (1982) which later advanced by Horne and Balinas (1986). For all frequencies interval $0-1 d^{-1}$ we have find a maximal peak in $\nu = 0.00265 \pm 0.00005 d^{-1}$, which is corresponded to the period $P_1 = 377^d \pm 10^d$.

In Fig.2 a fragment of light curves in range 1992 – 2004 was presented. V -values fitted with sinusoidal curve with period 377 days (solid line). A characteristic minimum in 1995 marked with the arrow.

In Fig3 phase diagrams for period 377 day have presented. In the up panel all measurement before 1983 and on the second panel all data after 1983 are described. We can see that before to event 1983 periodicity is not clear, but after 1983 obtained periodicity are well described all data's. It is showed that after 1983 events a character of the light variability of the

star is changed. After the deepest minimum in 1995 there was some change in system therefore, since, fluctuations with amplitude about 1^m are continued, the phase of the period founded before to this minimum was shows some displacement.

It is necessary to pay attention to that fact, that variation of average value V -magnitudes in different years can considerably deform the common picture of short-term periodicity. For exception of the contribution of a long-term component of light variation we have deducted season (a time interval in the year which less than 6 month) average values V_a from all V -values of the given season and get the parameter $\Delta m_V = V - V_a$. Obtained all data Δm_V divided to two massive M1 and M2 and periodicity for each its was searched. In booth of this massive we had obtained new period $P_2 = 146 \pm 3$ days with confidence at 40%. Possible there is a seasonal periodicity of the star.

The UV spectrum of the star has been investigated on the spectrograms taken from IUE archive data. It has been used 14 SWP and 86 LWP type spectrograms. Spectral resolution is at 6 Å. For avoiding the account of interstellar reddening in spectral lines, and also additional mistakes because of heterogeneity of the received spectrograms we applied a classical method of processing of spectrograms in which measurement is made in relative units: after setting of a level of the spectral continuum the central depths (residual - intensity) $R_\lambda = 1 - I/I_0$ and half widths ($(\Delta\lambda_{1/2} - \text{FWHM})$) of lines were determined. There, I - an absolute intensity at top of the line, I_0 - an absolute intensity of line at the level of continuum. In such measurements the mainly error in intensity of the line arises because of wrong carrying out of a level of the spectral continuum. Therefore, we carried out procedure of setting of the spectral continuum level very carefully, achieving a constancy of carrying out of a continuum through stable points of the spectrum. On the standard stars measurements mean deviations are in intensity at 5 %, and in half widths at 15-20 %.

In Fig.4 time variability of residual intensities R_λ for unresolved doublet MgII λ 2800 Å lines was presented. It is shows that for 10 year observations R_λ shows variability both from day to day and for a long time with characteristic time 5-6 year.

More rich massive contained 86 points of the parameter R_λ for emission lines MgII λ 2800 Å. We have carried out a periodogram, and have found a period 23.2 ± 0.3 days with more than 30% confidence. In Fig.5 phase diagram of the R_λ for lines MgII λ 2800 Å was presented.

3. Conclusions.

1. Firstly we have showed that in a time interval of 1983 – 2004 in V -band light of the star has cyclic character variations with the period of 377 ± 10 days, moreover a periodic radiation of the star sometimes was destroyed by flare like events.

2. After the deepest minimum in 1995 there was some change in system therefore, since, fluctuations with amplitude about 1m are continued, the phase of the period founded before to this minimum was shows some displacement.

3. After cleaning of average values of brightness for each year we have find a seasonal period of variability 146 ± 3 days.

4. Some variability of emission line intensities from night to night was obtained. For UV spectral range we have determined a periodical variability of intensities of MgII λ 2800 Ålines with period $P = 23.3 \pm 0.3$ days.

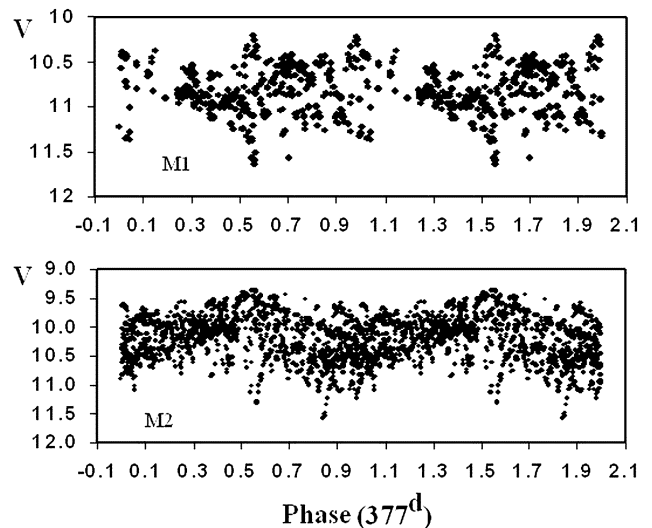


Figure 3: Phase diagrams for period 377 day have presented. In the up panel all measurement before 1983 and on the second panel all data after 1983 are described.

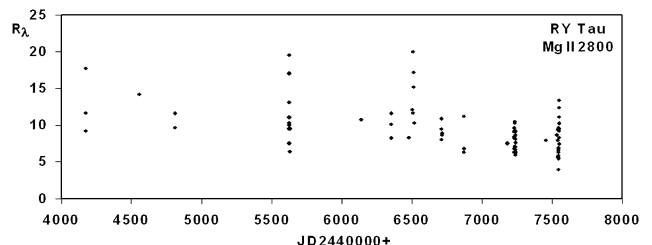


Figure 4: Time variability of intensities R_λ for MgII λ 2800 Å emission lines in the spectrum of RY Tau.

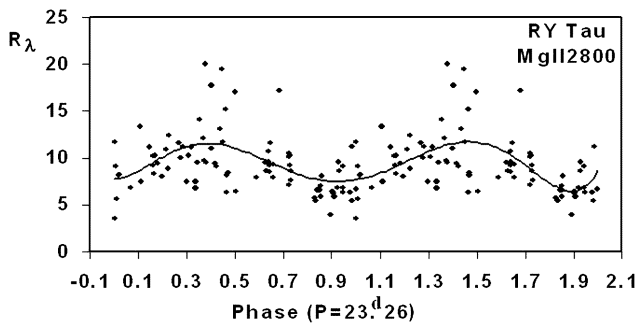


Figure 5: Phase diagram variations of the parameter R_λ for MgII λ 2800 Å emission.

References

- Bouvier J., Cabrit S., Fernandez M. et al.: 1993, *As.Ap.*, **272**, 176.
- Bouvier J., Covino E., Kovo O. et al.: 1995, *As.Ap.*, **299**, 89.
- Cabrit S., Edwards S., Strom S.E., Strom K.M.: 1990, *Ap.J.*, **354**, 687.
- Cohen M., Kuhl L.V.: 1979, *Ap.J.S.S.*, **41**, 743.
- Gomez de Castro A.I., Verdugo E.: 2007, *Ap.J.*, **654**, 91.
- Grankin K.N., Melnikov S.Yu., Bouvier J., et al.: 2007, *As.Ap.*, **461**, 183.
- Herbig G.H.: 1977, *Ap.J.*, **214**, 747.
- Herbst W., Booth C.F., Koret D.L. et al.: 1987, *A.J.*, **94**, 137.
- Herbst W., Koret D.L.: 1988, *A.J.*, **96**, 1949.
- Herbst W., Stine P.C.: 1984, *A.J.*, **89**, 1716.
- Herbst W.: 1986, *P.A.S.P.*, **98**, 1088.
- Herbst W., Shevchenko V.S.: 1999, *A.J.*, **118**, 1043.
- Horne J.H., Balinas S.L.: 1986, *Ap.J.*, **302**, 757.
- Ismailov N.Z.: 2005, *A.Zh.*, **82**, 347.
- Petrov P.P., Zajtseva G.V., Efimov Yu.S. et al.: 1999, *As.Ap.*, **341**, 553.
- Scargle J.D.: 1982, *A.J.*, **263**, 835.
- Zajtseva G.V.: 1986, *Afz.*, **25**, 471.
- Zajtseva G.V., Kolotilov E.A., Petrov P.P. et al.: 1985, *Pisma v Azh.*, **11**, 275.

IRON ABUNDANCES IN THE ATMOSPHERES OF HD10700 & HD146233

O.M. Ivanyuk¹, Ya.V. Pavlenko¹, J.S. Jenkins², H.R.A. Jones³, Yu. Lyubchik¹,
B. Kaminsky¹, M. Kuznetsov¹,

¹ *Main Astronomical Observatory of NASU*

² *University of Santyago, Chile*

³ *University of Hertfordshire, UK*

ABSTRACT. There are many different means to determine physical parameters of stars and their abundances by spectral analysis. In our work we draw our attention to the rotational and microturbulence velocities as well as metallicities for the stars of known effective temperature and surface gravity. We carried fits of LTE synthetic spectra to the observed spectra of HD10700 and HD146233. These stars are known as solar-twins except slightly higher rotational velocities in both cases and higher magnetical activity in HD10700. We adopted ABEL software (Pavlenko Ya.V.) to fit to HD10700, HD146233 spectra obtained on Camino Observatory, Chile. Selected stars look like. We compare our results with previous work of Valenti & Fischer (2005).

Key words: solar-type stars, properties, abundances;

1. Introduction

The majority of spectral research begins with effective temperature and surface gravity determinations, which are based on data of photometry and astrometry. Having defined these values usual analysis continues with solving Radiation Transfer Equation for selected number of elements in order to match equivalent widths and/or profiles of spectral lines (Pavlenko 2003). Our approach assumes direct fits to observed spectra instead of equivalent width measuring. Along with iron abundances determination we used our technique to determine microturbulence and rotational velocity.

2. Observational Spectra

Our stars are similar to the Sun. One is G8 type and another is F8. We may see their basic parameters in table below.

Name	Sp Class	T_{eff} (Model)	Log g	[Fe/H]
HD10700	G8V	5513 348 (5283)	4.59	-0.5
HD146233	F8V	6074 470 (5791)	4.41	0.0

Spectroscopic observations ($R=46000$) and maintenance data were obtained using Fibred Extended Range Optical Spectrograph (FEROS) installed on 2.2m Max-Planck Telescope at the European Southern Observatory (La Silla site in Chile). The exposure time was about 120-480 seconds. Each observing night commenced with collecting collateral data for further spectra reduction, i.e. flat-fields, bias, arc frames, in accordance with the standard ESO calibration plan, see Jenkins et. al. (2008).

3. Synthetic Spectrum

Plane-parallel LTE model atmospheres with 1D convection mixing and no energy divergence were computed using SAM12 program (Pavlenko 2003) which is based on ATLAS12 (Kurucz 1999). Opacities calculations are based on Sneden et al. (1976) approach. VALD2 line list (Kupka et.al. 1999) was used for our synthetic spectra computations. For absorption line profile we adopted Voigt function.

All synthetic spectra were computed with step

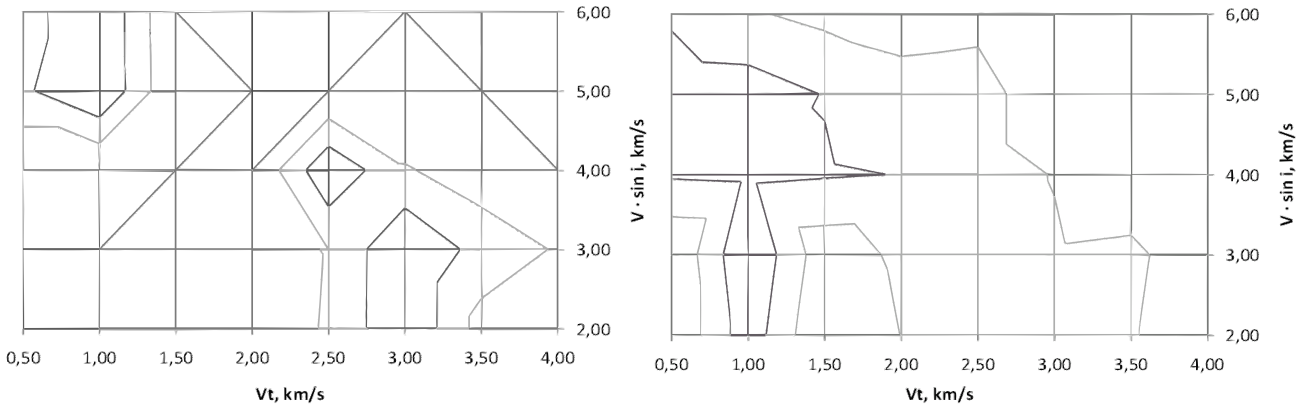
$$\Delta\lambda = 0.025\text{\AA}$$

using WITA6 and ABEL8 programs (Pavlenko 2003). We carried out the set of semi-automatic fits to observed spectra for a grid of adopted $V \sin i$, V_t values and Fe I/Fe II abundances.

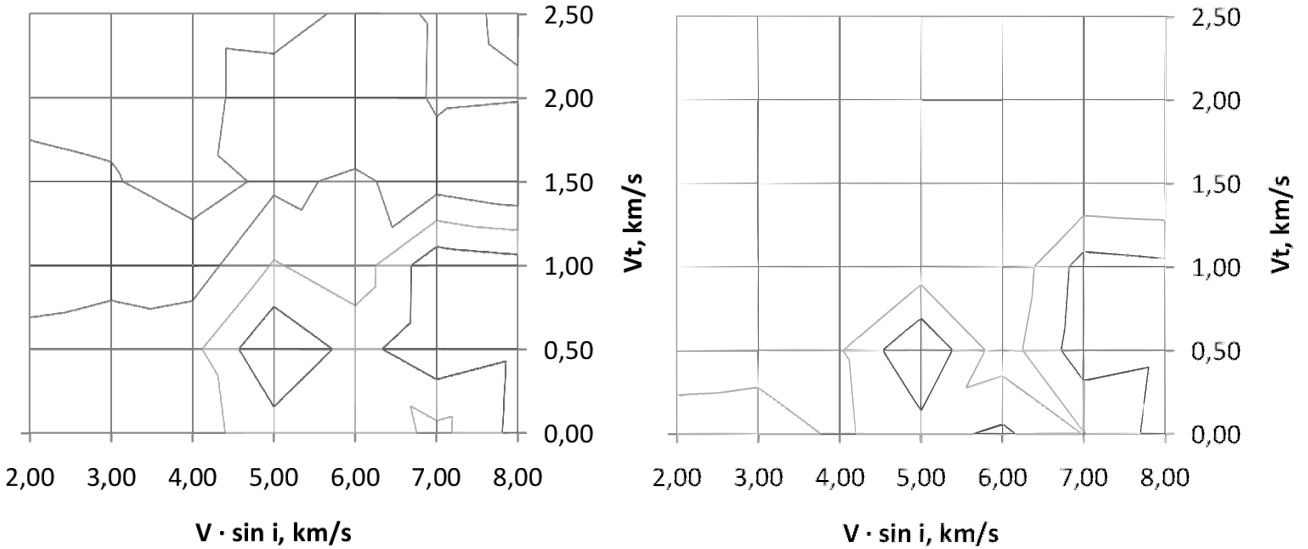
Quality of our fits characterizes by function of projected rotational velocity (v_i), microturbulence (v_t) and normalization factor (n):

$$S(f_{v_i}, f_n, f_{v_t}) = \sum_{\nu} (F_{\nu} - (F_{\nu}^x)^2)$$

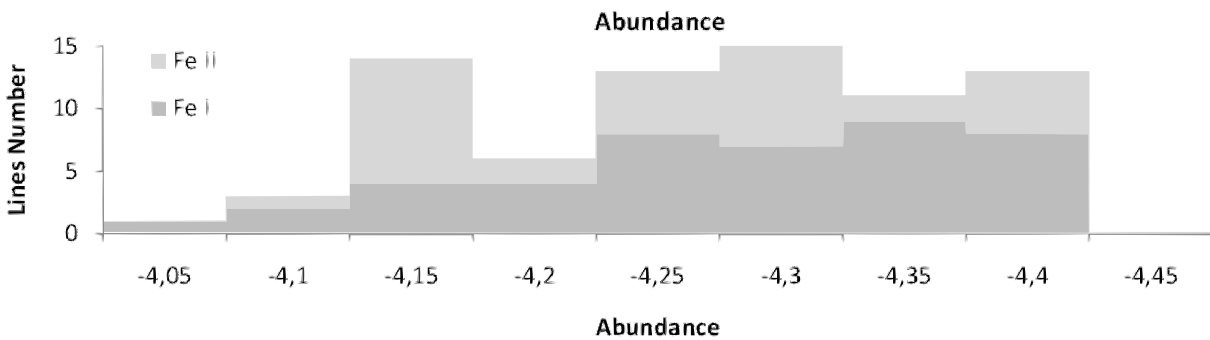
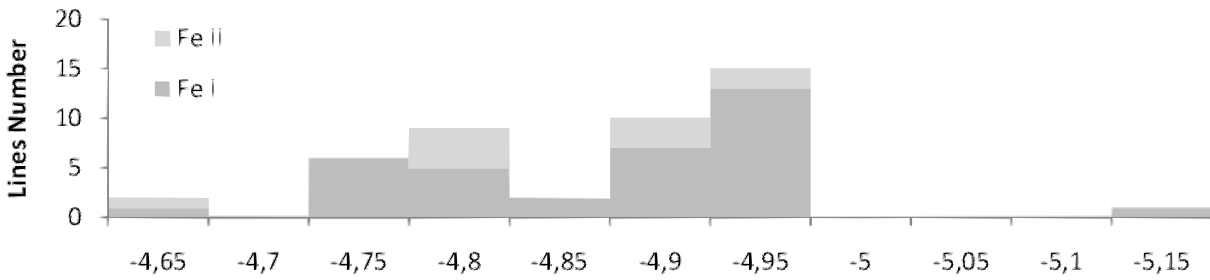
Each combination of n , v_i , v_t and [Fe/H] gives us



Figures 1 and 2. HD10700. Dependence of S values on rotational velocity and microturbulence velocity. Minimum of S corresponds to $V_t=1.0\text{km/s}$ and $V \sin i=5.0 \text{ km/s}$ for both Fe I and Fe II lines.



Figures 3 and 4. HD146233. Dependence of S values on rotational velocity along with microturbulence velocity. Minimum of S corresponds to $V_t=0.5\text{km/s}$ and $V \sin i=5.0 \text{ km/s}$ for both Fe I and Fe II lines



Figures 5 and 6. Histograms show number of lines that indicate $\log N(\text{Fe})$ for HD10700 and HD146233 respectively.

more or less good fit to observational spectra. The best fit characterizes by minimum of S.

It is important to note that we did not account lines that weaker than average noise level, in our case it is about 3%. Also were excluded lines that fit worse than on 30%. In most cases it is induced by blends in observed spectra and by mistakes in line lists.

4. Results & Conclusions

Results represent abundances for metal-deficient star HD10700 and star-like HD146233 in comparison with previous work (Valenti 2005). Contour surface below shows S distribution for different sets of v_i and v_t . The point of minimum indicates most appropriate values of projected rotational velocity and microturbulence.

Our analysis was done for neutral and one-time ionized Iron to verify log g of our model atmosphere. Histograms below show how many lines give us that or another log N(Fe) for selected star.

As we can see from the table our results in a good agreement with Valenti and Fischer work with only discrepancy in determined V sin i values, which can be explained by different sets of examined lines.

HD10700	Our Result	Valenti & Fischer
V_t	1.0 km/s	0.85 km/s (fixed)
V sin i	5.0 km/s	2.0 km/s
Fe/H	-0.5 dex	-0.52 dex

HD146233	Our Result	Valenti & Fischer
V_t	0.5 km/s	0.85 km/s (fixed)
V sin i	5.0 km/s	2.6 km/s
Fe/H	0.1 dex	0.03 dex

Acknowledgements. This work was supported by the FP7 project RoPACS (ROPACS PITN-GA-2008-213646) and the program Cosmomicrophysics of NAS of Ukraine.

References

- Allende Prieto C.: 2004. *Astronomische Nachrichten*, **325**, 604.
- Jenkins J. S., Jones H. R. A., Pavlenko Y., Pinfield D. J., Barnes J. R., Lyubchik Y.: 2008, *A&A*, **485**, 571.
- Kupka F., Piskunov N., Ryabchikova T.A., Stempels H.C., Weiss W.W.,: 1999. *Astron. Astrophys. Suppl.*, **138**, 119.
- Pavlenko Ya.: V. 1997, *Astron. Astrophys. Sci.*, **253**, p. 43
- Pavlenko Ya.V., Jones H.R.A., Longmore A.J.: 2003, *MNRAS*, **345**, 311
- Snedden C., Johnson H.R., Krupp B.M.: 1976, *ApJ*, **204**, 218.
- Valenti J.A., Fischer D.A.: 2005, *The Astrophysical Journal*, **159**, 141

TiO ISOTOPES BANDS IN THE M DWARF SPECTRA

O. Ivanyuk¹, Ya.V. Pavlenko¹, H.R.A. Jones², D. Pinfield², J.R.A. Clarke²

¹ *Main Astronomical Observatory of NASU*

² *University of Hertfordshire, UK*

ABSTRACT. A few TiO isotopes are responsible for formation different molecular features in M-Dwarfs. We present spectral analysis for molecular spectrum TiO (Schwenke 1998) consists of 5 Titanium isotopes: ⁴⁶Ti, ⁴⁷Ti, ⁴⁸Ti, ⁴⁹Ti, ⁵⁰Ti. Results denote most influent isotopes in our observational spectrum. Our main aim is to find some remarkable isotope features in the observed spectra of M Dwarf.

Key words: : late-type stars, molecular spectra;

1. Introduction

TiO is the most abundant of the 3D oxides present in the spectra of M and S class stars (Merrill et. al. 1962). TiO bands are used for spectral classification of cold stars (Morgan et. al. 1973). The distribution of intensities in the rotational structure of TiO bands can be used to determine the temperature of stellar atmospheres (Phillips 1973).

2. Observational Spectrum

M Dwarf 2MASS J02495798-2147267 is a potential Moving Group member which is good for understanding cool and low gravity atmospheres. Distanc is 26-40 pc, apparent magnitude is 13.27 ± 0.03 , spectral type is M6.0 (Clarke et. al. 2009).

3. Synthetic Spectrum

Model Atmospheres. We used LTE/1D model of atmosphere with these parameters $T_{eff} = 2800K$ and $\lg g = 5$, $[Fe/H] = 0$ (Hauschildt et. al. 1999). Synthetic spectra were computed using WITA6 (Pavlenko 2003). Rotational profile has been applied with $V \sin i = 1.5$ km/s.

TiO Linelist. Our synthetic spectra is computed for TiO list developed by Shwenke (1998) There is a number of constraints that limits its features. One is the inclusion of only a small number of electronic states. Another is the incompleteness in the electronic structure calculations, including the neglect of smaller relativistic corrections to the Hamiltonian. Finally,

there can be inaccuracies in the parameters determining the potential-energy curves. These are mostly obtained from experimental analysis. List includes lines for all five Ti isotopes bound with ¹⁶O. Next table shows the adopted relative abundances of Ti isotopes.

Ti Isotope	Relative Abundance
⁴⁶ Ti	0.0793
⁴⁷ Ti	0.0793
⁴⁸ Ti	0.7393
⁴⁹ Ti	0.0552
⁵⁰ Ti	0.0534

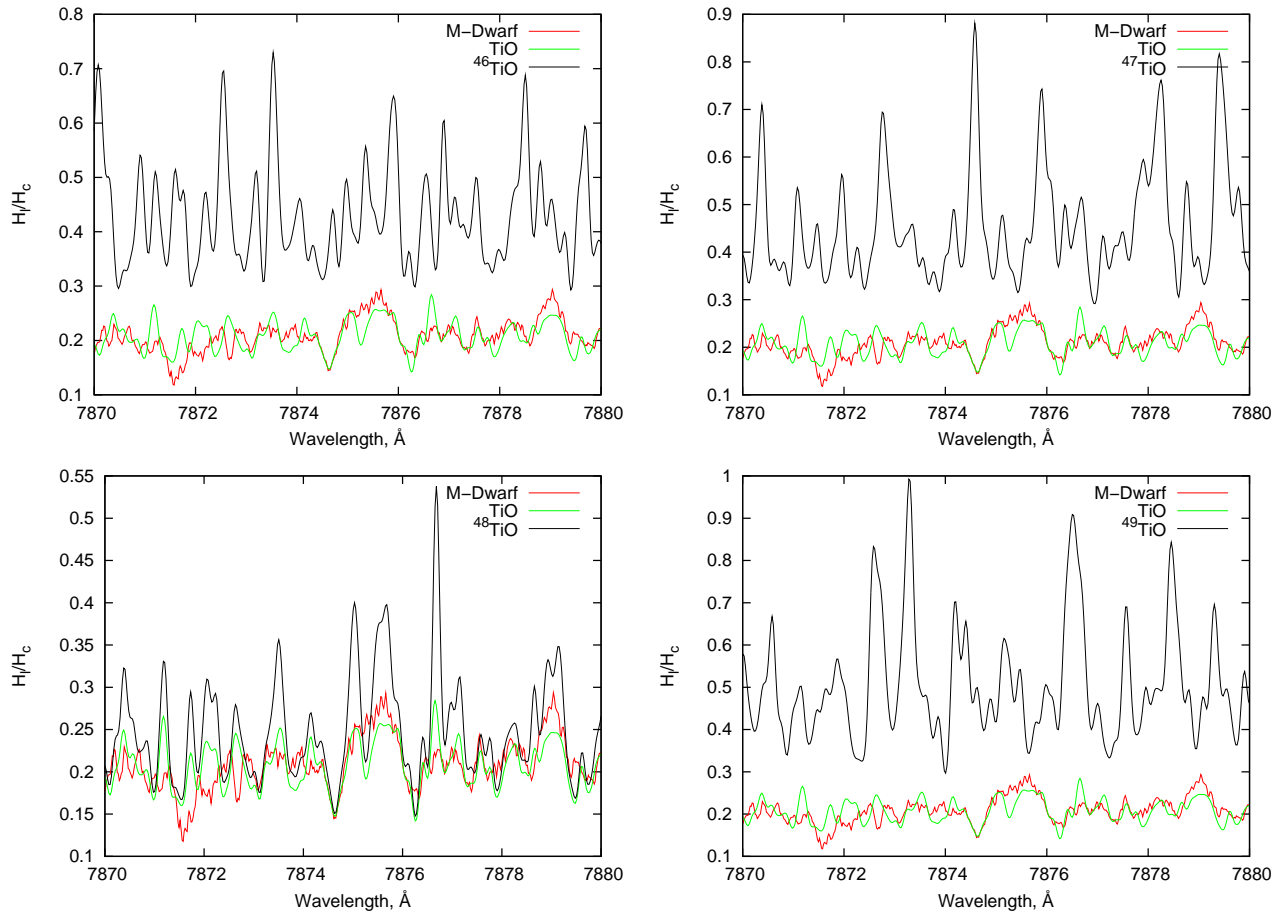
4. Results

Each figure denotes comparison of observational and TiO isotopes spectrum. We didnt account atomic spectrum due to its of much weaker intensities. First figure shows smoothed TiO and observed 2MASS J02495798-2147267 spectrum. Only small fraction of lines is in a good agreement with observational data. That could be explained with linelist constrains and not well-known metallicity values. Anyway, we can clearly distinguish the individual TiO isotope lines.

Most abundant ⁴⁸Ti isotope demonstrates the largest contribution in common Titanium spectrum. However, not all details can be described by only ⁴⁸Ti. We tried to find any relationship with other isotopes. Next figures portray each isotopes shape in a comparison with observed spectra in an attempt to dig these details.

We belive that we able to separate lines of different Titanium isotopes, despite their much smaller contribution in the combined spectrum. It proves our ability of further research we are intend to conduct on late type M dwarfs and TiO molecule.

Acknowledgements. This work was supported by the FP7 project RoPACS (ROPACS PITN-GA-2008-213646) and the program Cosmomicrophysics of NAS of Ukraine.



Figures 1, 2, 3 and 4. Spectra of ^{46}Ti , ^{47}Ti , ^{48}Ti and ^{49}Ti isotopes relatively to composite TiO and M Dwarf spectra.

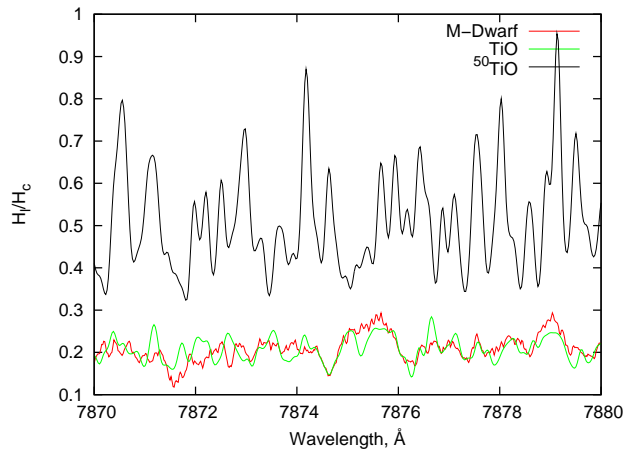


Figure 5. Spectra of ^{50}Ti isotope relatively to composite TiO and M Dwarf spectra

References

- Chavez J., Lambert D.L.: 2009, *ApJ*, **699**, 1906
- Clarke J.R.A.: 2009, *MNRAS*, **402**, 575
- Hauschildt P.H., Allard F., Baron E.: 1999, *ApJ*, **512**, 377
- Merrill P.W., Deutsch A.J., Keenan Ph.C.: 1962, *ApJ*, **136**, 21
- Morgan W.W., Keenan P.C.: 1973, *Annual Review of Astronomy and Astrophysics*, 11, p. 29
- Pavlenko Y.: 2003, *IAUS*, **211**, 365
- Phillips J.G.: 1973, *ApJ*, **26**, 313
- Schwenke D.W.: 1998, *Faraday Discuss.*, **109**, 321

FOUR NEW VARIABLE STARS NEAR CL AURIGAE. II

Chun-Hwey Kim¹, Jae Woo Lee², Duck Hyun Kim¹, Ivan L. Andronov³

¹ Department of Astronomy and Space Science, and CBNU Observatory,

Chungbuk National University, Cheongju 361-763, Korea, *kimch@chungbuk.ac.kr*

² Korea Astronomy and Space Science Institute, Daejeon 305-348, Korea, *jwlee@kasi.re.kr*

³ Department "High and Applied Mathematics", Odessa National Maritime University, Odessa, Ukraine, *il-a@mail.ru*

ABSTRACT. We report on a discovery of four new variable stars (USNO-B1.0 1234-0103195, 1235-0097170, 1236-0100293 and 1236-0100092) in the field of CL Aur. The stars are classified as eclipsing binary stars with orbital periods of 0.5137413(23) (EW type), 0.8698365(26) (EA) and 4.0055842(40) (EA with a significant orbital eccentricity), respectively. The fourth star (USNO-B1.0 1236-0100092) showed only one partial ascending branch of the light curves, although 22 nights were covered at the 61-cm telescope at the Sobaeksan Optical Astronomy Observatory (SOAO) in Korea. Fourteen minima timings for these stars are published separately. In an addition to the original discovery paper (Kim et al. 2010), we discuss methodological problems and present results of mathematical modeling of the light curves using other methods, i.e. trigonometric polynomial fits and the newly developed fit "NAV" ("New Algol Variable").

Key words: Variable stars: eclipsing: EA, EW -type; Data analysis: "NAV" algorithm.

During a study of the eclipsing binary CL Aur, we have discovered four new variable stars. The observations were made on 22 nights from 2003 November to 2005 February. The CCD camera has 2048×2048 pixels and an FOV of about 20'5 × 20'5. The filter set is attached to the 61 cm reflector at Sobaeksan Optical Astronomy Observatory (SOAO) in Korea. The exposure times were 75~140 s for *B*, 45~85 s for *V*, 33~65 s for *R*, and 30~60 s for *I*, respectively. A 2×2 binning mode was used. The nearby stars GSC 2393-1424 and GSC 2393-1418, imaged on the chip at the same time as the variable, were chosen as comparison and check stars, respectively. The co-ordinates (2000.0) of the comparison are 05^h13^m27^s.48, +33°26'46.3". Unfortunately, there is no multicolor calibration for the comparison star, so the photometry is in differences "var-comp". The discovery paper was published by Kim et al. (2010). The star USNO-B1.0 1236-0100092 is an EA-type star

with $T_0 = 2453412.0000(5)$ and $P_{orb} = 4.^d0055842(40)$. Here in brackets are the error estimates in units of last decimal digit. The secondary minimum is not covered completely by observations, but significantly shifted from the phase 0.5, indicating an elliptic orbit. USNO-B1.0 1234-0103195 shows only one ascending branch typical for EA-type stars, but, for determination of elements, new observations are needed.

USNO B1.0 1236-0100293: EW -type

The object is an EW-type binary system. For analysis, we used an trigonometric polynomial (TP) fit $m_s(t)$ of order s :

$$m_s(t) = C_{s,1} + \sum_{j=1}^s (C_{s,2j} \cdot \cos(j\omega t) + C_{s,2j+1} \cdot \sin(j\omega t)),$$

where $\omega = 2\pi f$, $f = 1/P$ is trial frequency. The test function is defined as

$$S(f) = \frac{\sigma_{O-C,s}^2}{\sigma_{O-C,0}^2}, \quad \sigma_{O-C,s}^2 = \sum_{k=1}^N (m_k - m_s(t_k))^2,$$

where $\sigma_{O-C,s}^2$ is variance of deviation of observational points from the s -th order fit. The value $S(f)$ is a square of the correlation coefficient between the observed and calculated (for a given f) values. Detailed discussion of statistical properties of this test function, coefficients was presented by Andronov (1994, 2003). For the periodogram analysis, we have used the computer program "Multi-Column View" (MCV) described by Andronov and Baklanov (2004).

The periodogram (dependence of the test function $S(f)$ on trial frequency is shown in Fig. 1. Taking into account the EW type of variability, the first approach is TP fit with $s = 2$, which corresponds to a double wave and different depth of minima and (in a case of O'Connell effect). Thus the most prominent peak at the periodogram occurs at the orbital period P_{orb} , and the second one (in height) at a double frequency (half-period).

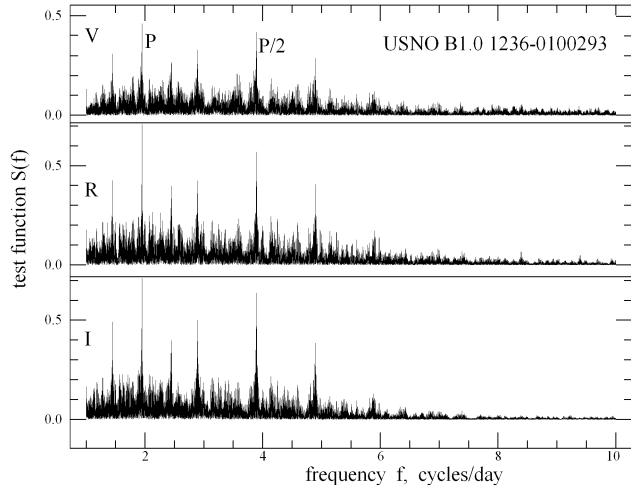


Figure 1: Periodogram of VRI observations (from top to bottom) of USNO B1.0 1236-0100293 computed using the 2-nd order trigonometric polynomial fit

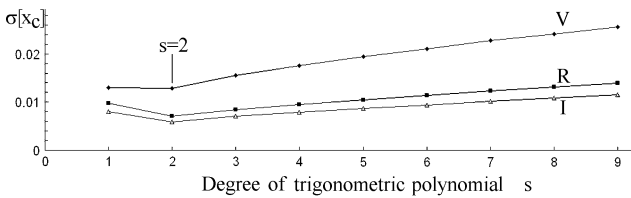


Figure 2: Dependence of the r.m.s. error estimate of the smoothing curve on the degree s of trigonometric polynomial for filters VRI.

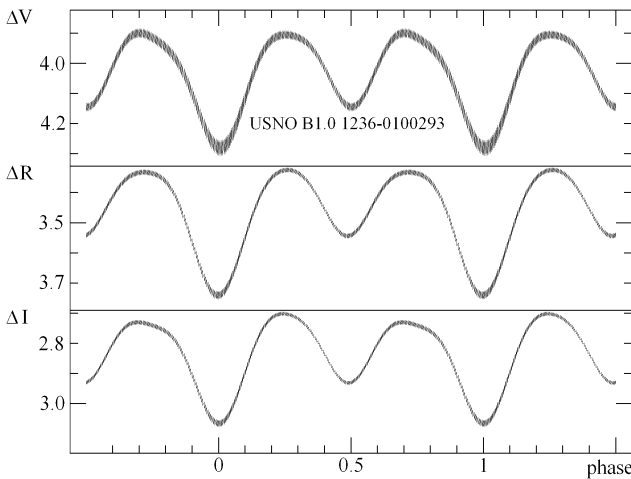


Figure 3: 4-th order trigonometric polynomial fit to the VRI observations of USNO B1.0 1236-0100293. The thickness of the line corresponds to the “ 1σ ” corridor. The ephemeris for the primary minimum is $\text{Min.HJD} = 2453215.5773 + 0.5137405 \cdot E$.

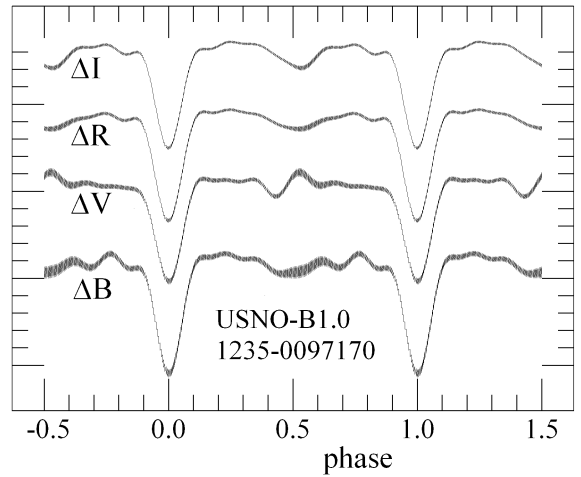


Figure 4: Trigonometric polynomial fits of 7-th order for BVRI observations of USNO-B1.0 1235-0097170 with “ 1σ ” corridor.

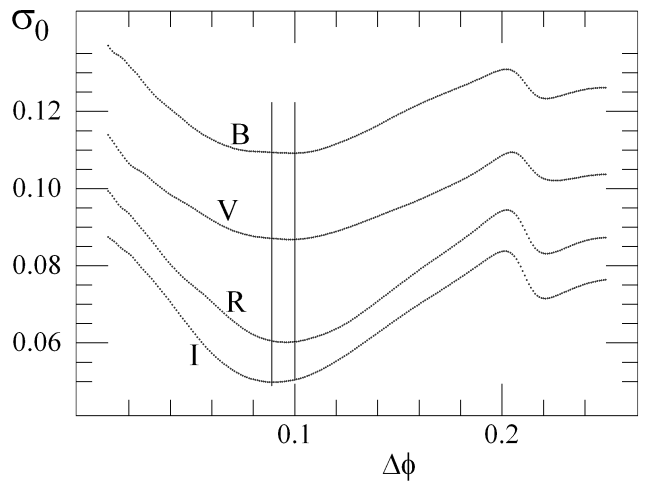


Figure 5: Dependence of the “unit weight error” on the eclipse half-width $\Delta\phi$ for filters BVRI.

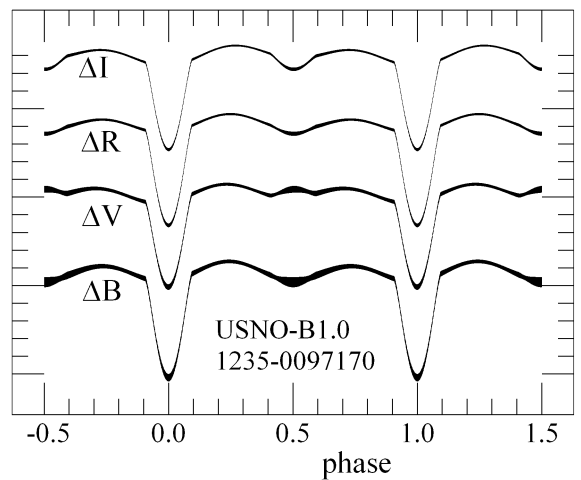


Figure 6: “NAV” fits to the BVRI observations of USNO-B1.0 1235-0097170 with “ 1σ ” corridor. The ephemeris for the primary minimum is $\text{Min.HJD} = 2453208.8503 + 0.8698365 \cdot E$.

Due to statistical errors and non-orthogonality of the basic functions, the best fit values of the period and coefficients ($C_{s,i}$ are generally dependent on s even for the same i . Kim et al. (2010) used the method of Scargle (1982) with a least squares approximation

$$m_c(t) = \bar{m} + C_{s,2} \cdot \cos(\omega t) + C_{s,3} \cdot \sin(\omega t),$$

with $C_{s,1} = \bar{m}$ (sample mean of the observations) instead of a least square solution in TP-1. Moreover, the estimates of period and other coefficients are dependent on the photometric system. For the TP-2 fit, we obtained for VRI the period estimates of $0.^d5137397(68)$, $0.^d5137347(36)$, $0.^d5137469(32)$. The weighted mean value is $P_{orb} = 0.^d5137413(23)$, is slightly different from that of $0.^d5137580(5)$ published by Kim et al. (2010). The initial epoch for the primary minimum is $T_0 = 2453215.57299(83)$.

In Fig. 2, the dependence of the r.m.s. error estimate of the smoothing curve $\sigma[x_C]$ ($= \sigma_{obs}$ in Eq. (18) of Andronov (1994)) is shown as a function of the degree s of trigonometric polynomial. For all three filters, the minimum of this function is seen at $s = 2$. Additional analysis using the program FDCN (FOUR-N) by Andronov (1994) had shown, that the coefficients $C_{s,2j}$ are statistically significant up to $j = 4$. Thus we have chosen $s = 4$, which corresponds to physically better phase curve (i.e. more sharp minima than maxima). For this $s = 4$, the period estimates are $0.^d5137419(70)$, $0.^d5137332(37)$, $0.^d5137454(32)$. The mean weighted value is $P_{orb} = 0.5137405(23)$ and $T_0 = 2453215.5773(13)$. We also computed a “mean weighted” periodogram

$$G(f) = \sum_{i=1}^3 w_i \cdot (1 - S_i(f))$$

with weights proportional to $w_i = (n - 1 - 2s)/(1 - S_{max,i})$, where $S_{max,i}$ is maximal value of the periodogram for a given filter i . The minimum of this function occurs at $P = 0.^d5137404(85)$. Although the period estimate is fairly close to a mean weighted value, the error estimate is significantly larger.

The phase light curves and the corresponding 4-th order trigonometric polynomial fits are shown in Fig. 3. The depth of the primary minimum in different filters is $\Delta_1 V = 0.^m382(13)$, $\Delta_1 R = 0.^m415(7)$, and $\Delta_1 I = 0.^m363(6)$, i.e. very similar. The amplitude is at small maximum in the filter R. The depth of the secondary minimum is $\Delta_2 V = 0.^m240(13)$, $\Delta_2 R = 0.^m219(8)$, $\Delta_2 I = 0.^m229(6)$ is the same within error estimates.

The phase-averaged mean brightness is $C_1 = 4.^m035(6)$, $3.^m365(3)$ and $2.^m836(3)$ for V,R,I, respectively. Although there is no calibration of the comparison star, so the color indices of the object are available only in respect to this comparison star. The differences $((V - R)_{var} - (V - R)_{comp}) = 0.^m570(7)$ and

$((R - I)_{var} - (R - I)_{comp}) = 0.^m629(4)$ are rather large, indicating that the comparison star is a blue one, and the variable is yellow or red. This is in an agreement with expectations for W UMa - type stars (e.g. Tsesevich 1971).

USNO-B1.0 1235-0097170: EA -type

This star was classified as an Algol - type variable. The coefficients of the trigonometric polynomial fit are statistically significant while $s \leq 7$. The TP-7 fits are shown in Fig. 4. The mean weighted values are $P_{orb} = 0.^d8698365(26)$ and $T_0 = 2453208.8503(9)$. For each of these fits, 16 parameters are determined using least squares, with estimates for the r.m.s. accuracy of the fit of $\sigma[x_C] = 0.^m0214$, $0.^m0154$, $0.^m0105$, $0.^m0085$. However, one may see apparent waves at the light curve, especially when at phases badly covered by observations. Such phenomenon is a common problem for signals with very asinusoidal shape. To improve accuracy of fits for EA variables, Andronov (2010) proposed a “New Algol Variable” (NAV) fit, which was also tested by Virnina (2010). The free parameter is the eclipse half-width $\Delta\phi$. We adopted value $\beta = 2$. To determine its statistically optimal value, we computed dependence of the “unit weight error” σ_0 on $\Delta\phi$ for filters BVRI, which is shown in Fig. 5. The minima of this test function appeared at $\Delta\phi$ from 0.089 to 0.100 with a weighted mean of 0.094. The corresponding values $\sigma[x_C]$ of $0.^m0128$, $0.^m0098$, $0.^m0066$, $0.^m0053$ are by a factor of ~ 1.6 better than for the TP fit. The fits are shown in Fig. 6. One may see a significant ellipticity effect arguing that the red star is tidally distorted, and (because of small depth of the secondary minimum) much larger than another component.

Acknowledgements. This work was supported by the Korea Research Foundation (KRF) grant funded by the Korea government (MEST)(No. 2010-0016968) and has been done as part of a cooperative project between Chungbuk National University and the Korea Astronomy and Space Science Institute.

References

- Andronov I.L.: 1994, *OAP*, **7**, 49
 Andronov I.L.: 2003, *ASPC*, **292**, 391
 Andronov I.L.: 2010, <http://www.astrokarpaty.net/kolos2010abstractbook.pdf>
 Andronov I.L., Baklanov A.V.: 2004, *Astronomy School Reports*, **5**, 264, <http://uavso.pochta.ru/mcv>
 Kim Chun-Hwey, Lee Jae Woo, Kim Duck Hyun, Andronov I.L.: 2010, *OEJV*, **126**, 1
 Scargle J.D.: 1982, *ApJ*, **263**, 835
 Tsesevich V.P. (ed.): 1971, *Instationary stars and methods of their investigation. Eclipsing variables*, Moskva: Nauka, 352 p., *1971isme.conf.....T*
 Virnina N.A.: 2010, *OEJV*, **129**, 1

ATLAS OF LIGHT CURVES OF FAINT MIRA-TYPE STARS. STATISTICAL RELATIONS BETWEEN THE CHARACTERISTICS OF SMOOTHED PHASE LIGHT CURVES

L.S. Kudashkina, I.L. Andronov

Department "High and Applied Mathematics", Odessa National Maritime University,
Odessa, Ukraine, kudals04@mail.ru, il-a@mail.ru

ABSTRACT. We propose a set of the photometric parameters which could be useful for the classification of the pulsating Mira-type stars and related objects and determination of the EAGB and TPAGB stages of the stellar evolution.

To solve this problem, the light curves of faint Mira-type stars and of the semi-regular variable V411 Sct were approximated using the program FDCN, which computes a trigonometric polynomial of a statistically optimal degree (I.L.Andronov, 1994, 2003). The atlas of statistically optimal fits of the phase curves of 34 long-period is presented, based on digitized data from the scanned "Atlas" by P. Maffei and G.Tosti (<http://astro.fisica.unipg.it/atlasmaffei/main.htm>).

Some statistical relations between the parameters of the trigonometrical polynomial approximation of the phase curve are analyzed. For an additional criterion of detailed classification of long-periodic variables, we used various parameters, e.g. "period", "amplitude", "asymmetry", "slope of the ascending branch", "characteristic time of brightening by 1^m ". Discussion of the results is presented.

Key words: Variable stars: pulsating: Mira-type.

Earlier we had approximated light curves of 62 variable Mira-type stars based on the observations obtained by the members of AAVSO between 1974 and 1977 using the trigonometrical polynomial with optimum values of number of harmonics and the period (Kudashkina and Andronov, 1996). The atlas of smoothed curves was compiled.

On the basis of this research, for more detailed classification of the Mira-type stars and related semiregular variable red giants and supergiants of an asymptotic branch (for example, at stellar evolutionary stages EAGB and TPAGB), we have introduced three groups of parameters: *t*_{basic} (the period, amplitude, asymmetry of a light curve), additional (degree of a trigonomet-

rical polynom, amplitudes of harmonics, phase shifts in relation to the main wave of a light curve), slope parameters (an inclination of ascending and descending branches of a light curve, time interval of brightness increase by 1^m , difference of this parameter from a corresponding sinusoid). The correlation analysis of 25 parameters from listed above had been carried out. More than 60 dependences have a correlation coefficient of ≥ 0.6 and above. All these dependences were presented in the papers: Andronov, Kudashkina and Rudnitskij (1989); Kudashkina and Andronov (1994, 1996, 1998ab); Andronov and Kudashkina (2006, 2008). In particular, it is noticed that stars RT Cyg, S UMi, T Cas, R Aql, most likely, are at the stage of first helium flash, or they are at the stage of the double shell source; and the stars X Aur, U CMi, possibly, only recently have come to AGB, and the stars T Cam and especially W And are for a long time already at the AGB stage and can undergo multiple flashes in a shell source (Kudashkina, 1999).

In the present work we continue similar research for 34 more stars using the observations of same authors - Paolo Maffei and Gino Tosti (<http://astro.fisica.unipg.it/atlasmaffei/main.htm>). Also the atlas of smoothed light curves was compiled. Examples of light curves for stars representatives of two from three groups of the periods (less than 250 days, from 250 till 350 days and more than 450 days) are shown in Fig. 1,2. The parameters are listed in Table 1.

Contrary to previous papers, it should be noted that here the parameters of a slope of branches ($m_i = (dm/dt)_{asc.br.}$, $t_i = (dt/dm)_{asc.br.}$) are calculated in the middle between the maximum and minimum. In earlier researches where the same parameters were computed at a phase of the largest slope. Correlation coefficients between the pairs of key parameters are listed in the Table 2.

Thus, we don't see significant correlations among the calculated parameters of smoothed light curves.

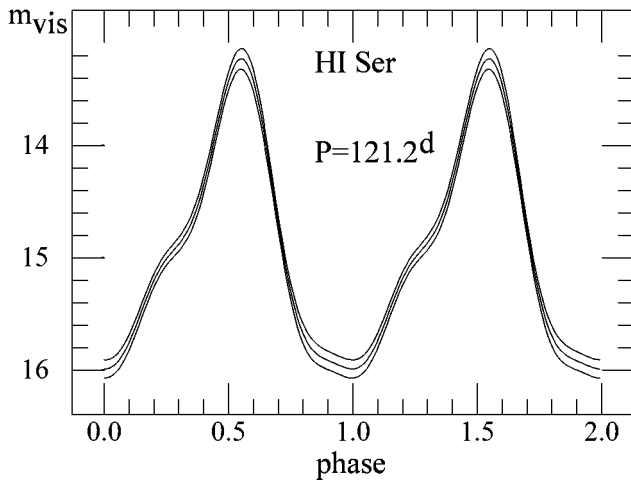


Figure 1. Smoothed light curve of HI Ser.

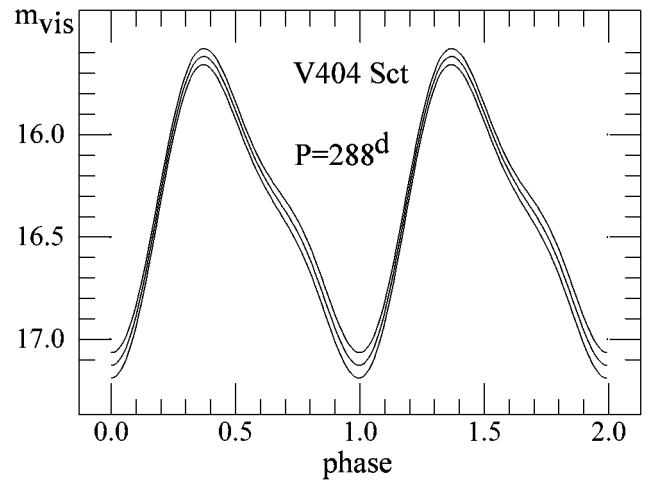


Figure 2. Smoothed light curve of V404 Sct.

Table 1: Characteristics of smoothed phase light curves of faint Mira-type stars

Star	P , d	Δ mag	f	m_i	t_i
LL Ser	250	1.68±.12	0.248±.021	–	–
GI Ser	254	3.93±.09	0.500±.001	-0.049	20.6
LP Ser	258	1.79±.06	0.444±.052	-0.027	36.4
V 420 Sct	261	2.67±.07	0.450±.010	-0.011	90.6
V 1970 Sgr	272	2.10±.06	0.428±.019	-0.029	34.0
GH Ser	272.5	1.56±.06	0.329±.027	–	–
GN Ser	273.5	2.47±.04	0.435±.013	-0.034	29.8
IZ Ser	278	1.68±.08	0.482±.016	-0.009	110.4
V 404 Sct	288	1.51±.04	0.372±.013	-0.010	102.5
V 383 Sct	289	2.58±.07	0.420±.014	-0.029	35.0
V 3926 Sgr	290	2.60±.06	0.398±.0.25	-0.030	33.4
GP Ser	292	3.38±.11	0.509±.014	-0.008	127.3
V 3939 Sgr	292	1.62±.05	0.502±.016	-0.008	120.6
V 3938 Sgr	297	2.59±.06	0.445±.016	-0.028	35.6
GW Ser	298.8	2.97±.11	0.482±.015	-0.024	41.2
V 384 Sct	454	3.15±.06	0.283±.021	–	–
V 411 Sct	457	1.31±.06	0.584±.077	-0.011	94.1
IY Ser	463	3.75±.12	0.595±.017	–	–
ET Ser	463	2.03±.06	0.409±.034	-0.026	38.4
KM Ser	469	4.18±.11	0.429±.017	-0.052	19.2
V 1977 Sgr	469	4.75±.11	0.376±.013	-0.041	24.4
V 409 Sct	469	3.86±.08	0.452±.019	-0.026	38.5
KU Ser	472	3.68±.10	0.586±.008	-0.007	151.0
V 424 Sct	474	4.50±.11	0.500±.001	-0.030	33.6
HH Ser	476	3.25±.08	0.418±.021	-0.034	29.5
V 392 Sct	480	2.49±.05	0.639±.009	–	–
HI Ser	121.2	2.76±.06	0.552±.025	-0.032	31.5
V 3925 Sgr	151.5	3.09±.13	0.486±.028	-0.057	17.4
NSV 10266	168.5	2.21±.07	0.414±.020	-0.040	25.1
GV Ser	230.5	1.47±.05	0.486±.017	-0.008	118.5
NSV 10251	236.5	1.85±.05	0.489±.013	-0.008	126.5
HO Ser	237	1.18±.07	0.512±.020	–	–
LR Ser	239	1.67±.05	0.428±.020	-0.021	48.0
NSV 10642	243	1.77±.08	0.623±.012	–	–

Earlier used parameters of slope of branches, defined at phase of maximum slope correlate better with period and amplitude, than the ones at the middle between maximum and minimum.

Table 2: Correlations between three groups of parameters: 1) “key”: period, amplitude Δ mag and asymmetry f for 34 weak Mira-type stars; 2) “key”: period, amplitude Δ mag and asymmetry f for all stars, including earlier investigated and 34 stars from Table 1.; 3) “parameters of a slope of branches” and amplitude.

Pair of parameters	ρ	σ_ρ	ρ/σ_ρ	N
Δ mag – f	0.058	0.176	0.33	34
P – Δ mag	0.508	0.152	3.34	34
P – f	0.077	0.176	0.44	34
Δ mag – f	-0.278	0.099	-2.80	96
P – Δ mag	0.183	0.102	1.780	95
P – f	-0.095	0.103	-0.93	96
Δ mag – m_i	-0.275	0.011	-2.49	78
Δ mag – t_i	0.308	0.109	2.82	78

References

- Andronov I.L.: 1994, *OAP*, **7**, 49
Andronov I.L.: 2003, *ASPC*, **292**, 391
Andronov I.L., Kudashkina L.S., Rudnitskij G.M.: 1989, IAU Symp. No. 131 Planetary nebulae, 451
Andronov I.L., Baklanov A.V.: 2004, *Astronomy School Reports*, **5**, 264, <http://uavso.pochta.ru/mcv>
Kudashkina L.S., Andronov I.L.: 1994, *KFNT*, **10**, 1, 41
Kudashkina L.S., Andronov I.L.: 1996, *OAP*, **9**, 108
Kudashkina L.S., Andronov I.L.: 1998, Asymptotic Giant Branch Stars, IAU Symp. 191 Poster Session, P2-16, held in Montpellier, France, Aug 28 - Sept 1, 1998
Kudashkina L.S.: 1999, *Vestnik OGU*, **4**, 4, 53
Andronov I.L., Kudashkina L.S.: 2006, *JAAVSO*, **35**, 1, 85
Andronov I.L., Kudashkina L.S.: 2008, *Open European Journal on Variable Stars*, **2008**, **84**, 1

PERIODOGRAM AND WAVELET ANALYSIS OF THE SEMI-REGULAR VARIABLE SUPERGIANT Y CVN

L.S. Kudashkina, I.L. Andronov

Department "High and Applied Mathematics", Odessa National Maritime University,
Odessa, Ukraine, *kudals04@mail.ru, il-a@mail.ru*

ABSTRACT. Time series analysis of the bright cold carbon SR-type star Y CVn was studied. The star belongs at a rare subclass "J" and has a separate asymmetric envelope. It is assumed that no "s" process takes place in this star. Due to this, Y CVn may belong not to the AGB, but to the RGB stage, or to a stage of helium burning in a nucleus after a helium flash. The data from the published international databases of AFOEV (France) and VSOLJ (Japan) were studied using the periodogram and wavelet analysis and the "running sine" approximation. The cycle of variations is 267^d (varying from 247^d to 343^d which are superimposed on 1000^d-10000^d waves.

Key words: Variable stars: pulsating: Semi-regular: Y CVn.

The star Y CVn has other designations HR 4846 =HD 110914 =SAO 44317 =PPM 53169 =HIP 62223 =BD +46 01817 =GC 17342 =TYC 03459-2147 1 =GSC 03459-2147.

This bright carbon cold star of rare J-type has an isolated asymmetric envelope. The star is located not precisely in the center, brightness of an envelope in the western part is smaller. Thickness of an envelope is $(2-5) \cdot 10^{17}$ cm, and an internal radius of the envelope is $7 \cdot 10^{17}$ cm. Distance to the star is 250 parsecs. Rate of mass loss has decreased during recent 14,000 yrs by two orders. Similar variations are present in stars U Hya, U Ant. But Y CVn does not show absorption line of technetium. It is suggested, that there is no s-process in the star. Due to this, Y CVn may be classified not as AGB, but as RGB or being at a stage of stationary burning of helium in nucleus after a helium flash (Izumiura et al., 1996).

Models of stellar pulsations were reviewed by Zhevakin (1963, 1975), Cox (1983).

For the analysis, we have used the observational database of visual observations of the French Association of Variable Star Observers (AFOEV, [ftp://cdsarc.u-strasbg.fr/pub/afoev](http://cdsarc.u-strasbg.fr/pub/afoev)) and of the Vari-

able Star Observers League of Japan (VSOLJ, <http://vsolj.cetus-net.org>) and methods of analysis of multi-periodic oscillations published by Andronov (1994, 2003). Totally, after filtration of "bad" and "fainter than" points, we analyzed 7428 observations obtained during the time interval from JD 24 23904 to 24 51081 (1924-1998 yrs). The observations are distributed in time very irregularly. Especially rare are observations are from JD 24 30115 to 24 38875 (1940-1965 yrs.) with an obvious absence of observations during the Second World war.

Periodogram analysis was carried out using the sine approximation for a trial period. As the test function, we have used $S(f) = r^2$, where r is a correlation coefficient between the observed and calculated values. For the analysis, we have used the programs FO (Four-1), FDCN (Four-N) described by Andronov (1994) and MCV (Andronov and Baklanov, 2004). The periodogram are shown in Fig. 1. The most prominent peak corresponds to a long period of 5150^d. However, it seems to be not a "true" (relatively stable) photometric cycle, but a characteristic value of the cycle length. There are also some other peaks at the periodogram which are listed in Fig. 1. There are two peaks near the value of 365^d, the year duration. These peaks may be interpreted as beat periods between the annual period of observations and a long-term photometric cycle. Interesting peaks occur at 985^d, 159^d.

To check their reliability, we have made a same analysis of artificial data defined at the same moments, as real observations have. The magnitudes were computed as $m(t_i) = m_0 - r \cos(2\pi(t_i - T_0)/P) + \varepsilon_i$, where the mean m_0 , semiamplitude r , initial epoch T_0 and period P are model parameters, and ε_i is normally distributed random value with variance σ_ε^2 . For our analysis, we adopted the period of $P = 267^d$, which is statistically optimal for the wavelet periodogram (see below) and a corresponding initial epoch of JD 24 42114.7. The formal semi-amplitude is 0.^m046(5) is statistically significant, but seems to be underestimated, if the period is not stable. The characteristic (r.m.s.) amplitude was arbitrarily set to $\sigma_\varepsilon = r$.

The periodogram for this artificial data set is also shown in Fig 1. One may note a strong peak corresponding to the model period, but also bias peaks at 995^d and 154^d . Thus we assume that the peaks seen at the periodogram for the observations of Y CVn close to these periods, are just biases and do not correspond to real physical variability of the star.

As the artificial signal did not contain a $\sim 5000^d$ periodicity, nothing significant was seen at the periodogram for the artificial set.

Assuming that the variations may show significant (and multiple) period variations, we have made additional analysis. The initial data set was splitted into 3 intervals of similar duration, which are relatively good covered by the observations, namely JD 2400000+ (24910 - 29965), (41059 - 46384), (46413 - 50718). The corresponding periodograms are shown in Fig. 2. The peaks are often occur at close (but not equal) periods. In this paper, we have used a “mean” periodogram computed as $S(f) = W(t)/(1 + W(t))$, where $W(t)$ is a geometric mean of $W_i(f) = S_i(f)/(1 - S_i(f))$, and $S_i(f)$ is the value of the test-function $D(f)$ for the interval i . The test function $W_i(f)$ has a sense of “signal-to-noise” ratio, i.e. ratio of variance of computed data to the variance of residuals. As the peaks at the periodograms show some shift, the resulting “mean periodogram” seems to be very close to zero (except the $\sim 5500^d$ “period”). The three other peaks again correspond to $\sim 264^d$ period and its annual biases.

Next method was the wavelet analysis using the program WWZ based on the algorithm by Andronov (1998). The “Morlet-based” wavelet periodograms (weighted averages of the wavelet map over time interval) are shown in Fig. 3. Besides a “standard” value of the decay coefficient $c = 0.0125$, we also have used smaller values 0.00125 and 0.000125 , which correspond to increasing period resolution. Generally, the structure of peaks is in an agreement with that at the periodogram. Also annual biases are present at the wavelet periodogram for the “artificial data”. So we adopted the value of the period of $P = 267^d$, which was used for the artificial data set. The number of peaks increases with decreasing c , indicating that the periods are not stable.

To check stability of period and other characteristics, we have used finally another complementary algorithm, So the “rectangular weight function” wavelet with a fixed period (=“running sine”, Andronov (2003)) was computed. The local fit $m_C(t) = m_0 - r \cos(2\pi((t - T_0)/P - \phi))$ was computed for each trial value of t_0 using the data in the interval from $(t_0 - \Delta t)$ to $(t_0 + \Delta t)$. For such a “running approximation”, we have used a filter half-width of $\Delta t = 0.5P_1$. The “initial epoch” for maximum magnitude (minimum brightness) is $T_0 = 24\,41981.2$, and $P = 267^d$. The parameter ϕ is the phase of maximum brightness (minimum magnitude).

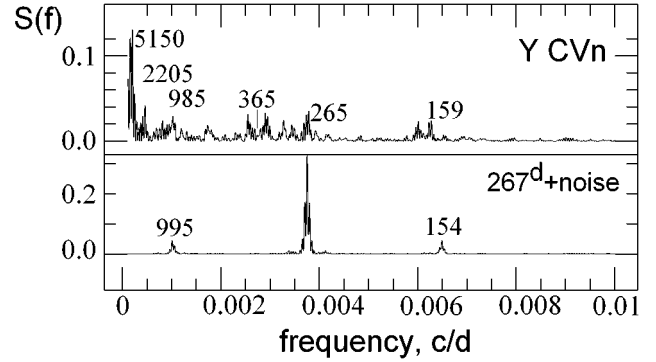


Figure 1: Periodograms for observations of Y CVn for all data (up) and for simulated “sine+noise” data. The numbers mark period values corresponding to some prominent peaks.

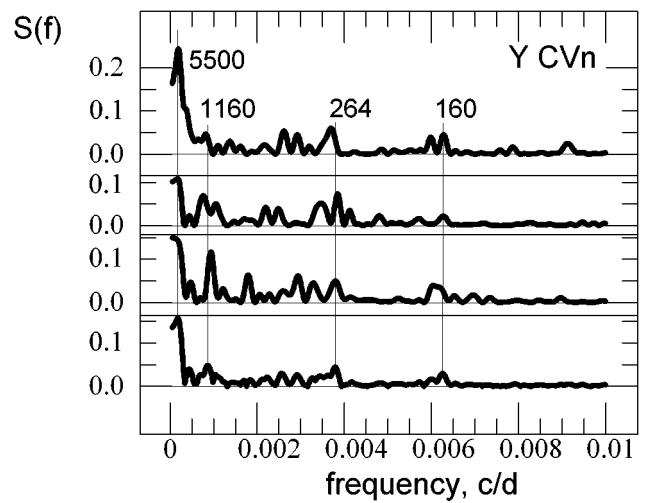


Figure 2: Periodograms for observations of Y CVn for three time intervals best covered by the observations. At bottom, there is a “mean” periodogram. The numbers mark period values corresponding to some prominent peaks at the “mean” periodogram.

The dependence of characteristics of the “running sine” approximation on trial time are shown in Fig. 4 as well as the original observations at the same scale. To study long-term variations, the best variable parameter is m_0 . It shows drastic variations from $5.^m43$ to $6.^m15$ at most prominent timescales of 1000^d and 10000^d . The semi-amplitude r sometimes reaches $r = 0.^m44$, but also vanishes down to $0.^m001$. Not unexpectedly, at these times of “constancy”, the phase may undergo jumps. The variations of phase show “linear parts” corresponding to “stable period,” but the values differ from 247^d (JD 24 45322-46499) to 343^d (JD 24 24362-27129).

Acknowledgements. The authors thank the observers and the staff of the AFOEV and VSOLJ international databases. for the free access.

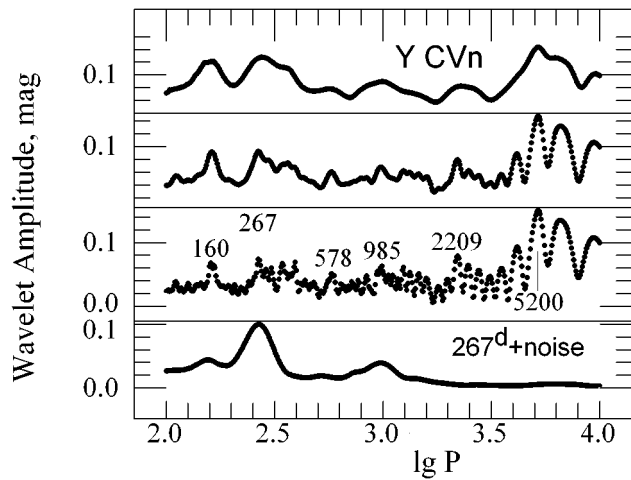


Figure 3: “Wavelet periodogram” for all data values for different values of the decay coefficient c (0.0125, 0.00125 and 0.000125 from top to bottom, respectively. The bottom curve corresponds to the noisy periodic data and $c = 0.0125$.) The numbers mark period values corresponding to some prominent peaks for $c = 0.000125$ - the wavelet with best period resolution.

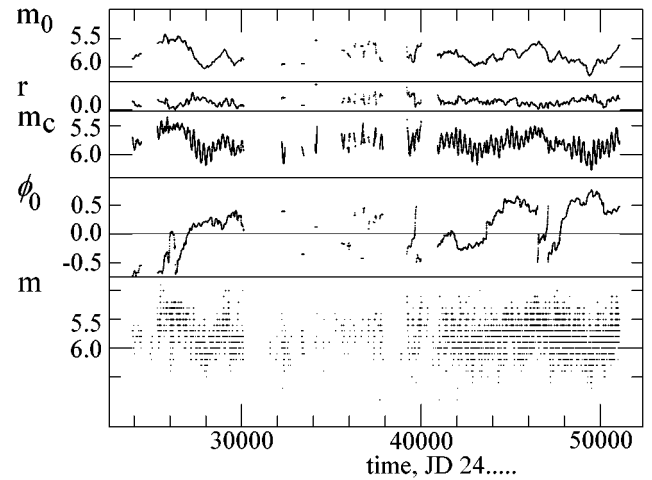


Figure 4: Dependence of the characteristics period and amplitude on trial time for different values of c .

References

- Andronov I.L.: 1994, *OAP*, **7**, 49
 Andronov I.L.: 1998, *KFNT*, **14**, 490
 Andronov I.L.: 2003, *ASPC*, **292**, 391
 Andronov I.L., Baklanov A.V.: 2004, *Astronomy School Reports*, **5**, 264, <http://uavso.pochta.ru/mcv>
 Cox J.P.: 1980, *Theory of stellar pulsations*, Princeton Ser. in Ap.
 Izumiura H., Hashimoto O., Kawara K., Yamamura I., Waters L.B.F.M.: 1996, *As.Ap.*, **315**, L221
 Zhevakin S.A.: 1963, *ARAA*, **1**, 367
 Zhevakin S.A.: 1975, *Theory of Stellar Pulsations*, in: Pulsating Stars. Ed. B.V. Kukarkin, J.Wiley & Sons, N.Y., 1

ONE-METER TELESCOPE IN KOLONICA SADDLE - 4 YEARS OF OPERATION

I. Kudzej¹, P.A. Dubovsky²

¹ Vihorlat Astronomical Observatory Humenne, Slovakia, *vihorlatobs1@stonline.sk*

² Vihorlat Astronomical Observatory Humenne, Slovakia, *var@kozmos.sk*

ABSTRACT. The actual technical status of 1 meter Vihorlat National Telescope (VNT) at Astronomical Observatory at Kolonica Saddle is presented. Cassegrain and Nasmyth focus, autoguiding system, computer controlled focusing and fine movements and other improvements achieved recently. For two channel photoelectric photometer the system of channels calibration based on artificial light source is described. For CCD camera FLI PL1001E actually installed in Cassegrain focus we presents transformation coefficients from our instrumental to international photometric BVRI system. The measurements were done during regular observations when good photometry of the constant field stars was available. Before FLI camera acquisition we used SBIG ST9 camera. Transformation coefficients for this instrument are presented as well.

In the second part of the paper we presents results of variable stars observations with 1 meter telescope in recent four years. The first experimental electronic measurements were done in 2006. Both with CCD cameras and with two channel photoelectric photometer. Starting in 2007 the regular observing program is in operation. There are only few stars suitable for two channel photoelectric photometer observation. Generally the photometer is better when fast brightness changes (time scale of seconds) must be recorded. Thus the majority of observations is done with CCD detectors. We presents an brief overview of most important observing programs: long term monitoring of selected intermediate polars, eclipse observations of SW Sex stars. Occasional observing campaigns were performed on several interesting objects: OT_J071126.0+440405, V603 Aql, V471 Tau eclipse timings, Z And in outburst.

Key words: Stars: binaries: cataclysmic, eclipsing; Telescopes; stars: individual: Z And, V603 Aql, TT Ari, VW Ari, MU Cam, BG CMi, V471 Tau.

1. Introduction

Vihorlat National Telescope (VNT) is the main instrument of The Astronomical Observatory at Kolonica

Saddle. Its main parameters are listed below.

Table 1: Main technical parameters

Main mirror diameter	= 1000 mm
Cassegrain focus focal length	= 9000 mm
CCD camera FLI PL1001E,	
Pixel scale with binning 2x2:	1 px = 1.10 arcsec

The telescope can work in 4 different operational modes:

- PEP - photoelectric photometry in Cassegrain focus and autoguiding through photometer.
- CCD photometry in Cassegrain focus and autoguiding on Pointer telescope.
- CCD photometry with Pointer telescope, simultaneous photoelectric photometry and autoguiding in Cassegrain focus of VNT.
- Visual observation in Nasmyth focus.

The detailed description of the telescope and detectors can be found in Kudzej et al. 2007.

2. Description of the instrument

2.1. Differential photometry with 2 channel photometer

The typical observing run looks as follows: Automatic sky measurement through diaphragm with diameter 30 arcsec every 100 - 200 exposures. The number of exposures is generated randomly in the range stated by observer. Star measurements through diaphragm #3 - diameter 40 arcsec. Exposure time 10 sec. Filter B, V or R. Calibration on constant star only in good photometric nights. Calibration on artificial light source (diode) during the observing run 3 - 5 times.

Typical serie:

5K,[5Vsky, 100-200Vstar,5Vsky]..... [5Vsky, 100-200Vstar,5Vsky],5K.

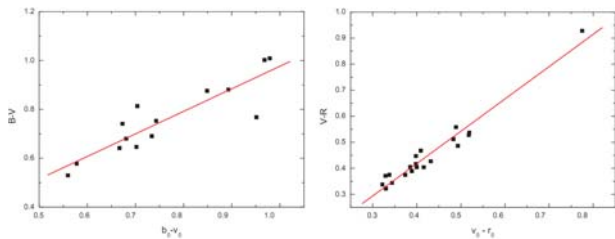


Figure 1: Dependency of $(b - v)$ vs. $(B - V)$ and $(v - r)$ vs. $(V - R)$ for combination of VNT and FLI camera. Observations made in January 2010.

2.2 Autoguiding system

Autoguiding of the VNT is carried out by TV Guider constructed by M. Myslivec from Czech Republic.

2.3 Autofocusing

The possibility of remote control of focusing has big impact on quality of observation. We have focusing system based on synchronous motors on secondary mirror of VNT. The control is carried out by the same software we control the CCD camera - Maxim DL.

2.4 Transformation coefficients for CCD photometry

We use transformation equations: $V = v + \zeta_v(B - V)$, $B - V = \zeta_{bv}(b - v)$, $V - R = \zeta_{vr}(v - r)$, where we denote b , v and r above-atmosphere instrumental magnitudes for used filters and B , V and R corresponding standard magnitudes. The following results were obtained analyzing images obtained during regular observations of enigmatic polar OT J071126.0+440405. Values of standard stars are from Henden's photometry (Henden & Honeycutt 1995).

Table 2: Weighted transformation coefficients with errors in parenthesis for BVR filters for used combinations of telescopes and CCD cameras.

Instrument	ζ_v	ζ_{bv}	ζ_{vr}
Pointer+FLI	0.002(8)	0.993(24)	1.005(19)
VNT+SBIG ST9	0.004(12)	0.991(29)	0.993(17)
VNT+FLI	0.001(7)	0.994(24)	1.007(17)

3. Observing results with two channel photoelectric photometer

3.1. Asteroseismology with 2 channel photometer

In 2007 we have performed campaigns on two low amplitude Delta Scuti type pulsating variables V2314

Oph and VW Ari. Our results were compared with the light curves and frequency patterns from the other observatories and presented at Kolos conference in 2007.

3.2. High time resolution photometry of TT Ari

There are rapid brightness variations in the active state of this cataclysmic star. We made 5 observations with 2 channel photometer on VNT with time resolution 1 second during the autumn 2007. One observation was simultaneous measurements with VNT (Photometer) and Pointer (CCD camera) telescopes.

4. Observing results - CCD photometry

4.1. Inter-Longitude Astronomy (ILA) long term monitoring of intermediate polars

The goal of the campaign is to monitor the selected intermediate polars for spin period changes (Andronov et al. 2003). Detailed data analysis is done by Prof. Andronov team including data from Korea, Crimea and USA. The list of targets is in the Table 3.

Table 3: Selected targets of the Interlongitude Astronomy monitoring

Star	P_{orb} [min]	P_{spin} [sec]	V
RXJ2133.7+5107	431.58	571	16.0
MU Cam	283.12	1187	15.0
BG CMi	194.04	913	14.5
PQ Gem	311.56	834	14.0
1RXS J063631.9+353537	201	1008	17.0
1RXS J070407.9+262501	250	481	17.0
DO Dra	238.14	528	14.5
V795 Her	155.88	950?	12.5
1RXS J180340.0+401214	160.21	1520.51	17.0
1RXS J192626.8+132153	291?	938.6	18.0
FO Aqr	290.96	1254.284	14.0
AO Psc	215.46	805	14.0
V603 Aql permanent superhumper	198.85	-	12.0
V1432 Aql asynchronous polar	201.94	202.50 min	12.0

Some interesting results up to now are depicted in figures 2 - 5.

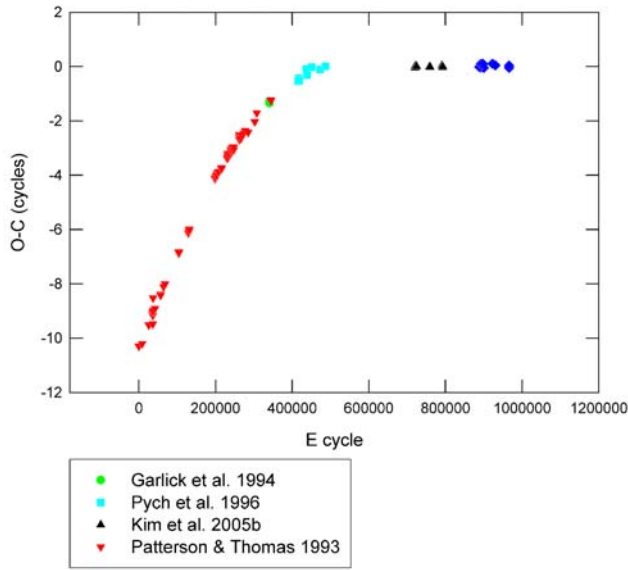


Figure 2: **BG CMi**. O-C diagram of pulse maxima calculated with the linear ephemeris $HJD_{max} = 2453105.31448 + 0.01057257716 \times E$. Cycle counting according Kim et al. 2005b. *DPV* means observations made by co-author P.A.D with VNT.

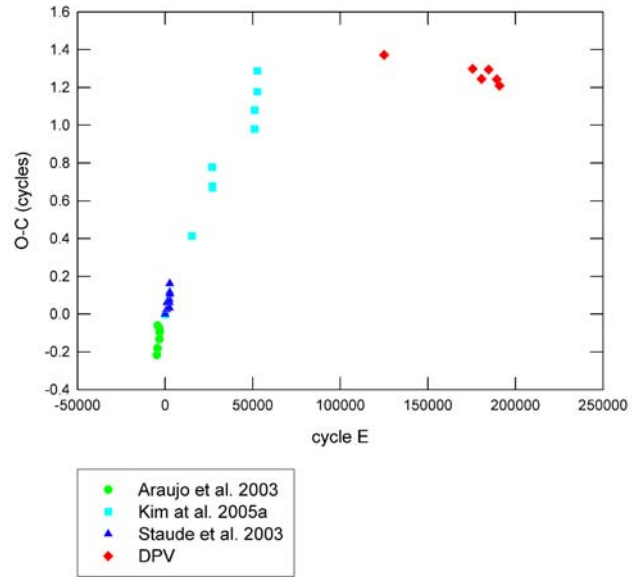


Figure 4: **MU Cam** = 1RXS J0625+7334. O-C diagram of pulse maxima calculated with the linear ephemeris: $HJD_{max} = 2452682.4181 + 0.0137408 \times E$. - 1 cycle after E=26826.

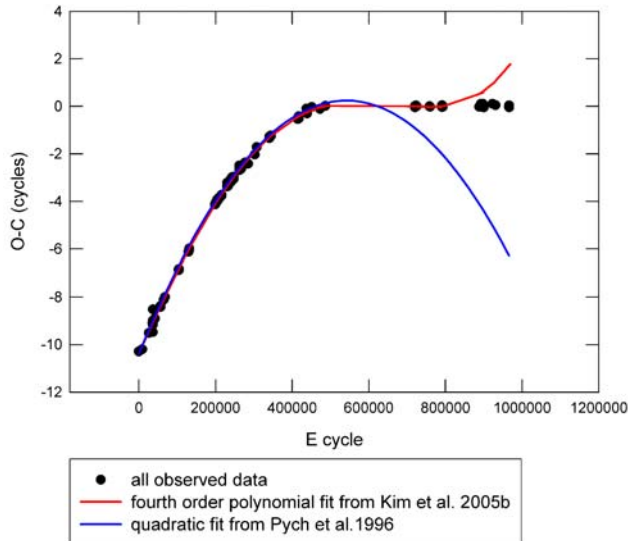


Figure 3: **BG CMi**. Comparison with previously published models. No one from previously published quadratic, cubic or even fourth-order polynomial ephemeris fits new data.

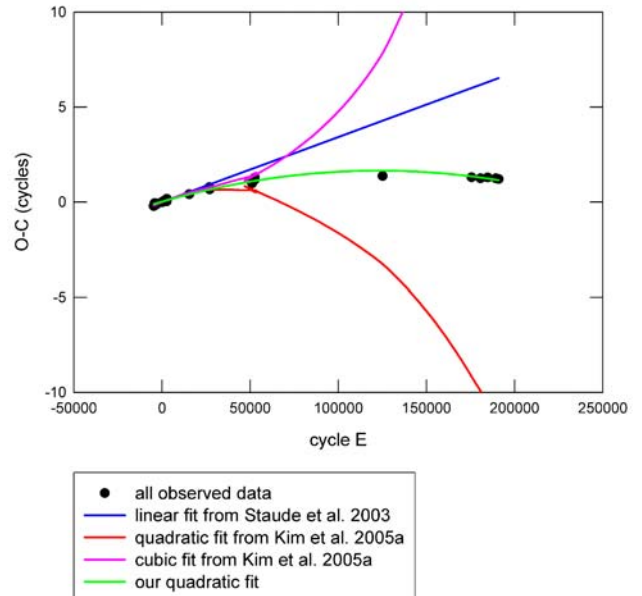


Figure 5: **MU Cam**. Comparison with previously published models.

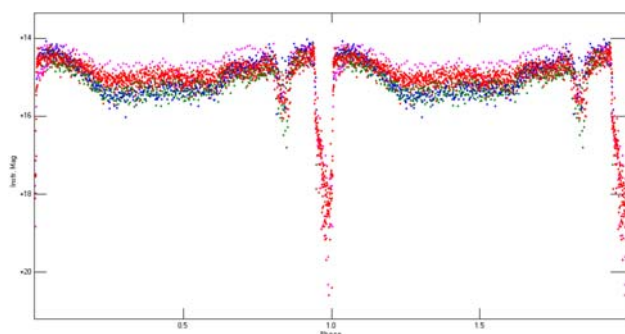


Figure 6: *OT J071126.0+440405*. Folded light curve. Different color corresponds to different filter used.

4.2. Inter-Longitude Astronomy campaign

OT J071126.0+440405

This object was discovered in January 2009 by Catalina Sky Survey (Drake et al. 2009) as relatively bright polar with deep eclipses. In the active state there is a pre-eclipse dip at phase -0.13 interpreted as eclipse caused by accretion stream falling toward white dwarf. Total 3 types of eclipses and 3 distinctly separate luminosity states were observed during the intense observing campaign during the spring 2009.

4.3. *V603 Aql*

In the summer 2009 N. Virnina carried out observing campaign with VNT on this nova like variable. Total 14 light curves with R and V filter interchanged. Rapid brightness variations were covered with 30 s time resolution. No important color variations were observed.

4.4. Eclipse mapping of *SW Sex* stars

The SW Sextantis stars compose a group of nova-like cataclysmic variables. The main goal of observing program proposed by A. Halevin (Odessa) is to observe the shape of the eclipse and to model the accretion disc using eclipse mapping method. Our list of observed eclipsing systems:

- LX Ser
- TT Tri
- HS0455+8315
- HS0728+6738

4.5. *Z And*

The prototype of symbiotic stars showed low amplitude irregular variations during autumn 2009 outburst. We have collected 5 light curves with VNT or Pointer telescopes in B, V, and Rc filters.

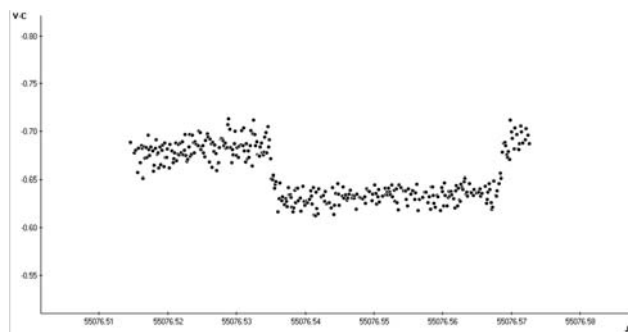


Figure 7: **V471 Tau**. 20.08.2009.

4.6. *V471 Tau*

Eclipsing pre cataclysmic system with eclipses observable only in U and B filter. The start and the end of

eclipse is very sharp. So we needed good time resolution. We used exposure time 10 s in B filter. Our results confirmed sinusoidal character of O-C diagram.

Acknowledgements. The work was supported by the Ukrainian MON grant No M/153-2006 and the Bilateral APVV grant SK-UK-01006, as also the Grant of the Slovak Research and Development Agency LPP-0049-06 and LPP-0024-09 and The National Scholarship Programme of the Slovak Republic. SBIG ST9 camera was kindly provided by K. Petrik from Hlohovec Observatory.

References

- Andronov I.L., Antoniuk K.A., Augusto P., et al.: 2003, *As. Ap. Transact.*, **22**, 793.
- Araujo-Betancor S., Gaensicke B.T., Hagen H.J., et al.: 2003, *A&A*, **406**, 213.
- Drake A.J., Djorgovski S.G., Mahabal A., et al.: 2009, *ApJ*, **696**, 870.
- Garlick M.A., Rosen S.R., Mittaz J.P.D., et al.: 1994, *MNRAS*, **267**, 1095.
- Henden A.A., Honeycutt K.T.: 1995, *PASP*, **107**, 324.
- Kim Y., Andronov I.L., Park S.S., et al.: 2005, *JA&SS*, **21**, 191.
- Kim Y., Andronov I.L., Park S.S., et al.: 2005, *JA&SS*, **22**, 197.
- Kudzej I., Karetnikov V.G., Dubovsky P.A., et al.: 2007 *OAP*, **20**, 100.
- Patterson J., Thomas G.: 1993, *PASP*, **105**, 59.
- Pych W., Semeniuk I., Olech A., et al.: 1996, *AcA*, **46**, 279.
- Staude A., Schwöpe A.D., Krumpke M., et al.: 2003, *A&A*, **406**, 253.

SPECTRAL INVESTIGATIONS OF CM DRA

M.K. Kuznetsov¹, Y.V. Pavlenko¹, D. Pinfield², H. Jones²

¹ Main Astronomical Observatory of National Academy of Sciences
27 Zabolotnoho, Kyiv-127, 03680 Ukraine, *astro@paco.odessa.ua*

² Centre for Astrophysics Research, University of Hertfordshire
College lane, Hatfield, AL10 9AB, UK

ABSTRACT. We present an analysis of a high resolution ($R=47000$) echelle spectra of the low-mass eclipsing binary CM Draconis, which were obtained on the 4.2-m William Herschel Telescope. Spectra were obtained for various phases of the orbit. There are some difficulties in echelle spectra processing of cool stars, since it is hard to get energy distribution in a large scale in such spectra. We proposed an efficient method for making the continuum of spectrum of cool stars. We refined the parameters (effective temperature, rotational velocity and metallicity) of the components of the system CM Dra using the method of stellar atmospheres. The data that we obtained are in good agreement with the results obtained by other authors. It is indicate on efficiency of our technique. The errors of temperature and metallicity determinations is about 100 K and 0.3 dex respectively.

Key words: Stars: binary: eclipsing binary, fundamental parameters: stars, low-mass: stars; stars: individual: CM Dra

1. Introduction

The CM Dra is low-mass eclipsing binary system. It is classical double-lined spectroscopic binary. Period of the system is $P = 1.268$ day (Metcalf et al. 1996). CM Dra is high proper motion object, it can be attributed to Population II (Lacy 1977). The orbits eccentricity of CM Dra is $e = 0.00051$ (Morales et al. 2009). This may indicate the presence of a third component in the system. Components of CM Dra are almost identical cool dwarfs. Their spectral types are estimated as dM4.5 (Metcalf et al. 1996). Both components of CM Dra are metal poor stars (Viti et al. 2002). Masses and radii for the components are known with high accuracy. $M_1 = 0.23M_{sun}$; $M_2 = 0.21M_{sun}$; $R_1 = 0.25R_{sun}$; $R_2 = 0.23R_{sun}$ (Morales et al. 2009) It makes CM Dra good test object for studying models of cool dwarfs atmospheres and spectra processing methods.

2. Observations and reduction

High-resolution spectral observations of CM Dra were carried out on the 4.2-m William Herschel Telescope using the echelle high-resolution spectrograph (UES). The spectra were obtained during queue observing runs from 20 to 23 May 1997 in different phase. In the course of this work we used 64 spectra of CM Dra. Resolution of obtained spectra is $R=47000$, spectral range is 4500 -10000 AA. In the observed spectrum we resolve spectral lines of both components. In case of the echelle spectra we lost information about energy distribution in a large scale in the spectra, which is important for analysis of cool dwarf spectra. It is possible to use only a few strong atomic lines which can be identified against the background of TiO bands in spectra M dwarfs. In fact, we can work here with pseudocontinuum formed by the haze of molecular lines. In the framework of this work we used spectra of divisor for determination of pseudocontinuum level. We found the good enough agreement between synthetic and reduced observed spectrum.

3. Atmosphere models of components and synthetic spectra of CM Dra

Synthetic spectra were calculated for different T_{eff} and abundances. A rotational velocity $V \sin(i) = 10$ km/s and microturbulent velocity $V_{turb} = 3$ km/s was adopted. We used NextGen models (Hauschildt et al. 1999) as stellar atmospheres models. Synthetic spectra were computed by program WITA6 (Pavlenko 1997) for both components. We used the line list of atomic line from VALD (Kupka et al. 1999) and the line list of TiO from Plez et al. 1998.

To account the duality of the system, i.e. we composed synthetic spectra of the components according to their radial velocities. From the best fitting theoretical to observed spectra of CM Dra in regions of NaI (8185 AA, 8197 AA), RbI (7818 AA) and CaI (6719 AA) we determined $T_{eff} = 3100$ K and metallicity $[M/H] = -0.5$ dex for each component. The

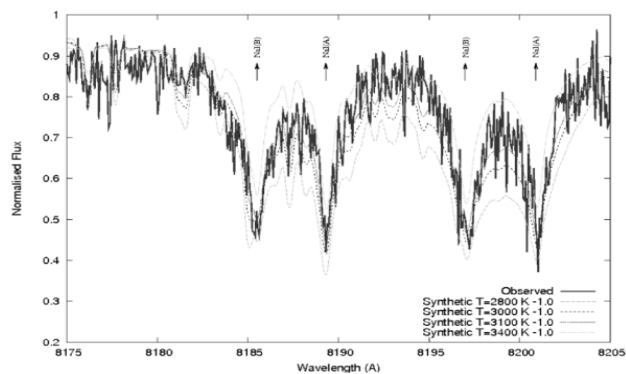


Figure 1: Fits of CM Dra synthetic spectra computed with different T_{eff} in the region of NaI 8185, NaI 8197 lines $T_{eff}=2800$ K; $T_{eff}=3000$ K; $T_{eff}=3100$ K; $T_{eff}=3400$ K; $V_{sin(i)}=10$ km/s; $V_{turb}=3.0$ m/s

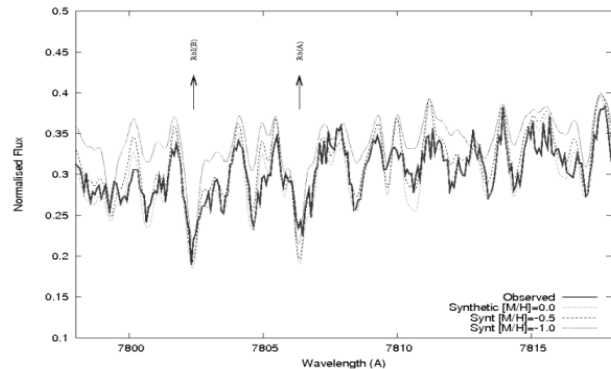


Figure 2: Fits of CM Dra synthetic spectra of computed with different $[M/H]$ in the region of Rb 7802 line $[M/H]=0.0$; $[M/H]=-0.5$; $[M/H]=-1.0$

errors of temperature and metallicity determinations is about 100 K and 0.3 dex respectively. These results are in good agreement with previous studies.

4. Conclusions

We determined effective temperature and metallicity of CM Dra components. Effective temperature of both components is $T_{eff}=3100$ K \pm 100 K and metallicity is $[M/H]=-0.5 \pm 0.2$. Our results are in good agreement with previous studies. Thus we can be confident of the effectiveness of our methodology for the analysis of stellar atmospheres of binary systems. In the near future investigations we investigate some interesting effects due to the interaction between the components, such as overheating of the the part of atmosphere of one component by the irradiation by the second component, etc.

Acknowledgements. This work was supported by the FP7 project RoPACS (ROPACS PITN-GA-2008-213646) and the program Cosmomicrophysics of NAS of Ukraine.

References

- Haushildt P., Allard F., Baron E.: 1999 *Astrophys. J.*, **512**, 337
 Kupka F., Piskunov N., Ryabchikova T.A., Stempels H.C., Weiss W.W.: 1999 *A&A Suppl.*, **138**, 119
 Lacy C.H.: 1977 *Astrophys. J.*, **218**, 444
 Morales J.C., Ribas I., Jordi C. et al.: 2009 *Astrophys.J.*, **691**, 1400
 Metcalfe T.S., Mathieu R.D., Latham D.W., Torres G.: 1996 *Astrophys. J.*, **456**, 356
 Pavlenko Ya.V.: 1997 *Ap&SS*, **253**, 43
 Plez B.: 1998 *A&A*, **337**, 495
 Viti S., Jones H.R.A., Maxted P., & Tennyson J.: 2002 *MNRAS*, **329**, 290

THE PHOTOMETRIC INVESTIGATION OF THE ACTIVE POST-NOVA CP LAC IN HIGH AND LOW STATE OF BRIGHTNESS IN 2006-2008 YRS

A.A. Litvinchova^{1,2}, E.P. Pavlenko¹

¹ Crimean Astrophysical Observatory
Nauchny, Crimea 98409, Ukraine, *litanya@ukr.net*

² Tavrida National V. Vernadsky University
Simferopol, Crimea 95007, Ukraine

ABSTRACT. We present the result of investigations of the quasi-periodic and periodic light variations of the CP Lac connected with different sources in the binary system. We found that CP Lac in 2006 was brighter on $\sim 1^m$ in comparison with 2008. The amplitude of the light variations in 2006 is growing with decreasing of the wave-length. The amplitude in B = $0^m.3$, in V = $0^m.2$. The mean brightness of CP Lac in 2008 varies from night to night during all interval of observation with amplitude $0^m.5$ in unfiltered light. Data of observations in 2006-2008 have a general period 0.037(5) day that is possibly related to the period of rotation of white dwarf.

Key words: Stars: binary: cataclysmic; stars: individual: CP Lac.

1. Introduction

CP Lacertae=Nova Lac 1936 is a non-eclipsing close binary system consists of a late-type red dwarf secondary losses its matter onto a white dwarf primary component via accretion disk. This system showed small-amplitude outbursts of dwarf nova-type. Our photometric investigation this star in 2003-2005 did not shows period 0.127 day suggested by Rodrigues-Gil and all (2005). We found that 1/0.127 cycle/day photometrical frequency found by Rodrigues-Gil and Torres obviously is a one-day alias of the frequency that is very close to the orbital one (6.89 day) (Pavlenko et al. 2007). To study the photometric behavior of this star and confirm the orbital period we have undertaken the long-term observations between 2006-2008.

2. Observations and data reduction

The photometric observations of CP Lac have been

carried out in the Crimean astrophysical observatory in the primary focus with the 2.6-m Shajn telescope (ZTSh) and with the Cassegrain 38cm (K-380) telescope between 2006 and 2008. The observations were made in the *BV* - Johnson system in 2006 November 20, in the *V* - Johnson system in 2007 August 29, without filter - white light in 2008 January-February during 11 nights and in 2008 May 21. The time scale of exposure was 5 sec for observations of the ZTSh, and from 60 sec to 180 sec for observations of the K-380. The data reduction was made using the aperture photometry package by Goranskij and program of MaxIm DL V4. The accuracy of a single observation varied from $0^m.01$ (ZTSh) to $0^m.05$ (K-380). We used the star from the catalogue USNO B1.0 1456-0394402 as the comparison star.

3. Analysis of the Light Variations of the CP Lacertae

Figures 1-4 show the nightly light curves for each of the year discussed here.

The examples of nightly light curves in 2006 are present in Fig.1. The light curves are dominated by intense and rapid variations (tens of minutes time scale). The amplitude of the light variations is growing with decreasing of the wave-length: amplitude in B-band = $0^m.3$, in V-band = $0^m.2$. For this data we calculated the color-index B-V (the amplitude is equal to the $0^m.2$). As decrease brightness of star its color index B-V is most blue.

The amplitude of the CP Lac light variations in 2007 is $0^m.35$ (Fig.2).

In Fig.3 the individual unfiltered light curves of CP Lac in 2008 are given. Light curves are highly variable from night to night. The amplitude variations could reach $0^m.5$ in some cases. All these data are combined together and shown in this plot. One could see that

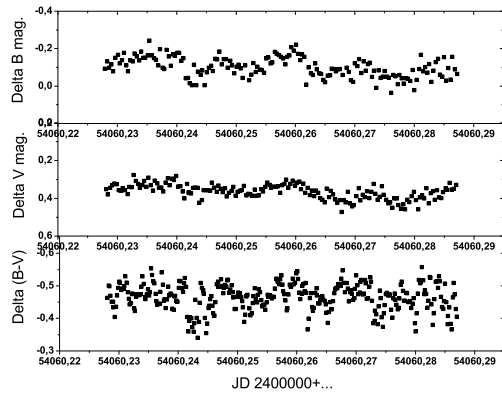


Figure 1: The example of the BV-data in 2006.

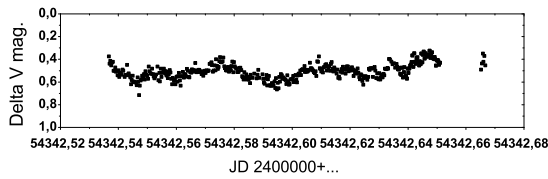


Figure 2: V-band light curve of CP Lac in 2007.

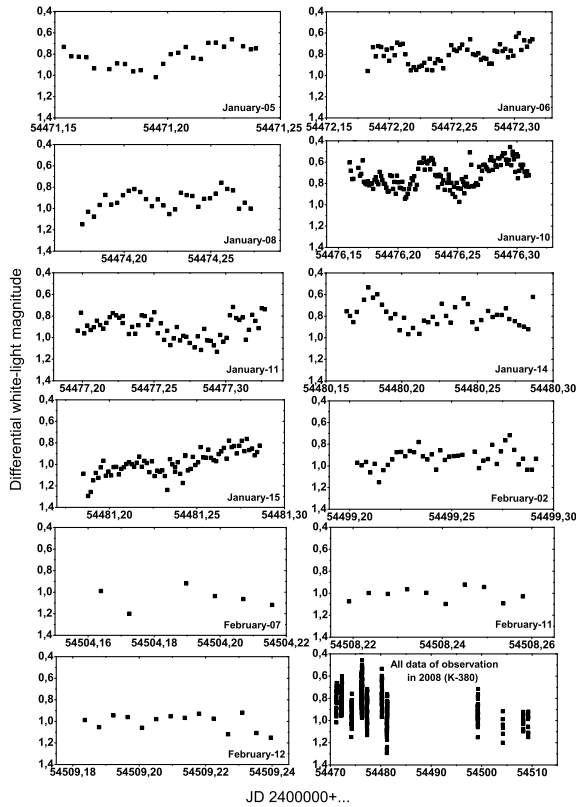


Figure 3: Unfiltered light curves of CP Lac obtained with the K-380 in 2008.

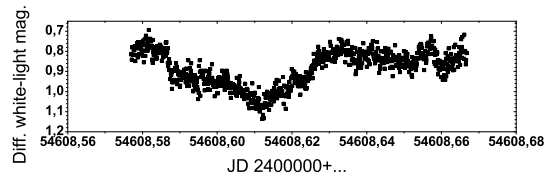


Figure 4: Periodograms computed from all the CP Lac light curves in 2006-2008

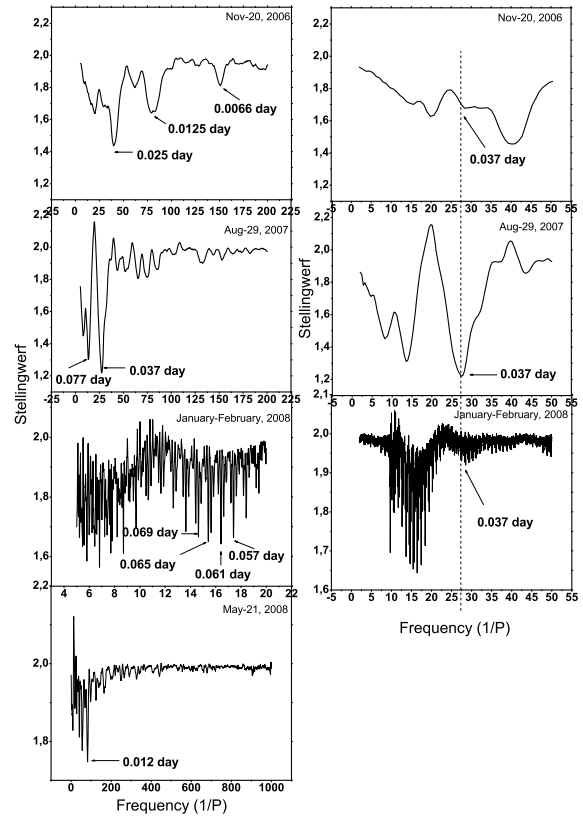


Figure 5: Unfiltered light curves of CP Lac obtained with the ZTSh in 2008.

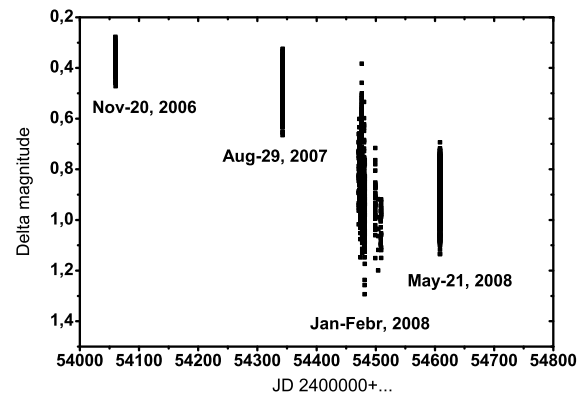


Figure 6: Long-term light curve of CP Lac. The plot shows a variation of the mean brightness from year to year.

the mean brightness varies from night to night during all intervals of observation in 2008. High-amplitude light curve for May 21 in 2008 is present in Fig.4. The amplitude of the light variations is $0^m.4$.

To search for periodicities in the light curves, we computed periodograms with ISDA package (Pelt 1992) using the Stellingwerf method after subtracting the nightly average trend. The resulting Fourier transform is present in Fig.5. The periodogram was constructed in the region of the 0.005-0.2 days for 2006-2007 years; in the region of the 0.05-0.2 days for January-February 2008. For construction of periodogram for May 21, 2008 we subtracted a period 0.084 day with four harmonics (Fig. 5, left panel). Right panel shows low-frequency part of spectrum (in the region of the 0.02-0.5 days).

The periodograms displays the series of significant peaks separated by day^{-1} , where the most significant peaks were marked by arrows for each year. The period 0.037 day (53 min) is present on all data observations of CP Lac between 2006 (ZTSh), 2007 (ZTSh), 2008

(K-380) (Fig.5, right panel). We supposed that this period to connected with the period of rotation of the white dwarf. Within the limits of errors this period coincides with period registered by Rodrigues-Gil et al (0.0435 \pm 0.0002 d)(2005).

The long term light curve of CP Lac is shown in Fig.6. The mean brightness is modulated with a periodicity of a few years. CP Lac in 2006 was brighter on $\sim 1^m$ in comparison with 2008.

Acknowledgements. This work was partially supported by the grant of the Ukrainian Fund of Fundamental Research F 25.2/139 and F28.2/081.

References

- Pavlenko E.P., Litvinchova A.A., Katysheva N.A. & Shugarov S.Yu.: 2007, *ASP Conf. Ser.*, **370**, 324.
Pelt Ja.: 1992, *Irregularly Spaced Data Analysis*, Helsinki.
Peters C.S. & Thorstensen J.R.: 2006, *PASP*, **118**, 687.
Rodríguez-Gil P. & Torres M.A.P.: 2005, *Astron & Astrophys.*, **431**, 289.

MODELING THE OPTICAL SPECTRUM OF ROMANO'S STAR IN MINIMUM BRIGHTNESS

O. Maryeva¹, P. Abolmasov²

¹ Stavropol State University, Stavropol 355001, Russia, *olga.maryeva@gmail.com*

² Sternberg Astronomical Institute, Moscow 119292, Russia

ABSTRACT. V532, known as Romano's star, is an interesting variable star located in the M33 galaxy. We study its spectral variability and the optical spectrum in minimum brightness. Using the non-LTE radiative transfer code CMFGEN we model the structure of its expanding atmosphere and stellar wind. The calculations show that all the observed properties of the object are well described by a late WN star model with high hydrogen abundance. We find that the luminosity of the object is $L = (0.8 \pm 0.2) \cdot 10^6 L_{\odot}$, its mass loss rate is $(4.5 \pm 0.5) \cdot 10^{-5} M_{\odot}/\text{year}$ and the terminal wind velocity is $400 \pm 100 \text{ km/s}$. We also find that H/He is $1.3 \div 1.8$.

Key words: stars: individual:Romano's star (M33); stars: Wolf-Rayet

1. Introduction

Luminous Blue Variables (LBVs) are broadly accepted as very massive and energetic stars emitting close to the Eddington limit, evolving from Of towards Wolf-Rayet stars. But the links between LBV, nitrogen-rich Wolf-Rayet (WN) and hydrogen-rich WN (WNH) stars are uncertain. Studying LBVs in nearby galaxies is very important for understanding stellar evolution and mass loss in different environments.

Romano's star is named after Italian scientist Giuliano Romano who was the first to notice its irregular variability (Romano, 1978). This object ($\alpha = 01^{\text{h}}35^{\text{m}}09.^{\text{s}}71$, $\delta = +30^{\circ}41'57''.1$, epoch 2000) is located in the outer spiral arm of the M33 galaxy. Now V532 is classified as an LBV star because it demonstrates both photometric and spectral variability (Kurtev et al. (2001), Viotti et al. (2007), Maryeva & Abolmasov (2010)).

In this article we study the spectral changes of V532 using archival data. We investigate the optical spectrum in minimum brightness using the non-LTE radiative transfer code CMFGEN. We describe the data and data reduction process in the next section. Spectral variability is presented in section 3, results

of modeling in section 4. In section 5 we make the conclusions.

2. Observations and Data Reduction

We use archival data from the 6m telescope of the Special Astrophysical Observatory (SAO) of Russian Academy of Sciences (RAS) and the SUBARU telescope. The 6m telescope data were obtained with the Multi Pupil Fiber Spectrograph (MPFS) (Afanasiev et al., 2001) and with the SCORPIO multi-mode focal reducer in the long-slit mode (Afanasiev & Moiseev, 2005). The data from SUBARU were obtained with the Faint Object Camera (FOCAS) (Kashikawa et al., 2002) in the Cassegrain focus.

All the spectra were reduced using IDL-based software. The reduction process includes all the standard reduction steps.

3. Spectral Evolution

Figure 1 shows all the spectra of V532 in the blue range (4000-5500 Å) analysed in this work, obtained between 2002 and 2007 at different spectral resolutions. It also shows a spectrum obtained by Szeifert (Szeifert, 1996) at Calar Alto with TWIN in 1992.

All the spectra obtained between 2002 and 2008 were classified using the classification of Smith, Crowther & Prinja (1994) for WN6-11 stars based primarily on relative strengths of NV $\lambda\lambda 4604 - 20$, NIV $\lambda 4058$, NIII $\lambda\lambda 4634 - 41$ and NII $\lambda 3995$ emission lines. The method has low dependence on elemental abundances, because only helium and nitrogen lines (preferably, ratios of the lines of one element) are used. The results of spectral classification are given in table 1.

We classified the spectra obtained in maximum of optical brightness (2004-2005) as WN11. From the middle of 2005 Romano star evolves along the sequence of late WN stars. The spectra in the minimum in 2007-2008 are classified as WN8. Combined with the data published by Szeifert, our results show that the object changes from a B emission-line supergiant in the photometrical maximum (1992), through Ofpe/WN

Table 1: Spectral classes identified via the scheme of Smith, Crowther and Prinja (1994)

B, mag	Spectral subtype	Date
17.5	WN10.5	2002/10/05
16.9	WN11	2004/11/13
17.1	WN11	2005/01/17
17.15	WN11	2005/02/06
17.3	WN10	2005/08/30
17.6	WN9	2005/11/08
18.3	WN8	2006/08/03
18.4	WN8	2007/08/10
18.5	WN8	2007/10/05-08
	WN8	2008/01/08-10

The photometric data were provided by Vitalij Goranskij

(these lines form both in the stellar atmosphere and in the nebula) and $HeII\lambda 5411/HeI\lambda 4713$, where contribution of the nebula is negligibly small.

Bright hydrogen lines are present in the spectra. Equivalent width ratios of hydrogen and helium lines are similar to those for the WN9h star BE381 (Brey 64) that has $H/He \simeq 2$ (Crowther & Smith, 1996). Therefore we calculate models with $H/He = 0.75 \div 2.6$ that is typical for hydrogen WR stars.

5. Results and Conclusions

Our results show that the object changes from a B emission line supergiant in the optical maximum, through Ofpe/WN (WN10, WN11) to WN9 and further towards a WN8 star in deep minimum.

We model the low-luminosity state spectrum of V532 having the highest available resolution of about 1\AA . Figure 3 shows the best-fit model spectrum, redshifted and diluted for the distance towards M33. The parameters of the model are: luminosity $L = 8 \cdot 10^5 L_{\odot}$, mass loss rate $4.2 \cdot 10^{-5} M_{\odot}/\text{year}$, hydrogen abundance $H/He = 1.3$, effective temperature at hydrostatic radius $T_{*} = 34600K$ ($R_{*} = 25R_{\odot}$) and $T_{\tau=2/3} = 28200K$.

Abundance pattern is consistent with the moderately sub-solar metallicity of M33 ($[Fe/H] \sim -0.5$), but nitrogen is significantly over-abundant (~ 2.4 solar). The latter value is consistent with the existing

evolutionary models and with data on other nitrogen-rich WR stars (Herald et al., 2001). Models are most sensitive to the mass-loss rate and the luminosity and practically unaffected by changes in the mass of the star. This is expected, because the density structure of the wind and optical depths are defined by the velocity law rather than by gravity, as for ordinary stars.

Increasing the number of models and refining the fitting procedure will help to better understand the physics and evolutionary status of V532.

Acknowledgement. We are grateful to Vitaliy Goransky, Elena Barsukova and Alla Zharova for providing us with photometrical data.

References

- Afanasiev V.L., Dodonov S.N., Moiseev A.V.: 2001, in *Stellar dynamics: from classic to modern*, Eds. Osipkov L.P., Nikiforov I.I., Sobolev Astronomical Institute, Saint Petersburg, 103
- Afanasiev V., Moiseev A.: 2005, *Astronomy Letters*, **31**, 194
- Crowther P.A., Hillier D.J., Smith L.J.: 1995, *A&A*, **293**, 172
- Crowther P.A., Smith L.J.: 1996, *A&A*, **305**, 541
- Herald J.E., Hillier D.J., Schulte-Ladbeck, R.E.: 2001, *ApJ*, **548**, 932
- Hillier D.J., Miller D.L.: 1998, *ApJ*, **496**, 407
- Kashikawa N., Aoki K., Asai R., et al.: 2002, *PASJ*, **54**, 819
- Kurtev R., Sholukhova O., Borrisova J., Georgiev L.: 2001, *Rev.Mex. AA*, **37**, 57
- Maryeva O., Abolmasov P.: 2010, *Rev.Mex. AA*, **46**, 279
- Romano G.: 1978, *A&A*, **67**, 291
- Smith L.J., Crowther P.A., Prinja R.K. 1994, *A&A*, **281**, 833
- Smith L.F., Shara M.M., Moffat F.J.: 1996, *MNRAS*, **281**, 163
- Szeifert T.: 1996, In: *Wolf-Rayet Stars in the Framework of Stellar Evolution* Eds. J.M.Vreux, A.Detal, D.Fraipont-Caro, E.Gosset and G.Rauw. 33rd Liege Institute Astroph. Coll., Liege, 459
- Viotti R.F., Galleti S., Gualandi R., et al.: 2007, *A&A Letters*, **464**, L53

THE NEW ABSOLUTE PARAMETERS OF OU GEM - THE STAR OF BY DRA TYPE

T.V. Mishenina¹, L.V. Glazunova^{1,2}, C. Soubiran³, V.V. Kovtyukh¹

¹ Department of Astronomy, Odessa National University

T.G.Shevchenko Park, Odessa 65014 Ukraine, *astro@paco.odessa.ua*

² Odessa National Academy of Telecommunications, Kuznechnaya street 1, Odessa, 65029, Ukraine

³ Universite de Bordeaux - CNRS - Laboratoire d'Astrophysique de Bordeaux, France

ABSTRACT. The spectra of OU Gem were obtained with the fiber-fed echelle spectrograph SOPHIE at the 1.93-m telescope of the Observatoire de Haute-Provence (France). The temperatures of components of the system were defined and are equal to 5013 ± 15 K and 4486 ± 50 K for primary (A) and secondary (B) components, accordingly. The rotation velocity of components are measured: for primary component it is equal to 5.1 ± 1 km/s and $6.2 \pm$ km/s for the secondary one. The definition of radial velocities of components by LSD profile method and redetermination of spectral orbital elements were carried out. New absolute parameters of components were obtained too.

Key words: Spectroscopic: absolute parameters: binary of the BY Dra type; stars: individual: OU Gem

1. Introduction

HD 45088 (=OU Gem) is a BY Dra-type spectroscopic binary with an orbital period of 6.99 days and an eccentricity of 0.15 (Griffin&Emerson, 1975; Tomkin, 1980). The photometric variability has been found by Bopp et al. 1981, V - light variations are up to 0.05 m with a period of 7.36 days. Spectral type of components are K3V + K5V (Montes et al., 1995). The eclipse of the system didn't found (Tomkin, 1980) The purpose of the given work is redetermination of spectral orbital elements using 8 of the new high dispersion spectries and definition of absolute parameters of system.

2. Observations and the effective temperatures of star

The spectra of OU Gem were obtained in the region of the λ 3387–6940 Å and with S/N about 70–170 using the 1.93 m telescope at the Observatoire de Haute-Provence (France) equipped with the echelle-spectrograph SOPHIE (Perruchot et al., 2008), a re-

solving power is $R = 75\,000$. The spectral processing carried out by (Katz et al., 1998; Galazutdinov, 1992).

The effective temperatures T_{eff} for both components were estimated by line depth ratio method (Kovtyukh et al., 2003) for not blending lines. The temperatures of components of the system are equal to 5013 ± 15 K and 4486 ± 50 K for A and B components, accordingly. The microturbulent velocity V_t was determined using the Fe I lines and it is equal to 1.02 km/s for A and 2.1 km/s for B components.

3. Velocities of components and spectral orbital elements

To determine the radial and rotation velocities of the components, we employed the least square decomposed (LSD) profiles obtained using the method described by Glazunova et al. (2008). In this approach we use two line-lists optimized for the temperature of each component, A (5000K) and B (4500K). The heliocentric radial velocities obtained from LSD profiles of primary and secondary components are presented in Table 1. The orbital radial velocities are shown in Figure 1. The radial velocities of the components of the system were obtained by averaging the radial velocities measured at the centre of LSD profile and its core. The solution, obtained solely on the basis of our radial velocity curve, is shown in column 4 of Table 2. The solution derived by Griffin&Emerson, 1975 data is given in column 2. Column 3 shows the orbital parameters obtained by Tomkin (1980). The orbital period of system and the epoch were refined. The rotation velocity is equal to 5.1 ± 1 km/s for A component and 6.2 ± 1 km/s for the secondary (B). For the visual demonstration of the contribution of components, we present in Figure 2 the LSD profiles constructed from the spectra obtained at phase 0.74. The LSD profile of the components yielded a Fourier expansion with a clear first minimum because we determined the projection of rotational velocity with good accuracy.

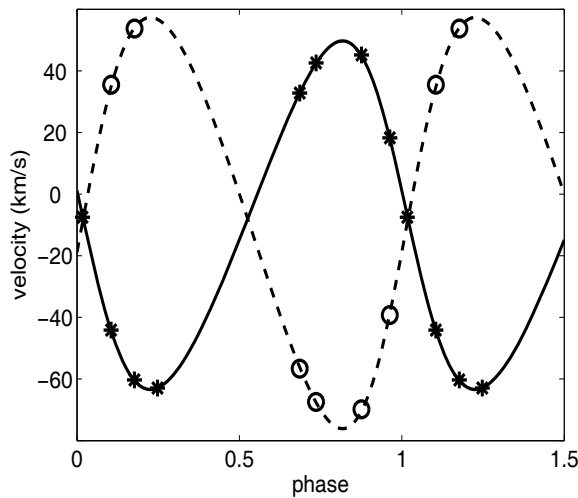
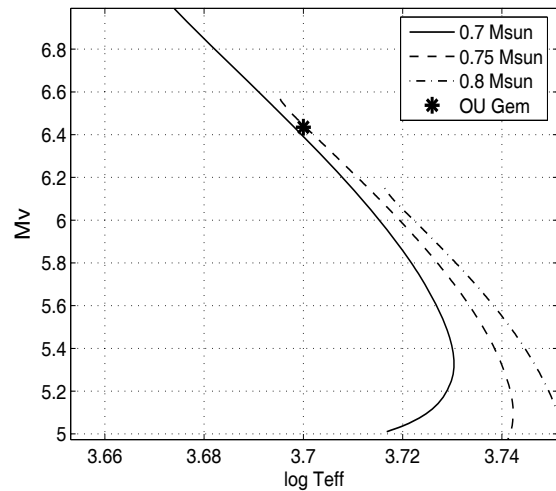
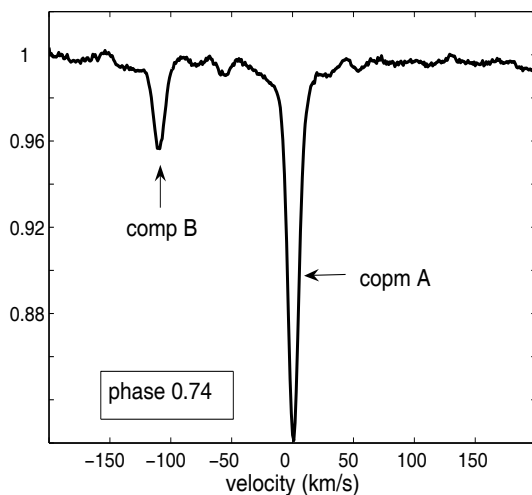
Figure 1: The observed and theoretical V_r .Figure 3: M_v vs. $\log(T_{\text{eff}})$.

Figure 2: LSD profile for phase 0.74.

4. The absolute parameters of systems OU Gem

$M_{\text{bol}} = 6.11^m$ and $M_v = 6.38^m$ were determined using $V = 6.79^m$, $B-V = 0.88^m$, distance 12 pc (Mishenina et al., 2009) and $BC = -0.268$ (Flower et al. 1996). The position of A component at the tracks (M_v vs. $\log(T_{\text{eff}})$, Pietrinferni et al., 2006) marked by asterisk in Fig.3. The radius of the A component ($R_A = 0.71 R_{\odot}$) was estimated using M_{bol} and T_{eff} .

To determine the mass of the components it need to know the angle of inclination i of the orbit in the visible plane. Using the radius and spectral elements of orbit we calculated the light curves for different angle of inclination by code for binary systems at <http://www.physics.sfasu.edu/astro/binstar.html>. Eclipse can occur, since the angle is $i = 86$ degrees (Fig.5). Hence, the minimal masses of components (Table 2) are equal to $M_A = 0.72$ and $M_B = 0.61 M_{\odot}$ and, consequently, the gravities are $\log g_A = 4.5$ and $\log g_B = 4.6$.

Conclusion

1. We determined the effective temperatures for both components system OU Gem using not blending lines.
2. We measured the rotation velocities of components with good accuracy by LSD method. The definition of radial velocities of components and redetermination of spectral orbital elements were carried out too.
3. We made an estimate for angle of inclination of the orbit in the visible plane and determined the absolute parameters of system.

References

- Bopp B. W., Noah P., Klimke A. et al.: 1981, *PASP*, **93**, 504.
Galazutdinov G.A.: 1992, *Preprint SAO RAS*, **92**, 1.
Glazunova L.V. et al.: 2008, *AJ*, **139**, 1736.
Griffin R.F., Emerson B.: 1975, *The observatory*, **95**, 23.

Table 1: Radial velocities of components depending on the phase.

JD 24+	VR_A (km/s)	σ	VR_B (km/s)	σ	New phase
54898.313	42.57	0.6	-67.43	0.97	0.74
54899.293	45.16	0.9	-69.84	1.05	0.88
54900.280	-7.52	1.2	-	-	0.02
54901.395	-60.32	1.04	53.74	2.1	0.18
55128.695	32.82	0.5	-56.62	1.5	0.69
55130.627	18.25	0.9	-39.20	1.3	0.96
55131.623	-44.11	1.5	35.55	1.8	0.11
55132.622	-62.96	0.8	56.41	0.9	0.25

Table 2: Spectral orbit elements

Parameters	G&E (A comp)	Tomkin (A+B)	ours
P (days)	6.99187±0.00007	6.9990±0.003	6.99185±0.00016
T(JD+24)	40203.163±0.029	43867.020±0.064	2454900.158±0.02
e	0.150±0.004	0.141±0.005	0.146±0.002
w (degre)	77.6±1.4	81.4±2.8	81.9±1.1
K_A (km/s)	56.55±0.21	55.97±0.25	56.57±0.17
K_B (km/s)		66.88±0.19	66.74±0.21
V_0 (km/s)	-8.40±0.15	-10.37±0.25	-8.01±0.11
$M_A \sin^3 i$ (M_\odot)		0.71	0.711±0.005
$M_B \sin^3 i$ (M_\odot)		0.59	0.603±0.004
A sin i (R_\odot)		12.68	11.68

Katz D., Soubiran C., Cayrel R. et al.: 1998, *A&A*, **338**, 151.

Kovtyukh V.V., Soubiran C., Belik S.I., Gorlova N.I.: 2003, *A&A*, **411**, 559.

Kurucz R.L.: 1993, *CD ROM n13*.

Mishenina et al.: 2009, *KFNTSuppl*, in pres.

Montes et al.: 1995, *A&A*, **294**, 165.

Perruchot et al.: 2008, *"The SOPHIE spectrograph Proceedings of the SPIE*, 7014.

Pietrinferni et al.: 2006, *ApJ*, **642**, 797.

Tomkin J.: 1980, *AJ*, **85**, 284.

Yushchenko A.V., Gopka V.F., Khokhlova V.L. et al.: 2004, *A&A*, **425**, 171.

SPECTRAL TYPE AND RADIAL VELOCITY VARIATIONS IN THREE SRC VARIABLES

K.E. Moncrieff¹, D.G. Turner¹, C.I. Short¹, P.D. Bennett¹, D.D. Balam², R.F. Griffin³

¹ Department of Astronomy and Physics, Saint Mary's University, Halifax, Nova Scotia, Canada *kathleen.moncrieff@gmail.com*

² Dominion Astrophysical Observatory, Victoria, British Columbia, Canada

³ The Observatories, Cambridge University, Cambridge, United Kingdom

ABSTRACT. SRC variables are M supergiants, precursors to Type II supernovae, that vary in brightness with moderately regular periods of order 100–1000 days. Although identified as pulsating stars that obey their own period-luminosity relation, few have been examined in enough detail to follow the temperature and spectral changes that they undergo during their long cycles. The present study examines such changes for several SRC variables revealed by CCD spectra obtained at the Dominion Astrophysical Observatory (DAO) during 2005–2009, as well as by archival spectra from the DAO (and elsewhere) for some stars from the 1960s to 1980s, and Cambridge radial velocity spectrometer measures for Betelgeuse. Described here is our classification procedure and information on the spectral type and radial velocity changes in three of the stars. The results provide insights into the pulsation mechanism in M supergiants.

Key words: Surveys; stars: individual: SRC variables: α Ori, α Her, S Per; stars: late-type.

1. Introduction

Type C semiregulars, or SRC variables, constitute a portion of the “forgotten” family of late-type variable stars located in the M supergiant region of the Hertzsprung-Russell diagram. The more irregular LC variables are close cousins, and both types are poorly studied, mainly because of their lengthy primary cycles of 200 – 900 days, although some also have superposed longer periods measuring thousands of days in duration. They are evolved stars, most being M supergiants, with a few bright giants and a few late K-type stars thrown into the mix. They have masses of order $15 - 20M_{\odot}$, effective temperatures below 4,000 K, and radii of at least several hundred R_{\odot} . Many are surrounded by large circumstellar dust shells created by their ongoing mass loss. SRC variables are also believed to be the precursors to most Type II supernovae.

Recent summaries of the properties of SRC variables were presented by Turner (2006), Rohanizadegan et al. (2006), and Turner et al. (2006), the last two studies in connection with the luminous M3 Ia variable BC Cyg. The stars appear to obey their own period-luminosity relation (Turner et al. 2006). Spectroscopic studies of a large sample of M supergiants were made by Levesque et al. (2005), including many of the SRC variables, and a study of period changes in BC Cyg reveals erratic changes of period in excess of what is typical of stars of late spectral type (Turner et al. 2009). It was demonstrated by Stothers (1969) forty years ago that pulsation can account for the primary periods of variability in such stars. But observational confirmation has been lacking, and detailed observational studies of the stars are few in number, mainly restricted to a limited spectroscopic and radial velocity survey by Joy (1942), the photometric survey of BC Cyg by Rohanizadegan et al. (2006) and Turner et al. (2006), and a brief survey of α Ori by Gray (2008).

In an attempt to remedy that situation, a spectroscopic survey of northern hemisphere SRC variables was initiated in 2005 using the 1.85m Plaskett telescope of the Dominion Astrophysical Observatory (DAO), Herzberg Institute of Astrophysics. Examination of archival photographic spectra for bright SRC variables, some from the David Dunlap Observatory (DDO), and scans of many of the original DAO plates have also been made, as well as a search for unpublished spectroscopic observations of the stars. Included are previously-unpublished radial velocity measures for Betelgeuse obtained by Griffin with the Cambridge radial velocity spectrometer. A comprehensive survey of the variables holds the promise of learning more about the basic properties of an intriguing group of massive stars, objects that may explode as supernovae within a few hundred years. This study examines changes in spectral type and radial velocity in three SRC variables: α Orionis, α Herculis, and S Persei. It is part of a larger project designed to improve our understanding of the pulsation mechanism in M

supergiants and the evolutionary changes in SRC variables.

2. Data Reduction

CCD spectra from the DAO were reduced with IRAF, first by applying bias corrections, trimming the spectra, and removing bad pixels with the *CCDPROC* package. Iron-argon arc spectra were used for wavelength calibration, and flat fielding was done with the *APFLATTEN* package. The *DOSLIT* package was used to extract one-dimensional (1-D) spectra from the two-dimensional (2-D) CCD output, as well as to wavelength-calibrate and dispersion-correct the former. The spectra were then normalized using IRAF's *CONTINUUM* package, which fits a polynomial to the data to find the continuum, and then outputs the ratio of the input spectra to the fitting function.

2.1. Spectral Classification

Luminous M stars have been notoriously difficult to classify, primarily because most of the available spectral standards are SRC variables (Keenan & McNeil 1976). A fairly straightforward scheme of temperature classification was set up by Keenan (see Gray & Corbally 2009), based upon the visibility of specific band heads of TiO in blue-green spectra of the stars: $\lambda 4954$ at M0, $\lambda 4761$ at M1, $\lambda 4804$ at M2, $\lambda 4584$ at M3, $\lambda 4626$ at M4, $\lambda 4352$ at M5, $\lambda 4395$ at M6, $\lambda 4310$ at M7, and distinct TiO absorption longward of $\lambda 4100$ at M8. That same scheme was employed here, along with the use of a VaO feature at $\lambda 4389$ that is a useful luminosity discriminant for warmer M supergiants. Table 1 summarizes the lines used to determine spectral type and luminosity class for this study.

Table 1: Lines used for spectral classification.

λ (Å)	Species	Behavior
4861	H β	Appears to strengthen with decreasing temperature when compared with nearby continuum, which is suppressed by the TiO band head.
4953	TiO band head	Strengthens with decreasing temperature. $\lambda 4953$ and other band heads are the primary determinants of spectral type for M stars. The $\lambda 4953$ band head is easiest to use.
4389	VaO blended with Fe I	Strengthens with increasing luminosity when compared with nearby Fe I line at $\lambda 4383$ Å.

2.2. Radial Velocity Determination

The IRAF package *RVIDLINES* was used to calculate radial velocities from the CCD and photographic spectra. *RVIDLINES* uses the differences between

observed wavelengths in a spectrum and rest wavelengths of the same lines to calculate a radial velocity. The user creates a list of rest wavelengths, then marks several lines in the spectrum and enters the rest wavelengths of the marked lines. The software then uses the user-created list to identify as many more lines in the spectrum as possible, and computes a velocity from the average wavelength shift, along with an associated uncertainty. When the software is run in heliocentric mode, it uses the observatory location keyword in the header along with the date and time information to apply a heliocentric correction to the computed velocity automatically.

3. Results

3.1. α Orionis

Table 2: α Orionis observations.

HJD	Phase	V_r (km/s)	Sp. Type	Source
2433937	0.4036	...	M1.5-2 Iab	DDO
2437957	0.9526	...	M2 Iab	DDO
2439921	0.6167	...	M1.5-2 Iab	DDO
2441043	0.2829	$+19.9 \pm 0.4$	M1 Ia	DAO pg
2441132	0.4943	$+3.7 \pm 0.1$	M1 Ia	DAO pg
2441233	0.7342	$+10.3 \pm 0.2$	M2 Iab	DAO pg
2442458	0.6439	-21.9 ± 0.8	M3 Ib	DAO pg
2442819	0.5014	-22.6 ± 0.1	M3 Ib	DAO pg
2454041	0.1562	+23.5	...	Griffin
2454057	0.1942	+23.8	...	Griffin
2454079	0.2464	+23.3	...	Griffin
2454124	0.3530	+22.6	...	Griffin
2454186	0.5023	+18.5	...	Griffin
2454360	0.9140	+18.7	...	Griffin
2454391	0.9888	+22.3	...	Griffin
2454414	0.0421	+24.7	...	Griffin
2454421	0.0587	+24.9	...	Griffin
2454429	0.0797	+24.7	...	Griffin
2454443	0.1110	+24.7	...	Griffin
2454472	0.1797	+22.2	...	Griffin
2454490	0.2246	+21.8	...	Griffin
2454508	0.2673	+21.4	...	Griffin
2454523	0.3029	+21.0	...	Griffin
2454757	0.8571	+22.8	...	Griffin
2454779	0.9091	+25.1	...	Griffin
2454804	0.9683	+25.5	...	Griffin
2454845	0.0678	+26.6	...	Griffin
2454876	0.1415	+26.9	...	Griffin
2454897	0.1911	+26.3	...	Griffin
2454929	0.2670	+25.4	...	Griffin
2455114	0.7050	+25.1	...	Griffin
2455128	0.7383	+25.2	...	Griffin
2455167	0.8307	+23.9	...	Griffin
2455187	0.8780	+23.4	...	Griffin
2455214	0.9443	+23.2	...	Griffin
2455227	0.9729	+23.3	...	Griffin
2455258	0.0487	+25.2	...	Griffin
2455295	0.1364	+24.6	...	Griffin

A comparison of AAVSO photometric information on the star with newly-derived and available spectral type and radial velocity data indicates that α Ori reaches its latest spectral type and lowest luminosity

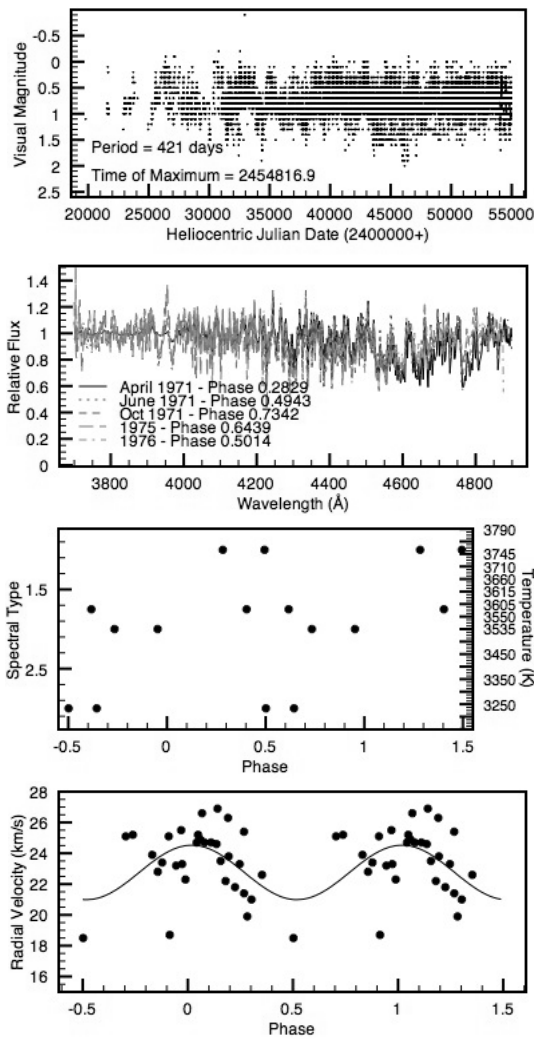


Figure 1: α Ori data. From top: visual light curve from AAVSO measurements, recent spectra, spectral types and temperatures as functions of phase, and radial velocity as a function of phase.

near light minimum. Radial velocity maximum (greatest photospheric recession) is reached near light maximum and the star reaches mean radial velocity (indicative of smallest dimensions) near light phase 0.27. Table 2 summarizes the spectroscopic results and Fig. 1 displays the available data for α Ori.

3.2. α Herculis

A comparison of AAVSO photometric information on α Her with newly-derived and available spectral type and radial velocity data indicates that it reaches smallest dimensions at phase 0.12 following light maximum. There is scatter in its spectral classifications, yet it appears to reach greatest luminosity at earliest spectral type. The star belongs to an optical triple. Table 3 summarizes the spectroscopic results and Fig. 2 displays the available data for α Her.

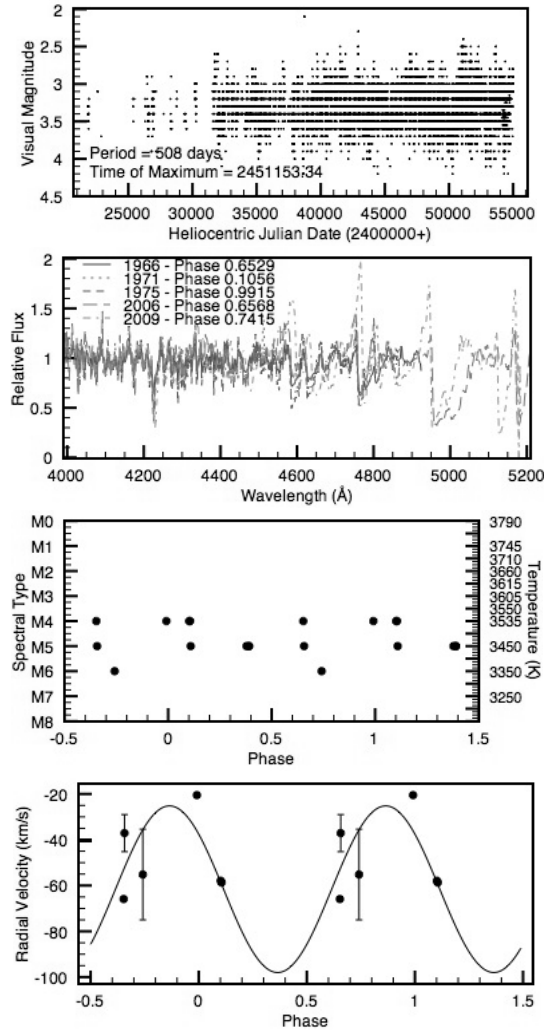


Figure 2: α Her data. From top: visual light curve from AAVSO measurements, recent spectra, spectral types and temperatures as functions of phase, and radial velocity as a function of phase.

3.3. S Persei

A comparison of AAVSO photometric information on S Per with newly-derived spectral type and radial velocity data indicates that it also reaches smallest dimensions at phase 0.11 following light maximum, and appears to reach greatest luminosity and earliest spectral type near light maximum. Table 4 summarizes the spectroscopic results and Fig. 3 displays the available data for S Per.

4. Conclusions

All three survey stars appear to reach their smallest dimensions following light maximum at photometric phases 0.11–0.27. The photospheric temperature changes follow the changes in overall size, with α Ori and S Per reaching their coolest photospheric temper-

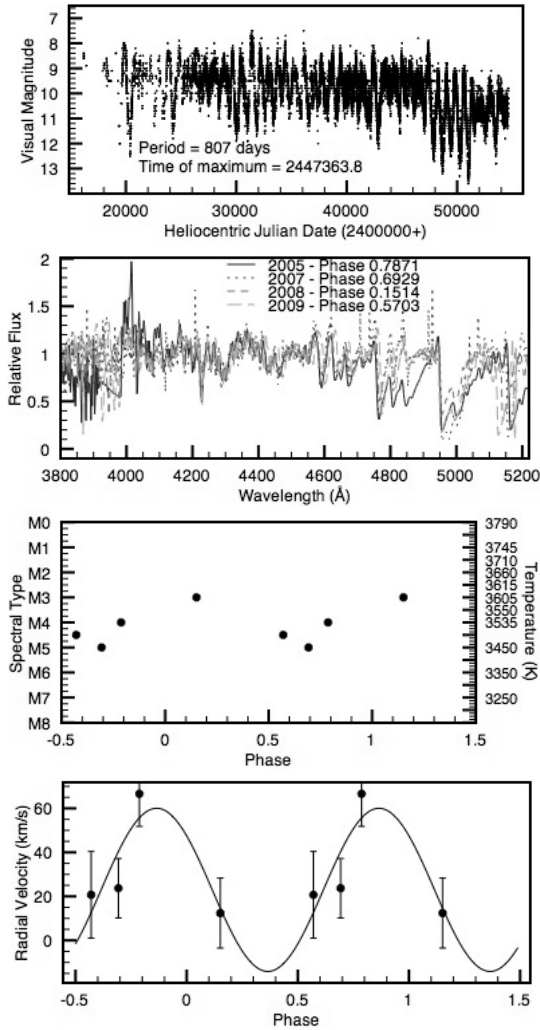


Figure 3: S Per data. From top: visual light curve from AAVSO measurements, recent spectra, spectral types and temperatures as functions of phase, and radial velocity as a function of phase.

atures near light minimum and greatest atmospheric extent. Like S Per, α Ori reaches its highest photospheric temperatures just prior to reaching its smallest overall dimensions. Scatter in the spectral classifications for α Her make it difficult to determine exactly when it reaches hottest photospheric temperature, but in all three stars greatest luminosity appears to be coincident with such phases, implying that the T_{eff}^4 term dominates the luminosity equation. Similar analyses are currently being performed on ~ 20 additional SRC variables, which will permit us to determine if other members of the class display the same general characteristics.

Table 3: α Herculis observations.

HJD	Phase	V_r (km/s)	Sp. Type	Source
2427978	0.3787	...	M5 Iab-Ib	DDO
2427984	0.3905	...	M5 Iab-Ib	DDO
2439293	0.6529	-65.9 ± 0.7	M4 Ia	DAO pg
2440033	0.1089	...	M5 Ib	DDO
2441047	0.1056	-58.7 ± 0.4	M4 Ia	DAO pg
2442513	0.9915	-20.5 ± 0.3	M4 Ia	DAO pg
2454027	0.6568	-37.1 ± 8.1	M5 Iab	DAO CCD
2455086	0.7415	-55.2 ± 19.8	M6 Ib	DAO CCD

Table 4: S Persei observations.

HJD	Phase	V_r (km/s)	Sp. Type	Source
2453648	0.7871	66.6 ± 14.8	M4 Ia	DAO CCD
2454379	0.6929	23.7 ± 13.5	M5 Iab	DAO CCD
2454749	0.1514	12.4 ± 15.9	M3 Ia+	DAO CCD
2455087	0.5703	20.7 ± 19.7	M4.5 Ia	DAOCCD

Acknowledgements. We are grateful to the DAO for allocating time on the 1.85-m telescope for this project. We also acknowledge with thanks the variable star observations from the American Association of Variable Star Observers (AAVSO) International Database contributed by observers worldwide and used in this research. This research used the POLLUX database (<http://pollux.graal.univ-montp2.fr>), operated at GRAAL (Université Montpellier II - CNRS, France) with the support of the PNPS and INSU.

References

Gray D.F.: 2008, *AJ*, **135**, 1450.
 Gray R.O., Corbally C.J.: 2009, *Stellar Spectral Classification*, Princeton Univ. Press.
 Joy A.H.: 1942, *ApJ*, **96**, 344.
 Keenan P.C., McNeil R.C.: 1976, *An Atlas of the Spectra of the Cooler Stars: Types G,K,M,S and C*.
 Levesque E.M., Massey P., Olsen K.A.G., et al.: 2005, *Ap. J.*, **628**, 973.
 Rohanizadegan M., et al.: 2006, *Odessa Astron. Publ.*, **18**, 87.
 Stothers R.: 1969, *ApJ*, **156**, 541.
 Turner D.G.: 1979, *JRASC*, **73**, 74.
 Turner D.G.: 2006, *Odessa Astron. Publ.*, **18**, 123.
 Turner D.G.: 2009, *AIP Conf. Series*, **1170**, 59.
 Turner D.G., et al.: 2006, *PASP*, **118**, 1533.
 Turner D.G., Percy J.R., Colivas T., et al.: 2009, *AIP Conf. Series*, **1170**, 167.

MODELLING OF LATE TYPE SPECTRA AND ABUNDANCES: NEW OBSERVED DATA AND APPROACHES

Ya.V. Pavlenko¹, J.S. Jenkins², H.R.A. Jones³

¹ *Main Astronomical Observatory of NASU, Ukraine*

² *University of Santyago, Chile*

³ *University of Hertfordshire, UK*

ABSTRACT. Spectrum of well known solar twins are interested for us in many aspects. We test the use the minimisation procedure to the observed spectrum of the Sun (Kurucz et al. 1996) in the wide spectral region $\lambda\lambda$ 4000 -8700 Å. For the Sun we obtained $\log N(\text{Fe}) = -4.40$, i.e the reference abundance (Gurtovenko & Kostik 1989), and microturbulence velocity $V_t = 1$ km/s.

Key words: Stars, spectroscopy.

1. Introduction

Studying stars which spectral type pretty close to solar but with a number of differences could help test new analyzing techniques. One of the examples is a work by Willie Soon et al. (1998) who tried gapped wavelet approach on studying clustering of surface features on magnetically-active rapidly rotating stars with solar characteristics in general.

Majority of another research conducted on this and other solar-type stars were focused on itemizing their parameters such as effective temperature, bolometric magnitude, radius, metallicity and color indices using different observational data, photometric and spectroscopic techniques (Glushneva et al 2002). However, the spectroscopic data obtained by instruments allows us to renew existing information to improve our vision of stellar nature through more precise modeling process.

Modern spectrographs (FEROS, HARPS) provide observational data of the solar quality. New procedures of the data reduction give us the chance to obtain more information of the solar-like stars with the high enough accuracy. However, the amount of the data is huge, traditional methods of the fine analysis of the stellar spectra are too time consumable to be the effective tool managing these data. This topic relates to the many problems of today astrophysics as search planetary systems, chemistry of the solar neighbourhood, chemistry evolution of our Galaxy, etc (see Jenkins et al. 2008, 2009).

The main aim of our work is to test some new approaches developed to get more information from the spectra of solar-like stars using the original minimisation procedure.

2. Observational data

We use Kurucz et al. (1984) spectrum of the Sun. It's worth noting that the atlas contains the low noise, high resolution ($R=500000$) data. However, some spectral regions are affected by telluric absorption. We excluded these regions from our consideration.

Procedure

2.1 Model atmospheres

We compute plane-parallel model atmospheres of the Sun (5777/4.47) in LTE, with no energy divergence, using the SAM12 program (Pavlenko 2003), which is a modification of ATLAS12 (Kurucz 1993). Chemical equilibrium is computed for molecular species assuming LTE. The opacity sampling approach Sneden et al. (1976) is used to account for absorption of atoms, ions and molecules (see more details in Pavlenko 2003). The 1-D convection mixing length theory modified by Kurucz(1993) in ATLAS12 was used to account for convection. The computed model atmosphere of the solar atmosphere is available <ftp://ftp.mao.kiev.ua/pub/users/yp/Results/0.5777.444.ja>.

Additionally, we used model atmospheres of the Sun HOLMU (Holveger, Muller 1974) and Kurucz (2010). Comparison of our computed 1D model structures with Kurucz (1993) and HOLMU are shown in Fig. 1.

2.2 Synthetic spectra

Synthetic spectra are computed with the WITA6 program Pavlenko (1997), using the same approximations and opacities as SAM12. To compute synthetic spectra we use line lists from VALD2(Kupka et al. 1999). The shape of each atomic line is determined using the

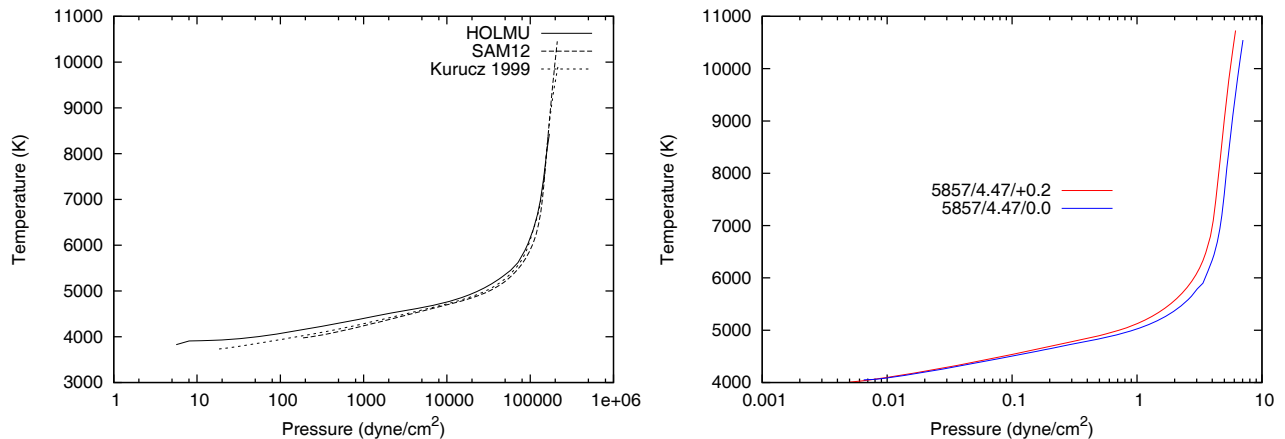


Figure 1: Left: comparison of temperature structures of model atmospheres of the Sun: HOLMU, Kurucz, SAM12. Right: changes of temperature structure of model atmosphere of due to the drop of metallicity by 0.2 dex

Voigt function. Damping constants are taken from line databases, or computed using Unsold's (Unsold, 1955) approach. A wavelength step $\Delta\lambda = 0.025 \text{ \AA}$ is employed in the synthetic spectra computations.

It is worth noting that atomic species provide different contribution to the formation of the spectrum of solar-like stars. As example, in Fig. 2 we show a few spectra formed by absorption of a few selected species in the whole spectral region of our interest. Iron lines are dominated across our spectrum.

2.3 Microturbulent velocity

In our computations we determine a microturbulent velocity on the stage of determination of the Fe abundance (see section 3). Afterwards that V_t can be used in the procedure of determination of other elements.

2.4 Abundance determination procedures

First of all, we developed our procedure which allows determine a limited number of parameters: V_t , $v \sin i$, abundance Fe(H) from the general fit to the observed spectrum. Absorption of iron dominates in the spectrum, therefore this procedure can be used for estimations of abundances.

From the observed spectral region we choose 11 spectral regions to be used in our analysis. It was done due to the different reasons:

- Synthetic spectra were computed with a fixed step for a limited number of wavelengths points (N=20000).
- We cropped spectral regions of strong telluric absorption.
- In our testing runs we found that a response of spectral regions on abundance variations differs with wavelengths.

Table 1: Spectral region splitting

N	λ_{min}	λ_{max}
1	4000.00	4400.00
2	4400.00	4800.00
3	4800.00	5200.00
4	5200.00	5400.00
5	5400.00	5800.00
6	5800.00	6300.00
7	6300.00	6800.00
8	6800.00	6865.00
9	6940.00	7160.00
10	7300.00	7590.00
11	7800.00	8130.00

In the Table 1 we show the list of our spectral regions.

To determine the best fit parameters, we compare the observed fluxes F_ν with the computed fluxes F_ν^x .

Namely, we find the minima of the 3D function

$$S(f_s, f_h, f_v) = \sum_{\nu} (F_\nu - F_\nu^x)^2,$$

where F_ν and F_ν^x are the observed and computed spectra respectively, and f_s , f_h , f_v are the wavelength shift, the normalisation factor, and microturbulent velocity, respectively.

The minimisation was done for every adopted abundance, and from the grid of the better solutions we find the $\log N(\text{Fe})$ and V_t at min S.

3. Abundance of Fe in atmosphere of the Sun

We determined the iron abundance in the atmosphere of the Sun for model atmospheres shown in Fig. 1.

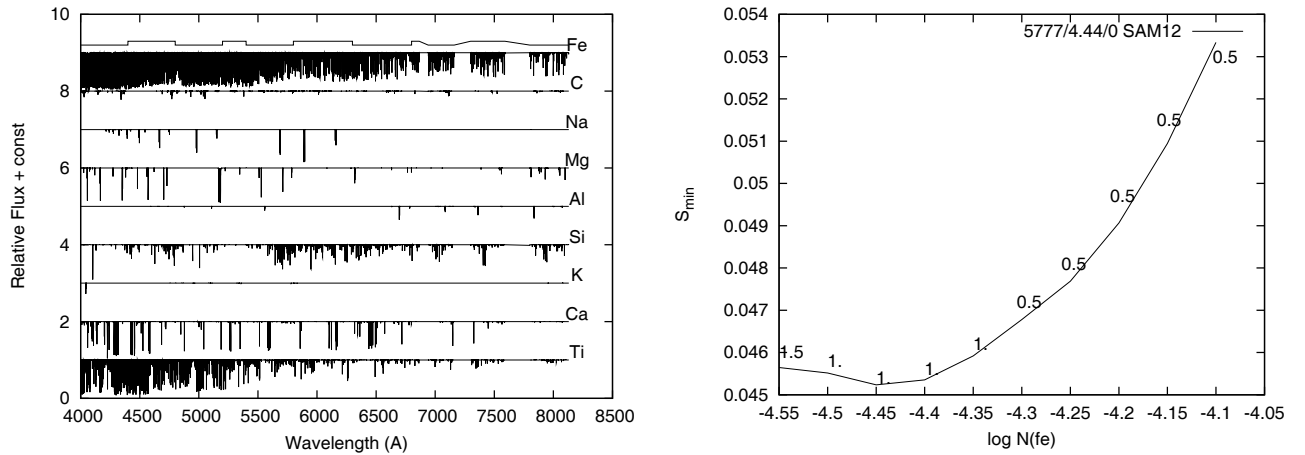


Figure 2: Left: absorption lines of a few atomic species in the theoretical solar spectrum. Computations were carried out for SAM12 model atmosphere and lines from the VALD database. Right: determination of V_t for the SAM12 model atmosphere of $T_{eff}=5777$ K, $\log g = 4.44$.

Table 2: Iron abundance determines for different model atmospheres of the Sun.

Model atm. (K)	Min S	$\log N(\text{Fe})$	V_t (km/s)
The Sun			
HOLMU	0.0465	-4.45	1.5
SAM12	0.0457	-4.50	1.0
Kurucz	0.0452	-4.45	1.0

Our procedure of the iron abundance determination in atmospheres of the Sun and HD1835 was carried out in the following steps:

1. we compute a small grid of synthetic spectra for $\log N(\text{Fe})$ from -4.9 with step 0.1 and 5 values of V_t from 0.5 with a step 0.5.

Only abundance on iron changes other abundances are adopted to be solar.

2. for every computed spectrum S was computed, min S determines a pair of parameters: $\log N(\text{fe})$ and V_t .

In Fig. 2 we show the dependence of the computed S_{min} with different V_t on $\log N(\text{Fe})$. The found iron abundances for three 1D model atmospheres of the Sun are shown in Table 2.

Theoretical model atmospheres show similar results agreed well with known values of the iron abundance and microturbulent velocity in the solar atmosphere.

4. Conclusions

We obtained a reference solar Fe abundance from analysis of all Fe I and Fe II lines in the atmosphere

of the Sun. The procedure can be used to determine abundances of other elements in atmospheres of solar twins. However, the procedure shows rather weak dependence of the minimisation factor on the iron abundance. Definitely it can be used in some specific cases:

- we know abundances of other elements in stellar atmosphere. Differences of observed and computed strengths of lines of other elements affect the S value for the element of our interest.
- the procedure does not distinguish lines if different ions of the element of our interest.
- the procedure is sensitive to the level of noise in the observed spectrum. In this paper we used well calibrated solar spectrum. Stellar spectra in most cases are more noisy.

However, the procedure works well for the determination of microturbulent velocity in stellar atmospheres. To determine V_t we use information about strong and weak lines which show different sensitivity on the parameter.

Now we develop new procedure of the automatic analyses of stellar spectra which separately analyses lines of different ions.

Acknowledgements. The work was partially supported by the Program of Comomicrophysics of NASU of Ukraine and PF7 Program Rocky Planets around cool stars (ROPACS PITN-GA-2008-213646).

6. References

- Gurtovenko E.A., Kostik R.I. 1989, Fraunhofer spectrum and solar system of oscillator strengths, *Kiev, Naukova dumka*, 1
- Jenkins J. S., Jones H.R.A., Pavlenko Y., Pinfield D.J., Barnes J.R., Lyubchik Y., 2008, *A&A*, **485**, 571.
- Jenkins J. S.; Ramsey L. W., Jones H. R. A.,

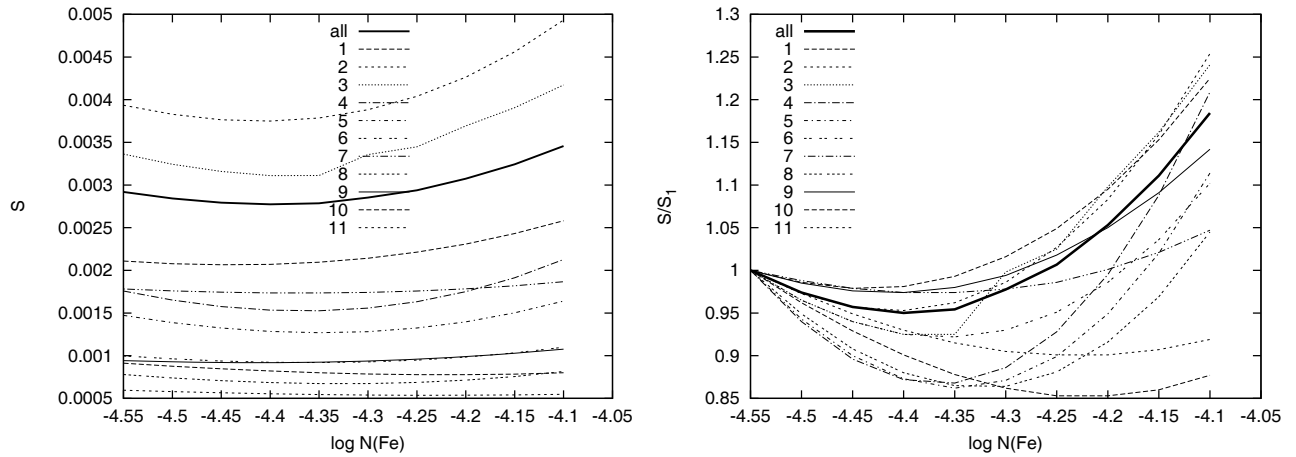


Figure 3: Left: dependence of S on $\log N(\text{Fe})$ computed for different spectral regions from the Table 1. Right: the same dependences shown in normalised S , i.e $S=1$ in the first point of the abundance grid.

- Pavlenko Y., Gallardo J., Barnes J. R., Pinfield D. J. 2009, *ApJ*, **704**, 975.
- Glushneva I. N., Shenavrin V. I., Roshchina I. A. 2002, *A&AT*, **21**, 317.
- Holweger H., Muller E.A. 1974, *Solar Phys.*, **39**, 19.
- Kupka F., Piskunov N., Ryabchikova T.A., Stempels H.C., Weiss W.W., 1999. *Astron. Astrophys. Suppl.*, **138**, 119.
- Kurucz R.L. 1993, in "Peculiar versus Normal Phenomena in A-type and Related Stars", eds. M.M. Dworetzky, F. Castelli, and R. Faraggiana, A.S.P. Conference Series vol. **44**, 87.
- Kurucz R. L., Furenlid I., Brault J., Testerman L. 1984, Solar flux atlas from 296 to 1300 nm, *National Solar Observatory Atlas, Sunspot*, New Mexico: National Solar Observatory, 198
- Pavlenko Ya. V. 1997, *Astron. Astrophys. Sci.*, **253**, p. 43
- Pavlenko Ya.V. 2003. *Astron. Rept.*, **47**, 59.
- Snedden C., Johnson H.R., Krupp B.M. 1976, *ApJ*, **204**, 218.
- Willie S., Peter F., Sallie B. 1982, 1999, *ApJ*, **510L**, 135.
- Unsöld A. 1955, *Physics der Sternatmosphären*, Springer: Berlin, 1.

SPECTRAL VARIABILITY OF THE UNUSUAL SOUTHERN Be STAR HD 152478

M.A. Pogodin¹, N.A. Drake², E.G. Jilinski^{1,3,4}, V.G. Ortega³, R. de la Reza³

¹ Pulkovo Observatory, St. Petersburg 196140, Russia, *pogodin@gao.spb.ru*

² Sobolev Astronomical Institute, St. Petersburg State University,
St. Petersburg, 198504, Russia

³ Observatório Nacional/MCT, Rio de Janeiro, 20921-400, Brazil

⁴ Instituto de Física, Universidade do Estado do Rio de Janeiro,
Rio de Janeiro, 200550-900, Brazil

ABSTRACT

We present results of the spectroscopic investigation of the unusual southern Be star HD 152478. Five echelle high-resolution spectra of the object were obtained in 2007 - 2009 with the FEROS spectrograph mounted at the 2.2 m telescope of the European Southern Observatory (La Silla, Chile). The star exhibits a specific remarkable variability of the numerous line profiles of such elements as H I, He I, Fe II, etc. The analysis of the spectral behaviour of the object has shown that the assumption of global oscillations in the rotating equatorial gaseous disk is not confirmed by the observations. The alternative hypothesis of a variable magnetized stellar wind of flattened geometry flowing close to the equatorial disk can qualitatively explain the observed profile variations.

Key words: Stars: Be: circumstellar matter; stars: spectroscopy; stars: individual: HD 152478

1. Introduction

The southern Be star HD 152478 was included in a program of identification and investigation of possible past supernovae events taking place in the region of the Scorpius-Centaurus OB association (Hoogerwerf et al., 2001). According to later spectroscopic study by Jilinski et al. (2010), this object may be considered as an eventual runaway star.

Nevertheless, this Be star demonstrates an unusual spectral behaviour. The goal of the present study was to investigate the spectroscopic activity of this star seen in a number of spectral lines.

In this report we consider the large-scale profile variability observed in optically thick H α and H β lines and in several optically thin Fe II lines.

2. Observations

Five high-resolution spectra were obtained in 2007 - 2009 using the echelle Fiberfed Extended Range Optical Spectrograph (FEROS) installed at the 2.2m telescope of ESO at La Silla, Chile. The FEROS spectral resolution is $R = 48\,000$, and the wavelength coverage is from 3600 Å to 9200 Å. A typical S/N ratio was from 100 to 200 depending on the spectral region. The dates of observations are given in Table 1.

Table 1: Observing dates.

N	Date	MJD
I	June 2, 2007	54253.162
II	Feb 23, 2008	54519.356
III	May 25, 2008	54611.154
IV	May 14, 2009	54965.118
V	July 28, 2009	55040.982

3. Spectral classification

We used the echelle spectra of the object to improve its former spectral classification published by Levenhagen & Leister (2006). Contrary to these authors, who used a rather limited number of observational criteria, we analysed a series of spectral parameters, such as:

- profiles of a number of helium lines in the blue part of the spectrum;
- numerous blends of such elements as ionized O, Fe, Si, etc.;
- wide absorption wings of the Balmer lines, free from the circumstellar (CS) influence.

Synthetic spectra, calculated with the code of Piskunov (1992), based on the LTE models of stellar atmospheres of Kurucz, were used for comparison

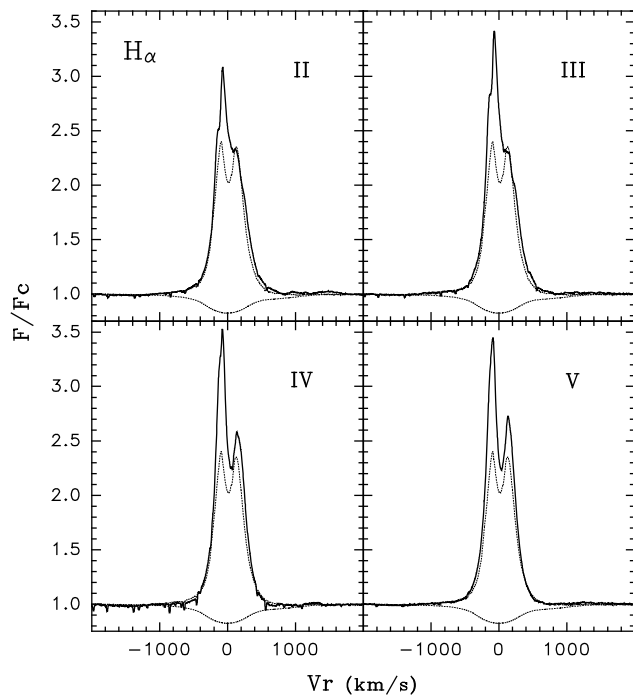


Figure 1: Normalized $H\alpha$ profiles in dates I - V. The profile for date I is shown by the dotted line.

with the observed spectra. Results of our estimates as well as the model parameters of Levenhagen & Leister (2006) are given in Table 2.

Table 2: Parameters of the atmosphere.

Model	T_{eff} (K)	$\log g$	$V \sin i$ (km s^{-1})
Former result	19 800	3.75	295
Our result	25 000	4.25	370

According to our estimates, the star is considerably hotter and rotates more rapidly than it was recognized earlier. Besides of that, a notable He overabundance of about $[\text{He}/\text{H}] = +0.35$ has been found.

4. Variability of line profiles

The temporal behaviour of the $H\alpha$ profile is shown in Fig. 1. Four fragments illustrate the profiles observed in dates II - V as compared with the double-peaked and symmetric profile obtained on date I (dotted line). The synthetic atmospheric profile is also given in this Figure (marked by the dotted line too). One can see that on dates II and III the emission profile becomes very asymmetric. The blue peak increases strongly in intensity, and the red wing shows an increase in its extension. In turn, on dates IV and V the red emission

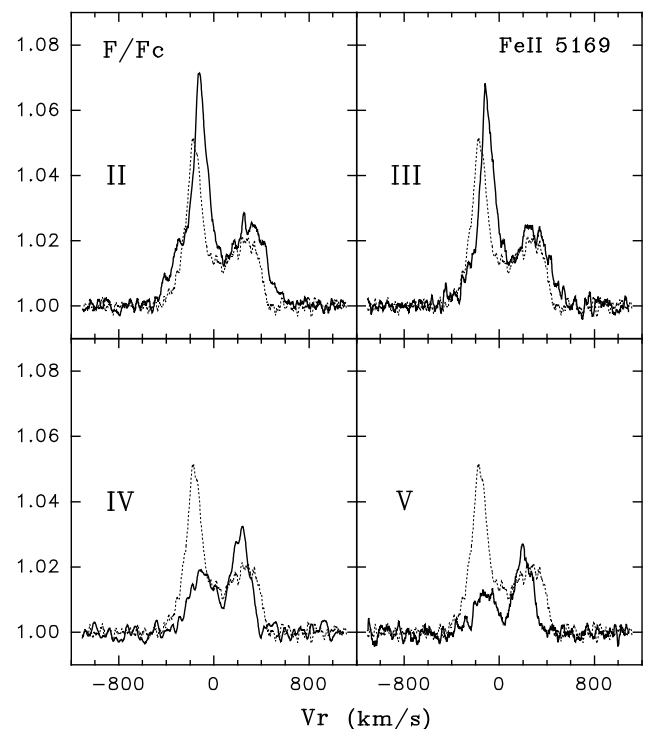


Figure 2: The same as in Fig. 1 but for the Fe II 5169 Å line profile.

peak starts to rise while the red wing looks again as on date I.

The temporal behaviour of the $H\beta$ line profile is similar to the behaviour of the $H\alpha$ profile.

Nevertheless, the character of the variations observed in the optically thin Fe II lines is quite different. The emission profiles of these lines are asymmetric already on date I with the blue peak being of greater intensity than the red one. On dates II and III the profiles remain approximately the same, but on dates IV and V the intensity of the lines decreases and the blue peak becomes even lower than the red one. As an example, this variability is illustrated in Fig. 2 for the Fe II 5169 Å line.

5. Possible interpretations of the spectral behaviour

The variability observed in HD 152478 is typical for a classical rapidly rotating Be star. In recent times, a prominent change of the V/R ratio is most commonly interpreted as a result of a drift of a so-called one-armed perturbation arising in the equatorial gaseous disk. According to the theory of global oscillations in disks of classical Be stars, a large-scale density and velocity inhomogeneities can be formed in the disk which is not co-rotating with the gas but is precessing ret-

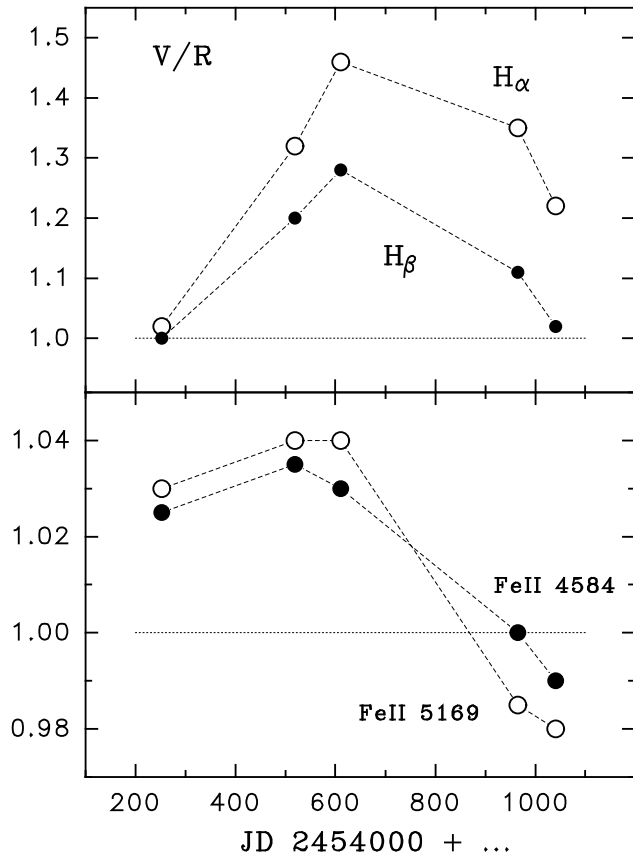


Figure 3: The V/R ratio variations observed in the Balmer and the Fe II lines.

rograde with a period of several years (Kato 1983, Okazaki 1991). Its drifting modulates profiles of CS lines, and a cyclic V/R ratio variability is observed.

In the paper of Hanuschik et al. (1995) it has been shown that:

- the V/R ratio variability takes place in the same phase in the optically thick $H\alpha$ and $H\beta$ lines as well as in optically thin Fe II lines;

- the V/R ratio variability is followed by no change of the EW of emission lines.

As seen in Fig. 3, the V/R ratio observed in the Balmer and Fe II lines in the spectrum of HD 152478, shows variations which can be assumed as long-term cyclic variations connected with the drifting of a large-scale perturbation. But they do not occur in the same phase. A phase shift is clearly seen here. The model of drifting perturbation alone cannot explain this phenomenon. Moreover, the observed profile transformations are followed by a high-amplitude change of EW (see Figs. 1 and 2). Besides, these variations are also not predicted by the oscillation theory. Finally, on dates II and III, when the Balmer line profiles become very asymmetric, the red emission wing becomes very extended (up to 1800 km s^{-1} for $H\alpha$). Such high ve-

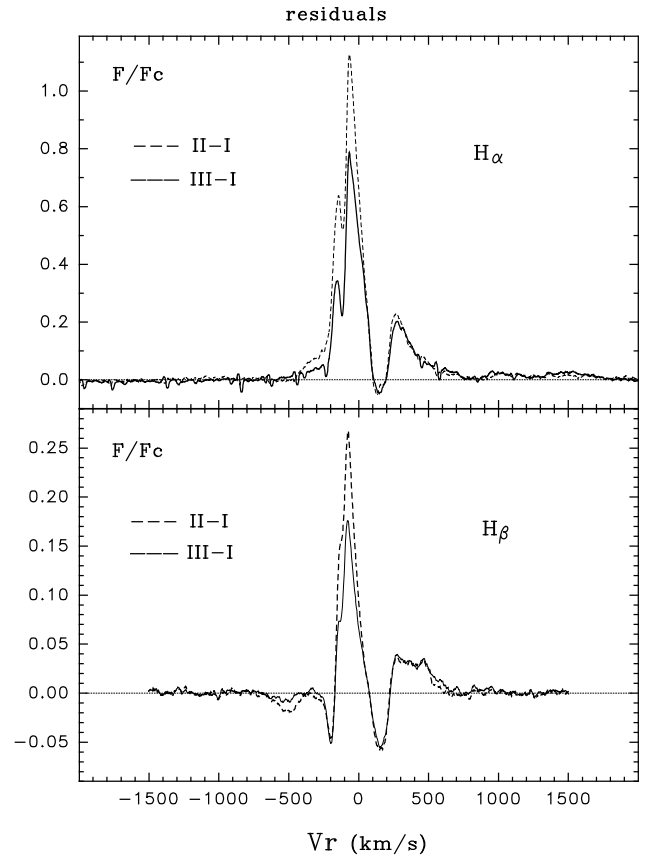


Figure 4: Residual $H\alpha$ and $H\beta$ profiles for dates II and III constructed by subtraction of the profiles for date I.

locities cannot exist in a nearly-Keplerian disk. The maximum velocity of the rotating gas near the inner boundary of the disk is only 650 km s^{-1} for a typical star of B1V spectral type. But such large velocity can be achieved in the radiatively-driven stellar wind flowing from a Be star at intermediate latitudes. This circumstance allows us to consider an alternative interpretation of the spectral behaviour of HD 152478 in the frame of the assumption on a variable stellar wind.

Some time ago it was shown that the Wind-Compressed Disk (WCD) theory of disk formation around Be stars (Bjorkman & Cassinelli 1993) together with a magnetic field of the order of 100 G introduced into the WCD model by Porter (1997), leads to a better agreement between the theory and observational data of Be stars. It should be mentioned, that such fields were already revealed in several classical Be stars using the spectropolarimetric method (Hubrig et al. 2009). According to calculations of Porter (1997), the wind zone in the WCD model with the presence of the magnetic field becomes flattened and concentrated towards the equator.

We tried to estimate a contribution of such magnetized wind in the whole emission line profile in a

qualitative level. It is clear that the red wing of the profile formed in the wind must be more intense and extended than the blue wing because the optically thick gas flowing towards the observer screens the star. And even the P Cyg-type structure is expected in the blue wing. If the orientation of the object is close to “edge-on”, as it is likely to be the case of HD 152478 with large $V \sin i$ (370 km s^{-1}), a local fall in intensity at moderate positive velocities can be expected in the red emission wing. It is connected with the fact that a considerable amount of the emitting gas flowing outwards the observer is screened by the stellar limb. This effect can be notable in the case of flattened magnetized winds and negligible for spherically symmetric geometry of the wind zone.

Fig. 4 shows the observational profiles of $H\alpha$ and $H\beta$ for dates II and III corresponding to the wind contribution to the whole emission profile by simple subtraction of the observed profile for date I. It is assumed that namely on date I the symmetric double-peaked profiles were formed mainly in the disk, and on dates II and III the wind contribution was maximum. One can see that the constructed residuals contain all principal features expected for a flattened magnetized stellar wind.

Therefore, we put forward the assumption on a variable magnetized wind as a possible interpretation of the spectral behaviour of HD 152478.

Acknowledgements. M. Pogodin would like to remark that his contribution to this work was sponsored by the Program of the Presidium of the RAS No 4, OFN RAS Program No 10104, RFBR (grant No 07-02-00535a) and Sci. School No 6110.2008.2. We also thank Anatoly Tarasov of Crimean Astrophysical Observatory for useful remarks during the discussion of our results.

References

- Bjorkman J.E., Cassinelli J.P.: 1993, *ApJ*, **409**, 429.
Jilinski E.G., Ortega V.G., Drake N.A., de la Reza R.: 2010, *ApJ*, **721**, 469.
Hanuschik R.W., Hummel W., Dietle O., Sutorius E.: 1995, *A&A*, **300**, 163.
Hoogerwerf R., de Bruijne J.H.J., de Zeeuw P.T.: 2001, *A&A*, **365**, 49.
Hubrig S., Schöller M., Savanov I., Yudin R.V., Pogodin M.A., Stefl St., Rivinius Th., Curé M.: 2009, *AN*, **330**, 708.
Kato S.: 1983, *PASJ*, **35**, 249.
Levenhagen R.S., Leister N.V.: 2006, *MNRAS*, **371**, 252.
Okazaki A.T.: 1991, *PASJ*, **43**, 75.
Piskunov N.E.: 1992, *Stellar Magnetism*, 92.
Porter J.M.: 1997, *A&A*, **324**, 597.

POSITIVE AND NEGATIVE SUPERHUMPS OF THE DWARF NOVA MN DRA

D.A. Samsonov¹, E.P. Pavlenko¹, M.V. Andreev², A. Sklyanov³, A.M. Zubareva⁴,
I.B. Voloshina⁵, V.G. Metlov⁵, S.Yu. Shugarov^{5,6},
A.V. Golovin⁷, O.I. Antoniuk¹

¹ Crimean Astrophysical Observatory, Nauchny, Crimea, 98409, Ukraine

² Terskol Branch of the Institute of Astronomy, Russian Academy of Sciences, Kabarda-Balkaria Republic, 361605, Russia

³ Department of Astronomy, Kazan' State University, 420008, Russia

⁴ Institute of Astronomy, Russian Academy of Sciences, Moscow, 119017, Russia

⁵ Sternberg Astronomical Institute, Moscow University, Universitetskiy pr. 13, Moscow, 119992, Russia

⁶ Astronomical Institute, Slovak Academy of Sciences, Tatranska Lomnica, 05960, Slovakia

⁷ Main Astronomical Observatory, National Academy of Sciences of Ukraine, Kiev, 03680 MSP, Ukraine

ABSTRACT. We present the result of O–C analysis of the dwarf nova MN Dra. It is based on the multi-site photometric observations that were made over 77 nights in August – November, 2009. The total exposure was 433 hours. During this time binary underwent two superoutbursts and five normal outbursts. In superoutbursts the positive superhumps decreased with extremely large $\dot{P} = -(3 - 8) \times 10^{-4}$ for SU UMa-like dwarf novae, confirming the known behavior of MN Dra in 2003.

MN Dra displayed large-amplitude (up to 1.4^m in quiescence and 0.1^m – 0.2^m in normal outbursts) negative superhumps. The improved value of negative superhump period is 0.095952(4) d.

Key words: Binary, cataclysmic stars, superhumps: MN Dra.

1. Introduction

Dwarf novae are a subclass of cataclysmic variable stars whose systems consist of a late-type star that loses matter through its inner Lagrange point to a non-magnetic white-dwarf. Degenerate companion, first forming an accretion disk around it. SU UMa stars are the shortest-period systems among cataclysmic variables, with orbital periods in the range 80–180 min. SU UMa stars also differ from other cataclysmic variables with longer periods: exhibiting two kinds of outbursts:

- (1) long-duration outbursts with amplitudes of 2^m – 6^m that last approximately two or three weeks;
- (2) fainter and shorter (3–5 days) outbursts.

The first type of outbursts is called superoutbursts and the second type, normal (or ordinary) outbursts. Short-period brightness variations, or positive superhumps, are observed during superoutbursts, whose periods are usually several percent longer than the orbital period. The positive superhumps have been successfully explained in the theory of tidal instability. They are caused by the apsidal precession of the accretion disk generated by gravitational perturbations of the secondary (Warner, 2005). Less common negative superhumps whose periods are slightly shorter than orbital period, are observed in a wide region of subclasses of cataclysmic variables (but only four dwarf novae have this property). The appearance of negative superhumps probably is caused by a retrograde precession of a tilted accretion disk (Montgomery and Bisikalo, 2010).

MN Dra was first discovered S.A. Antipin from the Moscow plate collection, and was originally designated as Var73 Dra (Pavlenko et al., 2010). To determine the nature of the variable it was observed in the Crimean Laboratory of the Sternberg Astronomical Institute in 2001. These observations confirmed that star is a dwarf nova, of the SU UMa type. Pavlenko et al. (2009) discovered in MN Dra the negative superhumps with period 0.0960 d.

2. Observations

Photometric observations were carried out in Crimean astrophysical observatory and Terskol obser-

vatory over 77 nights in August – November, 2009 in R band. The total exposure was 433 hours in integral light. Observations were done with a help of CCDs: FLI 1001E (Shajn 2.6-m telescope CrAO); PIXELVISION (60-cm telescope INASAN Terskol, Russia); SBIG ST-7 (38-cm telescope CrAO) and Zeiss 60-cm telescope in Crimean laboratory of the Sternberg astronomical institute. Total duration of observations was 433 hours (about 77 nights).

We reduced the observations in accordance with the aperture photometry technique using codes written by V.P. Goranskii and the MAXIM DL4 package. The accuracy of observations depended on the telescope used, the object's brightness and the weather conditions during the observations. We estimated its value from the brightness differences of several check stars relative to the comparison star. For the brightest state of the object and the brightness minimum, the accuracies were $0.^m007$ – $0.^m03$. We used the comparison star with coordinates $20^h23^m35.358^s$, $+64^\circ36'56.66$ (J2000.0) according to the USNO–A2.0 catalog (Monet et al., 2004).

3. General light curve

Our observations covered almost two supercycles including two superoutbursts and five normal outbursts (Fig. 1). The length of the supercycle was about 30 days. Typically three normal outbursts could occur during one supercycle. The amplitude of superoutbursts was $3^m.5$, its plateau lasts less than 10 d. The duration of normal outburst was rather long (~ 5 d) confirming those found by Antipin and Pavlenko (2002) and their amplitudes were in the range of 3^m – $3^m.5$. The scattering at plateau of superoutburst is caused by the positive superhumps and those in minimum – by the negative superhumps (Warner 1995).

3. O–C analysis

We determined the times of maxima for all positive and negative superhumps and analyzed their evolution separately. Note that negative superhumps have been seen both in normal outbursts and between them in minimum.

3.1 Positive superhumps

For the maxima of first and second superoutburst we obtained corresponded ephemeris as follows:

$$HJD_1Max = 2455023.28 + 0.105416 \cdot E \quad (1)$$

$$HJD_2Max = 2455023.41 + 0.105416 \cdot E \quad (2)$$

Using these ephemeris we calculated (O–C)s (see Fig. 2 and Fig. 3). It is seen that the period of positive superhumps for the first superoutburst decreases with

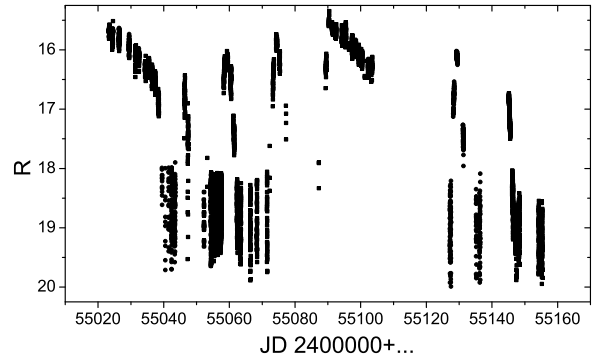


Figure 1: General light curve of MN Dra.

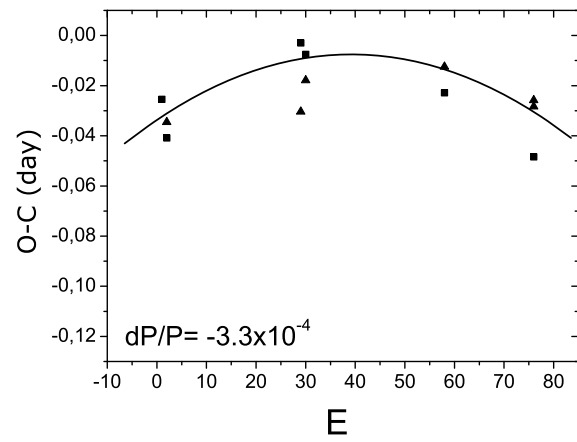


Figure 2: O–C diagram of the positive superhumps for the first superoutburst.

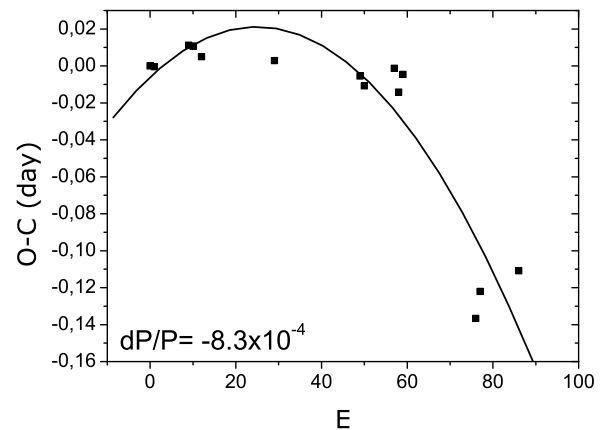


Figure 3: O–C diagram of the positive superhumps for the second superoutburst.

the $\dot{P} = -3.2 \times 10^{-4}$ during 80 cycles and for the second superoutbursts decreases with $\dot{P} = -8.3 \times 10^{-4}$ during 100 cycles. We could conclude that for both superoutbursts the rate of positive superhumps decrease is some different but coincides within the order of 10^{-4} .

3.1 Negative superhumps

Using ephemeris published by Pavlenko et al. (2010), we calculated O–C for all negative superhumps. The result is shown in Fig. 4. It is seen that the O–C behavior is rather complex. First is the long-term change that could be fitted by linear decrease. Using linear trend one could improve the initial period. The new value of the negative superhump period we obtained is 0.095952 d and corresponded ephemeris is:

$$HJDMax = 2454979.400(6) + 0.0959592(4)E \quad (4)$$

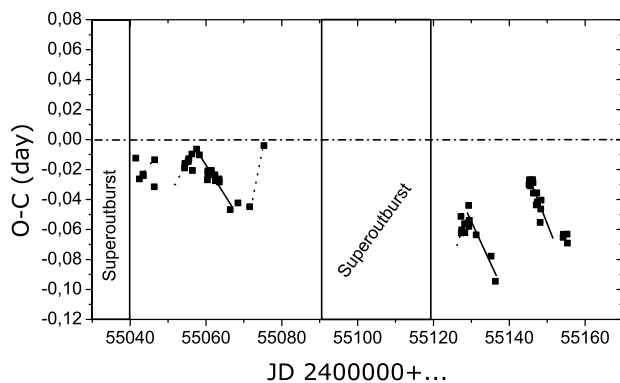


Figure 4: General diagram O–C.

Second, one could see that the O–C for maxima of negative superhumps vary cyclically in correlation with normal outbursts (see Fig. 4, 5). For comparison of time of outburst maxima and O–C maxima we drew vertical lines (the time of O–C maximum was obtained for intersection of fitting lines). Evidently, the times of these maxima do not coincide, and maximum O–C comes slightly before maximum of brightness MN Dra.

The O–C variations look like a jump switching of the period of negative superhumps from the longest value to the shortest one during the beginning of a normal outburst.

The O–C behavior could be even more complex. At some nights we got fast O–C variation: note the "bounced" but real $O - C = -0.3$ d in Fig. 6. This point is omitted in Fig.4.

4. Conclusion

Such correlation points to an impact of accretion on the period of negative superhumps. More observations are needed to understand the nature of this phenomenon.

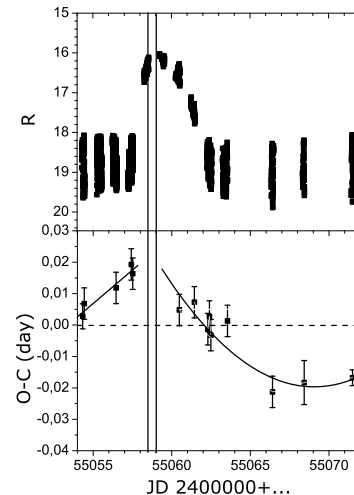


Figure 5: O–C of negative superhumps (lower part of figure) for one normal outburst (upper part of figure).

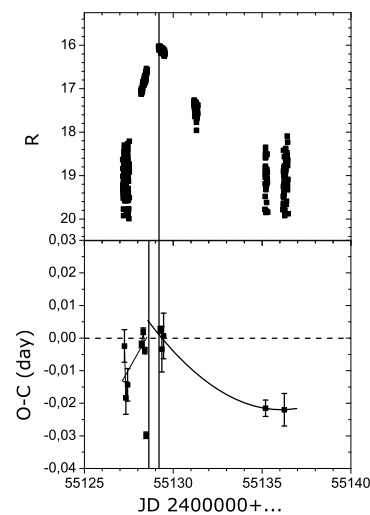


Figure 6: O–C of negative superhumps (lower part of figure) for other normal outburst (upper part of figure).

Acknowledgements. We are grateful to the LOC for possibility to participate in the conference. This work was partially supported by grants F 28.2/081 of Ukrainian Fund of Fundamental Researches, RFBR 10-02-90458.

References

- Antipin S., Pavlenko E.: 2002, *A&A*, **391**, 565
- Monet D. et al.: 1980, *USNO-A2.0. A catalog of Astrometric Standards*.
- Montgomery M., Bisikalo D.: 2010, *MNRAS*, **405**, 1397.
- Pavlenko E.P. et. al.: 2010, *Astronomy Reports*, **6**, 54.
- Warner B.: 1995, *Cataclysmic Variable Stars*, Cambridge University Press

NEW VARIABLE STARS IN THE FIELD OF 66 OPH ON DIGITIZED MOSCOW PLATES

N.N. Samus^{1,2}, S.V. Antipin^{2,1}, D.M. Kolesnikova¹, L.A. Sat², K.V. Sokolovsky^{3,4}

¹ Institute of Astronomy, Russian Academy of Sciences
48 Pyatnitskaya Str., Moscow 119017, Russia, *samus@sai.msu.ru*

² Sternberg Astronomical Institute, Moscow University
13 University Ave., Moscow 119992, Russia

³ Max Planck Institute for Radio Astronomy
Auf dem Hügel 69, Bonn 53121, Germany

⁴ Astro Space Center, Lebedev Physical Institute
84/32 Profsoyuznaya Str., Moscow 117997, Russia

ABSTRACT. Regular photographic observations at the Moscow Observatory began in 1895. The archive of direct and spectroscopic sky photographs kept at the Sternberg Astronomical Institute (SAI) currently contains more than 60000 photographs. The most important part of the Moscow plate stacks are about 22500 direct sky photographs acquired in 1948–1996 with a 40-cm astrograph, at different sites in Crimea and near Moscow (currently in Nauchny, Crimea). The size of its plates is 30×30 cm, corresponding to a $10^\circ \times 10^\circ$ sky field. The limiting magnitude is 17.5^m for good-quality plates.

Keywords: Variable stars, large surveys, discovery

To keep a large plate collection and to distribute information from it is a rather difficult task. After the transition to modern CCD imaging techniques, sufficiently effective algorithms of extracting data and analyzing information from panoramic sky images were developed, applicable, in a somewhat modified form, to old photographic images provided that they are digitized, also guaranteeing safe archive keeping and simple data transfer. Many observatories of the world have started projects on digitizing their plate stacks.

We began digitizing the Moscow collection of astronomical photographs in 2004 using two Creo EverSmart Supreme II scanners. The mode currently used for scanning provides a resolution of 2540 dpi (dots per inch).

The difference of our scanning program from those of other observatories is that, parallel to the process of scanning, we are developing and applying techniques of search for variable stars on a large scale.

The first area to be completely digitized in our program was the field centered at 66 Oph. This

star ($18^{\text{h}}00.3^{\text{m}}$, $+4^\circ 22'$, J2000.0) was the center of 254 plates taken in 1976–1995.

In this field, we discovered and studied 480 new variable stars, suspected brightness variations for more than 50 stars, and significantly improved information for 43 known variables. The statistics of our new discoveries shows a large number of new high-amplitude δ Scuti (HADS) stars in our sample: there are 11 of them in a field covering only 0.24% of the whole sky, while the General Catalogue of Variable Stars (GCVS) currently contains 121 stars of this type. The period distribution of eclipsing variables in our sample is considerably shifted towards short periods compared to the GCVS.

Hundreds of new variables found in a well-studied sky region demonstrate that archive photographs possess a large information potential, not realized till now, and that our techniques of semi-automated search for variables using digitized plates is rather efficient.

Our preliminary results for the northern half of the field were published in Kolesnikova et al. (2008). The complete version of this paper will be published in *Astronomy Reports*.

Acknowledgements. Our study was supported, in part, by the Russian Foundation for Basic Research (grant 08-02-00375) and by the Basic Research Program “Origin and Evolution of Objects in the Universe” of the Presidium of Russian Academy of Sciences. K.V. Sokolovsky wishes to thank the International Max Planck Research School (IMPRS) for Astronomy and Astrophysics at the universities of Bonn and Cologne.

References

Kolesnikova D.M., Sat L.A., Sokolovsky K.V. et al.: 2008, *Acta Astron.*, **58**, 279.

GENERAL CATALOGUE OF VARIABLE STARS: CURRENT STATUS AND NEW NAME-LISTS

N.N. Samus^{1,2}, E.V. Kazarovets¹, N.N. Kireeva¹, E.N. Pastukhova¹, O.V. Durlevich¹

¹ Institute of Astronomy, Russian Academy of Sciences
48 Pyatnitskaya Str., Moscow 119017, Russia, *samus@sai.msu.ru*

² Sternberg Astronomical Institute, Moscow University
13 University Ave., Moscow 119992, Russia

ABSTRACT. A short history of variable-star catalogs is presented. After the second World War, the International Astronomical Union asked astronomers of the Soviet Union to become responsible for variable-star catalogs. Currently, the catalog is kept electronically and is a joint project of the Institute of Astronomy (Russian Academy of Sciences) and Sternberg Astronomical Institute (Moscow University). We review recent trends in the field of variable-star catalogs, discuss problems and new prospects related to modern large-scale automatic photometric sky surveys, outline the subject of discussions on the future of the variable-star catalogs in the profile commissions of the IAU, and call for suggestions from the astronomical community.

Key words: Stars: variable; stars: catalogs.

1. Introduction

Variable-star catalogs have a long history. Probably the first list that can be called a variable-star catalog was published by E. Pigott in 1786, though it contained only 12 stars. The number of variable stars being discovered each year considerably increased after the introduction of astronomical photography. Between 1926 and 1942, the work on variable-star catalogs and ephemerides was organized by the German society “Astronomische Gesellschaft”, and a new catalog was published each year. The first of them contained 2906 variable stars and the last of them, 9476. Since 1943, the situation in the country involved in the war made German astronomers unable to continue publishing their catalogs.

After the World War II, the Executive Committee of the International Astronomical Union (IAU) decided to make astronomers of other countries responsible for several projects earlier fulfilled in Germany and important for the world astronomical community. One of the projects suggested to the Soviet Union was the General

Catalogue of Variable Stars (GCVS). The Executive Committee’s decision was preceded with an IAU inspection in Moscow, where a well-kept card catalog of variable stars founded by P.P. Parenago (1906–1960) and maintained by Parenago, B.V. Kukarkin (1909–1977), and their collaborators was available. It was decided to issue a new catalog once in several years, with supplements, containing only new variables and stars with important changes in the catalog data, printed between the major editions.

The new Soviet compilers of variable-star catalogs were able to publish the first, one-volume edition of the GCVS already in 1948 (Kukarkin and Parenago, 1948). In the style of Soviet scientific publications of that period, the title page of the book mentions only two authors, though an author team (listed in the Russian version of the two-language Introduction) already existed. This catalog contained 10930 variable stars, only slightly more than the last German catalog.

2. The GCVS

The GCVS work is now continued by a joint team of researchers in the Institute of Astronomy of the Russian Academy of Sciences and in the Sternberg Astronomical Institute of Moscow University.

Despite the name, the GCVS actually never was a genuine “general” catalog. First of all, originally it was not intended to contain galactic Novae or Supernovae; there were several exceptions due to tradition. In astronomy of the first half of the 20th century, researchers tried to distinguish between variable stars and Novae. By 1950, it was clear that Novae and Supernovae were also variability types, like other numerous existing classes of variable stars. Soon after the start of the Soviet GCVS project, historical galactic Novae and Supernovae were added to the catalog, and after that, all further Novae of our Galaxy acquired GCVS names (we did not have a Supernova for centuries). Also, as a rule,

extragalactic variable stars were not included (and are not included, with the exception of several traditional cases, like S Dor, S And, or Z Cen, and a special list in Volume V of the 4th GCVS edition – see below). Currently, there are no comprehensive catalogs of all known extragalactic variable stars; only the situation with catalogs of extragalactic Supernovae is good (see <http://www.sai.msu.su/sn/sncat/>).

Probably the most strange tradition limiting the scope of the GCVS is not to include variable stars in the globular star clusters of our Galaxy (variables in open clusters are included). These stars are listed in special catalogs of variable stars in globular clusters, prepared and published in Canada, now only in electronic form (cf. Clement et al., 2001; Clement, 2010). We highly appreciate this work. Nevertheless, we have recently opened a possibility to add those stars that meet the GCVS criteria also to our catalog, having determined accurate equatorial coordinates for many variable stars in globular clusters earlier listed only with rectangular coordinates with respect of their cluster centers (Samus et al., 2009).

The GCVS is intended to contain only proven and more or less well-studied variable stars. Currently, the criterion for the star to be considered studied well enough for the GCVS is the possibility to ascribe it at least a tentative variability type or to decide that the star is “unique” (possibly belongs to a type not yet introduced). Earlier, the rules used to be even stricter, like, for a periodic variable, the requirement of the period being known. Variable stars not meeting the GCVS criteria are called “suspected variables”, even if their photometric variations are beyond doubt, and listed in special catalogs. After the World War II, such catalogs are also a responsibility of the GCVS team in Moscow.

The fourth edition of the GCVS, surely the last one to consist of printed books, started with the “New Catalogue of Suspected Variable Stars” (the NSV catalog) with 14810 entries (Kholopov, 1982). A supplement to the NSV catalog, with 11206 additional entries, was published by Kazarovets et al. (1998). After the NSV catalog, five GCVS volumes appeared in 1985–1995. The first three of them (Kholopov, 1985–1987) are the catalog of galactic variables proper, containing 28435 stars. After them, two more books (Samus, 1990, 1995) appeared. The most important part of the first of them, devoted to different auxiliary tables, are cross-identification tables that permit a user to find the GCVS name for an object of interest if its name in one of the major astronomical catalogs is known. The second of them is the GCVS team’s first and only attempt, initiated by P.N. Kholopov, to add extragalactic variables to the GCVS and thus make the catalog more “general”. This book contains some 12000 entries for extragalactic variables, including Supernovae. Immediately after its publication, the flow of new discoveries

of extragalactic variables became too strong to permit the GCVS team, with its limited human power and funds, to further pursue this direction of work.

Till 1994, the IAU provided some financial support to the GCVS project. These funds did not reach the GCVS team but permitted it to rely on better attitude of local administrative bodies. Unfortunately, the support was discontinued, just at the time of a serious funding crisis and just when it became possible to make the IAU money available directly to the scientific group compiling the catalog. The IAU Commissions 27 and 42 (now Division V) continue to provide their moral support of our effort.

Currently, it is too expensive to continue the GCVS in the form of printed books, and the role of printed catalogs also has become secondary compared to electronic catalogs. The fourth GCVS edition, with corrections, is available electronically at the Strasbourg data center. The most recent electronic version of the GCVS can be found at our web site (<http://www.sai.msu.su/groups/cluster/gcvs/gcvs/>). The site also has a search engine permitting to retrieve GCVS information by the star’s name (in the GCVS or in other catalogs), coordinates, variability type, and other parameters.

Stars are added to the GCVS via Name-Lists. The last one published so far was No. 79 (Kazarovets et al., 2008), it makes the number of GCVS stars as high as about 41500. The GCVS+NSV system now contains more than 60000 Galactic variable stars. The GCVS data base contains stars from the fourth GCVS edition as well as stars from the subsequent Name-Lists, but, until recently, information provided in the data base for Name-List stars used to be incomplete. We have now started preparing catalogs of Name-List variables in the complete GCVS format. Recently, the first catalog of this kind (Kazarovets et al., 2009) has been published for the 79th Name-List.

We have now finished selecting stars for the Name-List No. 80. The number of stars selected is so large that we are forced to subdivide the list into several parts, to be published separately. The first part, for right ascensions (J2000) between 0 and 6 hours, will appear before the end of 2010. It will contain about 2000 variables.

For a number of constellations (it should be reminded that the traditional naming system of the GCVS relies on each star’s constellation), the web version of the GCVS now contains completely revised information on variability types, magnitude ranges, light elements, with new remarks. This revision will be continued.

3. Current GCVS Problems

These days, very many new variable stars are being discovered in modern automatic photometric sky sur-

veys. Some of the surveys provide their own catalogs of variable stars. In the near future, automatic surveys, especially those from space, will be able to discover millions of new variable stars each year.

For several reasons, it is not easy to incorporate the stars of variable-star catalogs of automatic surveys into the GCVS. First of all, most ground-based automatic sky surveys use wide-field, small-focal-length instruments, and thus the variable-star coordinates in their catalogs are not precise enough.

Note that the GCVS is ready for automatic identifications with newly-discovered stars having accurate coordinates. In 2002–2006, we checked identifications of all “old” GCVS variable stars using published as well as unpublished finding charts and other sources of information and provided accurate coordinates (to about $1''$) for virtually all of them (Samus et al., 2006 and references therein). In the process of identification, we revealed many cases of very wrong coordinates, with mistakes as large as about 10° in several exceptional instances. Only about 200 cataloged variable stars seem to be lost forever because of poor-quality coordinates in their discovery announcements and lacking finding charts.

In several important automatic surveys, like ASAS-3 (Pojmanski, 2002) or ROTSE-I/NSVS (Woźniak et al., 2004), the angular resolution is $15''$ – $30''$, and if a variable star is in a pair, its cataloged coordinates can be wrong by a dozen of arcseconds. Thus, in many cases, automatic-survey catalogs contain quite reliable variable stars at formal positions between two stars separated by $10''$ – $15''$, so that it is impossible to be sure which of the two stars varies. We strongly prefer not to worsen the standard of coordinate accuracy now established in the GCVS and not to add such stars to the GCVS till the true variable in the pair is reliably identified.

As a rule, variability types quoted in the variable-star catalogs of automatic surveys were determined also automatically. They do give some idea of what is observed, but the GCVS classification is much more detailed and informative. Algorithms for automatic variable-star classification still provide a large percentage of erroneous classifications. On the other hand, the GCVS classification system requires serious modification, taking into account current astrophysical ideas but not making it too complex and clumsy. We presented our suggestions to the IAU Division V (Variable Stars) at the General Assemblies of the IAU in 2006 and 2009. In 2006, the IAU Commission 26 established a working group to study the future of variable-star catalogs. We invite everyone interested in the problem to join the discussion on classification as well as on all other issues of future variable-star catalogs. Some materials of the working group can be found at our web site (<http://www.sai.msu.su/gcvs/future/future.html>).

Variable-star catalogs of large automatic surveys may be considered self-sufficient for the time being. Adding their stars to the GCVS will be very effort-consuming. So far, the GCVS team finds it more important not to miss variable stars announced individually or as a result of minor surveys. We use to add stars from large automatic surveys to the GCVS if they are studied in detail in subsequent publications.

Several years ago, the American Association of Variable Star Observers (AAVSO) started a new large-scale project, the Variable Star Index (<http://www.aavso.org/vsx>). It is a kind of a general list of variable stars, with extensive search possibilities, access to finding charts, possibilities to introduce users' additions and corrections. In the opinion of the AAVSO leadership, it can become a future main entry point to the GCVS system. In April 2009, prospects of interaction between the VSX project and the GCVS were discussed in detail between the two teams. After this discussion, the coordinates of GCVS variable stars in the two data bases were attentively compared, with a number of mistakes revealed and corrected in both of them. We invited the team of the SIMBAD data base (Strasbourg) to join our effort, and they have also started the mutually benefiting process of checking their coordinates of variable stars against those in the GCVS.

4. Conclusions

The GCVS project, initiated on behalf of the IAU in the second half of the 1940s, has a long and eventful history. The recent developments in astronomy have led to the necessity to solve a number of problems in order to enable future successful continuation of the project. The current GCVS problems can be summarized as follows.

- The GCVS is no longer (and actually never was) a true “general” catalog, even for variable stars in our Galaxy;
- no reliable software for automatic classification of variable stars exists;
- the GCVS classification scheme should be simplified but also improved according to the current state of variable-star astrophysics;
- individual approach of a human expert to each star, characteristic of the best catalogs in the past, will be impossible in future, but the experience of automatically updated catalogs shows that they contain too many mistakes;
- virtual data sources often have unpleasant imperfections, access to such sources is insufficiently standardized;
- light-curve-analysis software is not standardized, and the experience of automatic surveys evidences for low precision of periods and other derived parameters.

The discussion of these and other problems during the recent General Assemblies of the IAU shows that the astronomical community still wants quality variable-star catalogs. Thus, we need to seek solutions of the problems listed above most actively, with participation of variable-star experts worldwide.

Acknowledgements. Our GCVS work is supported, in part, by the Russian Foundation for Basic Research (grant 08-02-00375) and by the Basic Research Program “Origin and Evolution of Objects in the Universe” of the Presidium of Russian Academy of Sciences.

References

- Clement C.M.: 2010, in *Variable Stars, the Galactic Halo and Galaxy Formation*, Proceedings of the B.V. Kukarkin Centenary Conference, C. Sterken et al. (eds.), Moscow: Sternberg Astronomical Institute, p. 23.
- Clement C.M., Muzzin A., Dufton Q. et al.: 2001, *Astron. J.*, **122**, 2587.
- Kazarovets E.V., Samus N.N., Durlevich O.V. et al.: 2008, *Inform. Bull. Var. Stars*, No. 5422.
- Kazarovets E.V., Samus N.N., Durlevich O.V. et al.: 2009, *Astronomy Reports*, **53**, 1013.
- Kholopov P.N. (ed.): 1982, *The New Catalogue of Suspected Variable Stars*, Moscow: “Nauka”.
- Kholopov P.N. (ed.): 1985–1987, *General Catalogue of Variable Stars*, Fourth Edition, Vols. I–III, Moscow: “Nauka”.
- Kukarkin B.V., Parenago P.P.: 1948, *General Catalogue of Variable Stars*, First Edition, Moscow and Leningrad: Izdatel’stvo AN SSSR.
- Pojmanski G.: 2002, *Acta Atron.*, **52**, 397.
- Samus N.N. (ed.): 1990, *General Catalogue of Variable Stars*, Fourth Edition, Vol. IV (Reference Tables), Moscow: “Nauka”.
- Samus N.N. (ed.): 1995, *General Catalogue of Variable Stars*, Fourth Edition, Vol. V (Catalogue of Extragalactic Variable Stars; Catalogue of Extragalactic Supernovae), Moscow: Kosmosinform”.
- Samus N.N., Durlevich O.V., Zharova A.V. et al.: 2006, *Astronomy Letters*, **32**, 263.
- Samus N.N., Kazarovets E.V., Pastukhova E.N. et al.: 2009, *Publ. Astron. Soc. Pacific*, **121**, 1378.
- Woźniak P.R., Vestrand W.T., Akerlof C.W. et al.: 2004, *Astron. J.*, **127**, 2436.

OPEN QUESTIONS ON CEPHEIDS AND THEIR PERIOD-LUMINOSITY RELATIONSHIP

L. Szabados

Konkoly Observatory of the Hungarian Academy of Sciences
Konkoly Thege út 15-17, H-1121 Budapest XII, Hungary, *szabados@konkoly.hu*

ABSTRACT. Physical properties and pulsational behaviour of classical Cepheids can be studied in unprecedented details based on recent photometric and spectroscopic data. In spite of important new results, problems related to Cepheids still exist, such as metallicity dependence of their various properties, their mass loss and circumstellar environment, excitation of low-amplitude pulsation modes in such variables, etc.

Key words: Cepheids; Stars: binary; Stars: mass-loss; Stars: oscillations

Classical Cepheids are supergiant stars located in the Cepheid instability strip of the Hertzsprung-Russell diagram. Their main characteristic is a periodic radial oscillation of their atmospheric layers. This regularity gives rise to various relationships between the pulsation period and other physical properties (e.g., luminosity, radius, etc.) of Cepheids. The very accurate recent observational data, however, revealed that the pulsation may not be strictly regular. Deviations from perfect regularity and the individual behaviour in the pulsation of some Cepheids are topics of on-going investigations.

1. Introduction

Classical Cepheids are primary distance indicators via the famous period-luminosity ($P-L$) relationship, as well as key objects in studying stellar structure and evolution. The main aim of the recent Cepheid studies is to make progress in understanding the evolution of intermediate mass stars and to increase the precision of the calibration of the $P-L$ relationship, a fundamental tool in establishing the cosmic distance scale.

Major problems used to exist in explaining the behavior of Cepheids but the progress in the observational techniques and theoretical modelling of the internal structure, pulsation, and evolution of intermediate mass stars has normally led to the solution of these problems. Such long-standing problem was, e.g., the treatment of Cepheids as a homogeneous type of pulsators.

Classification into classical and Type II Cepheids solved the controversy in their distances. Another conundrum was how to explain the characteristic phase lag between the brightness and radial velocity variations of Cepheids.

A more recent problem of the discrepancy between the evolutionary and pulsation masses of Cepheids was largely mitigated by the new opacity values in the 1990s but a partial discrepancy still exists.

Unlike these historical problems, some more recent Cepheid related issues have remained unsolved. This paper summarizes the current picture and examples are listed for the still existing problems selected from the forefront of Cepheid research.

2. The $P-L$ relationship

The $P-L$ relationship has a century-long history with a permanent goal to improve its calibration. Assuming that the luminosity is a linear function of the decimal logarithm of the pulsation period, determination of two parameters is necessary for calibrating this relationship. Microlensing projects (e.g., OGLE, MACHO, and EROS) have resulted in long series of homogeneous photometric data on several thousand Cepheids in both Magellanic Clouds, therefore the slope of the $P-L$ relationship can be conveniently determined by the Magellanic Cepheids. The zero point of the relationship is usually determined by properly selected Galactic Cepheids of known distance/luminosity (see David Turner's review in this volume).

The ridge-line linear fit is, however, an approximation. In fact, Cepheids widely scatter along the fitted line. In addition to the observational errors, there are quite a few effects that contribute to the width of the $P-L$ plot:

- intrinsic colour of the Cepheid,
- pulsation mode,
- crossing mode,
- binarity,
- metallicity,
- helium content,
- non-linearity of the relationship,
- other effects (magnetic field, overshooting, blending, etc.).

It can be pointed out that the effective temperature of the Cepheid (corresponding to the location of the star within the instability strip) is an important parameter for the P - L relationship. Therefore, it is more appropriate to refer to P - L -colour relationship where colour means the intrinsic (i.e. dereddened) colour. For extragalactic Cepheids, the foreground (Galactic) and internal reddenings are superimposed. The effect of the average interstellar absorption is usually taken into account by calculating the Wesenheit function (Freedman & Madore 2010). The P - L plot for the Wesenheit magnitudes has smaller dispersion but its width is still non-negligible.

Magellanic Cepheids clearly show existence of separate P - L relationships for each mode. In the Magellanic Clouds, Cepheids pulsating in the fundamental mode and first overtone are ubiquitous, but single-mode Cepheids pulsating in the second overtone have also been identified (Udalski et al. 1999; Soszyński et al. 2008). In general, overtone pulsation can be readily identified in external galaxies because the luminosity of such Cepheids corresponds to the fundamental period but the actual pulsation period is shorter (the period ratio is known from double-mode Cepheids and pulsation models). In our Galaxy, however, a straightforward way for determining the pulsation mode is the Fourier decomposition of the light curve. The separation of various pulsation modes in the plots of Fourier amplitudes/phases vs. pulsation period is also demonstrated for Magellanic Cepheids (Soszyński et al. 2008b). The photometric amplitude itself is not a good indicator of the pulsation mode: although fundamental pulsators usually have a large amplitude, but companion stars decrease the observable amplitude, moreover large amplitude first overtone Cepheids are also known in the Magellanic Clouds. The most reliable indicator of the pulsation mode is the Fourier phase lag between the radial velocity and brightness variations (Szabó et al. 2007). A drawback to the application of this method is the lack of sufficiently precise radial velocity phase curves for a large percentage of Cepheids.

The P - L plot for a given pulsation mode still has a finite width. One of the causes of this dispersion is that intermediate mass stars cross the instability strip 3 (or for larger masses 5) times, and the excited pulsation period differs for each crossing. The pulsation period itself varies during crossing the instability strip, and the actual crossing mode can be inferred from the sign of the secular period change (increasing period during the 1st and 3rd crossings, decreasing period during the 2nd crossing) and the abundance of the heavy elements in the atmosphere of the given Cepheid (Turner et al. 2006).

The incidence of binarity among classical Cepheids exceeds 50% (Szabados 2003). Unresolved companions falsify the derived luminosity. When calibrating the

P - L relationship using Galactic Cepheids, presence of companion(s) has to be taken into account on an individual basis. In the case of external galaxies, unresolved optical companions and blending also increase the scatter in the P - L plot.

The calibration of the Hubble constant, H_0 , and the cosmic distance scale via extragalactic Cepheids was one of the Key Projects for the Hubble Space Telescope. The original intention to reach a 5% accuracy in calibrating the P - L relationship, however, could not be fulfilled mainly because of the uncertainty in the effect of metallicity on the luminosity of Cepheids. In spite of considerable theoretical and observational effort, studies of metallicity dependence of the P - L relationship for Cepheids have been still inconclusive (Marconi 2009, Romaniello et al. 2008).

Stellar luminosity also depends on the helium content of the Cepheid, especially in the case of long pulsation periods (Marconi et al. 2005). The helium abundance of Cepheids, however, can be hardly inferred from spectroscopic data.

The influence of the magnetic field and convection (including convective overshooting) on the luminosity needs thorough theoretical studies.

The effects of the interstellar extinction, binarity, and metallicity are much smaller in the infrared than in optical region. In addition, the photometric amplitude of Cepheids decreases towards longer wavelengths, so a reliable mean brightness can be determined from a few randomly obtained observations in the infrared. In view of these advantages, recently the near-infrared is the preferred region for photometry of Cepheids.

3. Other effects of metallicity

The chemical composition of the pulsating atmosphere has an influence on the Cepheid oscillations whose study was long delayed by absence of reliable spectroscopic abundance data. In the last decade, however, dedicated spectroscopic studies of Cepheids carried out by Andrievsky and his coworkers (Andrievsky et al. 2002a,b,c; 2004; 2005; Kovtyukh et al. 2005a,b) opened the possibility to detailed investigations of the effect of metallicity on pulsational properties of Cepheids.

On the one hand, the well known wavelength dependence of photometric amplitudes (decreasing amplitude towards longer wavelengths) has a metallicity dependence (Szabados & Klagyivik 2011). Similarly, the shape of the light curves is indicative of the iron content of the Cepheid via properly selected Fourier parameters (Szabados et al. 2011). On the other hand, the amplitude of the pulsational radial velocity variations itself is a function of the atmospheric iron content, especially for the short-period Cepheids (Szabados & Klagyivik 2011).

The period ratio of the excited modes in double-mode Cepheids is also sensitive to the atmospheric metal abundance. Theoretical calculations by Buchler & Szabó (2007) are in accord with the empirical formula obtained from Galactic beat Cepheids by Sziládi et al. (2007).

Recent theoretical calculations predict a larger mass loss rate via pulsation driven outflow for lower metallicity Cepheids, especially for shorter pulsation periods (Neilson & Lester 2009).

4. Problems related to the pulsation period

4.1. Period changes

Knowledge of the exact value of the actual pulsation period is essential for Baade-Wesselink type analyses to avoid phase mismatch (simultaneous V and K band photometry and radial velocity measurements seldom exist). Period changes have to be monitored, in some cases even permanently followed because of various reasons. Secular period variation may be indicative of stellar evolution. Although period noise has been superimposed on monotonous period changes during crossing the instability strip, evolutionary changes are apparent for a large number of Cepheids (see e.g., Fig. 1). Another kind of period changes is the cyclic variation in the pulsation period due to the light-time effect occurring in binary systems involving a Cepheid component.

Photoelectric and CCD photometric data obtained in the last decades are instrumental for revealing subtle period changes. Figure 2 shows an intriguing example: a phase jump (‘glitch’) superimposed on the monotonous period increase of Polaris (Turner et al. 2005). This phenomenon might be caused by a

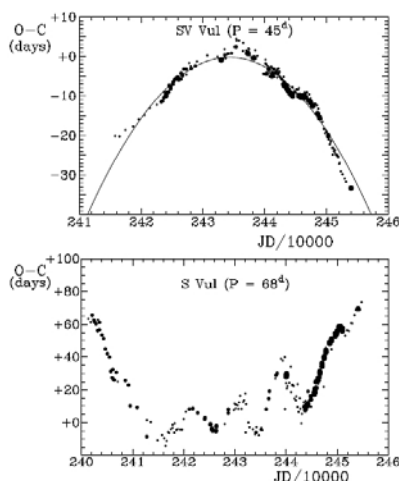


Figure 1: $O - C$ variations of long-period Cepheids SV Vul (upper panel) and S Vul (lower panel) with the size of individual residuals proportional to the weight assigned to the value (Turner et al. 2009).

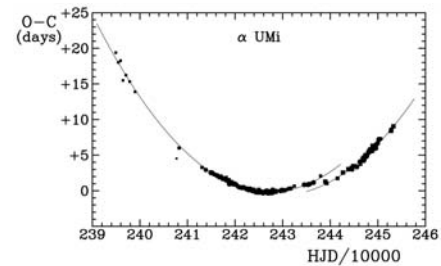


Figure 2: $O - C$ diagram of Polaris, a short period Cepheid. A sudden phase jump is clearly visible. (Turner et al. 2005).

trigger from the physical companion of the Cepheid. Continuous time series data recently obtained by photometric space probes allow one to investigate minute cycle-to-cycle changes in the pulsation period.

4.2. Double and multiple periodicity

Majority of Cepheids are monoperoiodic pulsators. Existence of additional periodicities is, however, important because the values of simultaneously excited frequencies bear information on the stellar interior. As an example, the dependence of the period ratio of the excited modes on the atmospheric iron abundance is mentioned (see Sect. 3).

Microlensing projects resulted in discovering more than 200 double-mode Cepheids in the LMC and over 150 such pulsators in the SMC, pulsating simultaneously in the fundamental mode and the first overtone, or in the first and second overtones. The number of the known beat Cepheids in our Galaxy (36) shows a deficiency as compared with their siblings in the Magellanic Clouds, in spite of the fact that recently Khruslov (2009a,b,c; 2010) discovered nine Galactic double-mode Cepheids analysing the ASAS photometric data base.

Double-mode Cepheids, especially those in external galaxies, are extremely important objects because the period ratio of their excited pulsation modes provides information on the metallicity of individual Cepheids without any spectroscopic observation (see Sect. 3).

Intriguing discoveries on additional periodicities were published by Moskalik & Kołaczowski (2009). They revealed slightly excited non-radial modes in Magellanic Cepheids. These appear either very close to the primary pulsation frequency or at a much shorter period (period ratio $\sim 0.60-0.64$). Such non-radial mode has been found in LMC Cepheids pulsating in the first radial overtone and some double-mode pulsators. No such oscillations have been observed in single-mode Cepheids performing fundamental-mode radial oscillations. Moreover, they also detected a Blazhko-type periodic modulation in 19% of double-mode Cepheids pulsating in the first two radial

overtones. Both modes are modulated with a common period, always exceeding 700 d. Variations of the two amplitudes are anticorrelated. They propose that the Blazhko phenomenon in Cepheids can be explained by a resonant interaction of one of the radial modes with a non-radial oscillation mode. Triple-mode Cepheids have also been found in the LMC by Moskalik & Kołaczowski (2009) and Soszyński et al. (2008a). These triple-mode Cepheids pulsate simultaneously either in the fundamental mode and the first two radial overtones or in the first three overtones.

5. Binarity among Cepheids

In view of the fact that at least 50% of the classical Cepheids are not solitary pulsators (Szabados 2003) (see also Fig. 3), binarity cannot be neglected when investigating Cepheid related relationships. Unresolved companions falsify the apparent brightness and the observable colour of the Cepheid, and they cause an adverse effect when determining the colour excess and deriving stellar radius by applying any version of the Baade-Wesselink method. It is, therefore, important to reveal and characterize companions to Cepheids, and correct for their effects when deriving the physical properties of individual Cepheids.

Eclipsing binaries with a Cepheid component are especially important because they provide an independent method of luminosity determination, thus facilitating the calibration of the P - L relationship. Cepheids in eclipsing systems have been found in both Magellanic Clouds: 4 in the LMC (Soszyński et al. 2008b), 2 in the SMC (Soszyński et al. 2010).

Companions affect astrometric measurements, as well. Though it was impossible to determine the astrometric orbit of the nearest Cepheids having a physical companion from the positional data of the Hipparcos astrometric satellite (with an angular resolution of about 1 milliarcsecond), the derived trigonometric parallaxes indicate the adverse effect of the companions: each (physically unrealistic) *negative parallax value belongs to binaries* (see Fig. 4). The ESA's next astro-

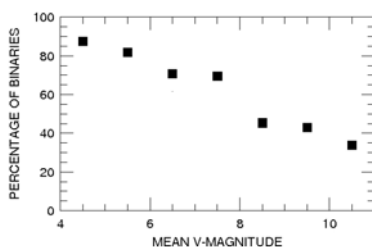


Figure 3: Frequency of known binaries (or multiple systems) among Cepheids. The diagram shows the presence of a strong observational selection effect: it is increasingly difficult to reveal companions of fainter Cepheids.

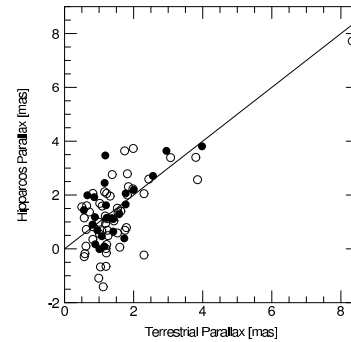


Figure 4: Hipparcos vs. ‘ground-based’ parallax of the nearest Cepheids. Open circles denote Cepheids with known companion(s). Cepheids without known companions are marked with black dots. Note that all negative parallax values belong to binaries.

metric satellite, Gaia, to be launched in late 2012 will be sufficiently sensitive to resolve these binary orbits with its angular resolution of several microarcseconds.

An on-line data base on Galactic binary (and multiple) Cepheids maintained by the author is available at the URL: <http://www.konkoly.hu/CEP/intro.html> (Szabados 2003).

6. Mass loss and circumstellar environment

The increasing importance of the infrared spectral region in Cepheid studies is further exemplified by interferometric studies of Cepheids in the near- and mid-infrared. A surprising result of these interferometric measurements is the discovery of circumstellar envelope around bright Cepheids. Extended envelopes surround α UMi and δ Cep (Mérand et al. 2006), Y Oph (Mérand et al. 2007), ℓ Car and RS Pup (Kervella et al. 2009). The presence of these envelopes so close to the Cepheids indicates on-going mass loss which offers an explanation for the still existing mass discrepancy (masses derived from the pulsational behaviour of Cepheids are smaller by about 15% than mass values deduced from stellar evolution – Keller 2008). However, the actual mass loss from Cepheids is unknown.

7. Determination of physical properties

The radial pulsation is instrumental in the process of determining physical properties of Cepheids. The application of the widely used Baade-Wesselink method for the determination of stellar radius and luminosity is, however, encumbered by the uncertainty in the value of the projection factor. This conversion factor between radial and pulsational velocities depends on the limb darkening effects, not properly known yet, the atmospheric velocity gradients, and the dynamical

structure of the Cepheid atmosphere (Nardetto et al. 2006). In addition, when carrying out Baade-Wesselink analysis, a special care must be taken for correcting the effects of the companions on a star-by-star basis.

Availability of precise spectroscopic abundance values facilitates studies of possible metallicity dependence of various Cepheid properties (see also Sect. 3).

Furthermore, interferometric observations in the near-infrared are indispensable for determining the rate of mass loss and its effects on the evolutionary properties of Cepheids. Strangely enough, the remaining mass discrepancy depends on the stellar mass (i.e., the pulsation period of Cepheids): it vanishes at higher masses. Keller (2008) pointed out that mild internal mixing in the main-sequence progenitor of the Cepheid would be sufficient to account for this mass discrepancy.

8. Ultra-low amplitude Cepheids

Recent ground- and space based photometric equipments facilitate discovery of extremely low amplitude pulsation. Among Cepheids, such oscillations may correspond to high-overtone radial modes that are trapped in the stellar atmosphere. These acoustic surface modes ('strange' modes) have been found in classical Cepheid models (Buchler et al. 1997). The pulsation in such modes can be linearly unstable to the left of the fundamental and first overtone blue edges and causes luminosity variations in the milli-magnitude range.

An observational confirmation of this prediction is the discovery of two low-amplitude variables in one MACHO field of the LMC whose periods are 5-6 times smaller than those of fundamental mode Cepheids of equal apparent magnitude (Buchler et al. 2005). These objects are thought to be Cepheids undergoing pulsations in a surface mode. They also found 7 ultra-low amplitude Cepheids (seven of them having a Fourier amplitude less than 0.006 mag). Further ultra-low amplitude

Cepheids have been revealed in the LMC by Soszyński et al. (2008b) and Buchler et al. (2009). These stars may be just entering or about leaving the Cepheid instability strip because theoretical calculations predict extremely low amplitude pulsation near either border of the instability region (Buchler & Kolláth 2002). Further low amplitude and strange Cepheid candidates have been found in the photometric data base of CoRoT satellite (Szabó et al. 2009).

9. Extragalactic Cepheids

Thanks to the HST Key Program on the calibration of the Hubble constant, H_0 , and the cosmic distance scale, Cepheid variables have been discovered in numerous galaxies. Moreover, projects aimed at revealing

extragalactic Cepheids (and then calibrating the $P-L$ relationship) have been carried out with ground based large and medium size telescopes from the 1990s. As a result, ~ 12000 Cepheids are now known in 81 galaxies. Almost 40 per cent of these Cepheids are beyond the Magellanic Clouds (including ~ 400 known Cepheids in galaxies belonging to the Virgo Cluster). The largest sample of Cepheids is known in the SMC (~ 4600), the second largest one in the LMC (~ 3400). The number of known classical Cepheids does not reach a thousand in each M31, M33, and our own Galaxy.

The period distribution of the known Cepheids is different for various galaxies. In addition to intrinsic differences (caused by e.g., the metallicity differences), an observational selection effect also contributes to this variety: in more remote galaxies only long-period Cepheids can be discovered yet.

10. New aspects of the $P-L$ relationship

The important question whether the $P-L$ relationship is universal has been unanswered yet. An interesting new aspect of this important relationship was revealed by Bird et al. (2009). Based on 18 Cepheids with periods exceeding 80 days, they pointed out that ultra-long period Cepheids have a relatively shallow $P-L$ relationship, thus being more suitable standard candles than shorter period classical Cepheids. Another advantage of such long period Cepheids is their high luminosity which makes them potential stellar distance indicators to galaxies up to at least 100 Mpc. The small sample studied by Bird et al., however, involved Cepheids in only 6 metal-poor galaxies. It would be important to repeat the investigation of the luminous end of the $P-L$ relationship based on an extended sample involving Cepheids in metal-rich galaxies, as well.

There is growing evidence that the $P-L$ relationship is better approximated with two linear sections, instead of a single line (Sandage et al. 2004; Kanbur & Ngeow 2004). Recent theoretical models also confirm nonlinearity of the relationship (Marconi 2009). Although the break is usually assumed to be at the period of 10 days, Klagyivik & Szabados (2009) pointed out that the dichotomy occurs at the limiting period of 10.49 days. Pulsation models, however, indicate that the nonlinearity of the $P-L$ relationship vanishes toward longer wavelengths (Marconi 2009).

11. Future tasks

Continuation of photometric observations (not only in infrared bands) are necessary to solve the problems of universality, dichotomy and fine structure of the $P-L$ relationship. To investigate metallicity dependence of the Cepheid pulsation, accurate spectroscopic abundance determinations are necessary for Galactic as well

as extragalactic Cepheids (within the Local Group). Interferometry of bright Cepheids and radial velocity measurements of faint Cepheids (including those in the Magellanic Clouds) are to be performed for revealing binarity and carrying out BW type analysis. Detailed studies of peculiar Cepheids (SU Crucis, V473 Lyrae, RS Pup, etc.) and beat (double and triple mode) Cepheids will shed light on some aspects of Cepheid pulsation to be clarified.

Ongoing space photometric studies (WIRE, CoRoT, Kepler) will certainly reveal unexpected phenomena in the behaviour of Cepheids. The Gaia astrometric satellite will result in discovery of thousands of new Galactic Cepheids, as well as determination of the astrometric orbit for binary systems involving a Cepheid component.

In addition to obtaining a three-dimensional map and kinematics of Galactic Cepheids with Gaia, the determination of cluster membership of Cepheids is also foreseen. The most important impact of the Gaia data will be undoubtedly a very accurate calibration of the P - L relationship taking into account metallicity effects.

Acknowledgements. This research was supported by the ESA and the Hungarian Space Office via the PECS programme (contract No. C98090). The author is indebted to Dr. M. Kun for her remarks on the manuscript.

References

- Andrievsky, S. M., Kovtyukh, V. V., Luck, R. E., et al.: 2002a, *A&A*, **381**, 32.
- Andrievsky, S. M., Bersier, D., Kovtyukh, V. V., et al.: 2002b, *A&A*, **384**, 140.
- Andrievsky, S. M., Kovtyukh, V. V., Luck, R. E., et al.: 2002c, *A&A*, **392**, 491.
- Andrievsky, S. M., Luck, R. E., Martin, P., & Lépine, J. R. D.: 2004, *A&A*, **413**, 159.
- Andrievsky, S. M., Luck, R. E., & Kovtyukh, V. V.: 2005, *AJ*, **130**, 1880.
- Bird, J. C., Stanek, K. Z., & Prieto, J. L.: 2009, *ApJ*, **695**, 874.
- Buchler, J. R. & Kolláth, R.: 2002, *ApJ*, **573**, 324.
- Buchler, J. R. & Szabó, R.: 2007, *ApJ*, **660**, 723.
- Buchler, J. R., Yecko, P. A., & Kolláth, Z.: 1997, *A&A*, **326**, 669.
- Buchler, J. R., Wood, P. R., Keller, S., & Soszyński, I.: 2005, *ApJ*, **631**, 151.
- Buchler, J. R., Wood, P. R., & Soszyński, I.: 2009, *ApJ*, **698**, 944.
- Freedman, W. L. & Madore, B. F.: 2010, *ARA&A*, **48**, 673.
- Freedman, W. L., Madore, B. F., Gibson, B. K., et al.: 2001, *ApJ*, **553**, 47.
- Kanbur, S. M. & Ngeow, C.-C.: 2004, *MNRAS*, **350**, 962.
- Keller, S. C.: 2008, *ApJ*, **677**, 483.
- Kervella, P., Mérand, A., & Gallenne, A.: 2009, *A&A*, **498**, 425.
- Klagyivik, P. & Szabados, L.: 2009, *A&A*, **504**, 959.
- Kovtyukh, V. V., Andrievsky, S. M., Belik, S. I., & Luck, R. E.: 2005a, *AJ*, **129**, 433.
- Kovtyukh, V. V., Wallerstein, G., & Andrievsky, S. M.: 2005b, *PASP*, **117**, 1173.
- Khruslov, A. V.: 2009a, *PZP*, **9**, 14.
- Khruslov, A. V.: 2009b, *PZP*, **9**, 17.
- Khruslov, A. V.: 2009c, *PZP*, **9**, 31.
- Khruslov, A. V.: 2010, *PZP*, **10**, 16.
- Marconi, M.: 2009, *Mem. SAI*, **80**, 141.
- Marconi, M., Musella, I., & Fiorentino, G.: 2005, *ApJ*, **632**, 590.
- Mérand, A., Kervella, P., Coudé du Foresto, V., et al.: 2006, *A&A*, **453**, 155.
- Mérand, A., Aufdenberg, J. P., Kervella, P., et al.: 2007, *ApJ*, **664**, 1093.
- Moskalik, P. & Kołaczowski, Z.: 2009, *MNRAS*, **394**, 1649.
- Nardetto, N., Fokin, A., Mourard, D., & Matthias P.: 2006, *A&A*, **454**, 327.
- Neilson, H. R. & Lester, J. B.: 2009, *ApJ*, **690**, 1829.
- Romaniello, M., Primas, F., Mottini, M., et al.: 2008, *A&A*, **488**, 731.
- Sandage, A., Tammann, G. A., & Reindl, B.: 2004, *A&A*, **424**, 43.
- Soszyński, I., Poleski, R., Udalski, A., et al.: 2008a, *Acta Astron.*, **58**, 153.
- Soszyński, I., Poleski, R., Udalski, A., et al.: 2008b, *Acta Astron.*, **58**, 163.
- Soszyński, I., Poleski, R., Udalski, A., et al.: 2010, *Acta Astron.*, **60**, 17.
- Szabados, L.: 2003, *IBVS*, **5394**.
- Szabados, L. & Klagyivik, P.: 2011, in preparation.
- Szabados, L., Klagyivik, P., & Kiss, Z. T.: 2011, in preparation.
- Szabó, R., Buchler, J. R., & Bartee, J.: 2007, *ApJ*, **667**, 1150.
- Szabó, R., Kolláth, Z., Molnár, L., et al.: 2009, *AIPC*, **1170**, 102.
- Sziládi, K., Vinkó, J., Poretti, E., et al.: 2007, *A&A*, **473**, 579.
- Turner D. G., Savoy, J., Derrah, J., et al.: 2005, *PASP*, **117**, 207.
- Turner D. G., Abdel-Sabour, M., & Berdnikov, L. N.: 2006, *PASP*, **118**, 410.
- Turner D. G., Majaess D. J., Lane D. J., et al.: 2009, *AIPC*, **1170**, 108.
- Udalski, A., Soszyński, I., Szymański, M., et al.: 1999, *Acta Astron.*, **49**, 45.

UNUSUAL ACCRETION DISK IN AN ALGOL - TYPE BINARIES - KU Cyg

T. Szymański¹, S. Zola^{1,2}, M. Siwak³, W. Ogłóża²

¹ Astronomical Observatory of the Jagiellonian University
ul. Orła 171, 30-244 Cracow, Poland

² Mt. Suhora Observatory, Pedagogical University
ul. Podchorążych 2, 30-084 Cracow, Poland

³ Department of Astronomy and Astrophysics, University of Toronto
50 St. George Street, M5S 3H4 Toronto, Canada

ABSTRACT. We present new results obtained from analysis of H α double peaked emission line observed at several phases. We confirm the results that KU Cyg harbours an eccentric shape, precessing accretion disk. The system mass ratio $q = 0.13$ may indicate that the 3:1 resonance can be responsible for changes in the accretion disk.

Key words: binaries: eclipsing stars: individual: KU Cyg.

1. Introduction

KU Cyg is a well studied Algol-type eclipsing binary. It has been observed both photometrically and spectroscopically since 1964 by Popper (1964,1965), Olson (1988,1991) and Olson et al. (1995). The first attempt to classify the components, resulting in F4p and K5 III spectral types, was made by Popper (1965). He suggested that the primary (the hotter) star was surrounded by gaseous matter of a relatively low temperature, creating a disk – like structure. He also pointed out that the secondary component likely fills its Roche lobe.

KU Cyg belongs to the group of long period Algol – type binaries, its orbital period derived from spectroscopic and photometric studies is $P = 38^d.4$. The radius of the primary, probably a Main Sequence star, is small enough and for such configuration the matter lost from the secondary star can not directly hit the primary but an accretion disk must be formed.

The spectroscopic results published by Olson and Etzel (1991) and Olson (1991) revealed in KU Cyg a double – peaked, hydrogen emission line, visible throughout the orbital cycle, confirming the hypothesis of a disk presence in this system (Smak 1984).

The main difficulty to obtain reliable orbital parameters of KU Cyg is due to uncertain properties of the primary component. Its mass and radius make it a Main

Sequence star with the expected spectral type around B7 V and the effective temperature of about 13 300 K. However, the observed spectral type of the primary is F4p (Popper 1964), resembling a supergiant, and its colours appear to indicate an effective temperature of only 7500 K (Olson 1988). On the other hand, the photometric solution by Zola (1992) gave $T_{e,1} = 10330K$. The discrepancy between those results could be due to absorption arising in a shell surrounding a star of earlier type (Popper 1964).

Smak(1997) calculated the orbital parameters from the analysis of the observed H α emission line profile originated from the disk. Though the analysis was based on only a single spectrum, he found that accretion disk is eccentric and determined the deformation of the disk from the circular shape: $a_d = 0.48 \pm 0.01$ (the major semi – axis of disk), $e_d = 0.31 \pm 0.07$ (the disk eccentricity) and $i = 86.0 \pm 0.1$ (the orbital inclination).

2. Spectroscopic Data

Spectroscopic observations of KU Cyg were collected at the David Dunlap Observatory (DDO), University of Toronto. The first observing run was done on 4th ($\phi \sim 0.220$), 10th ($\phi \sim 0.377$) and 12th ($\phi \sim 0.429$) December 2002 (Fig. 1), while the second one is more recent, data were taken on 1st ($\phi \sim 0.171$) and 2nd ($\phi \sim 0.197$) July 2008 (Fig. 1). The 1.9 m telescope and the Cassegrain focus spectrograph with dispersion of 10.8 \AA mm^{-1} , corresponding to about $0.2 \text{ \AA pixel}^{-1}$ or about $12 \text{ kms}^{-1} \text{ pixel}^{-1}$, were used for most observations.

The spectra were reduced with IRAF, the standard procedures were employed, which consist of calibrating the frames for bias, flat field, cosmic rays removal, extraction of one-dimensional spectra, wavelength calibration and rectification. After reduction, spectra were

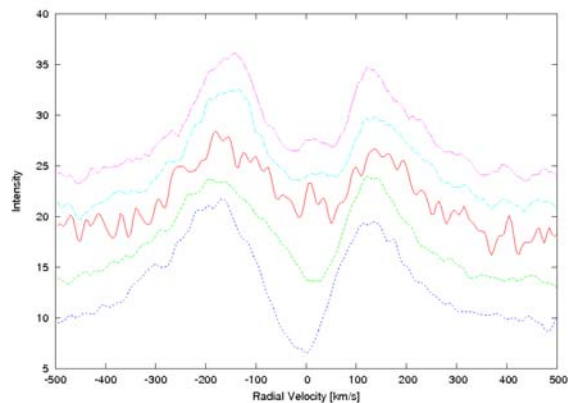


Figure 1: Double peak of H α emission line. Spectra correspond to the phases, from the top to phases 0.171, 0.197, 0.220, 0.377, 0.429 respectively. All data were shifted to show H α profile.

corrected by removing the γ velocity of whole binary system.

At the final result the observed velocity were corrected for the Earth rotation, the motion of the Earth around the Earth-Moon barycenter, and the orbit of the barycenter around the Sun.

Finally IRAF task (splot) were used to made Gauss fit to H α peak. From that task, peak velocity were collected (Table 1).

Table 1: Radial velocity of the center of Gauss fit for blue and red peak of H α

phases	blue peak	red peak
0.1707	-146.337	125.735
0.1711	-152.081	134.435
0.1967	-146.739	131.662
0.1971	-160.126	152.730
0.2204	-176.138	132.317
0.2207	-154.897	144.711
0.2212	-146.488	153.262
0.3774	-183.379	113.590
0.3518	-182.319	112.744
0.4291	-162.919	99.308
0.4296	-163.547	99.365

3. Model

In our model we use well know situation where in the circular, Keplerian disk, the observed peak velocities are almost the same as the Keplerian rotational velocities, at the outer edge of the disk (Smak 1981). We assumed that, it is also true in the case of an eccentric disk. In our work the disk is supposed to be restricted in the region close to the equatorial plan of

the star. Therefore we may simplify this problem to a two – dimensional case. In the calculations we use a polar coordinate system (r, ϕ) with its pole at the center of the primary star. We define the position angle θ_0 of the semi-major axis of the disk as follows: θ_0 equal 0° when the periastron is located between the two stars and θ_0 equal 90° when the periastron is locate between the primary and the observer, at the phase $\phi = 0.75$. For that model the radial velocity of a point placed by the angle θ in the orbit of disk semi – major axis a_d , disk eccentricity e_d and phases ϕ is given by well-know equation (e.g. Huang 1973)

$$V_r = C[\cos(\phi + \theta_0 + \theta) + e_d \sin(\phi + \theta_0)]$$

The constant C is equal to:

$$C = (GM_1/A_{ORB})^{(1/2)}[a_d(1 - e_d^2)] \sin i$$

For example the peaks velocity, corresponding to $\theta = \pm \pi/2 - (\phi + \theta_0)$, are:

$$V_{r,peak} = C[\pm + e_d \sin(\phi + \theta_0)]$$

where ± 1 corresponds to the red and the blue peak respectively (Smak 1997).

To compare radial velocity of the blue and red components of the emission line, coming from an eccentric disk with data of our model, the orbital motion K1 were taken into account.

Figure 2 shows variation of radial velocity curves at different parameters with $(\phi + \theta_0)$

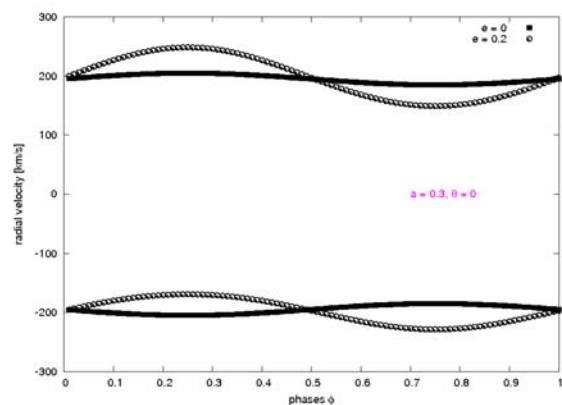


Figure 2: Variation of radial velocities of the blue and the red peaks at the different values of a_d, e_d, θ_0

4. Conclusion

The results of our model for the new spectra confirm the Smak's hypothesis that the disk shape is not circular. The resulting parameters are: inclination $i = 85.6 \pm 0.8$, the disk major semi – axis

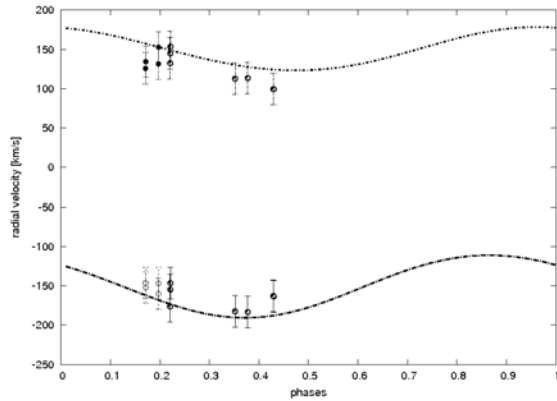


Figure 3: Observed points and theoretical velocity curves.

$a_d = 0.43 \pm 0.05$, disk eccentricity: $e_d = 0.21 \pm 0.08$, and the position angle $\theta_0 = 122 \pm 12$. The comparison of the theoretical versus observed velocities for all phases are shown in Figure 3. We were able to obtain a reasonable fit to the peak velocities for data taken in 2002 and 2008. It means that the disk size was similar in 2002 and 2008. The time scale of perturbation responsible for the growth of disk eccentricity is near 6 years, the same as in King (1994).

Using the inclination obtained from our model we determine the remaining system parameters (Table 2).

The mass ratio near 0.14 from our solution confirms another suggestion made by Smak(1997) about important role of the effects of 3:1 resonance. It can take the main role in the dynamic changes in the disk structure of the accretion disk. Further high precision spectral observations of the whole phases of this binary system are needed to resolve this problem.

Table 2: System Parameters of KU Cyg

$i[^\circ]$	$=85.6 \pm 0.8$
$q = M_2/M_1$	$= 0.136 \pm 0.01$
$r_1 = R_1/A_{orb}$	$= 0.041 \pm 0.004$
M_1/M_\odot	$= 3.88 \pm 0.07$
M_2/M_\odot	$= 0.53 \pm 0.07$
$A[10^{10} \text{ m}]$	$= 5.46 \pm 0.004$

References

- Hoang, S.-S.: 1973, *Astrophys. J.*, **183**, 541
 Kreiner J.M.: 2004, *Acta Astron.* **54**, 207-210
 King, A.R.: 1994, in: "The Evolution of X-Ray Binaries", ed. S.S.Holt, AIP Conf. Series, **308**, 515
 Olson E.C.: 1988, *AJ*, **96**, 1439
 Olson E.C.: 1988, *AJ*, **102**, 1423
 Olson E.C., Etzel P.B., Dewey M.R.: 1995, *AJ*, **110**, 2378
 Popper D.M.: 1964, *ApJ*, **139**, 143
 Popper D.M.: 1965, *ApJ*, **141**, 314
 Robinson E.L., Marsh T.R., and Smak J.: 1993, in: "Accretion Disk in Compact Stellar System", ed. J.C. Wheeler (Singapore: World Scientific), p.75
 Smak J.: 1981, *Acta Astron.*, **31**, 395
 Smak J.: 1984, *Acta Astron.*, **34**, 161
 Smak J.: 1997, *Acta Astron.*, **47**, 345
 Zola S.: 1992, *Acta Astron.*, **42**, 355

SPECTROSCOPIC ANALYSIS OF OSCILLATING ALGOL-TYPE SYSTEMS

A. Tkachenko¹, H. Lehmann¹, V. Tsymbal², D. Mkrtichian³

¹ Thueringer Landessternwarte Tautenburg, D-07778 Tautenburg, Germany

² Tavrian National University, Simferopol, Ukraine

³ Crimean Astrophysical Observatory, 98409 Nauchny, Ukraine

ABSTRACT. We analyze time-series of high-resolution spectra of RZ Cas, one of the brightest Algol-type stars where the primary shows δ Sct-like oscillations. Our investigation uses a variety of methods like the KOREL program to derive the orbital solution and to decompose the spectra of the binary components, the SynthV program to derive the elemental abundances of both components from the mean, decomposed spectra, and finally the newly developed Shell-spec07_inverse program to compute optimized stellar parameters from the composite line profiles observed at different orbital phases including the eclipse mapping.

Spectra of RZ Cas have been taken at two different epochs. In 2006, the system can be well modeled without including any Algol-typical effects like a gas stream or an accretion annulus into the calculations. We have only to assume that the secondary of RZ Cas shows a large dark spot on its surface pointing toward the primary, presumably originating from a cooling mechanism by the enthalpy transport via the inner Lagrangian point. The O-C residuals of our solution based on the spectra from 2001 show a complex distribution of circumbinary matter, however, pointing to the occurrence of an episode of rapid mass transfer. This assumption is supported by the deduced change of the orbital period of RZ Cas of 2 seconds between the two epochs of observations.

Numerical simulations of the spatial filtration effect that occurs during the primary eclipse showed that this effect can be used for an identification of the excited non-radial pulsation modes in terms of l and m numbers.

Key words: Stars: binary; eclipsing; Stars: variables; Algols; Stars: individual: RZ Cas.

1. Introduction

Algol-type systems are interacting, eclipsing binaries consisting of a more massive, main-sequence primary component of spectral type A-B and a less massive,

evolved F-K companion of luminosity class III-IV. The fact that the evolved component in the system is the less massive one completely contradicts our knowledge about stellar evolution and is called the Algol paradox. It was solved by realizing that currently less massive star initially was the more massive one but during the evolution of the system it filled its Roche-lobe and transferred a significant part of material to the companion. Algol-type systems are well known to show complex light curves effected by accretion disks, gaseous streams, and star-spots on the surface of the cool, evolved component indicating the occurrence of mass-transfer episodes and magnetic activity of the secondary component in the system.

The group of oEA stars was introduced by Mkrtichian et al. (2002) and means mass-accreting, eclipsing Algol-type systems with oscillating primary components. The stars lie in the instability strip showing δ Scuti-type pulsations. There are only about 40 such objects known so far. The co-existence of mass-transfer and oscillations of the primary components makes these objects to be of great interest for asteroseismic investigations. First, the occurrence of rapid mass-transfer episodes allows to study the evolution of the systems on a short time scale. Second, due to the change of the excited oscillation modes during phases of rapid mass-transfer, the changing structure of the outer layers of the mass-accreting primary can be investigated by asteroseismic methods. And third, the secondary acts as a spatial filter during the primary eclipse phases producing specific amplitude modulations of the excited oscillation modes which helps to identify these modes in terms of l and m numbers. Moreover, since oEA stars are eclipsing binaries, their atmospheric and system parameters can be determined with high accuracy from combined spectroscopic and photometric data which is very important for the subsequent construction of an asteroseismic model of the primary.

RZ Cas (A3 V+K0 IV) is a short-period ($P=1^d.1953$) Algol-type system and one of the best studied oEA stars. Narusawa et al. (1994) report that a partial

eclipse during primary minimum is observed. Olson (1982) and Varricatt et al. (1998) find evidence of circumstellar matter surrounding the primary component. Based on extended photometric investigations, Rodriguez et al. (2004) assume the existence of a gas stream between the components and the formation of a hot spot on the surface of the primary where the gas stream impacts its photosphere. Ohshima et al. (1998, 2001) detect the short-period light variability of the system for the first time. The authors find that the primary of RZ Cas is a mono-periodic pulsator with a dominant frequency of 64.2 d^{-1} . Later on, this conclusion is confirmed by Mkrtichian et al. (2003) and by Rodriguez et al. (2004).

The most extended spectroscopic investigation of the RZ Cas system is carried out by Lehmann & Mkrtichian (2004, 2008) based on two data sets taken in 2001 and 2006. The authors derive an orbital solution based on both data sets and find that the Rossiter effect (Rossiter 1924) observed in the radial velocities of the primary in 2001 is highly asymmetric whereas almost symmetric in 2006. They also report that the star changed its pulsation pattern twice: first, in 2001, it changed from mono- to multi-periodic behaviour with two dominant frequencies of 56.76 d^{-1} and 64.27 d^{-1} , and second, in 2006, when the third additional oscillation mode with the frequency of 62.41 d^{-1} is detected. These facts, together with the observed increase of the orbital period of about two seconds between 2001 and 2006, the authors attribute to the occurrence of a rapid mass-transfer episode in 2001.

In this paper we present a detailed spectroscopic analysis of the RZ Cas system using variety of methods. This, in particular, includes the newly developed computer program `Shellspec07_inverse` that is used for the fine-tuning of stellar and system parameters of RZ Cas based on the observed composite line profiles (Sect. 2). In Sect. 3 we represent our main results, while Section 4 is devoted to future prospects.

2. Methods

We used the `Shellspec07` code developed by Budaj & Richards (2004) as the basic engine for our program. This code does not solve the inverse problem of finding stellar and system parameters but serves for the computation of composite synthetic line profiles of interacting binaries based on a priori known input parameters. Mass-transfer typical phenomena like an accretion disk or a gas stream can be taken into account and are assumed to be optically thin. The stars are considered to emit either black-body radiation or their own intrinsic spectra while the effects of limb and gravity darkening are roughly approximated by analytical laws.

Our newly developed Fortran 90 code `Shellspec07_inverse` uses the core of the `Shellspec07` program

and is designed for an accurate estimation of stellar and system parameters of binary stars based on extended spectroscopic observations. According to this task, new input and output routines and a graphical representation of the results have been implemented in the program. The program can work in two different modes, optimizing the stellar and system parameters either based on the original, observed spectra or on spectra that have been averaged into a certain number of orbital phase bins.

With respect to the shape and position of the local continuum, `Shellspec07_inverse` is free of any approximations and provides an accurate normalization of the computed spectra, in contrast to the `Shellspec07` code which assumes the continuum to be a straight line between the outermost points of the considered spectral range. This is a poor approximation for two reasons. First, it is not for sure that the outermost points will be a part of the local continuum. And second, the shape of the continuum may significantly deviate from a straight line, especially for the broad Balmer lines. Instead, we compute both the line and continuum fluxes which makes the normalization of the synthetic spectrum to be a trivial task.

As mentioned at the beginning of this section, `Shellspec07` uses analytical laws to take the effects of limb and gravity darkening into account. In the case of limb darkening, the program uses a linear law assuming that the center-to-limb variation of intensity can be described by a constant limb darkening coefficient independent of line depth. In reality this is not the case and we solve the problem by computing intrinsic stellar line profiles for nine different values of the angle θ between the line-of-sight and the normal to the stellar surface and interpolate according to the desired position on the stellar disk. In a similar way, to count for the temperature variation over the stellar surface due to the effect of gravity darkening, we compute intrinsic line profiles for each point on the stellar surface for exactly the required temperature.

For the non-linear optimization we use the Levenberg-Marquardt algorithm (Levenberg 1944; Marquardt 1963), an iterative technique that determines the minimum of a χ^2 merit function realized as the sum of squares of non-linear functions. We use a modified, fast version of the algorithm (a detailed description can be found in Piskunov & Kochukhov 2002). For more details with respect to the program description see Tkachenko et al. (2009)

3. Results

We used `KOREL` (Hadrava 2004), a Fourier transform based program, to derive the orbital solution and to compute the mean, decomposed spectra of the components of the binary. Assuming circular orbits,

Table 1: Orbital elements of RZ Cas derived with KOREL and by Lehmann & Mkrtychian (2008).

	2001	2006	
P	1.19501(15)	1.195232(20)	d
K_1	71.55(26)	71.72(25)	km s^{-1}
K_2	200.50(69)	201.91(60)	km s^{-1}
q	0.3569(25)	0.3552(23)	
T	2193.39011(59)	3866.746(75)	

	2001+2006	L&M(2008)	
P	1.195243(19)	1.1952410(77)	d
K_1	72.01(25)	71.311(78)	km s^{-1}
K_2	199.03(59)	—	km s^{-1}
q	0.3618(23)	—	
T	2193.38931(57)	2193.38482(20)	
\dot{P}	0.66(39)	0.37(16)	s y^{-1}
\dot{K}	-0.104(87)	-0.135(27)	$\text{km s}^{-1} \text{ y}^{-1}$

we have computed three different orbital solutions: i) based on the spectra from 2001; ii) from 2006; iii) based on the combined 2001 and 2006 data. The results are presented in Table 1, together with those obtained by Lehmann & Mkrtychian (2008). The values of the orbital period derived from the two data sets separately differ significantly. For an additional test, we allowed for a linear trend in the orbital period when computing the orbital solution based on the combined 2001 and 2006 data. The obtained rate of period change of $\dot{P}=(0.66\pm 0.39)\text{ s y}^{-1}$ corresponds to a change of $(2.9\pm 1.7)\text{ s}$ during the total time span of 5 years. Alternatively, the orbital period change can be estimated from the orbital phase shift between the two data sets obtained when folding the radial velocities (RVs) obtained in the two different epochs with the period observed in 2006. The result is much more accurate than that obtained from the linear trend in the KOREL solution leading to a period change of $(2.0\pm 0.1)\text{ s}$ between the two epochs.

KOREL also delivers the mean decomposed spectra of the binary components. These spectra are normalized to the common continuum of both stars. We re-normalized them to their individual continua and then analyzed them with respect to the basic stellar parameters and individual abundances using the method of synthetic spectra. We used the SynthV code (Tsymbal 1996) for computing the synthetic spectra and the LLmodels program (Shulyak et al. 2004) for the calculation of atmosphere models for the hot primary component. For the cool secondary, MARCS atmosphere models (Gustafsson et al. 2008) have been used, together with an additional molecular line list taken from Kurucz CDs (Kurucz 1995).

For the primary, we obtained $v \sin i=(66.0\pm 0.5)\text{ km s}^{-1}$, $\xi_{\text{turb}}=(3.0\pm 0.2)\text{ km s}^{-1}$, and $T_{\text{eff}}=(8850\pm 25)\text{ K}$, with $\log g$ fixed to 4.35. We found that all abundances are close to solar ones except for silicon which is depleted by about -0.4 dex compared to the solar value. The mean error of mea-

surement is 0.03 dex. For the secondary we obtained $v \sin i=(81\pm 2)\text{ km s}^{-1}$ and $T_{\text{eff}}=(4800\pm 100)\text{ K}$, with $\log g$ fixed to 3.7. It was not possible to determine the micro-turbulent velocity for this late-type star, however, and thus we fixed it to 2.0 km s^{-1} . Our results show that the secondary of RZ Cas has a chemical surface composition close to the solar one, except for iron and chromium which are underabundant by about -0.4 dex and -0.6 dex, accordingly. The mean error of measurement for this cool object with its not so well determined continuum is of about 0.1 dex.

We used the Shellspec07_inverse program for the fine-tuning of the stellar and system parameters of RZ Cas. The starting values of the parameters have been taken from the orbital solutions and the analysis of the disentangled spectra. We started with an investigation of the data from 2006 where no hints to complex structures from a mass-transfer episode have been observed, assuming a spherical configuration of the primary and a Roche-lobe filling secondary. For the gravity darkening exponent of the secondary, we first assumed the value of $\beta=0.08$ as predicted by the theory in the case of a star with convective envelope (Lucy 1967). This model resulted in a smooth solution for all orbital phases except for a large region around secondary minimum where the computed line profiles appear to be stronger than the observed ones. We attribute this fact to an attenuation of the light of the secondary which can also be seen in form of a deviation of the RVs from the Keplerian orbital curve in our KOREL solution. Assuming that the observed deviation is an intrinsic property of the secondary, caused by an anomal temperature distribution on its surface, we tried to model this distribution using an unusually large value of $\beta=0.5$. This model fits the observed line profiles in the region around secondary minimum well but completely fails at phases close to the primary eclipse, where the calculated line profiles are much too weak. Finally, we divided the stellar surface of the secondary into two regions by using $\beta=0.5$ for the hemisphere pointing towards the primary and the normal value of $\beta=0.08$ for the opposite side. All spectra obtained around primary and secondary minima can be fitted well with this model. Thus, we conclude that a large dark spot on the surface of the secondary exists, located on the hemisphere that points towards the primary. We stress that an ultra-large value of $\beta=0.5$ has no physical meaning and is just used to model the temperature distribution on the surface of the secondary in the region of formation of a cool spot. Table 2 lists the parameters obtained from the final solution, assuming the two-hemispheres model.

In a next step, we applied the derived model to the spectra taken in 2001. The resulting solution indicates strong attenuation of the light of the primary along the full orbit most probably originating from the formation of accretion structures in the system. Our attempt to

Table 2: Parameters of the RZ Cas system derived with Shellpsec07_inverse.

T_1 (K)	T_2 (K)	$\log g_1$	$\log g_2$	R_1 (R_\odot)	R_2 (R_\odot)	M_1 (M_\odot)	M_2 (M_\odot)	q	a (R_\odot)	i (deg)
8907(15)	4797(20)	[4.35]	[3.7]	1.61(1)	1.93	2.01(2)	0.69(1)	0.342(2)	6.59(3)	82.0(3)

model this attenuation by introducing optically thin, circumprimary matter of disk-like structure provided a significantly improved solution inferring that a transient phase of rapid mass-transfer occurred shortly before the observing period in 2001. This is confirmed by the derived orbital period change of (2.0 ± 0.1) s between the two epochs of observations which we interpret in terms of angular momentum transfer between the accelerated rotation of the outer layers of the primary and the orbit.

4. Discussion

There is a unique event that is observed only in the oEA stars called the spatial filtration effect (SPE). It occurs when the secondary is passes in front of the oscillating primary during the primary eclipse phases. This effect causes specific amplitude and phase changes of the excited oscillation modes of the primary, in dependence on the corresponding l and m numbers. To examine whether or not SPE helps to identify the modes and if there are any basic correlations between the pulsation and system parameters, we did a spectroscopic investigation of this effect based on numerical simulations where we considered only the surface velocity field perturbations and neglected the influence of the temperature and projected surface area perturbations on the line profiles. The main conclusion of our study can be summarized as follows:

1. All sectoral modes show an increase of the amplitudes with the inclination of the rotation axis, whereas all modes with odd l, m combinations behave in the opposite way
2. RV amplitudes outside the eclipse decrease with increasing degree l
3. The sectoral modes give rise to a double-peaked amplification feature in the RV curves centered at primary minimum while the zonal and tesseral modes only produce a single peak
4. The amplification of the RV amplitudes is largest if the star is seen nearly equator-on

Our results show that there are two criteria that can be used for a mode identification based on SPE, namely the shape of the RV curve observed during primary eclipse and the amplification factor of the mode under consideration. Moreover, SPE provides an unique possibility to detect non-radial pulsation modes during the

eclipse phases although the pulsation amplitudes outside the eclipses may be below the detection limit.

In the future, we plan to implement the effects of surface temperature and area perturbations on the line profiles into the calculations and to derive the parameters of non-radial pulsations together with the stellar and system parameters from the observed time-series of spectra. Since most of the oEA stars are faint objects we want to enhance the signal-to-noise ratio (S/N) of our data by using the least-squares deconvolved technique (Donati et al. 1997) which allows to compute mean line profiles of high S/N from a large number of individual lines present in the spectra.

References

- Budaj J., Richards M.T.: 2004, *CoSka*, **34**, 167
Donati J.-F., Semel M., Carter B. D., et al.: 1997, *MNRAS*, **291**, 658
Gustafsson B., Edvardsson B., Eriksson K. et al.: 2008, *A&A*, **486**, 951
Hadrava P.: 2004, *Publ. Astron. Inst. ASCR*, **92**, 15
Kurucz R.L.: 1995, *ASPC*, **78**, 205
Lehmann H., Mkrichian D.E.: 2004, *A&A*, **413**, 293
Lehmann H., Mkrichian D.E.: 2008, *A&A*, **480**, 247
Levenberg K.: 1944, *Quart. J. Appl. Math.*, **2**, 164
Lucy L.B.: 1967, *Zs. f. Ap.*, **65**, 89
Marquardt D. W.: 1963, *J. Soc. Indust. Appl. Math.*, **11**, 431
Mkrichian D.E., Kusakin A.V., Gamarova A.Yu., et al.: 2002, *PASPC*, **259**, 96.
Mkrichian D. E., Nazarenko V., Gamarova A. Yu., et al.: 2003, *PASPC*, **292**, 113
Narusawa S.-Y., Nakamura Y., Yamasaki A.: 1994, *AJ*, **107**, 1141
Ohshima O., Narusawa S.-Y., Akazawa H., et al.: 1998, *IBVS*, **4581**
Ohshima O., Narusawa S.-Y., Akazawa H., et al.: 2001, *AJ*, **122**, 418
Olson E.C.: 1982, *ApJ*, **259**, 702
Piskunov N., Kochukhov O.: 2002, *A&A*, **381**, 736
Rodriguez E., Garcia J.M., Mkrichian D.E., et al.: 2004, *MNRAS*, **347**, 1317
Rossiter R.A.: 1924, *ApJ*, **69**, 15
Shulyak D., Tsymbal V., Ryabchikova T., et al.: 2004, *A&A*, **428**, 993
Tkachenko A., Lehmann H., Mkrichian D. E.: 2009, *A&A*, **504**, 991
Tsymbal V.: 1996, *ASPC*, **108**, 198
Varricatt W.P., Ashok N.M., Chandrasekhar T.: 1998, *AJ*, **116**, 1447

THE GALACTIC CALIBRATION OF THE CEPHEID PERIOD-LUMINOSITY RELATION AND ITS IMPLICATIONS FOR THE UNIVERSAL DISTANCE SCALE

D.G. Turner^{1,6}, D.J. Majaess^{1,2}, D.J. Lane^{1,2}, J.M. Rosvick^{3,6}, A.A. Henden⁴,
D.D. Balam⁵

¹ Department of Astronomy and Physics, Saint Mary's University, Halifax, Nova Scotia, Canada *turner@ap.smu.ca*

² The Abbey Ridge Observatory, Stillwater Lake, Nova Scotia, Canada

³ Thompson Rivers University, Kamloops, British Columbia, Canada

⁴ AAVSO, Cambridge, Massachusetts, U.S.A.

⁵ Dominion Astrophysical Observatory, Victoria, British Columbia, Canada

⁶ Visiting Astronomer, Dominion Astrophysical Observatory, Herzberg Institute of Astrophysics, National Research Council of Canada

ABSTRACT. The Galactic calibration of the period-luminosity (PL) relation for classical Cepheids is examined using trigonometric, open cluster, and pulsation parallaxes, which help establish independent versions of the relationship. The calibration is important for the continued use of classical Cepheids in constraining cosmological models (by refining estimates for H_0), for defining zero-points for the SNe Ia and population II (Type II Cepheids/RR Lyrae variables) distance scales, for clarifying properties of the Milky Way's spiral structure, and for characterizing dust extinction affecting Cepheids in the Milky Way and other galaxies. Described is a program to extend and refine the Galactic Cepheid PL relation by obtaining $UBVRIJHK_s$ photometry and spectra for stars in open clusters suspected of hosting classical Cepheids, using the facilities of the OAMM, DAO, AAVSO, and ARO.

Key words: Stars: fundamental parameters; stars: variables: Cepheids; Galaxy: structure.

1. Introduction

In the present era there is considerable interest in the distance scale established by classical Cepheid variables. The Cepheid period-luminosity relation is the primary standard candle used to establish the distances to galaxies hosting Type Ia supernovae, as well as to derive an accurate value for the Hubble constant H_0 , which is necessary for constraining a variety of cosmological parameters, including the nature of dark energy. A considerable amount of effort has been spent in attempts to solidify the calibration

and usefulness of the Cepheid distance scale, and yet the picture obtained from a perusal of the literature is that many questions about the zero-point and slope of the period-luminosity relation remain unanswered. Just how solidly established is the Cepheid distance scale?

2. The Empirical Approach

Many researchers refer to this method as the “theoretical” approach, but a better terminology would be “model dependent.” A good start is the effective temperature-colour relation derived by Gray (1992) from a comparison of model atmosphere determinations of effective temperature T_{eff} in bright non-variable stars with their unreddened $B - V$ colours:

$$\log T_{\text{eff}} = 3.988 - 0.881(B - V) + 2.142(B - V)^2 - 3.614(B - V)^3 + 3.2637(B - V)^4 - 1.4727(B - V)^5 + 0.2600(B - V)^6. \quad (1)$$

The relationship can be used to infer mean effective temperatures for Cepheids from $B - V$ colours corrected for reddening, even though the same colours in the case of variable stars are affected to a small degree by line blocking and line blanketing effects over the course of Cepheid pulsation cycles.

A sufficient number of Cepheids and Cepheid-like objects (V810 Cen, HD 18391) belonging to open clusters have been studied that one can obtain useful information on the Cepheids themselves from the empirical information gleaned for cluster stars. Such a study was made previously by Turner (1996), but

has been updated for this study using results from more recent studies (Turner, Pedreros & Walker 1998; Turner, Usenko & Kovtyukh 2006; Turner et al. 2007, 2009). A period-mass relation can be inferred for cluster Cepheids, for example, by establishing the masses of cluster stars at the main-sequence red turn-off (RTO), marking the termination of core H-burning, as tabulated by Meynet, Mermilliod & Maeder (1993) in their stellar evolutionary models. Results are presented in Fig. 1 for 19 Cepheids and Cepheid-like supergiants. In the original study (Turner 1996), the implied slope of the period-mass relation was 0.50 ± 0.02 , implying a simple relationship of the type $M/M_{\odot} \sim P^{\frac{1}{2}}$.

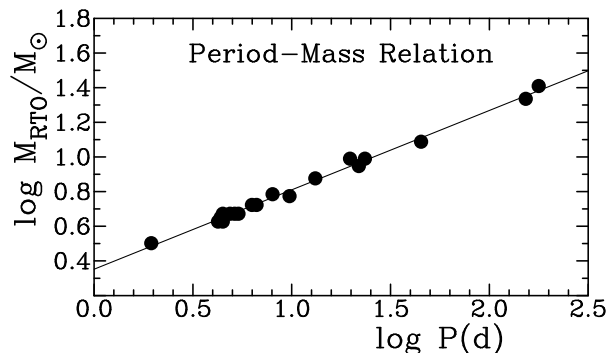


Figure 1: The period-mass relation for Cepheids and Cepheid-like supergiants in open clusters and associations. The slope of the relationship is 0.46 ± 0.01 .

In Turner (1996), cluster ages were derived from matching the upper ends of the resulting cluster colour-magnitude diagrams to best-fitting model isochrones by Meynet et al. (1993). For the present study, ages were inferred by the alternate technique of using the blue cluster turnoff points with the relations of Meynet et al. (1993). The results (Fig. 1) lead to a different slope for the relationship, namely 0.46 ± 0.01 , slightly different from the Turner (1996) results, but close enough to confirm them. It appears that the analysis may need to be repeated with more up-to-date stellar evolutionary model results that generate identical cluster ages from cluster turnoff points and from isochrone fitting. The main point is that many Cepheid parameters may be related in simple fashion to pulsation period.

A similarly straightforward parameterization applies to Cepheid radii, although that was not always the case. Cepheid radii can be established via the Baade-Wesselink (B-W) technique, in which phases of identical T_{eff} or surface brightness provide estimates for radius ratios at those phases via:

$$L_1/L_2 = 10^{-0.4(m_1-m_2)} = R_1/R_2. \quad (2)$$

Since the differences $R_1 - R_2$ can be established between those phases through integration of a Cepheid's radial

velocity changes, one can determine its mean radius using all phase pairs of identical T_{eff} .

Theory and practice differ, of course. For one thing, $B - V$ colour does not correlate well with effective temperature. Alternate choices have included the indices $V - R$, $V - I$, and $V - K$, and the Brigham Young University KHG index (Turner, Leonard & English 1987; Turner 1988). The KHG index, in particular, monitors atmospheric effective temperature in Cepheids using narrow-band filters tied to the Ca II K-line, $H\delta$, and the molecular G-band visible in Cepheid spectra, and has the advantage of being relatively independent of atmospheric and interstellar extinction. Use of the KHG index generates Cepheid radii (Turner 1988; Turner & Burke 2002) in which the basic premise of the Baade-Wesselink method is satisfied, something not normally tested with more sophisticated approaches, for example those using Bayesian Markov-Chain Monte Carlo code. When the B-W method is done correctly, a plot of radius ratios versus radius differences should describe a tight clockwise loop (Turner 1988) and not an open counterclockwise loop. The test fails when $B - V$ colour is used as the temperature indicator.

Table 1: Slope of the period-radius relation.

Slope	Source
0.70	Cogan (1978) theory
0.70:	Gieren (1981)
0.587–0.956	Fernie (1984) optimum 0.824
0.84	Gieren (1984)
0.63	Coulson, Caldwell & Gieren (1986)
0.77	Gieren (1986)
0.743	Gieren, Barnes & Moffett (1989)
0.750	Gieren, Fouqué & Gómez (1998)
0.751	Laney & Stobey (1995)
0.747	Turner & Burke (2002)

Results of past studies establishing the slope of the Cepheid period-radius relation are presented in Table 1. The derived slope varied widely from study to study in the early years, but eventually converged upon a value of 0.750 ± 0.003 a decade ago, as indicated by the results of Gieren et al. (1998), Laney & Stobey (1995), and Turner & Burke (2002). Data for the latter two provide a tightly defined period-radius relation, as indicated for the last two sources by the data of Fig. 2. The implication is that $\langle R \rangle / R_{\odot} \sim P^{\frac{3}{4}}$.

Not all results can be combined, however. That is because it is necessary to correct the measured radial velocity variations in Cepheids for projection effects arising from general envelope pulsation in the stars. The corresponding projection factor is close to 1.30, but has also varied significantly over the past 25 years. Since $\langle R \rangle$ scales the resulting radii, one source of Cepheid radii may scale differently from another because of dif-

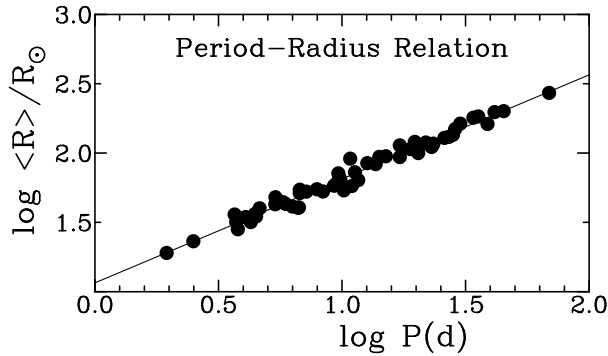


Figure 2: The period-radius relation delineated by data from Laney & Stobey (1995) and Turner & Burke (2002). The slope of the relationship is 0.75.

ferences in adopted p values. That results in a zero-point shift but not a change in slope. The manner in which the choice of p has varied over the years is indicated in Table 2. The abrupt increase in the parameter occurring in the mid 1980s has recently been reversed, and perhaps agreement will eventually settle upon the original values near 1.30–1.31. In fact, the exact value can be tested in simple fashion, as noted below.

Table 2: Estimates of the B-W projection factor p .

p	Source
1.412	Getting (1935)
1.31	Parsons (1972)
1.31	Karp (1975)
1.31–1.47	Hindsley & Bell (1986)
1.34–1.38	Gieren et al. (1989)
1.30–1.42	Gray & Stevenson (2007)
1.19–1.31	Laney & Jonev (2009)
1.30–1.31	Region of overlap (all studies)

The Cepheid period-luminosity relation can therefore be constructed from first principles without regard to observational data, provided one has a reliable bolometric correction scale to convert mean absolute visual magnitudes $\langle M_V \rangle$ to luminosities in solar units L/L_\odot . Such a technique was adopted by Turner & Burke (2002) and Turner (2010). An example is shown in Fig. 3 for stars of well-established reddening, where the colour excesses originate in studies such as those of Turner (2001), Laney & Caldwell (2007), and Kovtyukh et al. (2008), often with overlap between studies, many of which are based upon earlier studies of space reddening and spectroscopic reddening for Cepheids.

3. The Observational Approach

The observational approach to the problem has

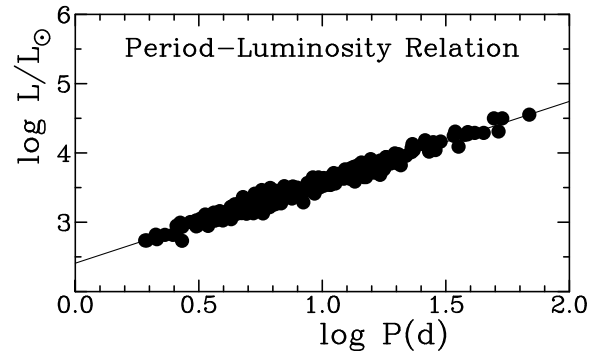


Figure 3: The period-luminosity relation defined by Cepheids of well-established reddening.

previously used observations for Cepheids in the Large Magellanic Cloud (LMC) to define the period-luminosity relation, with a few Galactic calibrators to tie down the zero-point. In many cases the results for cluster Cepheids are artificially “adjusted” to account for changes to the Hyades/Pleiades zero-point for zero-age main sequence (ZAMS) fitting or to increase the stated precision of the results. But that is no longer necessary. The Hubble Space Telescope (HST) program of Benedict et al. (2007) to derive parallaxes for 10 relatively nearby Cepheids and the study of Turner (2010) for 24 Cepheids in Galactic clusters provide by themselves a reasonably large sample of calibrators for the period-luminosity relation. The results, presented in Fig. 4, fit the identical relationship derived in Fig. 2 for Cepheids of well-established reddening:

$$\log L/L_\odot = 2.409 + 1.168 \log P. \quad (3)$$

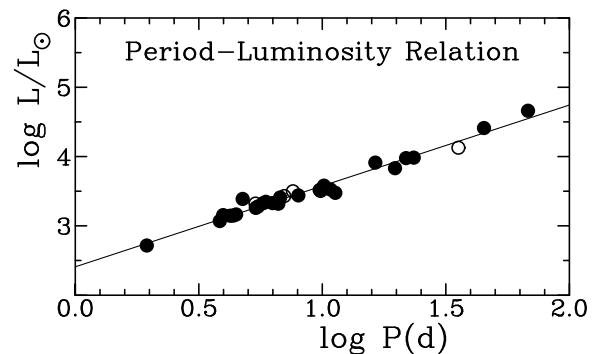


Figure 4: The period-luminosity relation defined by cluster (filled circles) and HST parallax (open circles) Cepheids.

Parallaxes from the Hipparcos catalogue prove to be less useful for such purposes (see Turner 2010), since there are peculiarities with the stated uncertainties, and in the parallaxes themselves, that create problems with the identification of proper pulsation mode (fundamental mode, overtone) for individual Cepheids.

Nevertheless, a few of the most reliable Hipparcos parallaxes appear to confirm the scale of Cepheid luminosities derived from cluster and HST parallaxes. A series of tests is presented by Turner (2010), the conclusion being that an observational approach to calibrating the period-luminosity relation using Cepheids in Galactic clusters and Cepheids with HST parallaxes strongly confirms the relationship inferred by empirical means, namely use of a $T_{\text{eff}} - (B - V)$ calibration, a well-defined period-radius relation, and a calibrated scale of bolometric corrections (Turner & Burke 2002). Incidentally, that conclusion in itself appears to confirm the choice of a projection factor of $p = 1.30 - 1.31$ for Cepheid B-W studies, as noted earlier. Galactic calibrators also span a wide range of pulsation periods ranging from 2^{d} to 68^{d} , making them ideal for calibration purposes, although a few cluster Cepheids fit the relationship somewhat poorly, even with colour spread in the instability strip taken into account (Turner 2010). That situation may improve with further study of the associated star clusters.

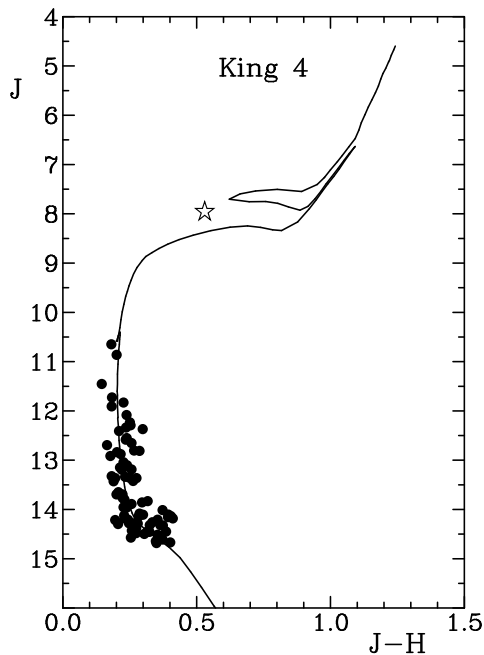


Figure 5: A preliminary 2MASS colour-magnitude diagram for the cluster King 4, with the Cepheid UY Per indicated by a star symbol. A 10^8 -yr Padova isochrone is shown for a reddening of $E(J H) = 0.25$ ($E(B V) = 0.89$) and $J M_J = 12.4$ ($V_0 M_V = 11.75$, $d = 2.24$ kpc).

A program has been initiated to increase the number of Galactic calibrators through the study of relatively unstudied open clusters that are spatially coincident, or nearly spatially coincident, with well-studied Cepheid variables. The program is rather ambitious and observations are being obtained from the Dominion Astrophysical Observatory (DAO), l'observatoire

astronomique du mont Mégantic (OAMM), the Abbey Ridge Observatory (ARO), and the Sonoma Research Observatory of the American Association of Variable Star Observers (AAVSO). Surprisingly, there are several good cases of cluster Cepheids that have yet to be studied extensively. The case for UY Per as an outlying member of the open cluster King 4 is shown as an example in Fig. 5.

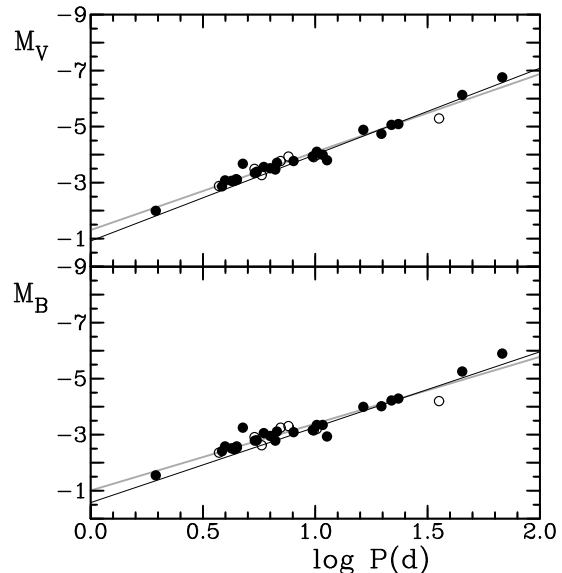


Figure 6: Absolute magnitudes M_V and M_B for Cepheids in open clusters (filled circles) and with HST parallaxes (open circles) produce the gray lines as best-fitting relationships, compared with the black lines predicted by the Sandage, Tammann & Reindl (2004) calibration.

A ramification of using the scale of Cepheid luminosities cited here and by Turner (2010) is that it affects distances derived for distant galaxies, for example from the distance scale of Sandage, Tammann & Reindl (2004). A comparison of Cepheid absolute magnitudes M_V and M_B derived from cluster and HST parallaxes with respect to the Sandage et al. (2004) Galactic calibration is shown in Fig. 6. Here the scatter is related to the location of each Cepheid in the instability strip. The best-fitting relationships for cluster and HST data from least squares and non-parametric fits are:

$$\langle M_V \rangle = -1.304 \pm 0.065 - 2.786 \pm 0.075 \log P, \quad (4)$$

$$\langle M_B \rangle = -1.007 \pm 0.087 - 2.386 \pm 0.098 \log P. \quad (5)$$

By comparison, the Sandage et al. (2004) relationships underestimate the luminosities of Cepheids with periods less than 20^{d} and overestimate the luminosities of Cepheids with periods in excess of 20^{d} . The latter, of course, are the objects most likely to be used to establish distances to galaxies hosting Type Ia supernovae. The effect appears small in Fig. 6, but is more

pronounced using a Wesenheit, or reddening-free, formulation, and can affect derived distances to galaxies by 10% or more in extreme cases. The effects on the Type Ia supernova calibration of Sandage et al. (2006) may be significant. For example, they can account for the difference between the value of $H_0 = 62.3 \pm 5.0$ km s⁻¹ Mpc⁻¹ derived by Sandage et al. (2006) for the Hubble constant applicable to galaxies hosting type Ia supernovae and the comparable value of $H_0 = 71 \pm 6$ km s⁻¹ Mpc⁻¹ derived by Freedman et al. (2001).

Another complication is that Cepheids at the limits of detectability in distant galaxies are frequently located in crowded fields where it can be difficult to extract uncontaminated light curves for the variables. Photometric errors can generate deleterious effects that may bias the determination of accurate period-absolute magnitude relations for Cepheids in such galaxies, thereby affecting their use as distance indicators. An example is provided by Turner (2010) for the galaxy NGC 4258. Wesenheit magnitudes for Galactic Cepheid calibrators exhibit a scatter of at most $\pm 0^m.5$ as a function of period, compared with a scatter in excess of $\pm 1^m.0$ for the Wesenheit magnitudes of Cepheids in the crowded inner regions of NGC 4258. The situation may worsen for more distant galaxies used to calibrate the distance scale for type Ia supernovae.

4. Type II Cepheids and RR Lyrae Variables

An additional complication for the classical Cepheid distance scale is the importance of metallicity to the zero-point of the period-luminosity relationship. An advantage gained from a Galactic calibration is that it applies to Cepheids of roughly solar metallicity, much like the expected metallicity of Cepheids in the sample of spiral galaxies used to calibrate the Type Ia supernova relation. Tests of the importance of metallicity have traditionally been done by comparing the luminosities of Cepheids in the metal-rich inner regions of galaxies with those in their comparably metal-poor outer regions. That makes the possibility of contamination by crowding an important consideration (Mochejska et al. 2004; Majaess 2010b).

An alternate approach can be made using Type II Cepheids and RR Lyrae variables, which sample an older population of galaxies, but which also appear to exhibit a tight relationship between luminosity and pulsation period, thereby permitting a comparison with galaxy distance moduli obtained from classical Cepheids (Majaess, Turner & Lane 2009c; Majaess 2010c). An example of their potential is displayed by the data of Fig. 7, which plots reddening-free Wesenheit magnitudes for Type II Cepheids and RR Lyrae variables in the LMC, using observations from Soszyński et al. (2008, 2009). The mean Wesenheit magnitudes for such stars appear to follow a

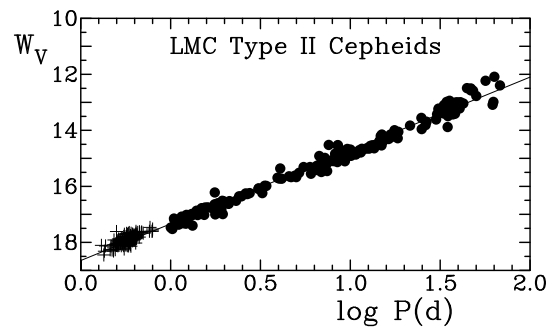


Figure 7: Mean brightnesses from OGLE data of LMC Type II Cepheids (filled circles: BL Her, W Vir, RV Tau variables) and RR Lyrae variables (crosses) as a function of fundamental mode pulsation period.

linear relationship that links the luminosities of short period RR Lyrae variables with those of longer period Type II Cepheids, although the linearity seems to break down for the long pulsation periods corresponding to RV Tauri variables (e.g., Majaess et al. 2010).

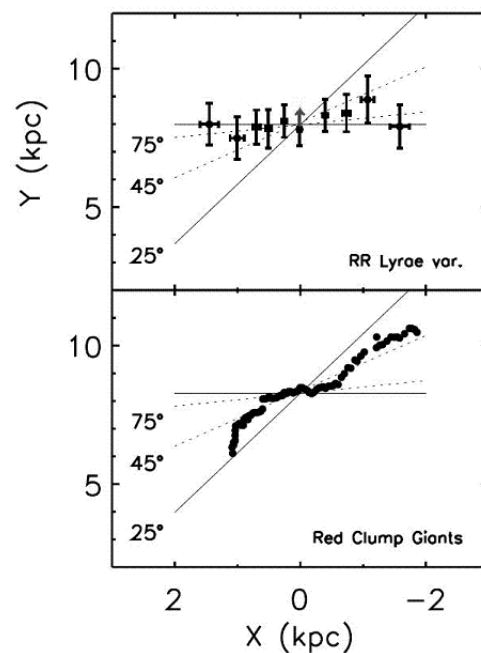


Figure 8: Mean distances from OGLE data for RR Lyrae variables in the Galactic bulge (upper) relative to peaks in the distribution of red clump stars (lower) mapped by Nishiyama et al. (2005).

Type II Cepheids also have the potential for use in other studies. Classical Cepheids, for example, have long been used to map the nearby spiral arms of the Galaxy, the most recent studies being those of Majaess, Turner & Lane (2009a,b) and Turner & Majaess (2010). Their Type II counterparts are more suitable for studying other characteristics of the Galaxy, for example by providing an independent estimate for the

distance to the Galactic centre (Majaess 2010a), or evidence for a Galactic bar. Fig. 8 is a plot of the mean distances of RR Lyrae variables detected in directions towards the Galactic centre, based upon *VI* photometry for RR Lyrae variables in the direction of the Galactic bulge from Collinge, Sumi & Fabrycky (2006). A comparison with the bar-like structure at the Galactic centre mapped by Nishiyama et al. (2005) using red clump stars reveals an apparent discrepancy, the distribution of RR Lyrae variables displaying no evidence for a bar, instead being concentrated concentrically within the Galactic bulge. Conceivably the bar of Nishiyama et al. (2005) formed much later than the mean epoch of formation for the precursors of the RR Lyrae variables, or possibly it is a simple difference in population types (Alcock et al. 1998), given that RR Lyrae variables are a common constituent of the Galactic halo.

5. Summary

As noted here, accurate period-luminosity or period-absolute magnitude relations for classical Cepheids can be constructed using only Galactic calibrators tied to the data of Benedict et al. (2007) and Turner (2010). The resulting linear relations closely match independent relationships derived using the Cepheid period-radius relation, a scale of Cepheid effective temperatures inferred from unreddened mean $(\langle B \rangle - \langle V \rangle)_0$ colours, and a reliable scale of bolometric corrections. Galactic calibrators also have the advantage of being bright and relatively nearby, whereas their counterparts in the Large and Small Magellanic Clouds are considerably fainter. The latter are used with Type II and RR Lyrae calibrators to test the importance of metallicity for the extragalactic distance scale.

References

- Alcock C., Allsman R.A., Alves D.R., et al.: 1998, *ApJ*, **492**, 190.
- Benedict G.F., McArthur B.E., Feast M.W., et al.: 2007, *AJ*, **133**, 1810.
- Cogan B.C.: 1978, *ApJ*, **221**, 635.
- Collinge M.J., Sumi T., Fabrycky D.: 2006, *ApJ*, **651**, 197.
- Coulson I.M., Caldwell J.A.R., Gieren W.P.: 1986, *ApJ*, **303**, 273.
- Fernie J.D.: 1984, *ApJ*, **282**, 641.
- Fouqué P., Arriagada P., Storm J., et al.: 2007, *A&A*, **476**, 73.
- Freedman W.F., et al.: 2001, *ApJ*, **553**, 47.
- Getting I.A.: 1935, *MNRAS*, **95**, 141.
- Gieren W.: 1981, *BAAS*, **13**, 871.
- Gieren W.: 1984, *ApJ*, **282**, 650.
- Gieren W.P.: 1986, *MNRAS*, **222**, 251.
- Gieren W.P., Barnes T.G., Moffett T.J.: 1989, *ApJ*, **342**, 467.
- Gieren W.P., Fouqué P., Gómez M.: 1998, *ApJ*, **496**, 17.
- Gray D.F.: 1992, *The Observation and Analysis of Stellar Photospheres*, Cambridge Astrophys. Series, **20**.
- Gray D.F., Stevenson K.B.: 2007, *PASP*, **119**, 398.
- Hindsley R., Bell R.A.: 1986, *PASP*, **98**, 881.
- Karp A.H.: 1975, *ApJ*, **201**, 641.
- Kovtyukh V.V., Soubiran C., Luck R.E., et al.: 2008, *MNRAS*, **389**, 1336.
- Laney C.D., Caldwell J.A.R.: 2007, *MNRAS*, **377**, 147.
- Laney C.D., Joner M.D.: 2009, *AIP Conf. Series*, **1170**, 93.
- Laney C.D., Stobie R.S.: 1995, *MNRAS*, **274**, 337.
- Majaess D.: 2010a, *ActA*, **60**, 55.
- Majaess D.: 2010b, *ActA*, **60**, 121.
- Majaess D.J.: 2010c, *AAVSO*, **38**, 100.
- Majaess D.J., Turner D.G., Lane D.J.: 2009a, *MNRAS*, **398**, 263.
- Majaess D.J., Turner D.G., Lane D.J.: 2009b, *AAVSO*, **37**, 179.
- Majaess D., Turner D., Lane D.: 2009c, *ActA*, **59**, 403.
- Majaess D.J., Turner D.G., Lane D.J., et al.: 2010, *AAVSO*, **38**, in press.
- Meynet G., Mermilliod J.-C., Maeder A.: 1993, *A&AS*, **98**, 477.
- Mochejska B.J., et al.: 2004, *ASPC*, **310**, 41.
- Nishiyama S., Nagata T., Baba D., et al.: 2005, *ApJ*, **621**, L105.
- Parsons S.B.: 1972, *ApJ*, **174**, 57.
- Sandage A., Tammann G.A., Reindl B.: 2004, *A&A*, **424**, 438.
- Sandage A., Tammann G.A., Saha A., et al.: 2006, *ApJ*, **653**, 843.
- Soszyński I., Udalski A., Szymański M.K., et al.: 2008, *ActA*, **58**, 293.
- Soszyński I., Udalski A., Szymański M.K., et al.: 2009, *ActA*, **59**, 1.
- Turner D.G.: 1988, *AJ*, **96**, 1565.
- Turner D.G.: 1996, *JRASC*, **90**, 82.
- Turner D.G.: 2001, *Odessa Astron. Publ.*, **14**, 166.
- Turner D.G.: 2009, *AIP Conf. Series*, **1170**, 59.
- Turner D.G.: 2010, *Ap&SS*, **326**, 219.
- Turner D.G., Burke J.F.: 2002, *AJ*, **124**, 2942.
- Turner D.G., Majaess D.J.: 2010, *BAAS*, **41**, 929.
- Turner D.G., Leonard P.J.T., English D.A.: 1987, *AJ*, **93**, 368.
- Turner D.G., Pedreros M.H., Walker A.R.: 1998, *AJ*, **115**, 1958.
- Turner D.G., Abdel-Sabour Abdel-Latif M., Berdnikov L.N.: 2006, *PASP*, **118**, 410.
- Turner D.G., Usenko I.A., Kovtyukh V.V.: 2006, *Observatory*, **126**, 207.
- Turner D.G., et al.: 2008, *MNRAS*, **388**, 444.
- Turner D.G., Kovtyukh V.V., Majaess D.J., et al.: 2009, *AN*, **330**, 807.

HDE 344787, THE POLARIS ANALOGUE THAT IS EVEN MORE INTERESTING THAN POLARIS

D.G. Turner^{1,6,7,8}, D.J. Majaess^{1,2}, D.J. Lane^{1,2}, J.R. Percy^{3,6}, D.A. English^{4,7},
R. Huziak⁵

¹ Department of Astronomy and Physics, Saint Mary's University, Halifax, Nova Scotia, Canada *turner@ap.smu.ca*

² The Abbey Ridge Observatory, Stillwater Lake, Nova Scotia, Canada

³ Erindale College, University of Toronto, Erindale, Ontario, Canada

⁴ Sir Wilfred Grenfell College, Memorial University, Corner Brook, Newfoundland, Canada

⁵ SED Systems, Saskatoon, Saskatchewan, Canada

⁶ Visiting Astronomer, Kitt Peak National Observatory, National Optical Astronomy Observatories, which is operated by the Associated Universities for Research in Astronomy, Inc. (AURA) under contract with the National Science Foundation

⁷ Visiting Astronomer, Dominion Astrophysical Observatory, Herzberg Institute of Astrophysics, National Research Council of Canada

⁸ Visiting Astronomer, Harvard College Observatory Photographic Plate Stacks

ABSTRACT. A collection of active photometric observations over the last half decade, archival data from the past 120 years, radial velocity observations from 1984, and recent monitoring through a pro-am collaboration reveal that the 9th magnitude F9 Ib supergiant HDE 344787 is a double-mode Cepheid variable of extremely small amplitude. It displays remarkably similar, but much more extreme, properties to the exotic Cepheid Polaris, including a rapidly-increasing period and sinusoidal light variations of decreasing amplitude suggesting that pulsational stability may occur as early as 2045. Unlike Polaris, HDE 344787 displays sinusoidal light variations at periods of both 5^d.4 and 3^d.8 days, corresponding to canonical fundamental mode and overtone pulsation. But it may be similar to Polaris in helping to define a small subgroup of Cepheids that display characteristics consistent with a first crossing of the instability strip. An update of 2010 observations of this remarkable star is presented.

Key words: Stars: variables: Cepheids; stars: individual: HDE 344787.

1. Introduction

HDE 344787 (BD+22°3786) is unusual in being an F9 Ib-II supergiant (Turner 1979; Shi & Hu 1999) lying on the outskirts (Fig. 1) of the 2×10^6 year-old cluster

NGC 6823 (Guetter 1992), but with a high membership probability from proper motions (Erickson 1971). An evolved intermediate-mass star in such close proximity to a very young cluster must be a spatial coincidence, which is testable by radial velocities. It has an optical companion 11'' southeast and six magnitudes fainter that is of probable B spectral type (Massey et al. 1995).

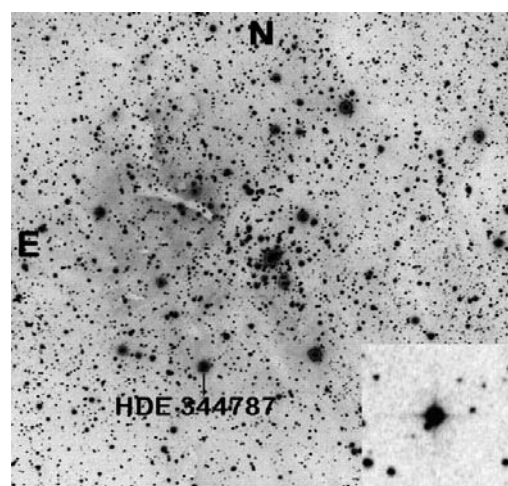


Figure 1: The $32' \times 32'$ field of the young cluster NGC 6823 and its H II region, showing the location of HDE 344787. The inset is an enlargement showing the close (11'') B-type companion to HDE 344787.

All-sky and differential photoelectric observations for the star were obtained in 1978, 1979, 1980, and 1981 with the 0.4m telescope at Kitt Peak National Observatory (KPNO) in a search for potential Cepheid-like variability, and radial velocity measures were obtained at the Dominion Astrophysical Observatory (DAO) in 1984. Initial examination of the data (Turner 1979) suggested a 4-day variation in brightness, although the observations are also consistent with light constancy! Tycho observations of the star (ESA 1997) are of low quality and were averaged. Additional data were obtained from the ASAS-3 survey (Pojmański 2002), from recent CCD imaging, mainly from the Abbey Ridge Observatory (ARO), and from examination of images in the Harvard College Observatory Photographic Plate Collection (HCO). Small brightness changes on the HCO plates were detected at the $0^m.05$ level, tied to a surrounding tight sequence of three stars of almost identical brightness and colour to HDE 344787, one slightly brighter and the other slightly fainter, thereby eliminating problems arising from differential extinction during plate exposures, which typically limits the accuracy attainable from eye estimates off photographic plates to $\pm 0^m.1$ or worse.

Absolute photometry of HDE 344787 from CCD imaging is rather challenging because of the star's small light amplitude. Since the reference and check stars for the Cepheid differ in colour from HDE 344787, it was necessary to account for atmospheric effects on the derived magnitude estimates. The procedure for that outlined by Turner et al. (2009) was followed.

2. Observational Results

The results were unexpected. Sample light curves for the Cepheid are shown in Fig. 2 along with fitted sine waves, indicating the low level of light variability at both photographic (B) and visual (V) wavelengths. The “variability” is presently only marginally larger than the scatter observed in reference stars of constant brightness (e.g., ASAS-3 2003, ARO 2006, 2008), was larger 30 years ago (e.g., KPNO 1979), and a century earlier was large enough to detect on photographic plates (e.g., HCO 1900, 1917, 1930). The variability is also seen in closely-adjacent Tycho observations combined into weighted means (e.g., 1990-93), and in radial velocity measures (DAO 1984, Fig. 3).

Fourier analysis of the magnitude estimates from the 1890-1951 Harvard plates, shown in Fig. 4, produced a dominant signal at $P = 3^d.8$, representing first overtone (OT) pulsation in the Cepheid, and a secondary peak at $P = 5^d.4$ (with aliases omitted), corresponding to fundamental mode (FM) pulsation. The $5^d.4$ period went unnoticed in the photoelectric observations because of limited durations for the observing runs.

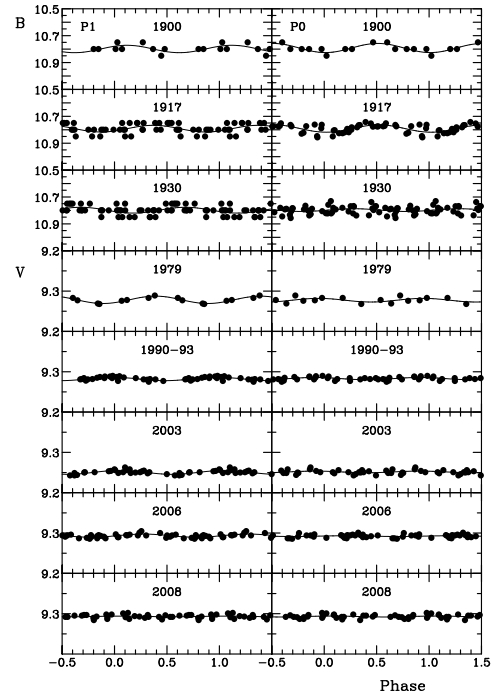


Figure 2: Sample light curves of HDE 344787 for FM (F0) and OT (F1) pulsation, derived from HCO estimates (1900, 1917, 1930), from KPNO observations (1979), from Tycho magnitudes (1990-93), from ASAS-3 (2003), and from the ARO (2006, 2008). Note the changing light amplitude over the past century.

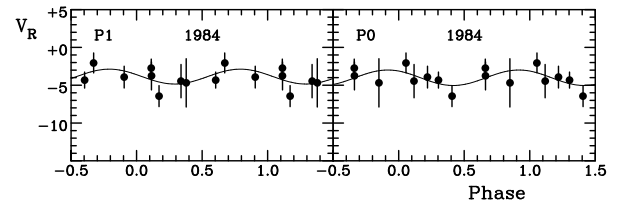


Figure 3: Radial velocity curves of HDE 344787 from observations with the DAO 1.85m telescope (1984).

A working ephemeris was constructed for HDE 344787 using maxima obtained from phasing the Tycho data as zero-points: $HJD_{\max} = 2448449.4642 + 5.4019E$ (for P0) and $HJD_{\max} = 2448447.4505 + 3.8011E$ (for P1), the stronger signal, where E is the number of elapsed cycles. The ephemerides were used to phase the observations in an O-C analysis presented in Fig. 5, although the individual light curves were phased using periods appropriate for the epochs of observation, given that the period is changing so rapidly. The HCO data from the early 1900s indicate that the phase of light maximum progresses through a complete cycle in less than a decade, with both periods increasing in phase at the same rate.

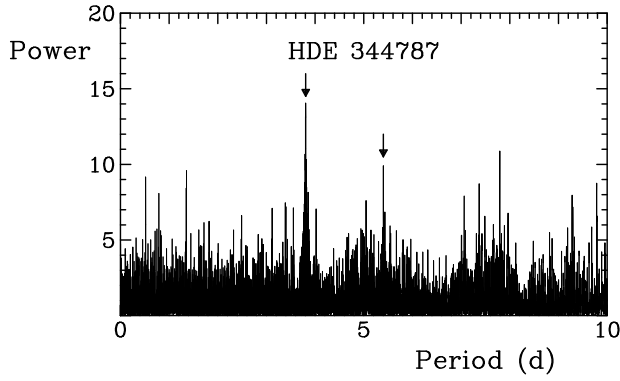


Figure 4: Fourier analysis of the power spectrum of HDE 344787 from HCO estimates, with peaks for OT pulsation (left arrow) and FM pulsation (right arrow).

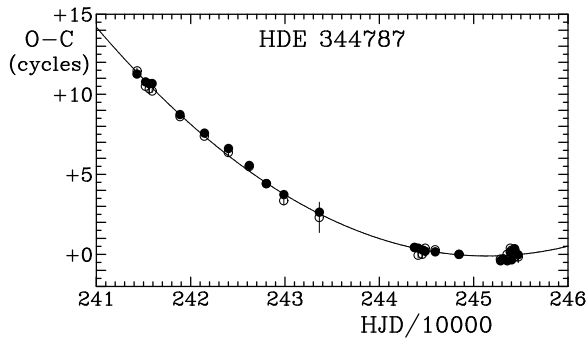


Figure 5: O-C variations of HDE 344787 for FM (open circles) and OT (filled circles) pulsation.

A regression analysis of the combined data sets is affected only weakly by the scatter in the O-C data for recent epochs, a result of the rapidly weakening light amplitude. A best fit parabolic trend implies a period increase for HDE 344787 of $12.96 \pm 2.41 \text{ s yr}^{-1}$ for P0. The rapid rate of period increase in HDE 344787 corresponds exactly with expectations from previous studies of Cepheid period changes (Turner et al. 2006), and predictions from stellar evolutionary models, for a star of solar metallicity crossing the instability strip for the first time (Fig. 6, see also Turner 2009). Temporal variations in light amplitude ΔV (with ΔB assumed equal to $1.5 \times \Delta V$ for comparison purposes) reveal a steady decrease in light amplitude (Fig. 8) that may represent the signature of a star about to leave the Cepheid instability strip.

The strongest signal seems to change between modes temporally, with the overtone mode dominating, but the total pulsation energy, as represented by a combination of the luminous signals into ΔV_{tot} (Fig. 9) is clearly waning. The star may cease to pulsate entirely by 2045, although the signal was barely detectable during the 2008-2009 observing seasons, and may have already been damped out by convection.

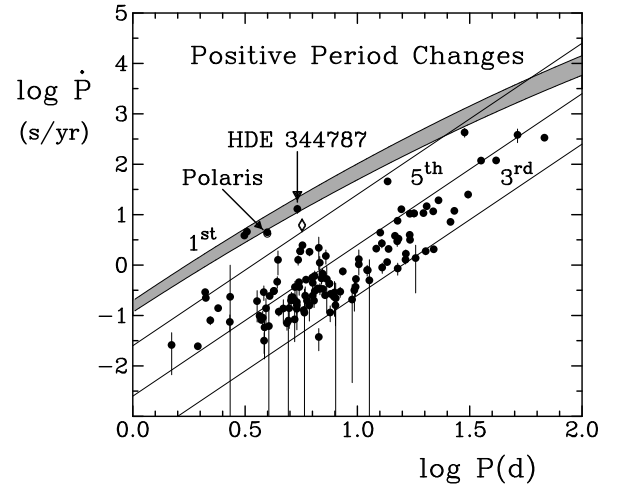


Figure 6: Rate of period change as a function of period for Cepheids with established period increases. Note the agreement of the observed rates for putative first crossers with expectations (gray region).

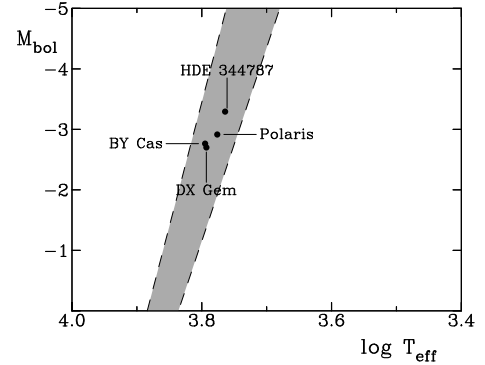


Figure 7: The location of putative first crossing Cepheids in the instability strip (gray region).

3. Comparison With Polaris

The following points can be noted when comparing HDE 344787 with Polaris, another F-type supergiant with a period of ~ 4 days that has a small light amplitude and may be crossing the instability strip for the first time: (i) HDE 344787 has a smaller light amplitude than Polaris, making it more difficult to observe, (ii) its rate of period increase of $12.96 \pm 2.41 \text{ s yr}^{-1}$ is ~ 3 times faster than that of Polaris (4.5 s yr^{-1}), but consistent with its longer fundamental mode pulsation period ($P_0 = 5^{\text{d}}.4$ versus 4^{d}), (iii) HDE 344787 is a double-mode pulsator, unlike Polaris, for which no secondary period is evident, (iv) the intrinsic colour for a F9 Ib-II supergiant (HDE 344787, Fig. 10) is $(B - V)_0 = +0.63$ (Kron 1978), versus $(B - V)_0 = +0.58$ for Polaris (Turner 2006), consistent with the difference in spectral type (Polaris is F7 Ib) and

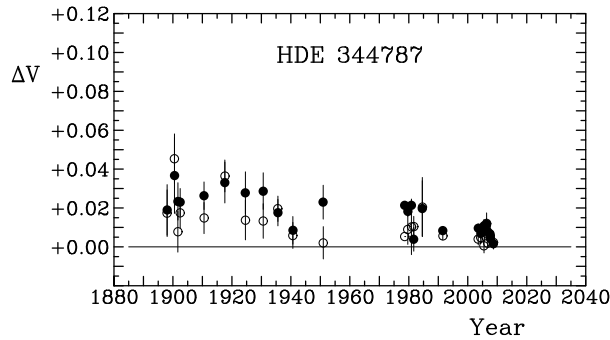


Figure 8: Light amplitude for HDE 344787 as a function of time for FM (open circles) and OT (filled circles) pulsation.

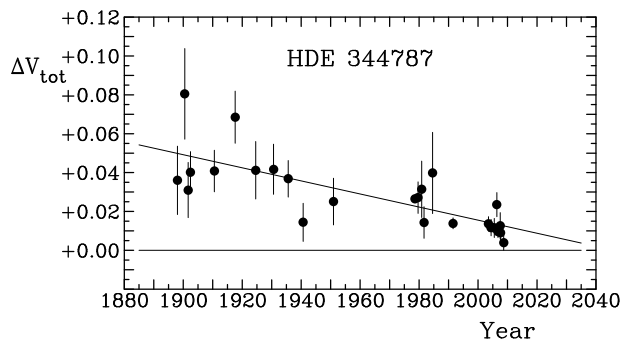


Figure 9: Total light amplitude for pulsation in HDE 344787 (FM + OT) as a function of time. The linear relation depicts the long-term declining trend.

difference in pulsation period, (v) the light amplitude of HDE 344787 has been in steady decline since 1890, whereas Polaris had a steady but slow decline in light amplitude prior to its unusual “glitch” in 1963–66 (Turner et al. 2005; Turner 2009), and is presently recovering erratically from a minimum in 1988, (vi) the putative first-crossing Cepheids, HDE 344787, Polaris, DX Gem ($P = 3^d.1$), and BY Cas ($P = 3^d.2$) have intrinsic colours that place them near the centre of the instability strip, consistent with model expectations (Alibert et al. 1999).

4. Discussion

Recent ARO observations of HDE 344787 (Fig. 11) reveal a level of variability in 2010 not significantly different from zero: $\Delta V = 0.002$ for FM pulsation and $\Delta V = 0.003$ for OT pulsation, the normal dominant mode. At that level the star would be an ideal target for Canada’s MOST space telescope, were it not for the fact that HDE 344787 lies outside the zone of continuous observation for MOST. As a consequence, it is difficult to determine if the star is still pulsating. Several recent sets of observations of the star have been made with facilities like the ARO and the campus

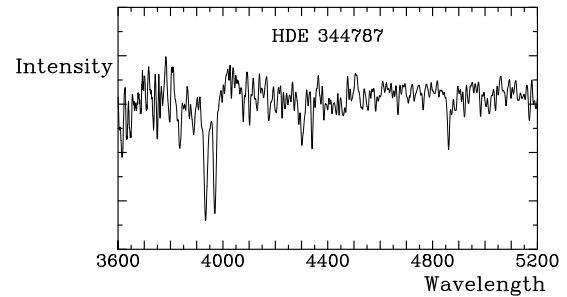


Figure 10: A spectrum of HDE 344787 taken at the DAO at a dispersion of 60 \AA mm^{-1} .

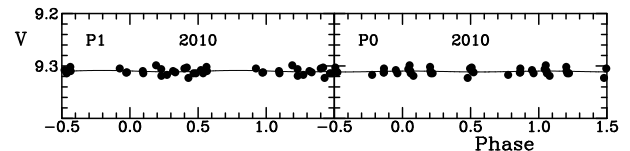


Figure 11: Recent ARO observations of HDE 344787, phased to FM (P0) and OT (P1) pulsation.

telescope in Saskatoon (Huziak), so it is a project for which even keen amateur astronomers can contribute. The star is better placed for observation than Polaris (North Celestial Pole), but its extremely low light amplitude makes it a challenging object to study, as it has been for more than a century now.

References

- Alibert Y., Baraffe I., Hauschildt P., Allard F.: 1999, *A&A*, **344**, 551.
 Erickson R.R.: 1971, *A&A*, **10**, 270.
 ESA: 1997, *The T ch Ca a g e*, ESA SP-1200.
 Guetter H.H.: 1992, *AJ*, **103**, 197.
 Kron G.E.: 1978, *AJ*, **83**, 1195.
 Massey P., Johnson K.E., DeGioia-Eastwood K.: 1995, *A J*, **454**, 151.
 Pojmański G.: 2002, *Ac a A* ., **52**, 397.
 Shi H.M., Hu J.Y.: 1999, *A&AS*, **136**, 313.
 Turner D.G.: 1979, *JRASC*, **73**, 74.
 Turner D.G.: 2006, *Ode a A . P b .*, **18**, 115.
 Turner D.G.: 2009, *AIP C f. Se ie*, **1170**, 59.
 Turner D.G., Savoy J., Derrah J., Abdel-Sabour Abdel-Latif M., Berdnikov L.N.: 2005, *PASP*, **117**, 207.
 Turner D.G., Abdel-Sabour Abdel-Latif M., Berdnikov L.N.: 2006, *PASP*, **118**, 410.
 Turner D.G., Kovtyukh V.V., Majaess D.J., Lane D.J., Moncrieff K.E.: 2009, *AN*, **330**, 807.

THE ONSET OF CHAOS IN PULSATING VARIABLE STARS

D.G. Turner^{1,5}, L.N. Berdnikov^{2,5}, J.R. Percy³ and M. Abdel-Sabour Abdel-Latif⁴

¹ Department of Astronomy and Physics, Saint Mary's University, Halifax, Nova Scotia, Canada *turner@ap.smu.ca*

² Sternberg Astronomical Institute, Moscow, Russian Federation

³ Erindale College, University of Toronto, Erindale, Ontario, Canada

⁴ National Research Institute of Astronomy and Geophysics, Helwan, Egypt

⁵ Visiting Astronomer, Harvard College Observatory Photographic Plate Stacks

ABSTRACT. Random changes in pulsation period occur in cool pulsating Mira variables, Type A, B, and C semiregular variables, RV Tauri variables, and in most classical Cepheids. The physical processes responsible for such fluctuations are uncertain, but presumably originate in temporal modifications of the envelope convection in such stars. Such fluctuations are seemingly random over a few pulsation cycles of the stars, but are dominated by the regularity of the primary pulsation over the long term. The magnitude of stochasticity in pulsating stars appears to be linked directly to their dimensions, although not in simple fashion. It is relatively larger in M supergiants, for example, than in short-period Cepheids, but is common enough that it can be detected in visual observations of the stars, as demonstrated by the example of Delta Cephei. Although chaos was discovered in pulsating stars 80 years ago, detection of its general presence in the group has only been possible in recent studies.

Key words: Instabilities; stars: oscillations; stars: variables: general.

1. Introduction

A well known problem in variable star studies is that it is impossible to predict exact moments for light maximum in some late-type pulsating variables, such as Miras and semi-regular variables, or to predict their amplitude on any given cycle (see Fig. 1 for AAVSO (American Association of Variable Star Observers) observations of the name star, *o* Ceti). The cyclical light patterns displayed in such stars are reasonably well defined over long time intervals and can be approximated closely with linear ephemerides, but the regularity of their pulsation is typically marked by other effects best revealed through careful O–C analysis.

A common complication is that of “random” fluctuations in pulsation period for a star from one cycle to another. Many years ago Eddington & Plakidis (1929)

developed an interesting technique for establishing the importance of random fluctuations in pulsation period for Mira variables, and it has been revived frequently in recent years (Percy & Hale 1998; Percy & Colivas 1999, Percy et al. 1993, 2003, 2007) in order to establish the importance of random changes in period for other Mira variables as well as for other types of cool and hot pulsating variables.

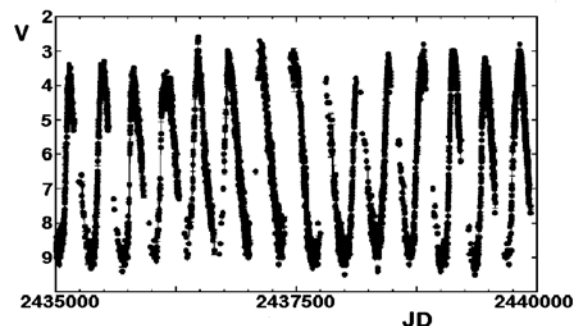


Figure 1: The visual light curve of Mira between JD 2435000 and JD 2440000 from AAVSO measurements.

The technique has been described previously in these pages (Turner & Berdnikov 2001), and involves computing, without regard to sign, the average accumulated time delays $\langle u(x) \rangle$ between light maxima separated by x cycles. If the deviations in the observed times of light maxima from their predicted times are dominated by random fluctuations in period, then the data for all available observed light maxima should display a trend described by:

$$\langle u(x) \rangle^2 = 2a^2 + xe^2,$$

where a is the average uncertainty in days for established times of light maxima and e is the magnitude of any random fluctuations in period. The technique could alternatively be formulated to represent e in terms of phase offset. A schematic representation

of expectations for a “typical” pulsating variable is presented in Fig. 2. But such expectations are never matched exactly in practice, since the dominant pulsation in such stars forces the random factor in the pulsations back into a regular pattern of variability after $\sim 50 - 200$ cycles.

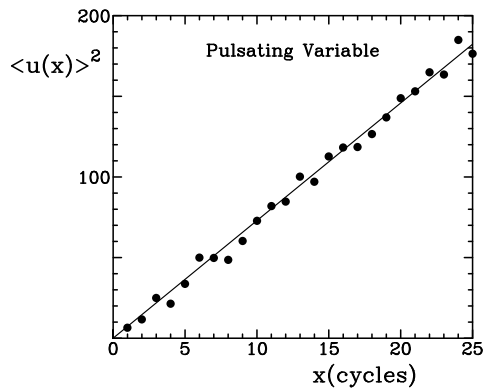


Figure 2: A schematic representation of an Eddington-Plakidis test for a pulsating variable with a randomness factor of $e = 2.7$ days and uncertainties of $a = 0.15$ day in measured times of light maximum.

2. Different Types of Pulsating Stars

Although the Eddington-Plakidis test was devised specifically to analyze random fluctuations in pulsation period for Mira variables, and later applications by Percy et al. (1993), Percy & Hale (1998), and Percy & Colivas (1999) included “Mira-like” stars (Miras, Type A and B semiregulars, and RV Turi variables), the same technique should be valid for all types of stars. The technique was also applied to short period pulsators of both Population types by Percy et al. (2003, 2007), and was extended to Cepheids in a number of studies (Turner & Berdnikov 2001, 2004; Abdel-Sabour Abdel-Latif 2004; Berdnikov et al. 2004, 2007, 2009a, 2009b; Berdnikov 2010, Berdnikov & Stevens 2010). Mostly negative results were found for short period Cepheids, but that is because individual light maxima are rarely observed for such stars and the individual times of light maximum tabulated in O–C analyses usually refer to data obtained over many adjacent cycles about the one cited. Since random fluctuations in period exist over several pulsation cycles, their effects on times of light maximum can easily be confused with other sources of scatter in the light curves when the data are averaged over many cycles.

Confirmation of that conclusion has recently come from space observations of Cepheids (Berdnikov 2010; Berdnikov & Stevens 2010). Since weather problems and limited observing windows are generally not a problem for space observations, it is possible to ob-

serve many consecutive light maxima for short period Cepheids and to derive observed times of light maxima from applications of Hertzsprung’s method. The results indicate that random fluctuations in period are relatively common even for short period Cepheids, and most likely apply to all radially pulsating stars, at least to some extent.

The same feature also appears in at least one SRC variable, the pulsating M3 Ia supergiant BC Cyg, a star for which the observed times of light maximum can vary by ± 84 days from those predicted by a quadratic ephemeris accounting for its long-term period decrease (Turner et al. 2009). The Eddington-Plakidis test for that star is replicated in Fig. 3 of this paper, which demonstrates that irregular pulsations in the star appear to return to a regular pattern after about 12 cycles or so (~ 23 years in the present case). In pulsating stars of shorter cycle length such regularity returns much sooner, a matter of a few years in the case of short period Cepheids (Berdnikov 2010).

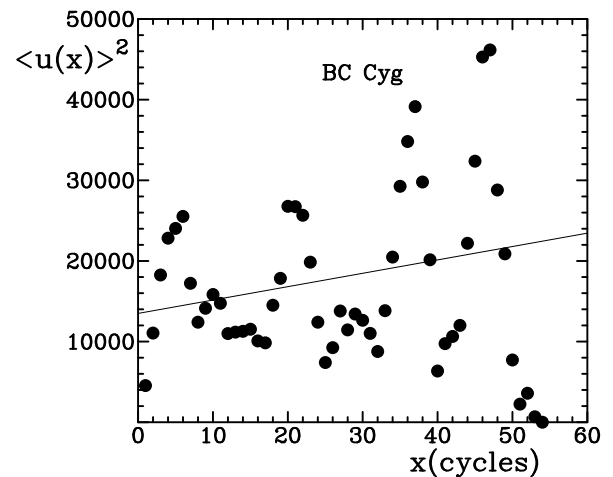


Figure 3: An Eddington-Plakidis test for the M3 Ia supergiant variable BC Cyg.

Evidence for random fluctuations in pulsation period on short time scales can also be seen in the results of Poleski (2008) for several Cepheids in the Large Magellanic Cloud. The evidence is revealed by offsets in the observed times of light maximum from cycle to cycle in Poleski’s O–C diagrams, although the deviations are typically rather small in comparison with much larger deviations observed over longer time intervals, where the evolutionary changes in mean radius become dominant (Turner et al. 2006).

3. Parameterizing the Randomness Factor

In their original tests on α Ceti (Mira) and χ Cygni, Eddington & Plakidis (1929) noted that the observed random fluctuations in period for both stars amounted

to about the same amount, 1.35–1.39% of the pulsation period. They clearly understood the importance of the star’s pulsation period to the magnitude of the stochastic processes producing the random fluctuations in period. Yet the cycle length for any pulsating star also depends directly on stellar radius through the period-radius relations applying to every type of pulsating star. Therefore, a better parameter for describing the stochastic processes arising in pulsating stars is the ratio e/P , although that is only to first order. The parameter e/P must be independent of radius if the variables obey similar period-radius relations.

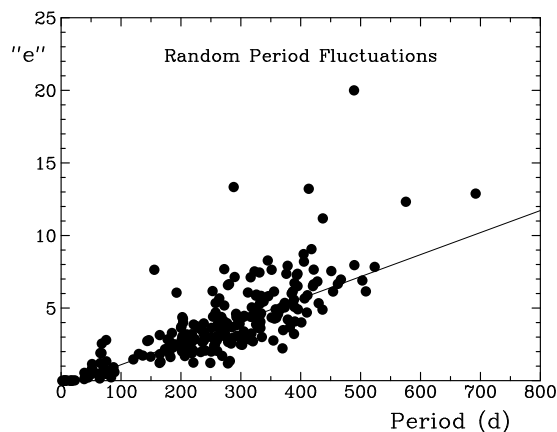


Figure 4: The observed trend of increasing randomness factor “ e ” with increasing pulsation period P .

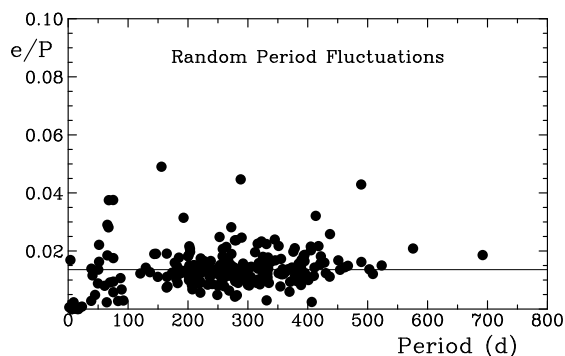


Figure 5: The nearly negligible trend of the parameter e/P with pulsation period.

Results to date for all Eddington-Plakidis analyses of pulsating stars (updated from Turner et al. 2009) are illustrated in Figs. 4 and 5, and confirm such an assumption. Note that Fig. 4 contains additional data from earlier versions plotted by Turner & Berdnikov (2001) and Turner et al. (2009). As seen in Fig. 5, the parameter e/P is indeed relatively independent of pulsation period, in other words independent of stellar radius, although there may be an additional trend with period, perhaps reflecting the increasing dominance of envelope convection with decreasing stellar

surface temperature in such stars. The parameter e/P has a mean value of 0.0136 ± 0.0005 (± 0.0069 s.d.), which matches the results of Eddington & Plakidis (1929) more than 80 years ago.

As noted earlier, the actual observed trends in the computed values of $\langle u(x) \rangle^2$ for all pulsating stars tested to date initially increase directly in proportion to increasing differences in cycle count, as predicted (Eddington & Plakidis 1929, see also Fig. 2). At larger cycle differences, however, the trend reverses as the dominant pulsation in such stars reimposes its regularity in the observed times of light maximum. Observed values of $\langle u(x) \rangle$ gradually become much smaller for large cycle differences, a characteristic also noted by Eddington and Plakidis in their original study of two Mira variables and seen in almost all of the Eddington-Plakidis tests cited earlier. The stochastic fluctuations in period that appear as a common feature in the cycle lengths of nearly all pulsating stars are therefore dominated by the regular pulsation in such stars. As noted above, the physical processes responsible for such characteristics are uncertain, but presumably originate in temporal modifications of envelope convection in such stars.

4. Discussion

The fact that random fluctuations in period are ubiquitous for all pulsating variables has important consequences. Standard O–C analyses of Cepheids, for example, will always display scatter in the individual O–C data, unless they are averaged over many adjacent cycles. Even then, the non-photometric source of scatter in light curve data points for individual cycles must also introduce a small source of uncertainty in the resulting O–C data based on light curves constructed from observations averaged over the same cycles. Likewise, the detection of sizable random fluctuations in period for long period variables means that the *P edic ed Da e f Ma i a a d Mi i a f L g Pe i d Va i a b e* issued regularly by the AAVSO must necessarily be inexact. Fortunately such predictions are generally issued within a cycle or two of the predicted dates, so they are likely to be only a few days off because of the stochastic processes occurring in the envelopes of such stars.

The AAVSO collection of data for Miras and long period variables was the basis for studies of random fluctuations in their pulsation periods by Percy et al. (1993), Percy & Hale (1998), and Percy & Colivas (1999), so it seems clear that such changes can be detected in long period variables from simple eye estimates. An interesting question to ask is whether or not such effects can also be detected from simple eye estimates for Cepheid variables. The lead author recently had an opportunity to address that question while

teaching an undergraduate course in astronomy. A decade previously, Turner (1999, 2000) demonstrated a simple procedure for obtaining precise estimates of magnitude for bright Cepheids from unaided observations by eye. The original observations from 1998-99 have been used frequently since then for instructional purposes, and the procedure was revived in October 2009 to provide a reference data set for a student attempting to follow the technique on his own. The results are illustrated in Fig. 6, where the data are phased using the same ephemeris adopted in 1998-99.

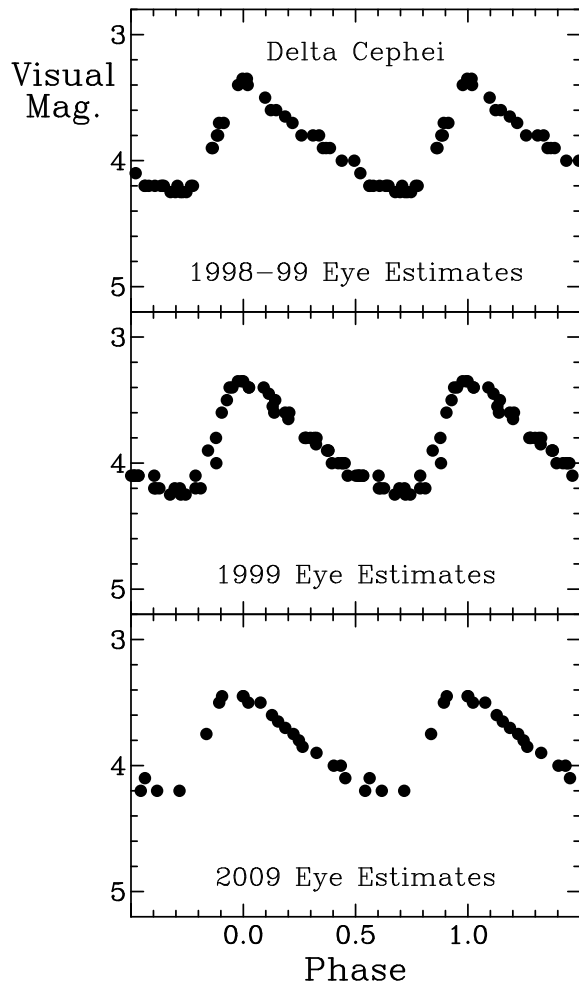


Figure 6: Observations by Turner with unaided eye of δ Cephei from 1998 to 2009.

The observed light maxima for δ Cephei in winter 1998-99 and fall 1999 fell very close to the times predicted from the adopted ephemeris for the star, and

the same conclusion applies to the observations from 2009. The Cepheid has a well-established period decrease (Turner 1999, 2000; Turner et al. 2006), so the times of light maximum should occur slightly earlier in 2009 than they did in 1998-99. But the O-C offset is effectively nil between the two dates, and no evidence for chaotic effects in pulsation period can be distinguished from our eye estimates for the star. The results of Berdnikov (2010) and Berdnikov & Stevens (2010) for other short-period Cepheids are consistent with such conclusions.

Acknowledgements. The authors acknowledge with thanks the variable star observations from the American Association of Variable Star Observers (AAVSO) International Database contributed by observers worldwide that are displayed in Fig. 1 of this study.

References

- Abdel-Sabour Abdel-Latif M.: 2004, Ph.D. Thesis, Cairo University.
- Berdnikov L.N.: 2010, In *Variable Stars, The Galactic Halo and Galaxy Formation*, p. 29.
- Berdnikov L.N., Stevens I.R.: 2010, In *Variable Stars, The Galactic Halo and Galaxy Formation*, p. 207.
- Berdnikov L.N., et al.: 2004, *PASP*, **116**, 536.
- Berdnikov L.N., et al.: 2007, *PASP*, **119**, 82.
- Berdnikov L.N., et al.: 2009a, *AstL*, **35**, 175.
- Berdnikov L.N., et al.: 2009b, *AstL*, **35**, 406.
- Eddington A.S., Plakidis S.: 1929, *MNRAS*, **90**, 65.
- Poleski R.: 2008, *AcA*, **58**, 313.
- Percy J.R., Colivas T.: 1999, *PASP*, **111**, 94.
- Percy J.R., Hale J.: 1998, *PASP*, **110**, 1428.
- Percy J.R., Bandara K., Cimino P.: 2007, *JAAVSO*, **35**, 343.
- Percy J.R., et al.: 1997, *PASP*, **109**, 264.
- Percy J.R., et al.: 2003, *PASP*, **115**, 626.
- Turner D.G.: 1999, *JRASC*, **93**, 228.
- Turner D.G.: 2000, *JAAVSO*, **28**, 116.
- Turner D.G., Berdnikov L.N.: 2001, *Odessa Astron. Publ.*, **14**, 170.
- Turner D.G., Berdnikov L.N.: 2004, *A&A*, **423**, 335.
- Turner D.G., Abdel-Sabour Abdel-Latif M., Berdnikov L.N.: 2006, *PASP*, **118**, 410.
- Turner D.G., et al.: 2006, *PASP*, **118**, 1533.
- Turner D.G., et al.: 2009, *AIP Conf. Series*, **1170**, 167.

PHOTOMETRY AND BLAZHKO EFFECT IN RR Lyr TYPE STAR DM Cyg

S.N. Udovichenko¹, P.A. Dubovsky², I. Kudzej²

¹ Astronomical Observatory, Odessa National University
T.G.Shevchenko Park, Odessa 65014, Ukraine, *udovich222@ukr.net*

² Vihorlat Observatory
Mierová 4, 06601 Humenné, Slovakia, *vihorlatobs1@stonline.sk*

ABSTRACT. The photometric CCD observations for RR Lyr type star DM Cyg in Astronomical stations near Odessa(Ukraine) and Kolonica(Slovakia) in 2008 and near Odessa in 2009 have been carried out. The light curves in V system were obtained and the frequency Fourier analyse was performed. From Fourier spectra of the light curves 18 frequencies were identified. The weak Blazhko effect was detected.

Key words: Stars: oscillations - stars; variables: RR Lyr - stars: individual: DM Cyg.

1. Introduction

The variability of the star was found by L. P. Tserasskaya in 1928. The star thoroughly was investigated by D. Ya. Martynov, which determined the primary elements of period. V. P. Tsessevich referred this star to type of the stars with suddenly variations of period. Visual observations in 20 century were carried out by Toronjadze, Esh, Martynov, Dombrovskiy, Selivanov, Gur'ev, Satyvaldyev, Born, Sofronevich, Alaniya, Lange, Lysova, Firmanuk, Braude at all, Tsessevich(1966). The period of Blazhko effect (26^d), found by Lysona & Firmanyuk (1980) was not confirmed (Sodor & Jurcsik 2005).

Now DM Cyg is known as RR Lyr-star type (RRab) with amplitude $10.^m93 - 11.^m99$ (V), has spectr A9-F6 and period $0.^d41986$, Kholopov et al. (1985).

2. Observations

The photometric CCD observations of DM Cyg in Astronomical stations near Odessa and Kolonica in 2008, and near Odessa in 2009 equipped with V filter have been carried out. Two stars were chosen as comparison and check stars (comp=Tycho 2707-01803, check=Tycho 2707-01687). The 48 cm reflector AZT-3 with the f/4.5 Newtonian focus and CCD photometer with CCD chip Sony ICX429ALL, Peltier cooler

and 28 cm reflector with Newtonian focus and CCD camera Meade DSI Pro with chip Sony ICX254AL were used respectively. More then 7140 CCD frames were gathered during two years. The reductions of the CCD frames were carried out using the MUNIPACK (<http://integral.sci.muni.cz/cmunicipack>) software. The procedures for the aperture photometry are composed of the dark-level and flat-field corrections and determination of the instrumental magnitude and precision. The relative magnitudes of DM Cyg measured to the magnitudes of comparison star ($V^T=12.07; 21:20:58 +32:12:59$ (2000.0)). The all set of observations are shown in fig.1. The errors on individual data points vary between 0.005 mag to 0.01 mag.

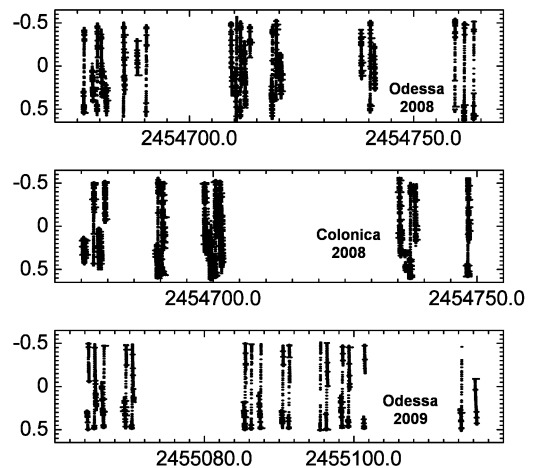


Figure 1: The all data set of observations DM Cyg in 2008-2009.

3. Results

For all observations of DM Cyg were determined the magnitudes comparatively of comparison star. The phase curves were computed from elements:

Max.HJD= 2442582.406 + 0.4198600 · E , Kholopov et al. (1985).

The light curve shows small amplitude modulations about 0.07 mag and phase modulations up to 0.01. The V light curves DM Cyg and the utmost case of amplitude modulation are shown on fig. 2. These small modulation determine the small Blazhko effect of the star.

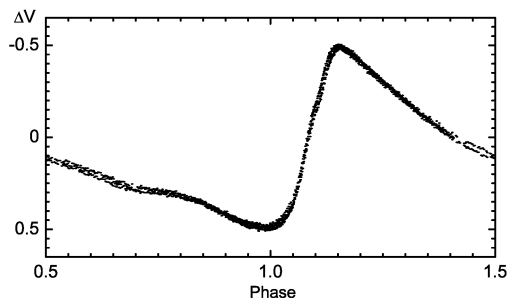


Figure 2: The two utmost case of amplitude modulation in the light curves DM Cyg.

The frequency analyses were performed using a package of computer programs with single-frequency and multiple-frequency techniques by using utilize Fourier as well as multiple-least-squares algorithms (program Period04, Lenz and Breger, 2004). The power spectra of all data set shown in Fig. 3.

The spectrum has been prewhitened for the pulsation component up to f_{12} . Do not all datas were used for frequency analyses. The differences between V instrumental system allow to take only a part data 2008 year and 2009 entirely. The Fourier amplitude and phases of the pulsation component identified in the spectra of the light curves of DM Cyg are presented in Table 1. The basic frequency denoted as f_0 , the modulation frequency of Blazhko effect denote as f_B . The errors of the amplitudes are 0.00024, the errors of frequencies and phases are given in table. With increasing order of frequencies the amplitudes of the pulsation are decrease. We find triplet of frequencies $f_0 \pm f_B$, but, perhaps, there are more frequencies in the pulsation spectra of DM Cyg. The amplitude of the component $f_0 + f_B$ is larger then the amplitudes $f_0 - f_B$ component. This fact have an influence on delay light curve and phase: the maximum of the amplitude modulation precedes the phase of the time delay of the maxima.

From obtained data the frequency of Blazhko effect amount 0.0947 c/d and period $10^d.56$. These values are agree with results, published Jurcsik et al.(2009).

4. Summary

DM Cyg, variable star of RR Lyr type, has pulsations in fundamental mode and small Blazhko effect. The difference of the amplitudes between min and max is about 0.07 mag, Blazhko period about $10^d.56$. The frequency Fourier analyse of light curves shows the components $f_0 \pm f_B$ of spectra up to 9 order.

There are three possible explanation of the Blazhko effect (Kovacs 1995):

- the *oblique pulsator* model, wich assumed that the Blazhko variable have a magnetic field which is oblique to the pulsation axis;
- *dynamical interaction* between the radial fundamental mode and a resonant non-radial mode;
- *steady resonant pulsation* in the radial fundamental mode together with a non-radial mode of low spherical degree with almost the same period. The amplitude modulation is caused by the rotation of the non-radial surface pattern.

The detection small-amplitude light curves modulation of DM Cyg and other RR Lyr stars may confirm the first model (oblique pulsator), so as the magnetic axis has a random distribution in spase, and we could be observe the small and large modulation. But this fact do not contradict to other explanations.

References

- Jurcsik J., Hurta Zs., Sodor A., et al.: 2009, *Mon.Not.R.Astron.Soc.*, **397**, 350
- Kovacs G.: 1995, *A&A*, **295**, 693
- Kholopov P. N., Samus N. N., Frolov M. C., Goransky V. P., Gorynya N. A., Kireeva N. N., Kukarkina N. P., Kurochkin N. E., Medvedeva G. I., Perova N. B., Shugarov S. Yu.: 1985, *General Catalogue of Variable Stars*.
- Lenz P., Breger M.: 2004, *Comm.in Asteroseismology*, **144**, 41
- Lysova L.E., Firmanyuk B.N.: 1980, *Astron.Tsirk.*, **1122**
- Sodor A., Jurcsik J., 2005, *IBVS*, **5641**
- Tsessevich V. P.: 1966, *RR Lyrae-Type Variable Stars*, Naukova Dumka, Kiev.

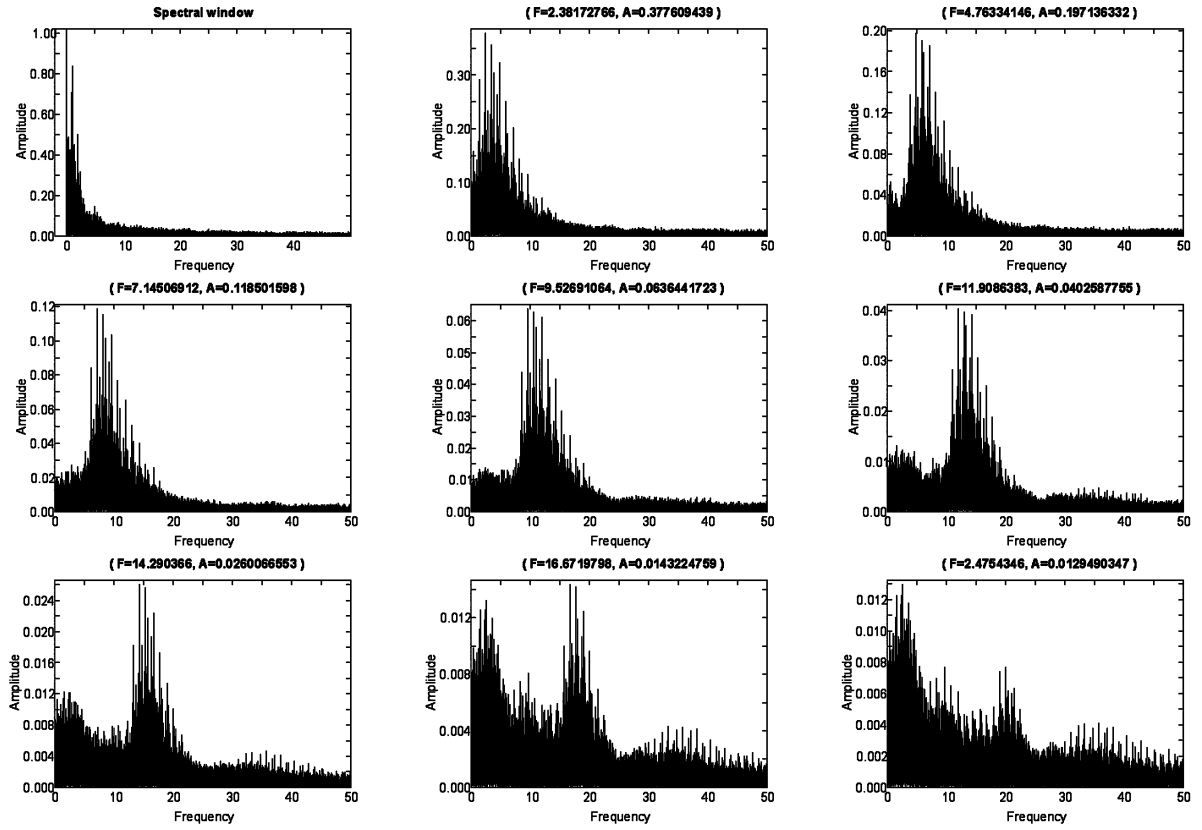


Figure 3: The spectral window and Fourier amplitude spectrum after the removal of the pulsation component (from f1 to f8).

Table 1: Identified Fourier amplitude and phases of the pulsation and modulation frequencies in light curves of DM Cyg.

	Identif.	Frequency	Sigma Fr.	Amplitude	Phase	Sigma Ph.
f1	f_0	2.381670	0.000079	0.335680	0.0837173	0.000114
f2	$2f_0$	4.763475	0.000014	0.181723	0.3182059	0.000212
f3	$3f_0$	7.145023	0.000023	0.1118295	0.2528553	0.000344
f4	$4f_0$	9.526944	0.000044	0.0598717	0.4594258	0.000643
f5	$5f_0$	11.90858	0.000072	0.0366815	0.1547723	0.001051
f6	$6f_0$	14.29043	0.000105	0.0251703	0.6956476	0.001531
f7	$7f_0$	16.67200	0.000188	0.0141136	0.4219310	0.002731
f8	f_0+f_B	2.475495	0.000221	0.0120192	0.7979833	0.003207
f9	$3f_0+f_B$	7.239372	0.000317	0.0083993	0.2286909	0.004590
f10	$8f_0$	19.05422	0.000331	0.00803232	0.8381523	0.004800
f11	$5f_0+f_B$	12.00350	0.000503	0.00529077	0.9015201	0.007287
f12	$7f_0+f_B$	16.76747	0.000566	0.00470369	0.9925396	0.008196
f13	f_0-f_B	2.285704	0.000394	0.00674569	0.2222793	0.005715
f14	$2f_0+f_B$	4.860136	0.000019	0.135926	0.1271544	0.000283
f15	$9f_0$	21.43453	0.000652	0.00408199	0.7569384	0.009445
f16	$4f_0+f_B$	9.617718	0.000641	0.00414875	0.0360648	0.009293
f17	$12f_0$	28.57882	0.001018	0.00261339	0.7852578	0.014753
f18	$9f_0+f_B$	21.53040	0.001006	0.00264637	0.0641502	0.014569

SPECTROSCOPIC INVESTIGATIONS OF CEPHEIDS IN CARINA

I.A. Usenko,¹ L.N. Berdnikov,² V.V. Kravtsov,^{2 3} A. Yu. Knyazev,⁴ R. Chini^{5 3},
V.H. Hoffmeister⁵, O. Stahl⁶, H. Drass⁵

¹ Astronomical Observatory, Odessa National University, T.G. Shevchenko Park,
Odessa 65014, Ukraine, *igus99@ukr.net*

² Sternberg Astronomical Institute, Moscow University, Moscow 119899, Russia,
lberdnikov@yandex.ru

³ Universidad Católica del Norte, Avenida Angamos 0610, Autofagasta, Chile,
vkravtsov@ucn.cl

⁴ South African Large Telescope, P.O. Box 9, Observatory, Cape Town 7935,
South Africa, *aknyazev@saaao.ac.za*

⁵ Astronomisches Institut, Ruhr-Universität Bochum, Bochum 44780, Germany,
chini@astro.rub.de vhoff@astro.rub.de hdrass@astro.rub.de

⁶ Landessternwarte, Heidelberg, Germany, *O.Stahl@sw.uni-heidelberg.de*

ABSTRACT. Spectroscopic investigations of seven southern Cepheids WW Car, SX Car, UZ Car, UY Car, GX Car, HW Car and YZ Car have been performed. It was founded out six objects have metallicities, close to solar one and their CNO-, odd elements and Mg content indicate that these objects are on the stage after the first dredge-up. Cepheid WW Car is an unusual objects because it has noticeable overabundance of $[C/H] = +0.3$ dex, $[N/H] = +0.95$ dex, whereas sodium is deficient ($[Na/H] = -0.46$ dex), and magnesium content is the largest ($[Mg/H] = -0.12$ dex) in comparison with other objects from this list having close pulsation periods.

Key words: Stars: Cepheids; stars: individual: WW Car, SX Car, UZ Car, UY Car, GX Car, HW Car, YZ Car.

1. Introduction

Region in Carina is still insufficiently explored among ones contained the classical Cepheids. Especially it concern to the faint objects. To fill up the gap in these explorations we have obtained some spectra of seven faint Cepheids (see Table 1). At that only two objects from this list have been more or less investigated in detail, - SX Car and YZ Car. SX Car have been regarded as a possible member of Ruprecht 91 open cluster in Carina, located on the its periphery, nevertheless it assumption was omitted (Turner et al., 2005). This Cepheid is a possible binary with companion of B6.5 spectral type (Turner, 1996). Its pulsational period is very stable, and O-C diagram do not

shows any significant increasing or decreasing. Instead YZ Car is a well-known binary system with orbital period 657.3 days (Pettersen, Cottrell & Albrow, 2004). Its Companion is a main-sequence star B8 V – A0 V with mass range from 2.2 - 2.9 M_{\odot} . (Evans & Butler, 1993). According to Pettersen et al. (2004) this Cepheid has $T_{eff} = 5900$ K; $L = 9350 L_{\odot}$, and $M = 7.7 M_{\odot}$. It, probably, is a supergiant on the stage of second crossing of Cepheids instability strip (Pettersen, Cottrell & Albrow, 2004).

2. Observations

Observations of these objects have been realized using 1.5m Hexapod telescope equipped by Bochum Echelle Spectrograph for OCA (BESO) (ESO, Chile): $\lambda\lambda$ 4961-8861 Å in 65 orders, and resolving power $R = 48\,000$, and S/N ratio from 25 to 75 (see Table 1). The exposition time consists 1800 s for the each spectrum.

The reduction was made using IRAF software, the MIDAS context ECHELLE modified for extraction of echelle spectra obtained with an image slicer (Yushkin & Klochkova 2005), DECH20 software (Galazutdinov, 1992).

3. Atmosphere parameters and chemical composition

Atmosphere parameters were determined:

1. T_{eff} : line depth ratio (Kovtyukh & Gorlova, 2000).

Table 1: Program stars spectra

Star	Period (days)	V (mag)	Spectral type	Num. of spectra	S/N
WW Car	4.67	9.748	F0	1	25
SX Car	4.86	9.090	F5II	1	50
UZ Car	5.20	9.331	G0	1	30
UY Car	5.54	8.949	?	3	75
GX Car	7.20	9.341	F8II	1	35
HW Car	9.20	9.128	G2 – G3Ib – II	1	65
YZ Car	18.16	8.711	G5	2	75

Table 2: Observations and atmosphere parameters

Star	Spectrum	HJD	T _{eff}	log g	V _t (km s ⁻¹)
		2450000+	(K)		
WW Car	042206	4944.597	5012±46	1.70	4.50
SX Car	042205	4944.574	5433±43	2.00	4.70
UZ Car	041705	4939.630	5374±58	2.00	4.20
UY Car	041503	4937.623	5900±30	2.20	4.20
	041807	4940.606	5550±30	2.10	4.20
	042204	4944.551	5700±30	2.00	3.40
GX Car	040709	4929.688	5451±26	2.00	5.40
HW Car	041808	4940.649	5702±28	1.70	4.50
YZ Car	041502	4937.600	5323±31	1.25	4.50
	041806	4940.584	5600±30	1.90	5.50

2. log g: by adopting the same iron abundance for Fe I and Fe II lines (accuracy: 0.15 dex).

3. V_t - by assuming abundances of the Fe II lines independent of the W_λ (accuracy: 0.25 km/s).

The mean atmosphere parameters are given in Table 2.

4. Chemical composition

All the atmosphere models and chemical composition for each spectrum were calculated using our version of the WIDTH9 code on the basis of the Kurucz (1992) grid with the “solar” log gf values, adopted from Kovtyukh & Andrievsky (1999). All the data about the element abundances for these Cepheids are given in Tables 3, 4, 5 and 6.

5. Conclusions

1. All these objects have metallicities, close to solar one (or slightly deficient), excepting WW Car with [Fe/H] = -0.3 dex.
2. Judging from the CNO-, odd elements, and Mg content, six Cepheids from the list are the objects on the stage after the first dredge-up.
3. Cepheid WW Car shows noticeable overabundance of carbon [C/H] = +0.3 dex nitrogen ([N/H] = +0.95 dex), whereas sodium demonstrate significant deficient in comparison with other ones having close pulsation periods ([Na/H]

= -0.46 dex), and magnesium content is the largest ([Mg/H] = -0.12 dex)! Therefore, WW Car is an unusual object among Cepheids.

4. α - elements abundances for these objects are close to solar ones, excepting Ca (small deficient), whereas Fe-group, “light” and “heavy” - s- process and r-process elements demonstrate either slight enhance or slight deficient.

5. Atmospheric parameters, obtained for YZ Car are close to ones derived from the model of Petterson et al. (2004).

References

- Evans N.R., Butler, J.: 1993, *PASP*, **105**, 915
Galazutdinov G.A.: 1992, *Preprint SAO RAS*, **92**
Kovtyukh V.V., Andrievsky S.M.: 1999, *A&A*, **351**, 597
Kovtyukh V.V., Gorlova N.I.: 2000, *A&A*, **358**, 587
Kurucz R.: 1992, *In: The Stellar Populations of Galaxies, (eds) B. Barbuy and A. Renzini, IAU Symp.*, **149**, 225
Petterson, O.K.L., Cottrell, P.L. & Albrow, M.D.: 2004, *MNRAS*, **350**, 95
Petterson O.K.L., Cottrell P.L., Albrow M.D. Fokin, A.B.: 2004, *MNRAS*, **362**, 1167
Turner D.G.: 1996, *JRASC*, **90**, 82
Turner D.G. Forbes D., Leonard P.J.T., Abdel-Latif, M.A., Majaess D.J., Berdnikov L.N.: 2005, *AJ*, **130**, 1194
Yushkin M.V., Klochkova V.G.: 2005, *Preprint SAO RAS*, **206**

Table 3: Elemental abundance for WW Car, SX Car and UZ Car. NL - number of elements.

El.	WW Car			SX Car			UZ Car		
	[E/H]	σ	NL	[E/H]	σ	NL	[E/H]	σ	NL
C I	+0.30	0.38	8	-0.41	0.19	10	-0.43	0.15	9
N I	+0.95	0.07	6	+0.62	0.31	5	+0.64	0.13	6
O I	+0.22	0.26	3	+0.12	0.11	2	+0.07	0.10	5
Na I	-0.46	0.18	4	-0.07	0.14	2	-0.14	0.14	3
Mg I	-0.12	0.28	7	-0.27	0.17	7	-0.28	0.13	7
Al I	-0.16	0.14	7	+0.11	0.10	7	-0.06	0.11	5
Si I	-0.07	0.21	36	-0.15	0.20	38	-0.12	0.24	41
Si II	+0.16	-	1	+0.07	0.28	2	-0.18	0.05	2
S I	+0.16	0.18	6	+0.04	0.22	6	+0.03	0.18	7
K I	+0.66	-	1	+0.63	-	1	+0.70	-	1
Ca I	-0.44	0.29	8	-0.30	0.20	11	-0.44	0.30	12
Sc I	+0.01	0.29	4	+0.30	0.24	3	-0.06	0.06	3
Sc II	-0.90	0.18	9	-0.42	0.17	7	-0.21	0.17	6
Ti I	-0.27	0.38	38	-0.13	0.33	59	-0.14	0.33	55
Ti II	-0.23	0.28	6	-0.54	0.09	7	-0.19	0.26	5
V I	-0.01	0.28	7	-0.23	0.32	14	-0.24	0.18	12
V II	-0.29	0.05	3	-0.07	0.08	4	-0.21	0.23	4
Cr I	-0.21	0.25	21	-0.15	0.27	27	+0.04	0.29	22
Cr II	-0.35	0.27	14	-0.12	0.19	12	-0.00	0.39	11
Mn I	-0.61	0.29	9	-0.38	0.29	13	-0.46	0.14	7
Fe I	-0.30	0.25	237	-0.16	0.20	264	-0.02	0.27	268
Fe II	-0.33	0.21	33	-0.18	0.17	42	-0.01	0.22	42
Co I	-0.33	0.35	19	-0.05	0.28	20	+0.04	0.31	31
Ni I	-0.32	0.31	73	-0.29	0.29	96	-0.32	0.31	85
Cu I	-0.53	0.33	3	-0.42	0.30	4	-0.26	0.47	4
Zn I	-0.50	-	1	-0.17	-	1	+0.21	-	1
Sr I	+0.18	0.31	3	+0.68	-	1	+0.40	0.05	2
Y I	-0.71	-	1	-0.16	-	1	-0.07	-	1
Y II	-0.17	0.30	6	+0.02	0.29	7	-0.07	0.09	6
Zr II	-0.11	0.09	3	+0.02	0.17	2	+0.00	0.16	4
Ru I	+0.34	-	1	+0.29	0.62	2	+0.03	-	1
La II	-0.29	0.29	2	-0.60	0.01	2	+0.01	0.02	3
Ce II	-0.55	0.11	5	-0.22	0.32	7	-0.13	0.13	4
Pr II	-0.30	0.20	2	-0.37	-	1	-0.17	0.01	3
Nd II	-0.36	0.19	9	-0.16	0.21	4	+0.09	0.24	11
Eu II	+0.09	0.20	2	+0.10	0.21	4	+0.24	0.43	2
Gd II	-0.36	-	1	-0.80	-	1	+0.01	0.00	1

Table 4: Elemental abundance for YZ Car.

Element	041502		041806		Mean		
	[E/H]	σ	[E/H]	σ	[E/H]	σ	NL
C I	-0.23	0.13	-0.55	0.16	-0.41	0.15	17
N I	+0.31	0.17	+0.25	0.25	+0.28	0.21	6
O I	+0.10	0.08	-0.01	0.16	+0.04	0.14	7
Na I	-0.13	0.17	-0.10	0.39	-0.05	0.26	7
Mg I	-0.33	0.13	-0.22	0.15	-0.25	0.15	12
Al I	+0.10	0.12	-0.13	0.19	-0.05	0.20	14
Si I	-0.08	0.17	-0.06	0.14	-0.07	0.15	78
Si II	+0.06	0.36	+0.05	-	+0.06	0.26	3
S I	+0.05	0.28	-0.06	0.17	-0.00	0.23	12
Ca I	-0.35	0.25	-0.32	0.15	-0.36	0.18	20
Sc I	-0.35	0.08	-0.11	0.12	-0.25	0.15	5
Sc II	-0.29	0.24	-0.23	0.09	-0.25	0.15	7
Ti I	-0.08	0.24	-0.11	0.28	-0.10	0.25	96
Ti II	-0.16	0.31	-0.16	0.15	-0.16	0.22	8
V I	-0.11	0.23	+0.03	0.19	-0.08	0.22	24
V II	-0.07	0.28	-0.06	0.18	-0.06	0.21	6
Cr I	-0.15	0.20	+0.04	0.26	-0.08	0.23	46
Cr II	-0.07	0.30	-0.04	0.13	-0.03	0.21	25
Mn I	-0.21	0.13	-0.29	0.29	-0.28	0.20	20
Fe I	-0.04	0.20	-0.08	0.24	-0.06	0.22	561
Fe II	-0.04	0.12	-0.10	0.15	-0.07	0.14	61
Co I	-0.06	0.22	+0.06	0.22	-0.00	0.23	51
Ni I	-0.16	0.27	-0.25	0.26	-0.20	0.26	172
Cu I	-0.23	0.15	-0.03	0.32	-0.21	0.13	7
Zn I	+0.07	-	-0.01	-	+0.03	0.05	2
Sr I	+0.57	-	+0.20	-	+0.39	0.26	2
Y I	+0.24	-	-	-	+0.24	-	1
Y II	+0.04	0.22	+0.05	0.19	+0.05	0.19	12
Zr II	+0.15	0.19	+0.17	0.12	+0.16	0.15	8
Ru I	+0.30	-	-	-	+0.30	-	1
La II	-0.19	-	+0.40	0.01	+0.21	0.34	3
Ce II	+0.02	0.28	-0.03	0.25	-0.00	0.26	9
Pr II	-0.23	0.11	-0.09	0.16	-0.16	0.15	6
Nd II	-0.10	0.16	+0.01	0.16	-0.05	0.16	26
Eu II	+0.21	0.05	+0.12	0.04	+0.17	0.06	6
Gd II	-	-	-0.76	-	-0.76	-	1

Table 5: Elemental abundance for GX Car and HW Car

Element	GX Car			HW Car		
	[E/H]	σ	NL	[E/H]	σ	NL
C I	-0.44	0.24	15	-0.48	0.27	15
N I	+0.46	0.20	4	+0.53	0.21	4
O I	+0.06	0.18	6	-0.17	0.14	4
Na I	-0.12	0.19	4	+0.07	0.07	2
Mg I	-0.44	0.27	6	-0.41	0.21	6
Al I	-0.03	0.14	7	+0.15	0.21	5
Si I	-0.09	0.19	49	-0.18	0.21	57
Si II	-0.07	0.07	2	-0.19	0.49	2
S I	-0.10	0.25	7	-0.02	0.17	7
K I	-	-	0	+0.57	-	1
Ca I	-0.35	0.19	11	-0.20	0.14	8
Sc I	+0.24	0.22	4	+0.03	0.19	4
Sc II	-0.14	0.21	7	-0.21	0.28	6
Ti I	-0.12	0.26	50	-0.04	0.23	63
Ti II	-0.25	0.25	4	-0.15	0.15	8
V I	-0.05	0.45	19	-0.11	0.12	13
V II	-0.11	0.17	5	-0.33	0.38	4
Cr I	-0.13	0.24	21	+0.03	0.28	32
Cr II	-0.05	0.23	13	-0.13	0.22	13
Mn I	-0.34	0.28	13	-0.15	0.22	15
Fe I	-0.12	0.24	294	-0.15	0.22	303
Fe II	-0.13	0.19	46	-0.16	0.12	42
Co I	-0.06	0.22	26	+0.14	0.41	31
Ni I	-0.23	0.31	90	-0.22	0.26	102
Cu I	-0.25	-	1	-0.00	0.32	4
Zn I	-0.25	-	1	-0.07	-	1
Sr I	+0.46	0.40	2	+0.44	-	1
Y I	-0.18	0.01	2	+0.14	-	1
Y II	-0.01	0.17	6	+0.01	0.06	6
Zr II	-0.05	0.18	5	+0.01	0.18	4
Ru I	+0.45	-	1	-	-	0
La II	+0.11	0.21	3	+0.27	0.07	3
Ce II	-0.12	0.23	4	-0.22	0.24	7
Pr II	-0.08	0.01	2	+0.04	0.01	2
Nd II	+0.02	0.16	15	-0.14	0.20	13
Eu II	-0.03	0.25	3	-0.12	0.10	2
Gd II	-0.07	-	1	-0.57	0.00	1

Table 6: Elemental abundance for UY Car

Element	041503		041807		042204		Mean		
	[E/H]	σ	[E/H]	σ	[E/H]	σ	[E/H]	σ	NL
C I	-0.47	0.27	-0.52	0.16	-0.31	0.17	-0.45	0.23	25
N I	+0.41	0.26	+0.35	0.04	+0.47	0.31	+0.39	0.21	14
O I	+0.01	-	+0.11	0.32	+0.11	0.13	+0.06	0.14	10
Na I	+0.03	0.29	-0.13	0.08	-0.02	0.07	-0.04	0.09	12
Mg I	-0.38	0.18	-0.27	0.08	-0.33	0.30	-0.33	0.25	16
Al I	-0.09	0.19	+0.08	0.16	-0.03	0.15	-0.01	0.18	19
Si I	-0.04	0.20	+0.04	0.23	+0.02	0.20	-0.00	0.20	134
Si II	-0.08	0.19	-0.07	0.21	-	-	-0.08	0.210	4
S I	+0.01	0.20	+0.05	0.23	-0.03	0.14	+0.01	0.18	21
K I	+0.12	-	+0.61	-	+0.71	-	+0.48	0.32	3
Ca I	-0.24	0.22	-0.18	0.35	-0.14	0.25	-0.18	0.27	35
Sc I	-	-	+0.08	0.05	+0.08	-	+0.08	0.05	3
Sc II	-0.20	0.18	-0.15	0.22	-0.17	0.07	-0.16	0.25	22
Ti I	-0.03	0.38	+0.08	0.24	-0.00	0.21	+0.03	0.27	143
Ti II	-0.15	0.15	-0.17	0.15	-0.10	0.20	-0.14	0.16	17
V I	+0.02	0.22	+0.02	0.24	-0.12	0.18	-0.01	0.22	33
V II	-0.12	0.18	-0.06	0.25	+0.10	0.18	-0.03	0.21	13
Cr I	+0.18	0.37	-0.02	0.33	-0.06	0.22	+0.03	0.32	77
Cr II	-0.02	0.22	-0.01	0.27	+0.09	0.23	+0.02	0.24	39
Mn I	-0.43	0.22	-0.24	0.27	+0.10	0.43	-0.22	0.33	34
Fe I	-0.07	0.23	-0.05	0.25	-0.06	0.22	-0.06	0.23	879
Fe II	-0.06	0.22	-0.06	0.22	-0.06	0.21	-0.06	0.22	138
Co I	-0.02	0.22	-0.04	0.27	+0.02	0.19	-0.00	0.21	69
Ni I	-0.15	0.24	-0.19	0.24	-0.09	0.27	-0.15	0.24	231
Cu I	-0.30	0.07	-0.18	0.21	-0.29	0.37	-0.21	0.17	14
Zn I	-0.08	-	-0.24	-	-0.04	-	-0.12	0.11	3
Sr I	+0.59	0.26	-	-	+0.59	0.22	+0.59	0.24	2
Y I	-	-	+0.67	0.14	+0.67	-	+0.67	0.14	3
Y II	+0.11	0.10	+0.03	0.08	-0.16	0.15	+0.01	0.13	15
Zr II	+0.01	0.18	+0.19	0.36	-0.01	0.11	+0.03	0.21	16
Ru I	-	-	+0.20	-	-	-	+0.20	-	1
La II	+0.24	0.06	+0.18	0.08	-0.07	0.25	+0.15	0.14	12
Ce II	-0.18	0.24	+0.06	0.16	+0.07	0.25	-0.02	0.25	20
Pr II	-	-	+0.29	0.28	+0.04	0.16	+0.17	0.22	4
Nd II	-	-	+0.09	0.25	+0.04	0.22	+0.07	0.24	26
Eu II	+0.02	0.09	+0.21	0.19	+0.18	0.35	+0.14	0.22	9
Gd II	+0.05	-	-0.13	-	-	-	-0.04	0.12	2

MAGNETIC FIELD OF POLARIS

I.A. Usenko¹, V.D. Bychkov², L.V. Bychkova², S.I. Plachinda³

¹ Department of Astronomy, Odessa National University

T.G. Shevchenko Park, Odessa 65014 Ukraine, *igus99@ukr.net*

² Special Astrophysical Observatory, Russian Academy of Sciences

Nizhnij Arkhyz, Karachaevo-Cherkessia, 369167 Russia *vbych@sao.ru*

³ Crimean Astrophysical Observatory, Nauchny, Crimea, 98409, Ukraine

ABSTRACT. 25 effective magnetic field (B_e) estimates of Polaris (α UMi) were obtained from July 1983 to December 2005 using 1m Zeiss and 6m BTA telescopes of SAO RAS, equipped by magnetometers. These data with added 7 ones from Borra et al. (1981), obtained in 1980 show that magnetizing force of Polaris vary from +162 to -109 Gauss do not depend on the changes of pulsational amplitude, but Fourier analysis reveal variability of magnetic field with period of 3.97586 days, close well with its pulsational period of 3.96961 days.

Key words: Stars.

1. Introduction

α UMi named Polaris is perhaps an unique Cepheid with measured magnetic field during its pulsational period (Borra et al., 1981). Since Polaris is an unique Cepheid itself due to its unusual pulsational activity (Ferne et al., 1993, Usenko et al., 2005), revealed in the increase and decrease of light and radial velocity pulsational amplitude, it would be interesting to observe its magnetic field behavior. Since Polaris is a multiple system with visual and spectroscopic main-sequence companions, therefore its unusual pulsational activity could be connected with its effect. Therefore we attempted during last a quarter of a century to observe for possible changes of its magnetic field.

2. Observations

Observations of these objects have been realized using:

1. 6m telescope BTA SAO RAS (Russia), - equipped by the main stellar magnetometer with Fabri-Perot standard, used Cr I 4254.33 line (Bychkov et al., 1988), and hydrogen magnetometer, used H_β hydrogen lines as an indicator of magnetic field (Shtol', 1991, Shtol', 1993).

2. 1m Zeiss telescope SAO RAS (Russia), - equipped by the circular polarization analyzer ACP before CEGS spectrometer used from 477 to 890 spectral lines (Bychkov et al., 2006, Bychkov, 2008).

In the Table 1 we represent the B_e data of Borra et al. (1981) attached to radial velocities data, obtained by Arellano Ferro (1983). In the Table 2 are the original unpublished data, obtained during 1983 - 1987, using 6m telescope SAO RAS. And in the Table 3, - the last data, obtained during 2005, using 1m Zeiss telescope SAO RAS.

3. Results and Discussion

So, we have obtained 25 B_e values and that with 7 ones from Borra et al. (1981) add up to 32 measurements. These B_e values vary from +162 to -109 Gauss, respectively. As seen from the measurements' results, the effective magnetic field of Polaris do not depend on the changes of pulsational amplitude, nevertheless, we have observed long-periodical changes of the mean value during one year. To search any periodicity on the magnetic field's variability, we have used the Fourier analysis technique (PERIOD 98 program, Sperl, 1998). Unfortunately, we have very small set of observational data, nevertheless the highest amplitude peak corresponds to period of 3.97586 days that agrees well with the pulsational one of 3.96961 days! Hence, magnetic field variability of Polaris connected only with its pulsational period and do not depend from the increasing and decreasing of pulsational amplitude.

References

- Arellano Ferro A: 1983, *ApJ*, **274**, 755
 Borra E.F., Fletcher J.M., Poeckert R.: 1981, *ApJ*, **247**, 569
 Brown C.F., Bochonko D.R.: 1994, *PASP*, **106**, 964
 Bychkov V.D., Gazhur E.B., Glagolevskij Yu., El'kin V.G., Nazarenko A.F., Naidenov I.D.,

Table 1: 1.2-m DAO (coude spectrograph) observations. The phase corresponds to the ephemeris of Brown & Bochonko (1994).

HJD 2440000+	B_e (Gauss)	σ (Gauss)	Phase*	RV ampl. (km s^{-1})	Remarks
4408.812	- 5.2	3.2	0.814	2.0 ± 1	July 1980
4442.829	- 7.0	4.2	0.383		Circular polarization
4444.837	+ 15.5	3.4	0.889		of 230 lines
4470.984	- 2.5	3.2	0.475	2.0 ± 1	August 1980
4471.744	- 3.5	4.8	0.667		ibid
4472.770	- 6.5	2.9	0.925		
4473.861	- 7.0	3.4	0.200		

Table 2: 6-m BTA, SAO RAS observations

HJD 2440000+	B_e (Gauss)	σ (Gauss)	Phase*	RV ampl. (km s^{-1})	Remarks
5545.390	+135	130	0.225	1.4 ± 0.3	July-August 1983
5546.355	- 56	64	0.468		Magnitometer 4254.33 Ca I line
5547.367	- 72	66	0.722		RV Kamper et al. (1984)
5929.483	- 34	36	0.983	3.0 ± 0.5	August 1984
5931.477	+104	70	0.486		RV Kamper (1996)
5932.519	- 48	76	0.748		
6633.337	- 29	36	0.295	1.5 ± 0.5	July 1986
6634.395	- 10	40	0.561		Hydrogen magnitometer H_β line
6635.412	+ 67	47	0.818		RV Kamper (1996)
6777.228	0	27	0.543	1.5 ± 0.5	December 1986
6780.283	- 55	26	0.313		Magnitometer 4254.33 Ca I line
6780.566	- 24	39	0.384		RV Kamper (1996)
7022.419	- 95	32	0.310	1.7 ± 0.4	August 1987
7023.183	- 28	62	0.503		RV Dinshaw et al. (1989)

Table 3: 1-m Zeiss SAO RAS observations

HJD 2450000+	B_e (Gauss)	σ (Gauss)	Phase*	RV ampl. (km s^{-1})	Remarks
3628.530	+ 34	40	0.490	2.4 ± 0.1	September 2005
3629.575	- 3	33	0.753		RV Usenko et al. (2008)
3632.584	+114	29	0.511		
3633.599	-109	52	0.767		
3636.598	+162	56	0.523		
3637.600	+ 14	29	0.775		
3638.499	- 88	97	0.002		
3665.606	- 9	24	0.831	2.4 ± 0.1	October 2005
3666.615	- 38	28	0.084		
3667.603	+ 44	30	0.333		
3692.644	- 19	20	0.642	2.4 ± 0.1	November 2005
3718.485	- 34	15	0.151		December 2005

- Romanyuk I.I., Chuntunov G.A., Shtol' V.D.: 1988, "Magnetic Stars", Leningrad, "Nauka", 12
- Bychkov V.D., Bychkova, L.V., Madej, J.: 2006, *MNRAS*, **365**, 585
- Bychkov V.D.: 2008, *Astroph. Bull.*, **63**, 83
- Dimshaw N., Matthews J.M., Walker G.A.H., Hill G.M.: 1989, *AJ*, **98**, 2249
- Fernie J.D., Kamper K.W., Seager S.: 1993, *ApJ*, **416**, 820
- Kamper K.W.: 1996, *JRAS Canada* **90**, 140
- Kamper K.W., Evans N.R., Lyons R.W.: 1984, *JRAS Canada*, **78**, 173
- Shtol' V.G.: 1991, *Bull. SAO RAS*, **33**, 143
- Shtol' V.G.: 1993, *Bull. SAO RAS*, **35**, 114
- Sperl M.: 1998, *PERIOD 98*, program
- Usenko I.A., Miroshnichemko A.S., Klochkova V.G. Yushkin M.V.: 2005, *MNRAS*, **362**, 1219
- Usenko I.A., Miroshnichemko A.S., Klochkova V.G. Panchuk V.E.: 2008, *OAP*, **21**, 127

NEW BINARY SYSTEMS WITH ASYMMETRIC LIGHT CURVES

N.A. Virnina

Department “High and Applied Mathematics”,
Odessa National Maritime University, Odessa, Ukraine, *virnina@gmail.com*

ABSTRACT. We present the results of investigation of the light curves of 27 newly discovered binary systems. Among the examined curves, there were 10 curves with statistically significant asymmetry of maximums, according the 3σ criterion for the difference between the maximal brightness. Half of these 10 curves have a higher first maximum, another half the second one. Two of these 10 curves, USNO-B1.0 1629-0064825 = VSX J052807.9+725606 and USNO-B1.0 1586-0116785, show the largest difference between magnitudes in maxima. The star VSX J052807.9+725606 also shows the secondary minimum, which is shifted from the phase $\varphi = 0.5$. The shape of the curve argues that the physical processes of this star could be close to that of well known short periodic binary system V361 Lyr, which has a spot on the surface of one star of the system. Another star, USNO-B1.0 1586-0116785, probably has a cold spot, or several spots, in the photosphere of one of the components.

Keywords: Variable stars: eclipsing, interacting binary, impactors

Introduction

Nowadays, using rather accurate CCD photometry, it is possible to detect fine features of the light curves. Weve noticed that among various shapes of the phase curves of close eclipsing binary systems the asymmetry shapes arent very unusual. Many authors points that there are binary systems with rather steady asymmetric curves, other noticed that the shape of the phase curve may change in different years. To make an investigation of this effect, we decided to determine the number of statistically significant asymmetric curves among those binary systems, which we discovered during 2009-2010. Weve examined all 27 phase curves of binary systems of different types, which were discovered and approved in this period. All observations were obtained using the remotely controlled telescopes of Tzec Maun observatory: -180 (D=180mm, F=1410mm) equipped with the

CCD camera SBIG STL-11000, the field of view was 87.5'x58.3', and FSQ-106 (D=106mm, F=527mm) equipped with the same CCD camera, the field of view was 233.8'x155.9'.

Statistical modeling

For the examined 27 binary systems all parameters needed for the General Catalog of Variable Stars (GCVS) were determined using the FDCN software (Andronov, 1994, 2003). This program computes the coefficients of the statistically optimal smoothing trigonometric polynomials using the least squares method routine and differential corrections for the period, which allowed determine all photometric parameters with corresponding errors. Some of these stars we already registered in the VSX catalog Variable Stars IndeX, operated by AAVSO. The information about the USNO-B.1 numbers of the stars, their coordinates, VSX numbers and types are given in the Table 1.

The information about the periods, magnitudes of maxima and minima was summarized in the Table 2. According to the 3σ criterion, the values which are marked in bold type correspond to the stars with statistically asymmetric curves.

Statistically significant asymmetry

From the Table 1 weve noticed that among the examined 27 light curves, there were 10 curves with statistically significant asymmetry of maxima. This means that more than 1/3 of our binary systems has asymmetric phase curves. We introduced two parameters. The first is the difference between magnitudes in maxima: $\Delta_{\max} = \text{Max}_{\text{II}} - \text{Max}_{\text{I}}$.

The second is the difference between the magnitudes in the primary minimum and in the secondary maximum: $A = \text{min}_{\text{I}} - \text{Max}_{\text{II}}$. Both these parameters are also given in the Table 2.

We looked for the different statistical dependences: 1. between Δ_{\max} and Δ_{\max}/A . The corresponding diagram is shown on the Fig. 1;

Table 1. Identifications and co-ordinates (2000.0) of new variable stars

No	USNO-B1.0	RA	DEC	VSX	Type
1	USNO-B1.0 0746-0450359	17 ^h 44 ^m 43. ^s 452	-15°20'14.12"	VSX J174443.4-152014	Ell:
2	USNO-B1.0 0746-0452118	17 ^h 45 ^m 09. ^s 615	-15°23'29.54"	VSX J174509.6-152329	EW
3	USNO-B1.0 1624-0096365	11 ^h 37 ^m 27. ^s 240	+72°24'03.43"	VSX J113727.2+722403	EW
4	USNO-B1.0 1611-0091801	11 ^h 48 ^m 36. ^s 524	+71°07'51.14"	VSX J114836.5+710751	EW
5	USNO-B1.0 1630-0091892	11 ^h 55 ^m 58. ^s 219	+73°00'25.33"	VSX J115558.2+730025	EW
6	USNO-B1.0 1611-0091333	11 ^h 40 ^m 30. ^s 022	+71°11'02.44"	VSX J114030.0+711102	EW
7	USNO-B1.0 1615-0092898	12 ^h 06 ^m 41. ^s 287	+71°32'46.93"	VSX J120641.2+713246	EW
8	USNO-B1.0 1229-0276915	14 ^h 13 ^m 40. ^s 556	+32°56'48.16"	VSX J141340.5+325648	EW
9	USNO-B1.0 1238-0228470	14 ^h 15 ^m 09. ^s 282	+33°52'22.12"	VSX J141509.2+335222	EB
10	USNO-B1.0 1017-0168554	08 ^h 53 ^m 48. ^s 933	+11°43'53.64"	VSX J085348.9+114353	EW
11	USNO-B1.0 1015-0165372	08 ^h 54 ^m 38. ^s 967	+11°33'00.23"	VSX J085438.9+113300	EW
12	USNO-B1.0 1629-0064825	05 ^h 28 ^m 07. ^s 975	+72°56'06.05"	VSX J052807.9+725606	E
13	USNO-B1.0 1634-0053325	05 ^h 33 ^m 00. ^s 072	+73°27'26.52"		EW
14	USNO-B1.0 1633-0056300	05 ^h 28 ^m 25. ^s 539	+73°21'14.57"		EW
15	USNO-B1.0 1635-0051301	05 ^h 35 ^m 14. ^s 565	+73°31'24.19"		EW
16	USNO-B1.0 1628-0064829	05 ^h 30 ^m 44. ^s 331	+72°51'13.67"		EA
17	USNO-B1.0 1624-0065083	05 ^h 25 ^m 43. ^s 672	+72°28'40.10"		EA
18	USNO-B1.0 1636-0050887	05 ^h 34 ^m 44. ^s 439	+73°40'06.37"		Ell
19	USNO-B1.0 1167-0308859	17 ^h 39 ^m 14. ^s 053	+26°42'43.19"		EW
20	USNO-B1.0 1165-0287124	17 ^h 38 ^m 22. ^s 563	+26°33'04.40"		E
21	USNO-B1.0 1165-0287544	17 ^h 39 ^m 14. ^s 265	+26°32'02.09"		EW
22	USNO-B1.0 1160-0265767	17 ^h 37 ^m 23. ^s 199	+26°02'51.73"		EA
23	USNO-B1.0 1161-0280071	17 ^h 39 ^m 52. ^s 694	+26°10'20.02"		EW
24	USNO-B1.0 1159-0264420	17 ^h 38 ^m 51. ^s 239	+25°57'46.69"		EB
25	USNO-B1.0 1164-0290487	17 ^h 38 ^m 59. ^s 968	+26°28'28.94"		EW
26	USNO-B1.0 1165-0287332	17 ^h 38 ^m 48. ^s 917	+26°34'37.20"		EW
27	USNO-B1.0 1586-0116785	11 ^h 28 ^m 25. ^s 293	+68°37'17.46"		EB

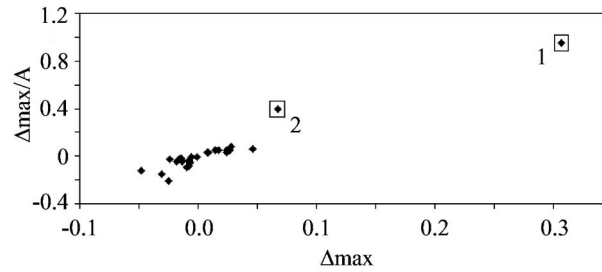
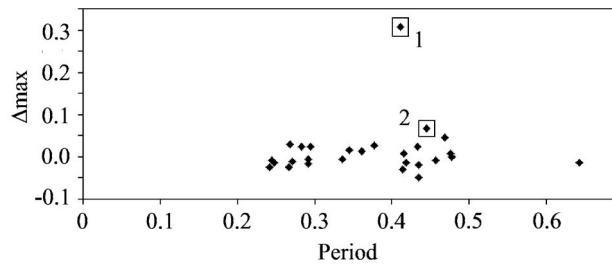
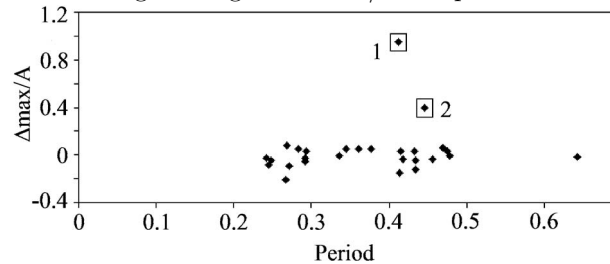
Fig.1. Diagram Δ_{\max}/A vs. Δ_{\max} .Fig.2. Diagram Δ_{\max}/A vs. periodFig.3. Diagram Δ_{\max} vs. period.

Table 2. Characteristics of new variable stars: number (as in Table 1), type, period P , initial epoch T_0 , brightness at maxima and minima (photometric system "clear R"), difference between the maxima $\Delta_{\max} = \max_{\text{II}} - \max_{\text{I}}$ and its ratio to the corresponding error estimate σ and amplitude A defined as $(\min_{\text{I}} - \max_{\text{II}})$.

No	Type	Period P	Initial epoch T_0	Max _I (CR)	Max _{II} (CR)	min _I (CR)	min _{II} (CR)	Δ_{\max}	$\frac{\Delta_{\max}}{\sigma}$	A	$\frac{\Delta_{\max}}{A}$
1	EII:	0.270841±0.000020	2454945.1622±0.0032	12.870±0.003	12.860±0.004	12.964±0.004	12.959±0.004	-0.010±0.005	2.000	0.104±0.006	-0.0962
2	EW	0.417856±0.000025	2454945.8432±0.0014	14.814±0.011	14.801±0.005	15.136±0.007	15.128±0.010	-0.013±0.012	1.083	0.335±0.009	-0.0388
3	EW	0.413660±0.000013	2455192.8152±0.0012	13.489±0.002	13.458±0.003	13.664±0.004	17.639±0.002	-0.031±0.004	7.750	0.206±0.005	-0.1505
4	EW	0.376831±0.000006	2455191.7896±0.0005	14.359±0.005	14.386±0.005	14.932±0.007	14.860±0.004	0.027±0.007	3.857	0.546±0.009	0.0495
5	EW	0.294039±0.000004	2455191.4051±0.0003	14.829±0.008	14.853±0.009	15.638±0.009	15.552±0.008	0.024±0.012	2.000	0.785±0.013	0.0306
6	EW	0.434912±0.000009	2455192.4772±0.0005	13.628±0.003	13.610±0.003	13.977±0.003	13.963±0.005	-0.018±0.004	4.500	0.367±0.004	-0.0490
7	EW	0.475366±0.000012	2455192.6380±0.0005	13.128±0.002	13.137±0.006	13.457±0.002	13.404±0.003	0.009±0.006	1.500	0.320±0.006	0.0281
8	EW	0.469085±0.000044	2455268.8822±0.0011	16.821±0.026	16.867±0.023	17.593±0.018	17.494±0.022	0.046±0.037	1.243	0.726±0.029	0.0634
9	EB	0.478130±0.000040	2455268.5270±0.0007	12.834±0.003	12.833±0.002	13.080±0.003	12.916±0.002	-0.001±0.003	0.333	0.247±0.004	-0.0040
10	EW	0.268768±0.000026	2455233.4364±0.0011	16.006±0.011	16.034±0.014	16.376±0.014	16.296±0.014	0.028±0.018	1.556	0.342±0.020	0.0819
11	EW	0.434548±0.000018	2455233.6290±0.0006	14.182±0.003	14.134±0.007	14.542±0.004	14.398±0.004	-0.048±0.007	6.857	0.408±0.008	-0.1176
12	E	0.411670±0.000054	2455261.8510±0.0015	15.920±0.010	16.227±0.016	16.550±0.016	16.341±0.011	0.307±0.019	16.158	0.323±0.023	0.9505
13	EW	0.345439±0.000049	2455262.1281±0.0011	15.884±0.009	15.901±0.009	16.226±0.008	16.181±0.010	0.017±0.013	1.308	0.325±0.012	0.0523
14	EW	0.415351±0.000024	2455261.9148±0.0006	14.545±0.005	14.553±0.003	14.798±0.003	14.796±0.003	0.008±0.005	1.600	0.245±0.004	0.0327
15	EW	0.456908±0.000028	2455261.8903±0.0010	14.523±0.004	14.515±0.004	14.761±0.003	14.756±0.004	-0.008±0.006	1.333	0.246±0.005	-0.0325
16	EA	0.336481±0.000020	2455261.9982±0.0005	15.318±0.006	15.312±0.005	15.918±0.007	15.798±0.007	-0.006±0.008	0.750	0.606±0.009	-0.0099
17	EA	0.642197±0.000012	2455261.1514±0.0014	15.732±0.026	15.718±0.032	16.401±0.016	16.385±0.016	-0.014±0.041	0.341	0.683±0.036	-0.0205
18	EII	0.292492±0.000019	2455261.8475±0.0005	14.120±0.002	14.113±0.002	14.246±0.002	14.240±0.002	-0.007±0.003	2.333	0.133±0.003	-0.0526
19	EW	0.245108±0.000006	2455312.3737±0.0006	15.614±0.004	15.606±0.002	15.700±0.003	15.682±0.003	-0.008±0.004	2.000	0.094±0.004	-0.0851
20	E	0.266685±0.000006	2455311.0962±0.0012	15.073±0.001	15.048±0.002	15.169±0.001	15.126±0.002	-0.025±0.002	12.500	0.121±0.002	-0.2066
21	EW	0.248007±0.000005	2455312.6068±0.0009	16.840±0.006	16.827±0.006	17.105±0.006	17.092±0.005	-0.013±0.008	1.625	0.278±0.008	-0.0468
22	EA	0.433131±0.000008	2455312.7456±0.0004	15.753±0.021	15.777±0.019	16.556±0.022	16.186±0.025	0.024±0.028	0.857	0.779±0.029	0.0308
23	EW	0.292380±0.000003	2455312.4524±0.0003	16.667±0.006	16.651±0.003	17.195±0.005	17.168±0.005	-0.016±0.007	2.286	0.544±0.006	-0.0294
24	EB	0.282757±0.000003	2455312.3299±0.0002	15.143±0.003	15.167±0.004	15.666±0.004	15.363±0.004	0.024±0.005	4.800	0.499±0.006	0.0481
25	EW	0.241996±0.000001	2455312.3475±0.0001	14.825±0.004	14.801±0.004	15.631±0.005	15.525±0.004	-0.024±0.006	4.000	0.830±0.006	-0.0289
26	EW	0.361080±0.000002	2455312.3549±0.0002	13.035±0.002	13.049±0.002	13.314±0.001	13.300±0.001	0.014±0.003	4.667	0.265±0.002	0.0528
27	EB	0.445393±0.000016	2455278.1853±0.0012	13.557±0.004	13.624±0.005	13.795±0.004	13.795±0.004	0.067±0.006	11.167	0.171±0.006	0.3918

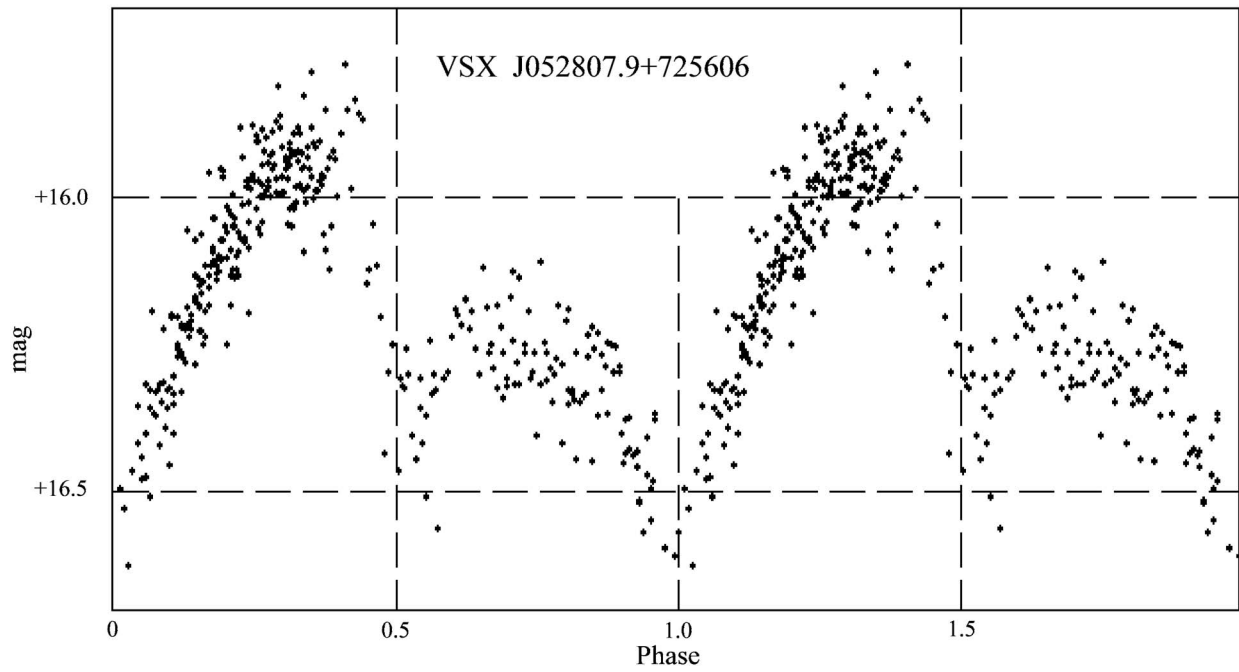


Fig.4. The phase curve of the star VSX J052807.9+725606.

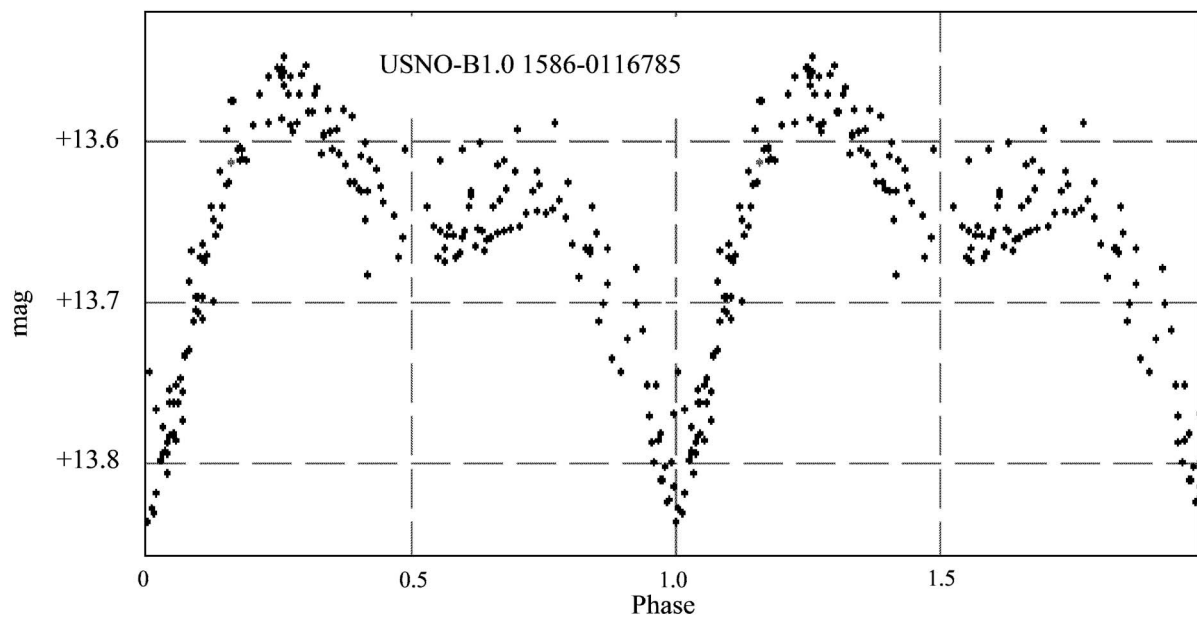


Fig.5. The phase curve of the star USNO-B1.0 1586-0116785.

2. between Δ_{\max}/A and the value of the period (Fig.2);
3. between Δ_{\max} and the value of the period (Fig.3).

We found no statistical dependence between the period and Δ_{\max}/A or Δ_{\max} . But there are 2 points, which are separated from the “main cloud”, they are marked by squares on the plots. The point No.1 corresponds to the star No 12 in the Tables 1 and 2, USNO-B1.0 1629-0064825 = VSX J052807.9+725606. The point No. 2 corresponds to the star No. 27, USNO-B1.0 1586-0116785.

The most unusual curves

Two stars, which marked on the Fig 1-3 exhibits the largest difference between magnitudes in maxima. The phase curve is shown on the Figure 4. The first of them, No.1 = VSX J052807.9+725606, is very similar to the well known binary system V361 Lyr. Both of these stars exhibit a huge difference in maxima, the first maximum is brighter than the second one. Besides, in both cases the phase of the first maximum is not 0.25, but 0.30, and the phase of the secondary minimum is not 0.50, but 0.52 for V361 Lyr and 0.54 for VSX J052807.9+725606. According to the classical model of V361 Lyr, the cause of this asymmetry is a presence of a hot spot in the photosphere of the first component. The accretion matter streams through the inner Lagrangian point from the second component to the first one, however it doesn't form the accretion disk, but, deviated by the Coriolis force from the line of centres, impacts into the photosphere of the accretor with a shift towards the orbital motion. The shock appears, which heats the surrounding plasma, and a hot spot is formed in the atmosphere. We assume that the same mechanism is present in VSX J052807.9+725606. The more detailed investigation of this star had been described in the paper “A New Binary System with an Unusual Asymmetric Light Curve” (Virnina and Andronov, 2010).

Another interesting binary system, which was marked by No. 2 (No. 27 in the Tables) shows rather big asymmetry too, but doesn't exhibit a confident shift of the secondary minimum. The phase curve of this star is shown on the Figure 5.

Taking into account the shape of the phase curve, we may assume the presence of a cool spot on one of the stars, which is visible near the phase of the second maximum. This version of the asymmetry could be confirmed during the further observations.

Conclusions

We've analyzed 27 newly discovered binary systems. Ten of them have the curves with statistically significant asymmetry of maximums, which means that more than 1/3 of the stars investigated in this paper have asymmetrical curves. One of the most probable solutions for these stars is the presence of a cold or a hot spot (or group of spots) in the photosphere of one or even both of the components. The question of stability of these spots could be solved due to further multicolor photometrical and spectroscopic observations.

Acknowledgments. This work is based on data collected with the Tzec Maun Observatory, operated by the Tzec Maun Foundation. The author is grateful to Ron Wodaski (director of the observatory) and Donna Brown-Wodaski (director of the Tzec Maun Foundation).

Also the author is thankful to Prof. Ivan L. Andronov for helpful discussions.

References

- Andronov I.L.: 1994, *OAP*, **7**, 49
 Andronov I.L.: 2003, *ASPC*, **292**, 391
 Andronov I.L., Richter G.A.: 1987, *AN*, **308**, 235
 Samus N.N. et al.: 2010, *General Catalog of Variable Stars*, <http://www.sai.msu.su/groups/cluster/gcvs/>
 van Rensbergen W., De Greve J.P., De Loore C., Mennekens N., 2008, *A&A*, **487**, 1129
 Virnina N.A., Andronov I. L.: 2010, *O&A*, **127**, 1
 VSX, <http://vsx.aavso.org/>
 Zhang X.B., Zhang R.X., Fang M.J., 2002, *A&A*, **395**, 587

PERIOD VARIATIONS IN THE CLOSE BINARY BM UMa

N.A. Virnina¹, E.A. Panko^{2,3,4}, O.G. Sergienko³,
B.A. Murnikov², E.G. Gubin², A.V. Klabukova², A.I. Movchan²

¹ Department "High and Applied Mathematics",
Odessa National Maritime University, Odessa, Ukraine, *virnina@gmail.com*

² Astronomical observatory, Odessa National University,
Odessa, Ukraine, *panko.elena@gmail.com*

³ Astronomical Observatory, Nikolaev National University, Nikolaev, Ukraine

⁴ Visiting Astronomer, Department of Astronomy, Saint Mary's University,
Halifax, Nova Scotia, Canada

ABSTRACT. We present the results of analysing of the light curve and O–C variations in the eclipsing system BM UMa, based on *V*-band observations which cover the period from JD 2454933 to 2454961 using two robotic remotely-controlled telescopes of Tzec Maun Observatory (USA) along with observations made with the RK-600 telescope of Odessa Astronomical Observatory. The full light curve displays a total primary eclipse with a duration 0.06 of the period, or 24 minutes, and a partial secondary eclipse, with both maxima of equal magnitude.

For our observations, we determined the statistically optimal values of the initial epoch of $T_0 = 2454944.2814 \pm 0.0001$ and orbital period of $P = 0.^d271226 \pm 0.000002$. The depths of primary and secondary minima are nearly equal, $0.^m838 \pm 0.006$ and $0.^m748 \pm 0.006$, respectively. The physical parameters of the system were calculated using the Wilson-Devinney code, appended with the Monte Carlo search algorithm. The result establishes BM UMa as a contact system (fillout factor 10.7%) with parameters: mass ratio 0.538 ± 0.001 , inclination $86.^{\circ}815 \pm 0.005$, and temperatures of components 4700 ± 20 K and 4510 ± 10 K. The more massive component is larger and cooler. The 72 archival and 11 newly-obtained times of light minimum cover the interval 1961-2010 and allowed us to exclude possible systematic period variations in BM UMa and to determine an initial epoch of HJD 2447927.382 and orbital period of $P = 0.^d2712209 \pm 0.0000006$.

Key words: Stars: eclipsing variables: period variations; stars: individual: BM UMa.

1. Introduction

The eclipsing variable BM UMa ($\alpha_{2000} = 11^h11^m20^s48$, $\delta_{2000} = +46^{\circ}25'47''.3$, type EW/KW,

$V_{\max} = 14.^m39$, $\Delta V_I = 0.^m9$) was selected for investigation by us as a star exhibiting period variations, but being poorly studied previously. A search of the literature on BM UMa by Kreiner et al. (2000) revealed 34 times of light minimum for the system, 14 primary minima and 20 secondary minima, covering the interval from 1961 to 1998. New observations of the system were therefore initiated to augment the available data, the major portion of our new observations being in the visual *V*-band. An *O* – *C* diagram for the system was constrained using the ephemeris:

$$\text{JDh}_{\min I} = 2444292.3413 + 0.2712222E$$

The variable BM UMa was discovered by Hoffmeister (1963), with Busch et al. (1966) originally classifying it as an "RRc" star due to a small difference between the depths of primary and secondary minima. Shugarov (1975) subsequently reclassified BM UMa as a W UMa variable and calculated a period of $0.^d27123$. Hoffman (1981) later analyzed *B* and *V* light curves for BM UMa obtained from photoelectric observations of the star over the course of one night. He determined two times of minimum light and derived the following elements:

$$\text{HJD}_{\min I} = 2437348.558 + 0.2712207E$$

That ephemeris was selected by Kreiner et al. (2000) as a standard formula for BM UMa, and O–C values linked to it allow one to examine both parabolic and periodic approximations for period variations in the system. From that ephemeris and the 32 times of light minima cited previously, Samec et al. (1995) derived parabolic variations for BM UMa based upon a linear ephemeris of:

$$\text{HJD}_{\min I} = 2444292.3496(8) + 0.27122009E$$

They used *VRI* photometry obtained over the course of one night for a detailed study of BM UMa and found

Table 1. The comparison stars

Star	$\alpha_{2000.0}$	$\delta_{2000.0}$	V
1	168°.00166	+46°.37723	12 ^m .486
2	167°.74274	+46°.30769	12 ^m .020
3	167°.83080	+46°.30388	12 ^m .905

a period decrease of $\sim 5 \times 10^{-8} \text{ d yr}^{-1}$ attributed to angular momentum loss arising from stellar winds. They also classified BM UMa as a W UMa-type system according to its *VRI* light curves, compared their data with synthetic light curves, and found that BM UMa is a contact binary consisting of two, early K-type components with a fillout factor of 20%, a temperature difference of 400 K, and a mass ratio of 0.5.

Our observations of BM UMa, obtained 18 years later, allow us to analyze the $O - C$ offsets for the system over a longer interval of time and with a resulting better accuracy.

2. Observations

New CCD observations of BM UMa were obtained by N.A.V. in April 2009 between JD 2454933 and 2454961 using two robotic remotely-controlled telescopes at the Tzec Maun Observatory (USA). The first telescope was a AP-206 astrophysical refractor ($F = 1620 \text{ mm}$), equipped with a SBIG STL-6K CCD camera. The second telescope was a 14" Maksutov-Newtonian ($F = 1410 \text{ mm}$), equipped with the same CCD camera. A standard Bessell *V*-filter was used for the observations, with 100 s exposures in both cases. These observations are published separately (Virnina, 2010).

Another set of observations was obtained on JD 2454939 using the Odessa Astronomical Observatory's RK-600 telescope ($D = 600 \text{ mm}$, $F = 4780 \text{ mm}$) located at the Observatory's Mayaki station. Integration times of 20 seconds were used in 5-frame series. A total of 815 *V*-magnitude estimates covering the full light curve of BM UMa were obtained with the robotic telescopes, and 207 *V*-magnitude estimates, including coverage of primary minimum, were obtained from Mayaki.

The reduction of the data was made in standard fashion including dark frame and flat field corrections. Original Julian dates for the observations were corrected to the barycenter of the Solar system.

The TASS Mark IV photometric catalog (Droege et al. 2006) was used to search for suitable comparison stars in the field. They are shown on Fig. 1 with coordinates and *V* magnitudes given in Table 1. The stars were used as reference objects for both series of observations. Individual minima timings obtained from the new observations are listed in Table 2. The Heliocentric Julian Dates (HJD) for the minima are listed

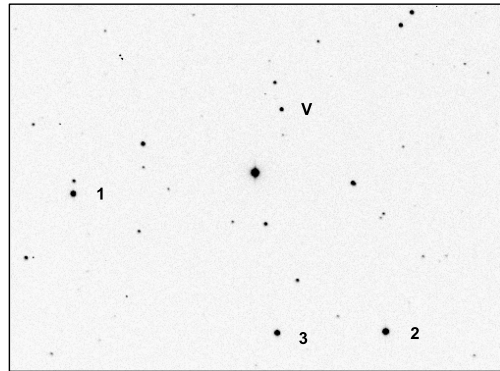


Figure 1: The finding chart ($18' \times 13'$) for BM UMa. Comparison stars are marked as 1, 2 and 3, and BM UMa as V.

in the first column, standard deviations for each value (σ), type of minimum, and observer are listed in the next columns. Observed, smoothed and synthetic light curves of BM UMa are shown in Fig. 2.

We determined the magnitudes in minima and in maximum, orbital period and initial epoch, using the program FDCN (Andronov, 1994, 2003): $min_I = 14.878 \pm 0.004$, $min_{II} = 14.788 \pm 0.004$, $Max = 14.040 \pm 0.005$, $P = 0^m271226(\pm 0.000002)$, $T_0 = 2454944.2814 \pm 0.0001$. The statistically optimal degree of the trigonometric polynomial fit is $s = 8$. The depths of primary and secondary minimum are nearly equal, $0^m838 \pm 0.006$ and $0^m748 \pm 0.006$ respectively. The differences in the shapes of primary and secondary minima allow us to infer that the primary eclipse is total, whereas the secondary eclipse is partial. The duration of totality is about 0.06 of the orbital period, or 24 minutes. That result agrees with the conclusions of Samec et al. (1995), where the possibility of total eclipses was noted. However, the same authors noted the possibility of a marginal O'Connell effect in BM UMa, which we do not observe: both light maxima are of identical magnitude.

3. Modeling

In order to obtain the physical parameters of BM UMa we used the Wilson-Devinney code (WD) (Wilson & Devinney 1973; Wilson 1979, 1993) appended with the Monte Carlo search algorithm. The procedure has been described in details by Kreiner, Rucinski, Zola et al. (2003) in the paper "Physical parameters of components in close binary systems. I". From the 2MASS photometric catalog (Skrutskie et al., 2006), we determined the color indexes: $J - H = 0^m501$, $H - K = 0^m119$, $J - K = 0^m62$, which confirms that the system belongs to the spectral class K. These

color indexes corresponds to the spectral class K3 and temperature 4700 ± 20 K. Thus, we fixed this parameter as a temperature of the hotter component. We used the gravity coefficient of 0.32 and reflection coefficient of 0.50 for both stars. Unfortunately there are no spectroscopic observations of BM UMa, and we can't evaluate the radial velocities and the mass ratio. Thus, all other parameters were adjusted. The statistically optimal solution corresponds to the following parameters: the inclination $i = 86.815 \pm 0.005$, the mass ratio $q = 0.538 \pm 0.001$, and the temperature of the secondary component $T_2 = 4510 \pm 10$ K. For contact binary systems, the potentials of the the atmospheres of stars are equal, in our case, $\Omega = 4.9861 \pm 0.0009$. This corresponds to the overflowing factor $f = (\Omega - \Omega(L_1))/(\Omega(L_2) - \Omega(L_1)) = 0.107$, where $\Omega(L_1)$ and $\Omega(L_2)$ are potentials at the inner (L_1) and outer (L_2) Lagrangian points.

The synthetic light curve is shown in the Fig. 2.

The geometry of the system with calculated parameters had been visualized using the software "Binary Maker - 3" (Bradstreet and Steelman, 2004, Bradstreet, 2005) and is shown on the Fig. 3.

4. $O - C$ Variations

We analyzed the $O - C$ variations in BM UMa using the 65 archival values in combination with the 11 newly-derived values in Table 2. 6 additional data (Busch et al., 1968) were used with correction according to Samec et al., 1995. We also checked all existing ephemerides, and found statistically significant linear trends with time, which implies the need for a small correction in the adopted orbital period of the system. Our best fit based on all 76 tabulated times of light minimum is:

$$\text{HJD}_{\text{minI}} = 2447927.382 + 0.2712209 \cdot E$$

with an error estimate of the period value of $\sigma = 5.7 \cdot 10^{-7}$. The ephemeris exhibits no linear or quadratic tendencies in the $O - C$ variations (see Fig. 3). Even corrected by Samec et al. (1995), the times of minima don't show systematic shifts in the $O - C$ values (see Fig. 4). So, we can not confirm quadratic term found by Samec et al. (1995).

5. Conclusions

BM UMa is found to be a contact binary system with a mass ratio of ~ 0.54 , an orbital inclination of 86.815 , effective temperatures of 4700 K and 4510 K for the primary and secondary, respectively, and a fill-out factor of 10.7%. The smaller component is the hotter star. The duration of totality during primary eclipse is about 0.06 of the period, or 24 minutes, and secondary

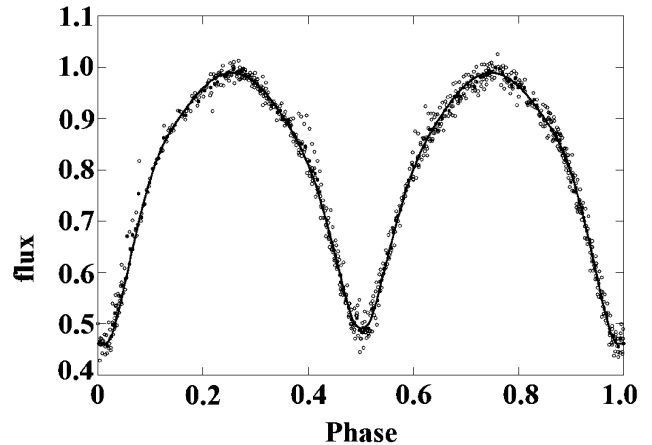


Figure 2: Observed (grey circles), smoothed (black circles) and synthetic (line) phase curves of BM UMa are shown in relative flux. The error estimates in the observed data are smaller than the symbol size.

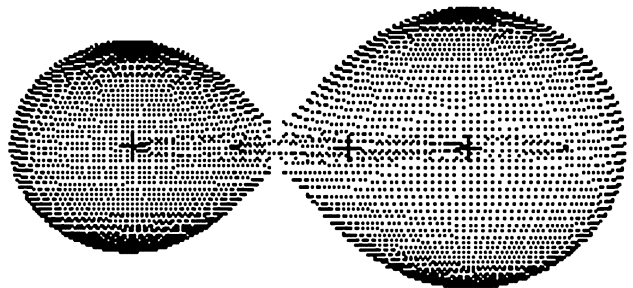


Figure 3: Visualization of the geometrical model of the system BM UMa using the "Binary Maker -3". Points at the common envelope of the system are shown in grey, the plus signs correspond to the centers of masses of each component and of the system, dashed lines show projections of the trajectories of the centers of components onto the celestial sphere (scaled to the dimensions of stars).

minimum corresponds to a partial eclipse. The absence of statistically significant non-linear $O - C$ trends appears to exclude the possibility of extensive mass loss or transfer. We also do not confirm the presence of spots on the components.

Given the low accuracy in the determination of times of minima from visual observations, we are not able to convincingly exclude the possibility of systematic period changes in BM UMa. The system is in need of future patrol observations for times of light minimum in order to examine that possibility with greater precision.

Acknowledgements. This research has made use of NASA's Astrophysics Data System and the "Variable

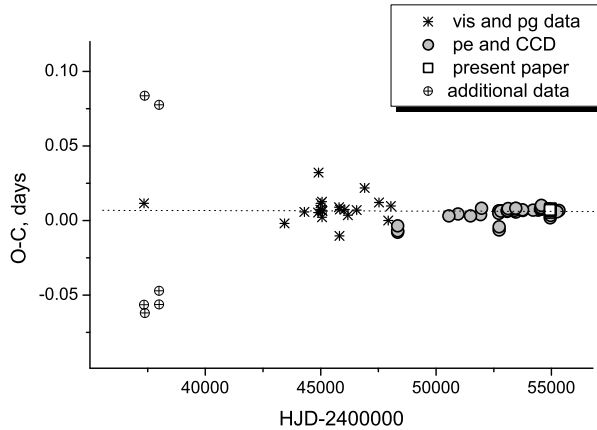


Figure 4: $O-C$ dependence for the full data set. Visual and photographic observations are shown as crosses, CCD and photoelectric as circles, and our data are represented as squares.

Star and Exoplanet Section of the Czech Astronomical Society” database. This work is based on data collected with the Tzec Maun Observatory, operated by the Tzec Maun Foundation. The authors are grateful to Ron Wodaski (director of the observatory) and Donna Brown-Wodaski (director of the Tzec Maun Foundation). This publication makes use of data products from the Two Micron All Sky Survey, which is a joint project of the University of Massachusetts and the Infrared Processing and Analysis Center/California Institute of Technology, funded by the National Aeronautics and Space Administration and the National Science Foundation.

EP thanks Saint Mary’s University for hospitality during her stays in Halifax.

NV thanks Staszek Zola for hospitality during her stay in the Astronomical Observatory of the Jagiellonian University.

The authors are thankful to Ivan L. Andronov for fruitful discussions.

Table 2. New minima of BM UMa

HJD	σ	Min.	Observer
2454933.973337	0.000280	I	Virnina
2454934.785961	0.000212	I	Virnina
2454939.669899	0.000081	I	Virnina
2454941.703916	0.000198	II	Virnina
2454955.671458	0.000215	I	Virnina
2454955.807005	0.000344	II	Virnina
2454958.791469	0.000337	II	Virnina
2454959.876600	0.000479	II	Virnina
2454960.824650	0.000615	I	Virnina
2454961.775360	0.000242	II	Virnina
2454939.669810	0.000237	I	Klabukova & Sergienko

References

- Andronov I.L.: 1994, *OAP*, **7**, 49
 Andronov I.L.: 2003, *ASPC*, **292**, 391
 Bessel M. S.: 1988, *PASP*, **100**, 1134
 Bradstreet D.H.: 2005, *SASS*, **24**, 23
 Bradstreet D.H., Steelman D.P.: 2004, *Binary Maker 3 Light Curve Synthesis Program*, (Contact Software, Norristown, Pennsylvania)
 Busch H., Haussler K., Lochel K., Memunger L., Wenzel W., Ziegler E.: 1966, *MVS*, **4(2)**, 19
 Droegge T.F., Richmond M.W., Sallman M.P., Creager R.P.: 2006, *PASP*, **118**, 1666
 Harmanec P.: 1988, *BAICz*, **39**, 6
 Hoffmann M.: 1981, *IBVS*, **1934**, 1
 Hoffmeister C.: 1963, *AN*, **287**, 169
 Kreiner J.M., Kim Ch.-H., Nha I.-S.: 2000, *An Atlas of O-C Diagrams of Eclipsing Binary Stars*, (Krakow, Poland)
 Kreiner J.M., Rucinski S., Zola S. et al.: 2003, *A&A*, **412**, 465
 Samec R.G., Gray J.D., Carrigan B.J., Kreidl T.J.: 1995, *PASP*, **107**, 136
 Skrutskie M.F. et al.: 2006, *AJ*, **131**, 1163
 Shugarov S.: 1975, *AZh*, **88**, 7
 Virnina N.A.: 2010, *VSNET-obs*, **69159**, <http://ooruri.kuastro.kyoto-u.ac.jp/mailarchive/vsnet-obs/69159>

SEARCH FOR SPECTROSCOPIC FAMILIES AMONG DIFFUSE INTERSTELLAR BANDS

B. Wszolek¹, A. Kuźmicz²

¹ Jan Długosz University, Institute of Physics, Częstochowa, Poland, *bogdan@ajd.czyst.pl*

² Jagiellonian University Astronomical Observatory, Kraków, Poland, *cygnus@oa.uj.edu.pl*

ABSTRACT. Diffuse interstellar bands (DIBs) await an explanation for many decades. One expects that significant progress in identification of DIBs' carriers will be possible when all the known DIBs are divided into families in such a way that only one carrier is responsible for all bands belonging to the given family. Analysing high resolution optical spectra of reddened stars we test a new method to find out the first true spectroscopic families among DIBs.

Keywords: Interstellar medium.

1. Introduction

One of the longest standing problems in astronomy and astrochemistry has been the inability to identify the diffuse interstellar band (DIB) carriers. It is debated whether the DIB carriers arise from the dust, the gas, or the large-molecule component of the interstellar medium (Sarre 2006, Herbig 1995). Furthermore, different strength ratios of major DIBs along different lines of sight, revealed a DIB origin in many carriers.

Any attempt to solve the mystery of DIBs' carriers must involve interdisciplinary collaboration between molecular physicists, chemists and astronomers. One expects that progress in this field will be possible when all known DIBs are divided into families in such a way that only one carrier is responsible for all bands belonging to a given family. The first trial on dividing DIBs into spectroscopic families were presented by Wszolek & Godłowski (2003). The authors noted that formal statistical attitude to DIBs' intensities measurements, without any additional supporting methods, is not sufficient to find out spectroscopic families. They proposed also some alternative methods as more adequate to the problem.

Among all known DIBs we can see only few relatively strong bands and many rather weak ones. With better quality spectra one can expect to find more weak DIBs. It is very probable that DIBs originated by the same carrier have different intensities; in one spectroscopic family we expect to find stronger bands as well as weak (and extremely weak) ones. Discovering new very weak DIBs may be therefore crucial when

we want to find complete spectroscopic families among DIBs. Extracting spectroscopic families of DIBs is a task to solve with use of astronomical spectra of the best quality. After extracting any spectroscopic family, its carrier will be to find by the way of laboratory search supported by quantum chemical considerations.

2. Looking for spectroscopic families - new method

We test a new method of extracting spectroscopic families of DIBs. This method may be summarized as follows:

1. We measure equivalent widths (EWs) of all accessible DIBs in the spectra of two different target stars. These stars should be slightly reddened and they should be sufficiently far away one from the other on the sky, to have slightly different chemistry in the corresponding interstellar clouds; this will enable to minimize the so called "noisy correlation" (see Wszolek & Godłowski 2003). We get series of measurements:

$EW_1^1, EW_2^1, EW_3^1, \dots, EW_n^1$
(for the first star, n - number of measured DIBs)

$EW_1^2, EW_2^2, EW_3^2, \dots, EW_n^2$
(for the second star)

2. We count the ratios of kind: $R_i = EW_i^1/EW_i^2$, (where $i = 1, \dots, n$) and we draw the diagram with R_i on vertical axis and i on horizontal one.

3. We look on the diagram for elongated (in horizontal direction) concentrations of points with almost constant R . If the commonly used assumption that intensity ratio for two DIBs originated by the same carrier should be constant (independently on direction to the target star) is valid, all points in such line-shaped concentration on diagram should correspond to DIBs

Table 1: The details concerning observed stars. In rows HD number is followed by spectral type, magnitude, reddening, air mass and the date of observation. First two items are for comparison stars.

HD	Sp	m(v)	E(B-V)	air mass	date
35497	B7 III	1.68	0.00	1.08	13.03.2010
120315	B3 V	1.85	0.02	1.02	23.06.2010
23180	B1 III/B3 V	3.82	0.3	1.25	12.03.2009
				1.7	13.03.2010
24760	B0.5 V/A2 V	2.9/3.9	0.1	1.27	13.03.2010
149757	O9 V	2.56	0.29	1.7	23.06.2010
184915	B0.5 III	4.96	0.22	1.9	23.06.2010
210839	O6 I	5.04	0.54	1.1	23.06.2010

belonging to the same spectroscopic family. Searching one diagram we may expect to find many spectroscopic families (different R).

EW ratios defined above will have much smaller errors than the ratios of type $r_{k,i}^m = EW_k^m / EW_i^m$ ($m = 1, \dots, n$), which were of common use before, since they avoid dividing very big numbers (for strong DIBs) over very small numbers (for weak DIBs). Furthermore, our method needs in principle only spectra for two stars; instead of a few dozens stars needed by other methods.

3. First trials

To test our method we used the echelle spectra taken by spectropolarimeter NARVAL coupled by Telescope of Barnard Lyot (TBL) at Pic du Midi Astronomical Observatory. We got spectra with S/N ratio of about 2000 and with resolution R of 67 000. For given pair of target stars observations were done during the same night to have the same atmospheric conditions. Observations with different air mass helped us to decide which weak absorption lines come from Earth atmosphere and which are extraterrestrial in their origin. To distinguish interstellar lines from weak stellar lines we observed moderately reddened spectroscopic binary (HD23180) during two subsequent nights. We observed also practically non-reddened comparison stars, which were helpful to indicate telluric lines. In Table 1 we summarize the details concerning the observed stars.

To minimize errors for ratio R we limited our measurements only to well confirmed DIBs which were additionally quite good visible in our spectra. Resulting diagrams look like this presented in Figure 1.

4. Final remarks

When watching the Figure 1 we can see that DIBs 4964, 5546 and 5819 tend to belong to the same

spectroscopic family with $R = EW(o \text{ Per}) / EW(\kappa \text{ Aql})$ of about 6. Similarly, DIBs 5766, 5850 and 5595 seem to represent the other spectroscopic family, with the ratio R of about 4. However, before qualifying DIBs as the same spectroscopic family members one has to check whether they show the same tendency for different pairs of stars, minimum for two of them. To exploit successfully the presented method we need to use spectra of very high original S/N ratio. Spectra, which are averaged from many single spectrograms taken in different time, may be slightly contaminated by weak telluric lines which are not to be fully removed when using traditional reduction procedures.

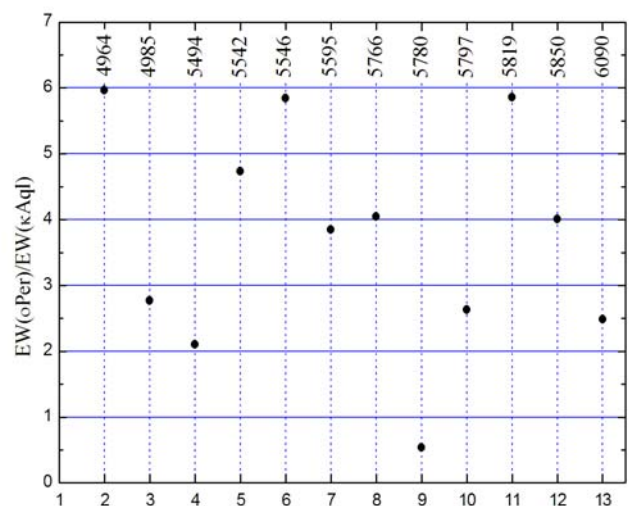


Figure 1: R^i/i diagram for the pair of stars: o Per (HD23180) - κ Aql (HD184915). On the top DIBs' names (in common notation - the profile wavelengths in angstroms) are written. On the bottom we have i-numbers describing individual DIBs.

References

- Herbig G.H.: 1995, *ARA&A*, **33**, 19
 Sarre P.J.: 2006, *J. Molec. Spectrosc.*, **238**, 1
 Wszolek B., Godłowski W.: 2003, *MNRAS*, **338**, 990

AUTHOR INDEX

- Abdel-Sabour Abdel-Latif M. 129
 Abolmasov P. 79
 Adygezalzade H.N. 46, 53
 Alentjev D.V. 6
 Alimardanova F.N. 46
 Andreev M.V. 98
 Andrievsky S.M. 41
 Andronov I.L. 8, 19, 27, 62, 65, 67
 Antipin S.V. 101
 Antoniuk K.A. 8
 Antoniuk O.I. 98
 Arkharov A. 13
 Baheddinova G.R. 46
 Baklanov A.V. 8
 Baklanova D.N. 11, 21
 Balam D.D. 86, 119
 Barsunova O. 13
 Basak N.Yu. 17
 Belik S.I. 17
 Bennett P.D. 86
 Berdnikov L.N. 129, 136
 Breus V.V. 8, 19
 Burwitz V. 8
 Butkovskaya V.V. 21
 Bychkov V.D. 23, 140
 Bychkova L.V. 23, 140
 Chekhonadskikh F.A. 29
 Chinarova L.L. 8, 25, 27
 Chini R. 136
 Chochol D. 8
 Chun-Hwey Kim 8
 Chuntonov G.A. 33
 Clarke J.R.A. 60
 Drake N.A. 94
 Drass H. 136
 Dubovsky P.A. 8, 19, 70, 133
 Durlevich O.V. 102
 English D.A. 125
 Glagolevskij Yu.V. 33
 Glazunova L.V. 83
 Godłowski W. 37
 Golovin A.V. 98
 Gopka V.F. 41
 Gorbaneva T.I. 44
 Griffin R.F. 86
 Grinin V. 13
 Gubin E.G. 27, 148
 Han W. 8
 Hegedus T. 8, 19
 Henden A.A. 8, 119
 Hoffmeister V.H. 136
 Hric L. 8
 Huziak R. 125
 Ismailov N.Z. 46, 49, 53
 Ivanyuk O. 57, 60
 Jenkins J.S. 57, 90
 Jilinski E.G. 94
 Jones H.R.A. 57, 60, 74, 90
 Kaminsky B. 57
 Kazarovets E.V. 102
 Khalilov O.V. 49
 Kim Chun-Hwey 62
 Kim Duck Hyun 62
 Kireeva N.N. 102
 Klabukova A.V. 148
 Knyazev A.Yu. 136
 Kolesnikov S.V. 8
 Kolesnikova D.M. 101
 Kovtyukh V.V. 17, 83
 Kravtsov V.V. 136
 Kudashkina L.S. 65, 67
 Kudzej I. 8, 19, 70, 133
 Kuźmicz A. 152
 Kuznetsov M.K. 57, 74
 Lane D.J. 119, 125
 Lee Jae Woo 62
 Lehmann H. 115
 Liakos A. 8
 Litvinchova A.A. 76
 Lyubchik Yu. 57
 Madej J. 23
 Majaess D.J. 119, 125
 Maryeva O. 79
 Metlov V.G. 98
 Mishenina T.V. 17, 44, 83
 Mkrtichian D.E. 6, 115
 Moncrieff K.E. 86
 Movchan A.I. 148
 Murnikov B.A. 148
 Niarchos P.G. 8
 Ogłóza W. 112
 Oksanen A. 8
 Ortega V.G. 94
 Panko E.A. 148
 Pastukhova E.N. 102
 Patkos L. 8
 Pavlenko E.P. 76, 98
 Pavlenko Ya.V. 57, 60, 74, 90
 Percy J.R. 125, 129
 Petrik K. 8, 19
 Pinfield D. 60, 74
 Pit' N.V. 8
 Plachinda S.I. 11, 21, 140
 Pogodin M.A. 94
 de la Reza R. 94
 Rosvick J.M. 119
 Samsonov D.A. 98
 Samus N.N. 101, 102
 Sat L.A. 101
 Schatilov A.V. 23
 Sergeev S. 13
 Sergienko O.G. 148
 Shakhovskoy N.M. 8
 Shavrina A.V. 33, 41
 Short C.I. 86
 Shugarov S.Yu. 13, 98
 Siwak M. 112
 Sklyanov A. 98
 Sokolovsky K.V. 101
 Soubiran C. 17, 83
 Stahl O. 136
 Szabados L. 106
 Szpanko M. 37
 Szymański T. 112
 Tkachenko A. 115
 Tsybal V. 115
 Turner D.G. 86, 119, 125, 129
 Udovichenko S.N. 133
 Ulyanov O.M. 41
 Usenko I.A. 136, 140
 Virnina N.A. 8, 143, 148
 Voloshina I.B. 98
 Wszółek B. 152
 Yonggi Kim 8
 Yoon J. 8
 Yushchenko V.A. 41
 Zola S. 8, 112
 Zubareva A.M. 98



Наукове видання

Вісті Одеської астрономічної обсерваторії

том 23 (2010)

Англійською мовою

Зав. редакцією *Т. М. Забанова*
Технічний редактор *М. І. Кошкін*
Комп'ютерна верстка: *С. Л. Страхова*

Підписано до друку 04.02.08. Формат 60x84/8.
Ум. друк. арк. 27.90. Друк офсетний. Папір офсетний. Тираж 300 прим. Зам. .

Надруковано з готового оригінал-макета
Видавництво і друкарня "Астропринт"
65091, м. Одеса, вул. Разумовська, 21.
Тел.: (0482) 37-07-95, 37-14-25, 33-07-17
www.astroprint.odessa.ua

Свідоцтво суб'єкта видавничої справи ДК №1373 від 28.05.2003 р.